

Adam Mickiewicz University in Poznan

Faculty of Biology

Department of Gene Expression

Uniwersytet im. Adama Mickiewicza w Poznaniu

Wydział Biologii

Zakład Ekspresji Genów

Katarzyna Agata Knop

Biogenesis of selected abiotic-stress responsive plant microRNAs

Biogeneza wybranych mikroRNA związanych z odpowiedzią rośliny na stresy abiotyczne



PhD thesis

Rozprawa doktorska

Supervisor: prof. dr hab. Zofia Szweykowska-Kulinska

Promotor: prof. dr hab. Zofia Szweykowska-Kulińska

Poznan, Poland 2017

Poznań, Polska 2017

FUNDING

This work was supported by the Polish National Science Center NCN (PRELUDIUM: 2012/05/N/NZ2/00955 and ETIUDA: 2015/16/T/NZ1/00022) and by the Polish Ministry of Science and Higher Education (for the KNOW RNA Research Center in Poznan (01/KNOW2/2014)).

PUBLICATIONS

Results presented within this PhD thesis have been published in the following paper:

1. Knop K*, Stepień A*, Barciszewska-Pacak M, Taube M, Bielewicz D, Michałak M, Borst J W, Jarmolowski A, Szweykowska-Kulinska Z. (2016). Active 5' splice sites regulate the biogenesis efficiency of Arabidopsis microRNAs derived from intron-containing genes. *Nucleic Acids Res* doi: 10.1093/nar/gkw895.

In addition, the following papers concerning the biogenesis and function of miRNAs have been published:

1. Stepień A*, Knop K*, Dolata J*, Taube M, Bajczyk M, Barciszewska-Pacak M, Pacak A, Jarmolowski A, Szweykowska-Kulinska Z. (2016). Post-transcriptional coordination of splicing and miRNA biogenesis in plants. *Wiley Interdiscip Rev RNA* doi: doi: 10.1002/wrna.1403.
2. Barciszewska-Pacak M, Knop K, Jarmolowski A, Szweykowska-Kulinska Z. (2016). *Arabidopsis thaliana* microRNA162 level is posttranscriptionally regulated via splicing and polyadenylation site selection. *Acta Biochim Pol* epub, No. 2016_1349, doi: 10.18388/abp.2016_1349.
3. Barciszewska-Pacak M, Milanowska K, Knop K, Bielewicz D, Nuc P, Plewka P, Pacak AM, Vazquez F, Karlowski W, Jarmolowski A, Szweykowska-Kulinska Z. (2015). Arabidopsis microRNA expression regulation in a wide range of abiotic stress responses. *Front Plant Sci* 6:410.
4. Zielezinski A*, Dolata J*, Alaba S*, Kruszka K*, Pacak A*, Swida-Barteczka A, Knop K, Stepień A, Bielewicz D, Pietrykowska H, Sierocka I, Sobkowiak L, Lakomiak A, Jarmolowski A, Szweykowska-Kulinska Z, Karlowski WM. (2015). mirEX 2.0 - an integrated environment for expression profiling of plant microRNAs. *BMC Plant Biol* 15:144.

*equal contribution

ŹRÓDŁA FINANSOWANIA

Niniejsza praca doktorska powstała dzięki dofinansowaniu w ramach grantów uzyskanych z Narodowego Centrum Nauki NCN (PRELUDIUM: 2012/05/N/NZ2/00955 i ETIUDA: 2015/16/T/NZ1/00022) oraz ze środków Ministerstwa Nauki i Szkolnictwa Wyższego (dotacja KNOW dla Poznańskiego Konsorcjum RNA (decyzja numer 01/KNOW2/2014)).

PUBLIKACJE

Wyniki badań objętych niniejszą pracą doktorską zostały przedstawione w artykule:

1. Knop K*, Stępień A*, Barciszewska-Pacak M, Taube M, Bielewicz D, Michalak M, Borst J W, Jarmołowski A, Szweykowska-Kulińska Z. (2016). Active 5' splice sites regulate the biogenesis efficiency of Arabidopsis microRNAs derived from intron-containing genes. *Nucleic Acids Res* doi: 10.1093/nar/gkw895.

Ponadto opublikowane zostały następujące prace dotyczące biogenezy i działania miRNA:

1. Stępień A*, Knop K*, Dolata J*, Taube M, Bajczyk M, Barciszewska-Pacak M, Pacak A, Jarmołowski A, Szweykowska-Kulińska Z. (2016). Post-transcriptional coordination of splicing and miRNA biogenesis in plants. *Wiley Interdiscip Rev RNA* doi: doi: 10.1002/wrna.1403.
2. Barciszewska-Pacak M, Knop K, Jarmołowski A, Szweykowska-Kulińska Z. (2016). *Arabidopsis thaliana* microRNA162 level is posttranscriptionally regulated via splicing and polyadenylation site selection. *Acta Biochim Pol* epub, No. 2016_1349, doi: 10.18388/abp.2016_1349.
3. Barciszewska-Pacak M, Milanowska K, Knop K, Bielewicz D, Nuc P, Plewka P, Pacak AM, Vazquez F, Karłowski W, Jarmołowski A, Szweykowska-Kulińska Z. (2015). Arabidopsis microRNA expression regulation in a wide range of abiotic stress responses. *Front Plant Sci* 6:410.
4. Zieleziński A*, Dolata J*, Alaba S*, Kruszka K*, Pacak A*, Świda-Barteczka A, Knop K, Stępień A, Bielewicz D, Pietrykowska H, Sierocka I, Sobkowiak L, Łakomiak A, Jarmołowski A, Szweykowska-Kulińska Z, Karłowski WM. (2015). mirEX 2.0 - an integrated environment for expression profiling of plant microRNAs. *BMC Plant Biol* 15:144.

*równocenne współautorstwo

REVIEWERS
RECENZENCI

Prof. dr hab. Włodzimierz Krzyżosiak

Department of Molecular Biomedicine

Institute of Bioorganic Chemistry

Polish Academy of Sciences

Poznan, Poland

Zakład Biomedycyny Molekularnej

Instytut Chemii Bioorganicznej

Polska Akademia Nauk

Poznań, Polska

Dr. Andreas Wachter

Center for Plant Molecular Biology

Eberhard Karls Universität Tübingen

Tübingen, Germany

Centrum Biologii Molekularnej Roślin

Uniwersytet Eberharda Karola w Tybindze

Tybinga, Niemcy

*With all of my heart I would like to thank all of the people,
without whom this work would not have been possible.*

*First of all to Professor Zofia Szweykowska-Kulinska
for giving me the opportunity of scientific development,
help, understanding, support, constructive criticism,
valuable discussions, and fruitful cooperation.*

*To Professor Artur Jarmolowski
for discussions, help, and scientific support.*

*To all of my colleagues, co-workers and professors
from the Adam Mickiewicz University in Poznan.*

*To all of the people from the Department of Gene Expression,
particularly to Agata Stepień, Maria Barciszewska-Pacak and Michał Taube
for their cooperation, invaluable support, inspiration,
and contributions that helped to foster a wonderful work environment.*

To my parents for their support and motivation.

*And a special thanks to my husband Michał
for his patience, understanding, and support during my moments of doubt.*

*Z całego serca pragnę podziękować Wszystkim,
bez których niniejsza praca nie mogłaby powstać.*

*Przede wszystkim pani Profesor Zofii Szweykowskiej-Kulińskiej
za możliwość rozwoju naukowego, wszelką pomoc,
zrozumienie, okazane wsparcie, krytyczne uwagi,
cenne merytoryczne dyskusje oraz owocną współpracę.*

*Panu Profesorowi Arturowi Jarmołowskiemu
za cenne dyskusje, okazaną pomoc oraz wsparcie naukowe.*

*Wszystkim znajomym, współpracownikom oraz profesorom
z Uniwersytetu im. Adama Mickiewicza w Poznaniu.*

*Wszystkim doktorom, doktorantom i pracownikom Zakładu Ekspresji Genów,
a w szczególności Agacie Stępień, Marii Barciszewskiej-Pacak oraz Michałowi Taube
za wspaniałą współpracę, nieocenione wsparcie,
inspirację oraz świetną atmosferę pracy.*

Moim Rodzicom za wsparcie i motywację.

*Szczególne podziękowania składam mojemu Mężowi Michałowi
za cierpliwość, wyrozumiałość oraz wsparcie w chwilach zwątpienia.*

TABLE OF CONTENTS

ABBREVIATIONS	11
SUMMARY	14
STRESZCZENIE	16
INTRODUCTION	18
1 MicroRNAs	18
1.1 MicroRNA biogenesis in plants	18
1.2 Plant microprocessor complex	21
1.2.1. DICER LIKE1 (DCL1)	22
1.2.2. SERRATE (SE).....	23
1.2.3. HYPONASTIC LEAVES 1 (HYL1)	24
1.2.4. CBC.....	25
1.2.5. Other components of the plant microprocessor complex	26
1.3 Distinct characteristics of miRNA pathways in plants and animals	29
1.4 Plant miRNA gene (<i>MIR</i>) structure.....	30
2 Splicing in plants	34
2.1 General overview of splicing principles.....	34
2.2 Alternative splicing	38
2.3 Pre-mRNA splicing in plants	39
3 Polyadenylation mechanism in plants	40
4 Posttranscriptional regulation of miRNA biogenesis	43
4.1 Crosstalk between miRNA biogenesis and splicing during maturation of exonic miRNAs derived from intron-containing genes in plants	43
4.2 Biogenesis of miRNAs located within introns of their host genes.....	44
4.2.1. Intronic miRNA maturation in mammals.....	44
4.2.2. Intronic miRNA biogenesis in plants	46
5 Plant miRNAs responsive to biotic and abiotic stress factors	50
6 Biogenesis of miR319b and miR319b.2 in <i>Arabidopsis thaliana</i>	53
THE AIM OF THE WORK	61
MATERIALS AND METHODS	62
1 Reagents	62
2 Plant material	64
2.1 Plant growth conditions.....	64
2.1.1. Plant culture on MS medium.....	64
2.1.2. Plant culture in soil.....	65

2.2	Plant transformation.....	65
2.2.1.	Transformation of <i>Arabidopsis thaliana</i> plants using the floral dip technique.....	65
2.2.2.	Selection of <i>Arabidopsis</i> transgenic lines using BASTA herbicide.....	66
2.2.3.	Transient expression in <i>Nicotiana benthamiana</i> leaves.....	66
2.3	Induction of <i>A. thaliana</i> plant response to selected abiotic stresses.....	67
2.3.1.	Heat stress.....	67
2.3.2.	Salinity stress.....	67
2.3.3.	Drought stress.....	67
2.4	Plant treatment with transcription inhibitor – cordycepin (3'-Deoxyadenosine)	68
2.4.1.	Heat-stressed <i>A. thaliana</i> 17-day-old seedling treatment with cordycepin.....	68
2.4.2.	Agroinfiltrated <i>N. benthamiana</i> leaf disc treatment with cordycepin.....	68
2.5	Plant treatment with splicing inhibitor – Herboxydiene (Gex-1A).....	69
3	Bacterial cultures.....	70
3.1	Bacteria strains.....	70
3.2	Bacterial culture media and reagents.....	70
3.3	<i>E. coli</i> cell transformation.....	71
3.3.1.	Preparation of competent <i>E. coli</i> cells.....	71
3.3.2.	Transformation of <i>E. coli</i> cells using heat-shock method.....	72
3.3.3.	Transformed <i>E. coli</i> cell growth conditions and selection.....	72
3.4	<i>A. tumefaciens</i> cell transformation.....	73
3.4.1.	Preparation of competent AGL1 cells.....	73
3.4.2.	Transformation of AGL1 cells using electroporation method.....	73
3.4.3.	Transformed AGL1 cells growth conditions and selection.....	73
4	Methods used during work with ribonucleic acid (RNA).....	75
4.1	Northern hybridization.....	75
4.1.1.	RNA isolation using TRIzol reagent.....	75
4.1.2.	RNA electrophoresis in agarose gel.....	76
4.1.3.	RNA electrophoresis in polyacrylamide gel.....	77
4.1.4.	RNA transfer from gel to membrane.....	77
4.1.5.	Radiolabeling of DNA oligonucleotides.....	78
4.1.6.	Hybridization of radiolabeled oligonucleotides with RNA.....	78
4.1.7.	Hybridization signal detection.....	79
4.2	cDNA preparation.....	80
4.2.1.	RNA isolation for cDNA preparation.....	80
4.2.2.	Removing genomic DNA contamination from RNA sample.....	80
4.2.3.	First-strand cDNA synthesis for RT-PCR/RT-qPCR analysis.....	80

4.2.4.	First-strand cDNA synthesis for 5' RLM-RACE PCR and 3' RACE PCR analyses	81
5	Methods used during work with deoxyribonucleic acid (DNA)	82
5.1	Genomic DNA isolation.....	82
5.2	PCR reactions.....	83
5.2.1.	PCR reactions using DreamTaq DNA Polymerase.....	83
5.2.2.	PCR reactions using Pfu DNA Polymerase	84
5.2.3.	Quantitative real-time PCR technique (RT-qPCR).....	85
5.2.3.1	Gene expression analysis using Power SYBR® Green PCR Master Mix ..	85
5.2.3.2	MiRNA accumulation level analysis using TaqMan® Universal Master Mix II with UNG.....	86
5.2.4.	Site-directed mutagenesis.....	87
5.2.5.	5' RLM-RACE PCR and 3' RACE PCR analyses	88
5.3	DNA electrophoresis in agarose gel.....	91
5.4	Genetic construct preparation	92
5.4.1.	DNA purification directly from PCR mixture or extraction from agarose gel	92
5.4.2.	Restriction cleavage of DNA	93
5.4.3.	Vector dephosphorylation.....	93
5.4.4.	DNA ligation.....	93
5.4.5.	Plasmid DNA isolation	94
5.4.6.	DNA sequencing	94
5.4.7.	LR clonase reaction.....	94
5.4.8.	Vectors	95
6	Oligonucleotides	95
7	Bioinformatic tools and databases.....	102
7.1	Programs	102
7.2	Databases	103
RESULTS		104
1	Biogenesis of intronic miRNAs in <i>Arabidopsis thaliana</i>	104
1.1	Characterization of Arabidopsis intronic miRNAs	104
1.2	Analysis of miR402 biogenesis in selected abiotic stresses.....	108
1.3	Intronic miR402 biogenesis regulation after splicing inhibitor treatment (Gex-1A)	117
1.4	Active 5'SS controls miR402 biogenesis.....	122
1.5	The effect of pre-miR402 stem-loop structure localization on miRNA biogenesis efficiency.....	129
1.6	The role of SERRATE protein in regulation of intronic miRNA maturation	136

2	Functional dissection of miR319b and miR319b.2 biogenesis in plants	139
2.1	Preparation of Arabidopsis transgenic lines carrying mutated versions of <i>MIR319b</i>	139
2.2	Detailed analysis of miR319b and miR319b.2 in selected transgenic lines.....	143
2.2.1.	Analysis of pri-miR319b and mature miRNA levels in <i>MIR319b</i> transgenic lines.....	143
2.2.2.	Analysis of selected target mRNA levels.....	145
	DISCUSSION	151
1	Biogenesis of intronic miRNAs in <i>Arabidopsis thaliana</i>	151
1.1	Plant intronic miRNA accumulation depends on developmental stage or environmental conditions tested	151
1.2	Plant intronic pri-miRNAs can be transcribed as independent transcription units from their host pre-mRNAs	152
1.3	Splicing inhibition stimulates intronic miRNA biogenesis efficiency	154
1.4	Active 5' splice site controls biogenesis of intronic miR402.....	157
1.5	Selection of polyadenylation site within pri-miRNA transcripts influences plant intronic miRNA biogenesis efficiency	158
1.6	SERRATE is key player in crosstalk between the plant microprocessor and spliceosome	159
1.7	Co-transcriptional regulation of intronic miRNA biogenesis in plants.....	164
2	Functional dissection of miR319b and miR319b.2 biogenesis in plants	165
	CONCLUSIONS	169
	FUTURE PERSPECTIVES	170
	LITERATURE	175

ABBREVIATIONS

3'SS	3' SPLICE SITE
5'SS	5' SPLICE SITE
A	ADENOSINE
aa	AMINO ACID RESIDUE
ABA	ABSCISIC ACID
ABF	ABSCISIC ACID RESPONSIVE ELEMENT-BINDING FACTOR
ACT	ACTIN
AF	AUXILIARY FACTOR
AGO	ARGONAUTE
AMP	ALTERED MERISTEM PROGRAM
APA	ALTERNATIVE POLYADENYLATION
APS	AMMONIUM PEROXYDISULFATE
AS	ALTERNATIVE SPLICING
ATP	ADENOSINE TRIPHOSPHATE
BASTA	GLUFOSINATE AMMONIUM
BP	BRANCH POINT
C	CYTOSINE
CBC	CAP-BINDING COMPLEX
CBP	CAP-BINDING PROTEIN
CE	CLEAVAGE ELEMENT
cDNA	COMPLEMENTARY DNA
CDS	CODING REGION OF THE GENE
DEPC	DIETHYL PYROCARBONATE
ChIP	CHROMATIN IMMUNOPRECIPITATION
DML	DEMETER-LIKE
DMSO	DIMETHYL SULFOXIDE
CPSF	CLEAVAGE AND POLYADENYLATION SPECIFICITY FACTOR
cry SS	CRYPTIC SPLICE SITE
CStF	CLEAVAGE STIMULATORY FACTOR
CTD	C-TERMINAL DOMAIN OF RNA POLYMERASE II
CYP	CYCLOPHILIN
DCL	DICER-LIKE
DRB	DOUBLE-STRANDED RNA-BINDING PROTEIN
dsRNA	DOUBLE-STRANDED RNA

EDTA	ETHYLENEDIAMINETETRAACETIC ACID
ER	ENDOPLASMIC RETICULUM
ES	EXON SKIPPING
FS	FULLY-SPLICED ISOFORM
FUE	FAR UPSTREAM ELEMENT
G	GUANOSINE
GAPDH	GLYCERALDEHYDE-3-PHOSPHATE DEHYDROGENASE
Gex-1A	HERBOXYDIENE
hc-siRNA	HETEROCHROMATIC SMALL-INTERFERING RNA
HEN	HUA ENHANCER
hnRNP	HETEROGENEOUS NUCLEAR RIBONUCLEOPROTEIN
HSP	HEAT-SHOCK PROTEIN
HST	HASTY
HYL	HYPONASTIC LEAVES
IR	INTRON RETENTION
kDA	KILODALTON
LB	LURIA-BERTANI MEDIUM
LEA	LATE EMBRYOGENESIS ABUNDANT
MIR	microRNA-ENCODING GENE
miRNA	microRNA
mRNA	MESSENGER RNA
MS	MURASHIGE & SKOOG MEDIUM
MYB	MYELOBLAST FAMILY
NCED	NINE-CIS-EPOXYCAROTENOID DIOXYGENASE
NLS	NUCLEAR LOCALIZATION SIGNAL
NMD	NONSENSE MEDIATED DECAY
nt	NUCLEOTIDE
NTC	NINETEEN COMPLEX
NUE	NEAR UPSTREAM ELEMENT
ORF	OPEN READING FRAME
PAB	POLY(A)-BINDING PROTEIN
PAP	POLY(A) POLYMERASE
PAZ	PIWI ARGONAUTE ZWILLE
PCR	POLYMERASE CHAIN REACTION
PolyA SITE	CLEAVAGE AND POLYADENYLATION SITE
PPT	POLYPYRIMIDINE TRACT
Pre-miRNA	microRNA STEM-LOOP STRUCTURE PRECURSOR

Pre-mRNA	PRECURSOR MESSENGER RNA
Pri-miRNA	microRNA PRIMARY PRECURSOR
PRP	Pre-mRNA-PROCESSING PROTEIN
PTB	POLYPYRIMIDINE TRACT BINDING PROTEINS
PTC	PREMATURE TERMINATION CODON
RAB	RESPONSIVE TO ABA
RACE PCR	RAPID AMPLIFICATION OF cDNA ENDS
RISC	RNA-INDUCED SILENCING COMPLEX
RLM-RACE PCR	RNA LIGASE MEDIATED RAPID AMPLIFICATION OF cDNA ENDS
RNA Pol II	RNA POLYMERASE II
RPM	REVOLUTIONS PER MINUTE
rRNA	RIBOSOMAL RNA
RT-qPCR	REVERSE TRANSCRIPTION FOLLOWED BY A QUANTITATIVE POLYMERASE CHAIN REACTION
SDS	SODIUM DODECYL SULFATE
SE	SERRATE
SF	SPLICING FACTOR
siRNA	SMALL-INTERFERING RNA
snRNP	SMALL NUCLEAR RIBONUCLEOPROTEIN
SPL	SQUAMOSA PROMOTER-BINDING PROTEIN-LIKE
SR	SERINE/ARGININE RICH PROTEIN
SS	SPLICE SITE
SWC	SOIL WATER CONTENT
T	THYMINE
ta-siRNA	TRANS-ACTING SMALL-INTERFERING RNAS
TEMED	N, N, N', N'-TETRAMETHYLETHYLENEDIAMINE
TF	TRANSCRIPTION FACTOR
TRIS	TRIS[HYDROXYMETHYL]AMINOMETHANE
TSPO	OUTER MEMBRANE TRYPTOPHAN-RICH SENSORY PROTEIN
TSS	TRANSCRIPTION START SITE
U	URIDINE
UTR	UNTRANSLATED REGION
X-Gal	5-BROMO-4-CHLORO-3-INDOLYL-D-GALACTOPYRANOSIDE

SUMMARY

MicroRNAs (miRNAs) are short, single-stranded, non-coding RNAs present in almost all eukaryotic cells that regulate the expression of many genes in cells at the posttranscriptional level. MiRNA biogenesis in plants is conducted by multicomponent machinery known as the microprocessor complex. Plant miRNAs are encoded by *MIR* genes, which can be complicated in-structure. For example, many of them contain introns which splicing has been shown to stimulate the production of mature miRNAs. Interestingly, in *A. thaliana* 29, miRNAs are located within the introns of protein-coding or non-coding RNA genes (host genes). However, knowledge concerning the mechanism of intronic miRNA maturation in plants still remains limited.

The main aim of the first part of the presented PhD thesis was to reveal the Arabidopsis intronic miRNA biogenesis mechanism. For intronic miR402, abiotic stress treatment caused upregulation of the miRNA level, which correlated with the lower efficiency of the miRNA-hosting intron splicing and with the highest proximal polyA site selection. Moreover, the inactivation of the constitutive 5' splice site (5'SS) of the miRNA-carrying intron (resulting in splicing inhibition) correlated with upregulation of the level of mature miR402, accompanied by a higher proximal polyA site selection. Besides, the position of the miRNA stem-loop structure regarding the nearest active 5'SS turned out to be relevant for miR402 biogenesis efficiency. The effect of the 5'SS was stimulatory or inhibitory when the pre-miR402 hairpin was located upstream or downstream from this splice site, respectively. What is more, further experiments revealed that the interactions between the microprocessor and spliceosome play an essential role in regulating the biogenesis of *A. thaliana* intronic miRNAs. Importantly, these connections seem to be relevant for intronic miRNA maturation under changed environmental conditions.

The main goal of the second part of this PhD thesis was the dissection of Arabidopsis miR319b and miR319b.2 biogenesis. Both of these miRNAs are located within the same pre-miR319b, but they differ in nucleotide sequences and targeted mRNAs. Analyses performed with the use of genetic transgenic lines carrying modified versions of pre-miR319b revealed that any alterations (mutations or deletions) introduced within miR319b/miR319b* sequences caused significant downregulation of pri-miR319b

and mature miR319b.2 levels. Moreover, analysis of the selected target mRNAs indicated that modifications of miR319b/miR319b*, besides the regulation of miR319b target mRNAs (TCP4, TCP10 and TCP24), can also influence the levels of TBL10 and the IR-isoform of RAP2.12 (miR319b.2 target mRNAs). A similar effect has been observed for modifications introduced within miR319b.2/miR319b.2* sequences. The presented results indicated that miR319b and miR319b.2 biogenesis might be mechanistically coupled, and both analyzed miRNAs can cross-regulate their target mRNA levels. However, to fully understand the mechanism of miR319b and miR319b.2 maturation and the biological functions of these two miRNAs in plant development, further experiments are necessary.

Keywords:

Arabidopsis thaliana, gene expression, microRNA, miRNA biogenesis, splicing, polyadenylation, abiotic stress, pri-miRNA posttranscriptional regulation

STRESZCZENIE

MikroRNA (miRNA) to krótkie cząsteczki RNA, powszechnie występujące w organizmach eukariotycznych, regulujące ekspresję wielu genów na poziomie potranskrypcyjnym. Za dojrzewanie roślinnych miRNA odpowiedzialna jest złożona maszyna białkowa, zwana kompleksem mikroprocesora. Cząsteczki miRNA kodowane są przez geny *MIR* charakteryzujące się złożoną budową. Wykazano między innymi, że mogą one zawierać introny, których splicing stymuluje dojrzewanie miRNA. Co ciekawe, u *A. thaliana*, 29 cząsteczek miRNA położonych jest w intronach tzw. genów gospodarzy kodujących funkcjonalne białka lub niekodujące RNA. Wiedza dotycząca mechanizmu powstawania intronowych miRNA u roślin nadal jest niewystarczająca.

Celem pierwszej części prezentowanej pracy doktorskiej było poznanie mechanizmu dojrzewania intronowych miRNA u *Arabidopsis*. W wybranych warunkach stresu abiotycznego zaobserwowano, że podniesiony poziom intronowej cząsteczki miR402 korelował z obniżoną wydajnością wycinania intronu goszczącego miRNA oraz z częstszym wyborem alternatywnego, proksymalnego miejsca poliadenylacji. Ponadto, inaktywacja konstytutywnego miejsca 5' splicingowego intronu zawierającego pre-miR402, która spowodowała zahamowanie splicingu tego intronu, skutkowałą podwyższeniem akumulacji miR402 oraz częstszym wyborem proksymalnego miejsca poliA. Co ważne, przeprowadzone eksperymenty ujawniły, że lokalizacja pre-miRNA w stosunku do najbliższego aktywnego miejsca 5' splicingowego ma kluczowe znaczenie dla wydajności dojrzewania miR402. Efekt ten był stymulujący lub hamujący, gdy pre-miR402 położony był odpowiednio powyżej lub poniżej aktywnego miejsca 5' splicingowego. Dalsze eksperymenty udowodniły, że oddziaływania pomiędzy maszyną biogenezy miRNA a splicingową odgrywają ważną rolę w regulacji dojrzewania miRNA u roślin, także podczas odpowiedzi rośliny na czynniki stresowe.

Głównym celem drugiej części niniejszej pracy doktorskiej była analiza biogenezy cząsteczek miR319b i miR319b.2 u *A. thaliana*. Obie cząsteczki zlokalizowane są w obrębie jednej struktury typu „*spinka do włosów*” pre-miR319b, aczkolwiek posiadają inną sekwencję nukleotydową oraz regulują inne docelowe mRNA. Analizy przeprowadzone w liniach transgenicznym zawierających zmodyfikowane wersje pre-miR319b wykazały, że modyfikacje sekwencji miR319b/miR319b* skutkowałą obniżeniem poziomu pri-miR319b i dojrzałego miR319b.2. Ponadto, analizy

poziomu docelowych mRNA wykazały, że modyfikacje te, oprócz zmiany poziomu mRNA *TCP4*, *TCP10* i *TCP24* (regulowanych przez miR319b) spowodowały także zmianę poziomu mRNA *TBL10* oraz izoformy splicingowej *RAP2.12* (kontrolowanych przez miR319b.2). Podobną regulację zaobserwowano w przypadku modyfikacji wprowadzonych w obrębie miR319b.2/miR319b.2*. Przedstawione wyniki wykazały, że dojrzewanie cząsteczek miR319b i miR319b.2 może być wzajemnie powiązane oraz że obie cząsteczki mogą współkontrolować poziom swoich docelowych mRNA. Do pełnego zrozumienia mechanizmu biogenezy miR319b i miR319b.2 i ich roli w regulacji wzrostu i rozwoju roślin niezbędne jest przeprowadzenie dodatkowych eksperymentów.

Słowa kluczowe:

Arabidopsis thaliana, ekspresja genów, mikroRNA, biogeneza miRNA, splicing, poliadenylacja, stres abiotyczny, potranskrypcyjna regulacja poziomu pri-miRNA

INTRODUCTION

1 MicroRNAs

1.1 MicroRNA biogenesis in plants

Other than siRNAs (small-interfering RNAs), microRNAs (miRNAs) are the second-most-abundant class of small noncoding RNAs present in eukaryotic cells. MiRNAs are short (19-24 nucleotides in length) and single-stranded (Carrington et al., 2003; Voinnet et al., 2009). MiRNAs regulate the expression of many genes at the posttranscriptional level via mRNA cleavage and degradation or by translational repression through base pairing to their target mRNAs. The first miRNA (*lin-4*) was identified in 1993 and described as a regulator of larval development in *Caenorhabditis elegans* (Lee et al., 1993; Wightman et al., 1993). In 2002, 16 *Arabidopsis* miRNAs exhibiting differential expression patterns during plant development were discovered (Reinhart et al., 2002). As of now, more than 400 miRNAs have been identified in *A. thaliana*, while more than 1000 miRNAs have been found in humans (Kozomara and Griffiths-Jones, 2014). MiRNAs are believed to exist in all multicellular organisms (excluding fungi) and are considered to be fundamental regulators of the expression of almost all of the genes in a cell (Voinnet et al., 2009; Kruszka et al., 2012).

Plant miRNA biogenesis is a multistep process that, in contrast to animal cells, occurs primarily in the cell nucleus (Park et al., 2005). MiRNA genes (*MIRs*) are transcribed by RNA polymerase II (RNA Pol II) to primary transcripts (pri-miRNAs). *MIR* transcription is controlled by many transcription factors (TFs); e.g., Mediator complex, NEGATIVE ON TATA2 (NOT2), and CELL DIVISION CYCLE5 (CDC5) (Kim et al., 2011; Wang et al., 2013; Zhang et al., 2013). These TFs are involved in the facilitation and recruitment of RNA Pol II to the promoters of miRNA genes. Moreover, within the plant *MIR* promoters, the binding sites of several other transcription factors have been identified that can play regulatory roles under specific conditions. These include SQUAMOSA PROMOTER BINDING PROTEIN-LIKE7 (SPL7) (binds to *MIR398b* and *MIR398c* promoters under copper deficiency) and MYB2 (binds to the *MIR399f* promoter under phosphate-deficiency stress) (Yamasaki et al., 2009; Baek et al., 2013). What is important is that, since *MIRs* are transcribed by RNA Pol II, they contain cap structures and a polyA tail at the 5' and 3' pri-miRNA ends,

respectively (Xie et al., 2005). To the cap structure of miRNA transcripts, CAP-BINDING COMPLEX (CBC) is binding; this consists of two proteins: CAP-BINDING PROTEIN 20 (CBP20) and CAP BINDING PROTEIN 80 (CBP80) (Izaurralde et al., 1994; Izaurralde et al., 1995; Kmiecik et al., 2002). The role of this complex in plant miRNA biogenesis is described more precisely in the next subchapter.

Pri-miRNA processing to mature miRNA occurs entirely in the nucleus in a two-step process and is conducted by multicomponent machinery called the microprocessor complex. The core of this complex consists of the RNase III ribonuclease - DICER-LIKE1 (DCL1), HYPONASTIC LEAVES 1 (HYL1, also known as DOUBLE-STRANDED RNA BINDING PROTEIN 1 (DRB1)) and SERRATE (SE) (Reinhart et al., 2002; Dong et al., 2008; Laubinger et al., 2008). DCL1 is an endonuclease that is responsible for both cleavages occurring during plant miRNA biogenesis: (1) when pri-miRNAs are processed to miRNA-containing stem-loop structures (pre-miRNAs); and (2) when miRNA/miRNA* duplexes are cut out from pre-miRNAs (Park et al., 2002). What is important is that HYL1 and SE are necessary for the efficient and correct processing of pri-miRNAs by the regulation of proper cleavage by DCL1 (Dong et al., 2008). Besides these three proteins, there are many other components of the microprocessor complex that are involved in miRNA maturation. A detailed description of all of these proteins is included in the next subchapter.

After excision, miRNA/miRNA* duplexes are methylated by methylase HUA ENHANCER 1 (HEN1) at the 3' ends, which protects them from degradation (Park et al., 2005). Next, methylated duplexes are exported from the nucleus to the cytoplasm by the action of exportin HASTY (HST) (Bollman et al., 2003). Then, the passenger strand of the duplex (miRNA*) is removed, and mature miRNA is incorporated into the RNA-induced Silencing Complex (RISC). The main component of the RISC complex is the ARGONAUTE 1 protein (AGO1) (Baumberger and Baulcombe, 2005). In plants, there are ten members of the AGO family, among which AGO1 is involved in the miRNA-guided target mRNA cleavage. Only miRNAs incorporated in RISC are able to regulate their target mRNA expression. For proper RISC formation, other proteins such as HEAT SHOCK PROTEIN 90 (HSP90) and CYCLOPHILIN 40 (CYP40) are also necessary (Iki et al., 2010; 2012). They facilitate the incorporation of miRNA/miRNA* duplexes into the RISC complexes via activation of the conformational changes of the AGO1 protein.

As mentioned above, miRNAs bind to the sequence-complementary regions of mRNAs and cause their degradation via cleavage or inhibit their translation to functional proteins. Up until now, the first mechanism is prevalent in plants and involves AGO1 slicing activity for the cleaving mRNA targets that have high base-pair complementarity to the miRNA embedded into the RISC complex (Parker et al., 2004). Although miRNA action in translation inhibition is most common in animal and human cells, there are few such examples described in plants. MiR156 and miR157 cause a reduction of the SPL3 protein level without affecting its mRNA transcript level (Gandikota et al., 2007). Moreover, it has been shown that miR172 can function in both pathways by cleavage or translation inhibition of its target mRNA APETALA 2 (Aukerman and Sakai, 2003). Unfortunately, the exact mechanism of this pathway in plants (which does not require perfect miRNA- target mRNA complementarity) is still unknown. There are suggestions that the selection between miRNA action modes can be dependent on DCL1 protein partners, since it has been demonstrated that the DRB1 (HYL1) and DRB2 proteins are required for target mRNA cleavage or miRNA-guided translation inhibition, respectively (Reis et al., 2015). What is more, it has been shown, that translation repression in plants occurs at the cytoplasmic face of the endoplasmic reticulum (ER) membrane and involves AGO1 association with ALTERED MERISTEM PROGRAM1 (AMP1), which is an ER integral membrane-associated protein (Li et al., 2013).

To sum up this chapter, the canonical miRNA biogenesis pathway in plants is presented in the figure below (Fig. 1).

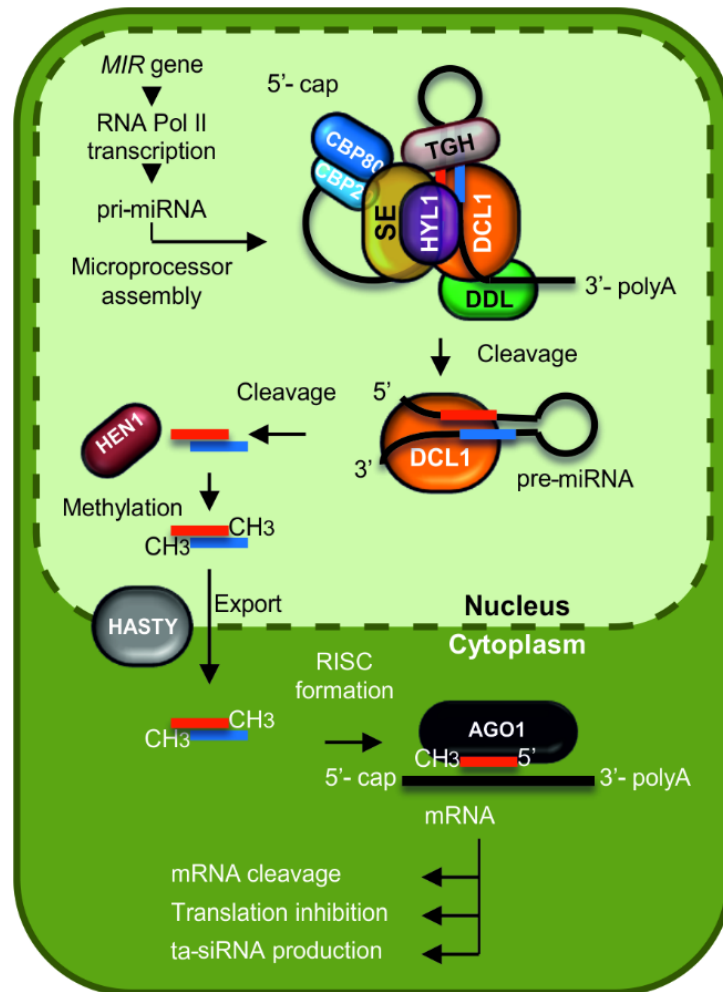


Figure 1. The canonical plant miRNA biogenesis pathway (Stepien, Knop, Dolata et al., 2016, modified). Red and blue lines - miRNA and miRNA*; stem-loop structure – pre-miRNA; black line – target mRNA. All protein abbreviations are listed in the text as well as in Table 1.

1.2 Plant microprocessor complex

As mentioned in the previous subchapter, miRNA biogenesis in plants is handled by the multicomponent microprocessor complex, whose core consists of three major components: DCL1, SE, and HYL1. It has been reported that plant miRNA maturation occurs primarily in the nuclear foci called dicing bodies (D-bodies), where DCL1, HYL1, and SE are located (Fang and Spector, 2007). In this subchapter, the most important plant microprocessor components and associated proteins are described.

1.2.1. DICER LIKE1 (DCL1)

DCL1 (DICER LIKE1), a human homolog of the Dicer 1 protein, is an endoribonuclease involved in both cleavage steps during miRNA biogenesis in plants (Park et al., 2002). It contains several domains important to its function: (1) two NLS signals (Nuclear Localization Signal); (2) the DExD/H-box RNA helicase domain (responsible for RNA recognition and cleavage); (3) the DUF283 domain (a novel RNA-binding domain); (4) the PAZ domain (characteristic for miRNA-pathway proteins); (5) two RNase III domains; and (6) two dsRNA-binding domains (Schauer et al., 2002; Qin et al., 2010).

Since null mutants of the DCL1 are embryo-lethal, it is clear that this protein plays an important role in plant cells (Schauer et al., 2002). Up until now, several weak Arabidopsis mutants containing mutations in different DCL1 domains have been described. In two of them (*dcl1-7* (single amino-acid substitution within the helicase domain) and *dcl1-9* (T-DNA insertion in the second dsRBD domain)), a strong inhibition of miRNA biogenesis has been reported (Kurihara et al., 2006). In both of these mutants, levels of pri-miRNAs increased with a concurrent downregulation of mature miRNA accumulation (Kurihara et al., 2006; Song et al., 2007; Zielezinski et al., 2015). Analysis of the protein variants present in DCL1 mutant plants revealed that the *dcl1-7* version is still able to interact with other components of the core microprocessor – HYL1 and SE proteins – while HYL1-DCL1 connections and DCL1 localization in D-bodies are lost in the *dcl1-9* variant (Fang and Spector, 2007; Fujioka et al., 2007). What is more, *dcl1-7* (Fig. 2) and *dcl1-9* plants show many phenotypic features characteristic for miRNA biogenesis mutants; e.g., growth retardation, late flowering, smaller leaves, and female fertility (Schauer et al., 2002).

Interestingly, it has also been reported that other proteins from the DCL family, like DCL3 (involved in heterochromatic siRNAs [hc-siRNAs] biogenesis) and DCL4 (required for trans-acting siRNAs [ta-siRNAs] production), may play an important roles in the miRNA maturation pathway in plants (Henderson et al., 2006; Rajagopalan et al., 2006; Vazquez et al., 2008).

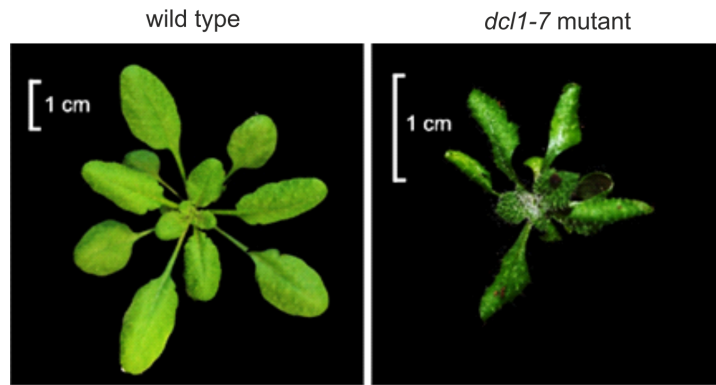


Figure 2. Phenotype comparison between rosette leaves of Arabidopsis wild-type and *dcl1-7* mutant plants (Zielezinski et al., 2015).

1.2.2. SERRATE (SE)

The SERRATE protein is about an 80-kDa (kilodalton) protein that consists of one structured fragment (the central part of the protein, called the core) and two unstructured fragments (located at both the N- and C-termini) (Machida et al., 2011). The core part is responsible for SE interactions with DCL1 and HYL1 and contains three domains: (1) an N-terminal domain; (2) a middle domain; and (3) a C2H2-type zinc finger domain (at the C-terminus). Moreover, the unstructured N-terminal part of SE has been shown to be involved in pri-miRNA binding (Iwata et al., 2013). It has also been reported that SE interacts with both subunits of the CBC complex (Raczynska et al., 2014).

As SERRATE plays a pivotal role in the plant cell, the null mutants of this protein are embryo-lethal (Lobbes et al., 2006). However, there are three weak hypomorphic SE mutants described in the literature: *se-1*, *se-2*, and *se-3* (Prigge and Wagner, 2001; Grigg et al., 2005). In *se-1*, the deletion of 20 C-terminal amino acids (aa) results in a serrated leaf shape (Fig. 3A-B) (Prigge and Wagner, 2001). More severe phenotypical changes (i.e., hyponastic leaves and growth retardation) are observed in the *se-2* mutant, in which the SE protein lacks 40 C-terminal aa residues (Fig. 3C) (Grigg et al., 2005). The most-severe phenotype alterations (like hypertrophic meristem and defective patterning of leaves that are upwardly curled) exhibit the *se-3* mutant (Fig. 3C). In all three mutants, increased levels of pri-miRNAs and a reduced accumulation of mature miRNAs have been detected (Prigge and Wagner, 2001; Grigg et al., 2005; Yang et al., 2006).

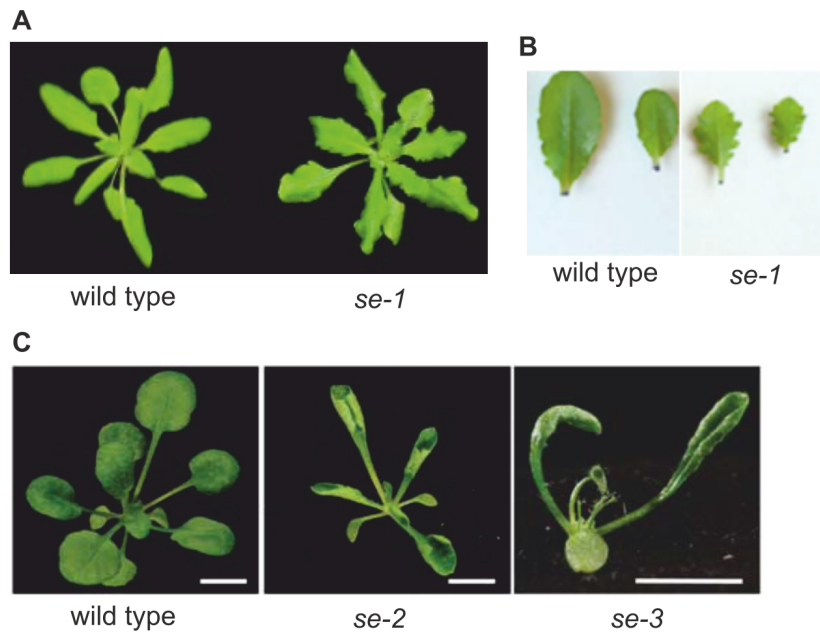


Figure 3. Phenotype comparison between Arabidopsis wild-type and (A-B) *se-1*, (C) *se-2*, and *se-3* mutant plants (Department of Gene Expression, AMU, Poznan; Grigg et al., 2005, modified; Laubinger et al., 2008, modified). The line bars =5 mm.

In addition to its function in miRNA biogenesis, SERRATE has also been shown to be involved in the splicing regulation of pre-mRNAs and pri-miRNAs (Laubinger et al., 2008; Raczynska et al., 2010, 2014). What is important is that, besides its localization in D-bodies, SE has also been found in nuclear speckles, that contain serine/arginine-rich proteins (SR proteins) (Ali et al., 2003; Fang and Spector, 2007).

1.2.3. HYPONASTIC LEAVES 1 (HYL1)

The third component of the plant microprocessor is the HYPONASTIC LEAVES 1 (HYL1) protein, which belongs to the family of proteins binding double-stranded RNAs (dsRNA) (DRBs) (Lu and Fedoroff, 2000; Hiraguri et al., 2005). Thus, it is also called the DRB1 protein. HYL1 consists of two dsRNA-binding domains: dsRBD1 and dsRBD2 (Yang et al., 2010). The second domain is necessary for DCL1-HYL1 and HYL1-SE core interactions as well as for HYL1 homodimerization (important for its activity during pri-miRNA processing). Both of these domains are sufficient for HYL1 action in miRNA biogenesis (Wu et al., 2007). Moreover, it has recently been demonstrated that, to efficiently act during pri-miRNA processing, HYL1 needs to be dephosphorylated (Manavella et al., 2012). In this process, the C-TERMINAL DOMAIN PHOSPHATASE LIKE 1 (CPL1) protein is involved (see Table 1).

In contrast to DCL1 and SE, the null mutant of the HYL1 protein (*hyl1-2*) is not lethal and shows characteristic phenotype features, like hyponastic leaves and growth retardation (Fig. 4) (Lu and Fedoroff, 2000; Vazquez et al., 2004). In *hyl1-2* plants, upregulated levels of pri-miRNAs and a reduced accumulation of mature miRNAs have been observed (Szarzynska et al., 2009).

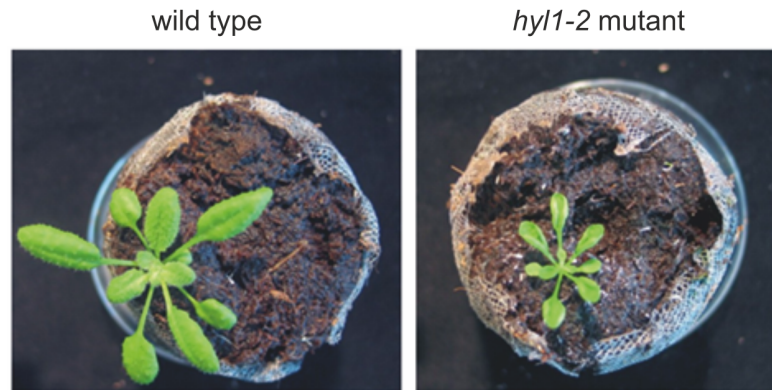


Figure 4. Phenotype comparison between rosette leaves of Arabidopsis wild-type and *hyl1-2* mutant plants (Department of Gene Expression, AMU, Poznan).

1.2.4. CBC

As mentioned above, the CBC complex consists of two components – CBP20 and CBP80 (Kmieciak et al., 2002). Both subunits interact with each other as well as with the SERRATE protein (Kierzkowski et al., 2009; Raczyńska et al., 2014). Null mutants *cbp20* and *cbp80* exhibit the same phenotype changes as the *se-1* mutant (Fig. 5) along with a higher level of pri-miRNAs and lower accumulation of mature miRNAs (Laubinger et al., 2008). Interestingly, CBP20, CBP80 and SE have been shown to also be involved in pre-mRNA and pri-miRNA splicing regulation (Raczyńska et al., 2010, 2014). According to this information, both CBC and SE seem to be the best communicators between the spliceosome and the microprocessor complex.



Figure 5. Phenotype comparison between rosette leaves of *Arabidopsis* wild-type and *cbc* mutant plants (Department of Gene Expression, AMU, Poznan).

1.2.5. Other components of the plant microprocessor complex

Besides DCL1, HYL1, SE, and CBC, there are many other players that affect plant miRNA biogenesis at the transcriptional/posttranscriptional level by regulating *MIR* transcription or pri-miRNA splicing efficiency (for example). The most important proteins (and their functions during miRNA maturation) are described in the table below (Tab. 1).

Table 1. Other proteins involved in plant miRNA biogenesis (adapted from Stepien et al., 2016)

Protein	Functions in miRNA biogenesis	Direct interactors	References
DAWDLE (DDL)	Stabilization of pri-miRNA during cleavage by DCL1	DCL1	Yu et al., 2008
TOUGH (TGH)	Binding of pri-miRNAs and pre-miRNAs; regulation of pri-miRNA processing; reinforcement of pri-miRNA-HYL1 interactions	DCL1, SE, HYL1	Ren et al., 2012 ^a
HEN1 SUPPRESSOR 1 (HESO1)	Bringing unmethylated miRNA/miRNA* duplexes to degradation by uridylation	Unknown	Ren et al., 2012 ^b

C-TERMINAL DOMAIN PHOSPHATASE LIKE 1 (CPL1)	Dephosphorylation of HYL1	SE, HOS5, RS40, RS41	Manavella et al., 2012; Chen et al., 2013; Chen et al., 2015
CONSTITUTIVE PHOTOMORPHOGENIC 1 (COP1)	Hindering of pri-miRNA processing by suppression of the protease X (specifically cleaves off two dsRBDs of HYL1)	Unknown	Cho et al., 2014
SICKLE (SIC)	Regulation of pri-miRNA processing	Colocalization with HYL1	Zhan et al., 2012
MODIFIER OF SNC1-2 (MOS2)	Binding to pri-miRNAs; pri-miRNA processing regulation	Unknown	Wu et al., 2013
HIGH EXPRESSION OF OSMOTICALLY RESPONSIVE GENES 5 (HOS5)	Present in complexes with pri-miRNAs; regulation of pri-miRNA processing	SE, HYL1, CPL1, RS40, RS41	Chen et al., 2013; Chen et al., 2015
ARGININE/SERINE-RICH SPLICING FACTOR 40/41 (RS40/RS41)	Present in complexes with pri-miRNAs; regulation of pri-miRNA processing	SE, HYL1, HOS5	Chen et al., 2013; Chen et al., 2015
STABILIZED 1 (STA1)	Regulation of pri-miRNA processing	Unknown	Chaabane et al., 2012
RECEPTOR FOR ACTIVATED C KINASE 1 (RACK1)	Stabilization of pri-miRNA; regulation of pri-miRNA processing	SE	Speth et al., 2013
GLYCINE-RICH RNA-BINDING PROTEIN 7 (GRP7)	Present in complexes with pri-miRNAs; regulation of pri-miRNA processing	Unknown	Koster et al., 2014
PLEIOTROPIC REGULATORY LOCUS 1 (PRL1)	Present in complexes with pri-miRNAs; regulation of pri-miRNA processing	DCL1, SE, HYL1, CDC5	Zhang et al., 2014
CELL DIVISION CYCLE 5 (CDC5)	Regulation of <i>MIR</i> transcription; regulation of pri-miRNA processing	DCL1, SE, PRL1	Zhang et al., 2013; Zhang et al., 2014

NEGATIVE ON TATA LESS 2a (NOT2a)	Regulation of <i>MIR</i> transcription	NOT2a, NOT2b, DCL1, SE, CBP80, CBP20, NRPB1	Wang et al., 2013
NEGATIVE ON TATA LESS 2b (NOT2b)	Regulation of <i>MIR</i> transcription	NOT2a, NOT2b, DCL1, SE, CBP80, CBP20, NRPB1	Wang et al., 2013
HIGH EXPRESSION OF OSMOTICALLY RESPONSIVE GENES 1 (HOS1)	Regulation of <i>MIR</i> 168b transcription	Unknown	Wang et al., 2015
CYCLING DOF TRANSCRIPTION FACTOR 2 (CDF2)	Regulation of <i>MIR</i> transcription; control of DCL1 binding to pri-miRNAs	DCL1, HYL1	Sun et al., 2015
ELONGATION PROTEIN 2 (ELP2)	Coupling transcription and pri-miRNA processing	SE, DCL1	Fang et al., 2015
ELONGATION PROTEIN 4 (ELP4)	Coupling transcription and pri-miRNA processing	DCL1	Fang et al., 2015
ELONGATION PROTEIN 5 (ELP5)	Coupling transcription and pri-miRNA processing	SE	Fang et al., 2015

1.3 Distinct characteristics of miRNA pathways in plants and animals

Although miRNAs are found in all eukaryotic cells, the mechanism of their biogenesis differs between plants and animals. The most substantial similarities and differences between these two kingdoms concerning; e.g., their microprocessor components and their ways of target mRNA recognition and regulation are presented in the table below (Tab. 2).

Table 2. Differences and similarities of miRNA biogenesis pathways between plants and animals

Properties	Plants	Animals	References
MIR transcription	RNA Pol II	RNA Pol II; RNA Pol III (subset of <i>MIRs</i>)	Lee et al., 2004; Park et al., 2005; Borchert et al., 2006
Subcellular localization	Nucleus	First step: nucleus Second step: cytoplasm	Park et al., 2005; Fang and Spector, 2007; Song et al., 2007
Microprocessor components	RNase III- type ribonucleases	DCL1	Drosha (in the nucleus) Dicer (in the cytoplasm) Park et al., 2002; Ketting et al., 2001; Kurihara and Watanabe, 2004; Lee et al., 2004
	Assisted proteins	HYL1, SE, etc. (Tab. 1)	DGCR8 TRBP Han et al., 2004a; Han et al., 2004b; Gregory et al., 2005; Lobbes et al., 2006; Yang et al., 2006; etc. (Tab. 1);
Nucleus-to-cytoplasm exporting protein	HASTY	XPO5	Yi et al., 2003; Park et al., 2005
miRNA/miRNA* duplex methylation	Yes (HEN1)	No	Park et al., 2002; Li et al., 2005

RISC composition	AGO 1 (slicing activity), HSP90, CYC40, bioinformatically predicted WG/GW proteins	AGOs1-4 (AGO2 – slicing activity), GW182, MOV10, TNRC6B	Meister et al., 2004; Baumberger and Baulcombe, 2005; Liu et al., 2005; Meister et al., 2005; Karlowski et al., 2010; Iki et al., 2010, 2012
Target mRNA recognition and regulation	High sequence complementarity between miRNA-target mRNA is required; mostly miRNA-directed mRNA cleavage	More mismatches between miRNA-target mRNA are allowed; mostly miRNA-guided translation inhibition	Rhoades et al., 2002; Lewis et al., 2003; Brennecke et al., 2005; Addo-Quaye et al., 2008; German et al., 2008

Abbreviations: DGCR8, DIGEORGE SYNDROME CRITICAL REGION 8; XPO5, Exportin-5; GW182, GLYCINE-TRYPTOPHAN PROTEIN OF 182 KDA; MOV10, PUTATIVE HELICASE MOV-10; TNRC6B, TRINUCLEOTIDE REPEAT-CONTAINING GENE 6B PROTEIN. Other abbreviations explained in the text or in Table 1.

1.4 Plant miRNA gene (*MIR*) structure

According to the latest data, there are 427 mature miRNAs identified in *Arabidopsis thaliana*, which are located within 325 pre-miRNA precursors (Kozomara and Griffiths-Jones, 2014). Among them, 82 *MIR* gene structures have been described for 87 miRNAs (Kurihara and Watanabe, 2004; Brown et al., 2008; Szarzynska et al., 2009; Zielesinski et al., 2015). Their lengths range from 319 base pairs (bp) (*MIR165a*) to 4975 bp (*MIR472*). In contrast to animals, plant *MIRs* mostly encode independent transcription units (called intergenic miRNAs) that are transcribed from their own promoters. Thus far, 55 such genes have been identified in *Arabidopsis*, and half of them possess at least one intron within the gene structure. In these *MIRs*, pre-miRNAs are mostly located in the first exons. Only seven examples have been identified in the subsequent exons. Another 29 miRNAs are located within the introns of genes that encode proteins or non-coding RNAs (called host genes) and are believed to be transcribed from the host promoters (Brown et al., 2008; Yan et al., 2012; Jia and Rock, 2013; Zielesinski et al., 2015). These miRNAs are mostly located within the first or last intron,

whose can be situated in either the untranslated (UTRs) or coding (CDSs) regions of the host gene. All identified *A. thaliana* intronic miRNAs are presented in Table 3. Several examples of the host gene structures for intronic miRNAs in Arabidopsis are depicted in the figure below (Fig. 6).

Table 3. Intronic miRNAs identified in *Arabidopsis thaliana* (based on *TAIR10*)

No.	miRNA	Host gene	miRNA localization within host gene	References	
1.	miR156d	<i>At5g10946</i>	Unknown protein	1 st intron	Zielezinski et al., 2015
2.	miR156f	<i>At5g26146</i>	Potential natural antisense gene, locus overlaps with <i>At5g26150</i>	1 st intron	Zielezinski et al., 2015
3.	miR162a	<i>At5g08185</i>	Unknown protein	2 nd intron	Hirsch et al., 2006; Brown et al., 2008
4.	miR400	<i>At1g32583</i>	Unknown protein	1 st intron	Yan et al., 2012
5.	miR402	<i>At1g77230</i>	Tetratricopeptide repeat (TPR)-like superfamily protein	1 st intron	Brown et al., 2008
6.	miR420	<i>At5g62850</i>	VEGETATIVE CELL EXPRESSED 1 (VEX1)	4 th intron	Zielezinski et al., 2015
7.	miR778	<i>At2g41620</i>	Nucleoporin interacting component (NUP93/NIC96-like) family protein	15 th intron	Zielezinski et al., 2015
8.	miR833	<i>At1g78476</i>	Unknown protein	3 rd intron	Zielezinski et al., 2015
9.	miR837	<i>At1g18880</i>	Major facilitator superfamily protein - NRT1/PTR family 2.9	1 st intron	Brown et al., 2008
10.	miR838	<i>At1g01040</i>	DICER-LIKE1 (DCL1)	14 th intron	Brown et al., 2008
11.	miR842	<i>At1g61224</i>	Non-coding RNA	1 st intron	Jia and Rock, 2013

12.	miR844	<i>At2g23348</i>	Unknown protein	1 st intron	Brown et al., 2008
13.	miR848	<i>At5g13890</i>	Family of unknown function (DUF716)	1 st intron	Brown et al., 2008
14.	miR850	<i>At4g13495</i>	Non-coding RNA	2 nd intron	Brown et al., 2008
15.	miR852	<i>At4g14500</i>	Polyketide cyclase/dehydrase and lipid transport superfamily protein	4 th intron	Zielezinski et al., 2015
16.	miR853	<i>At3g23325</i>	Splicing factor 3B subunit 5/RDS3 complex subunit 10	3 rd intron	Brown et al., 2008
17.	miR862	<i>At2g25170</i>	SWI/SWF nuclear-localized chromatin remodeling factor of the CHD3 group	14 th intron	Brown et al., 2008
18.	miR1886	<i>At2g37160</i>	Transducin/WD40 repeat-like superfamily protein	10 th intron	Zielezinski et al., 2015
19.	miR1888a	<i>At5g21100</i>	PLANT L-ASCORBATE OXIDASE	1 st intron	Zielezinski et al., 2015
20.	miR1888b	<i>At3g60960</i>	Tetratricopeptide repeat (TPR)-like superfamily protein	1 st intron	Zielezinski et al., 2015
21.	miR2112	<i>At1g01650</i>	SIGNAL PEPTIDE PEPTIDASE-LIKE 4 (SPPL4)	10 th /11 th intron	Zielezinski et al., 2015
22.	miR3434	<i>At5g22770</i>	ALPHA-ADAPTIN (ALPHA-ADR)	14 th /15 th intron	Zielezinski et al., 2015
23.	miR5014	<i>At1g65960</i>	GLUTAMATE DECARBOXYLASE (GAD2)	2 nd intron	Zielezinski et al., 2015
24.	miR5024	<i>At1g44100</i>	AMINO ACID PERMEASE 5 (AAP5)	2 nd intron	Zielezinski et al., 2015
25.	miR5026	<i>At4g13495</i>	Non-coding RNA	2 nd intron	Zielezinski et al., 2015
26.	miR5632	<i>At2g19390</i>	Unknown protein	8 th intron	Zielezinski et al., 2015
27.	miR5640	<i>At1g05570</i>	CALLOSE SYNTHASE 1 (CALS1)	23 rd intron	Zielezinski et al., 2015

28.	miR5650	<i>At2g48140</i>	EMBRYO SAC DEVELOPMENT ARREST 4 (EDA4)	2 nd intron	Zielezinski et al., 2015
29.	miR5656	<i>At1g05780</i>	Vacuolar ATPase assembly integral membrane protein, VMA21-like domain protein	1 st intron	Zielezinski et al., 2015

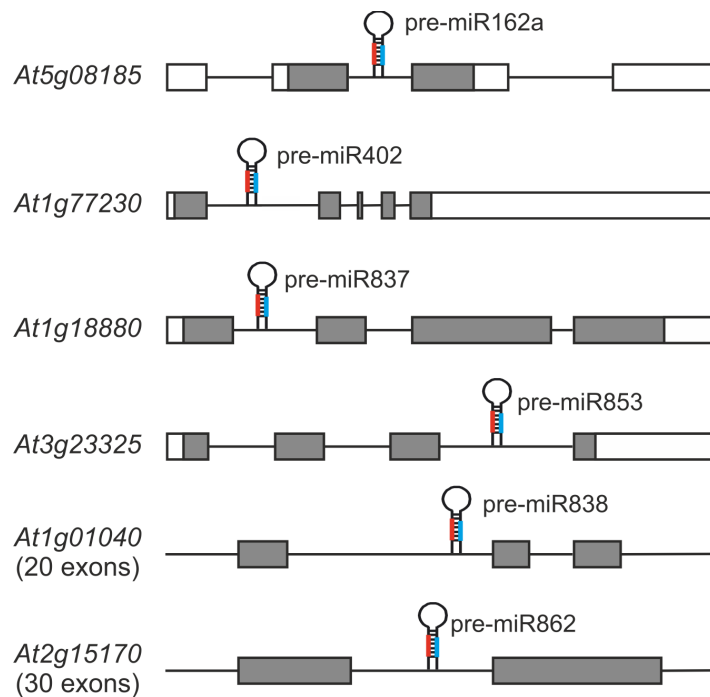


Figure 6. Schematic structures of several host genes of *A. thaliana* intronic miRNAs. Boxes – exons (protein-coding sequences – gray; UTRs – white); black lines – introns; red and blue lines – miRNA and miRNA*; stem-loop structures – pre-miRNAs.

As previously mentioned, *MIR* genes in plants are transcribed by RNA polymerase II. Within their promoters, typical 8-nt TATA box-like elements can be found, which are located in the closest proximity of their transcription start sites (TSSs) (Xie et al., 2005). What is more, elements responsive to different biotic and abiotic stress factors have been found in the promoter regions of many *MIRs* (Kruszka et al., 2012; Barciszewska-Pacak et al., 2015). Several miRNA genes (like *MIR170*, *MIR400*, and *MIR5014*) can be transcribed from different TSSs (Zielezinski et al., 2015). Interestingly, there are four identified Arabidopsis polycistronic miRNAs: miR400-miR5654, miR842-miR846, miR771-miR851, and miR5026-miR850-miR863a (Merchan et al., 2009; Yang et al., 2011; Meng et al., 2012; Jia and Rock, 2013; Zielezinski 2015). Also, there are two miRNAs located within the same pre-miRNA

hairpin structure in some cases; e.g., miR319a-miR319a.2, miR319b-miR319b.2, and miR319c-miR319c.2 (Zhang et al., 2010; Sobkowiak et al., 2012).

Complex structure of Arabidopsis miRNA-coding genes is not unique in the plant world. In barley (*Hordeum vulgare*), 16 *MIR* gene structures have been described thus far: 12 that encode independent transcription units, 2 located within the introns, and 2 within the 3'UTRs of the protein-coding genes (Kruszka et al., 2013, 2014). In *Physcomitrella patens*, 25% of the identified miRNAs are polycistronic (Axtell et al., 2007). Also in *Pellia endiviifolia*, the gene structure is known for 10 *MIRs* among the 26 identified pri-miRNAs (from which, 4 possess at least 1 intron) (Alaba et al., 2015).

Taking all of this data together, it is clear that the complicated structure of miRNA genes is an important factor in facilitating the regulation of miRNA biogenesis in plants. This process can be influenced by many additional processes, such as splicing, polyadenylation-site selection, or transcription-start-site selection (Zhang et al., 2015; Stepień, Knop, Dolata et al., 2016).

2 Splicing in plants

2.1 General overview of splicing principles

In Eucaryota, genes are composed of exons (mainly coding regions) that are separated by introns (non-coding regions). Although intron lengths differ between animals (5 kb on average) and plants (160 bp on average), consensus splicing sequences (e.g., the 5' splice site (5'SS), 3' splice site (3'SS) and branch point (BP)) are similar in both kingdoms (Fig. 7) (Brown et al., 1996; Simpson et al., 2002; Sakharkar et al., 2004; Reddy 2007; Iwata and Gotoh, 2011; Marquez et al., 2012; Meyer et al., 2015). Accordingly to the structure of these conserved sequences, two types of introns have been defined: the U2-type (containing GU and AG dinucleotide motifs at the 5' and 3' ends of the intron, respectively) and U12-type (possessing mostly non-canonical splice sites) (Brown et al., 1996; Lewandowska et al., 2004).

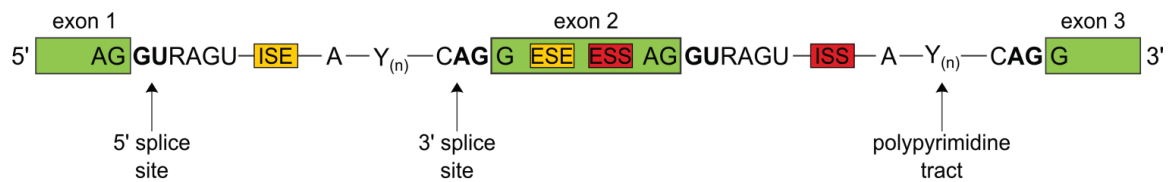


Figure 7. Consensus U2-type intronic sequences conserved in animals and plants (Meyer et al., 2015, modified). Introns are presented as short consensus sequences, 5' and 3' splice sites (R = Purine), Y_n – polypyrimidine tract (Y = Pyrimidine) (PPT), and A – branch point. Green boxes – exons. Additional sequence elements influencing pre-mRNA splicing efficiency: ISS – intronic splicing silencers; ISE – intronic splicing enhancers; ESS – exonic splicing silencers; ESE – exonic splicing enhancers.

Within the cell nucleus, nascent pre-mRNAs are edited to create mature mRNAs, which are next translated into proteins or become a source of non-coding RNAs. Assuming excision of the introns and ligation of the neighboring exons, this editing process is called pre-mRNA splicing. Splicing entails two steps (both S_N2-type transesterification reactions) that require the presence of functional groups from three reactive regions in pre-mRNA (Moore et al., 1993; Fica et al., 2013). During the first reaction, the 2'-hydroxyl group of the conserved adenine located in the intronic branch point (BP) attacks the 5' splice site, causing cleavage of the 5'SS phosphodiester bond (Fig. 8) (Moore et al., 1993). As a result, the 5' exon is released, and the intron forms a lariat structure through the creation of a new 5'-2' phosphodiester bond that links the first nucleotide of the intron with the BP adenosine. In the second step, the 3'-hydroxyl group of the 5' exon attacks the 3' splice site, triggering excision of the intron lariat and ligation of the 5' and 3' exons. This results in the release of mature mRNA and the intron lariat (which is, next, rapidly degraded).

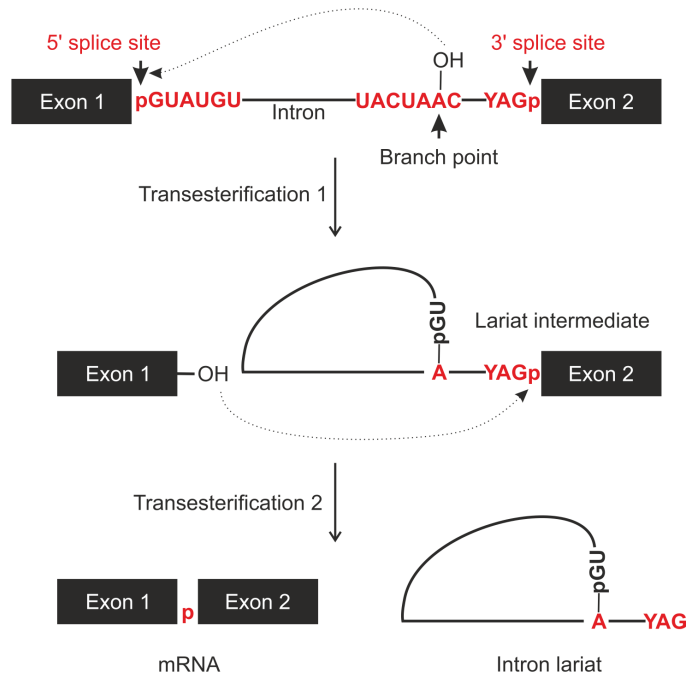


Figure 8. Two sequential transesterification reactions during pre-mRNA splicing (based on Chen and Cheng, 2012). Black boxes – exons; black lines – introns; black dashed arrows – nucleophilic attacks (on 5’SS terminal phosphodiester bond by 2’- hydroxyl group of branch point adenosine (A) (transesterification 1) and by 3’ - hydroxyl group of 5’ exon (transesterification 2), respectively).

The splicing reaction is accomplished by a large complex called the spliceosome, whose conformation and composition are highly dynamic. U2-type introns are spliced by the major spliceosome (U2-dependent spliceosome) while U12-type introns are spliced by the minor spliceosome (U12-dependent spliceosome) (Patel and Steitz, 2003). The major spliceosome is composed of small nuclear ribonucleoprotein complexes (snRNPs). SnRNPs consist of the following: (1) conserved Sm proteins; (2) snRNP-specific proteins; and (3) a variable number of small nuclear RNAs (snRNAs). These snRNAs are short non-coding and non-polyadenylated transcripts. SnRNPs are described as U1, U2, U5 (all containing one snRNA), and U4/U6 (containing two snRNAs) (Wang et al., 2004). The spliceosome assembly occurs in the exact order presented in the figure below (Fig. 9). At the beginning, the U1 snRNP binds to the 5’SS by complementary base-pairing (Kandels-Lewis and Seraphin, 1993). Then, the 35 kDa subunit of U2 auxiliary factor (U2AF) – U2AF³⁵ – binds to the 3’ splice site, while the 65 kDa subunit – U2AF⁶⁵ – interacts with the polypyrimidine tract. Subsequently, U2 snRNP binds to the branch point (Barabino et al., 1990). Next, the U4, U5, and U6 snRNPs (called the U4/U6.U5 tri-snRNP complex) associate to

U2 snRNP. After rearrangement, the U1 and U4 snRNPs dissociate from the spliceosome, and then the Nineteen complex (NTC) is bound (Chan et al., 2003). This supports the RNA-RNA interactions that form the catalytic core for the first step of splicing. As a result of the two catalytic steps of the splicing reaction, the mature mRNA and intron lariat are released by the action of the helicases, and the spliceosome complex dissociates (Company et al., 1991, Schwer and Gross, 1998). Then, the lariat is degraded, and all snRNPs are recycled to participate in the next spliceosomal cycle. Interestingly, there are also self-splicing introns and ribozymes that contain their own catalytic active sites, allowing for intron excision and exon ligation without spliceosome participation (Cech, 1990).

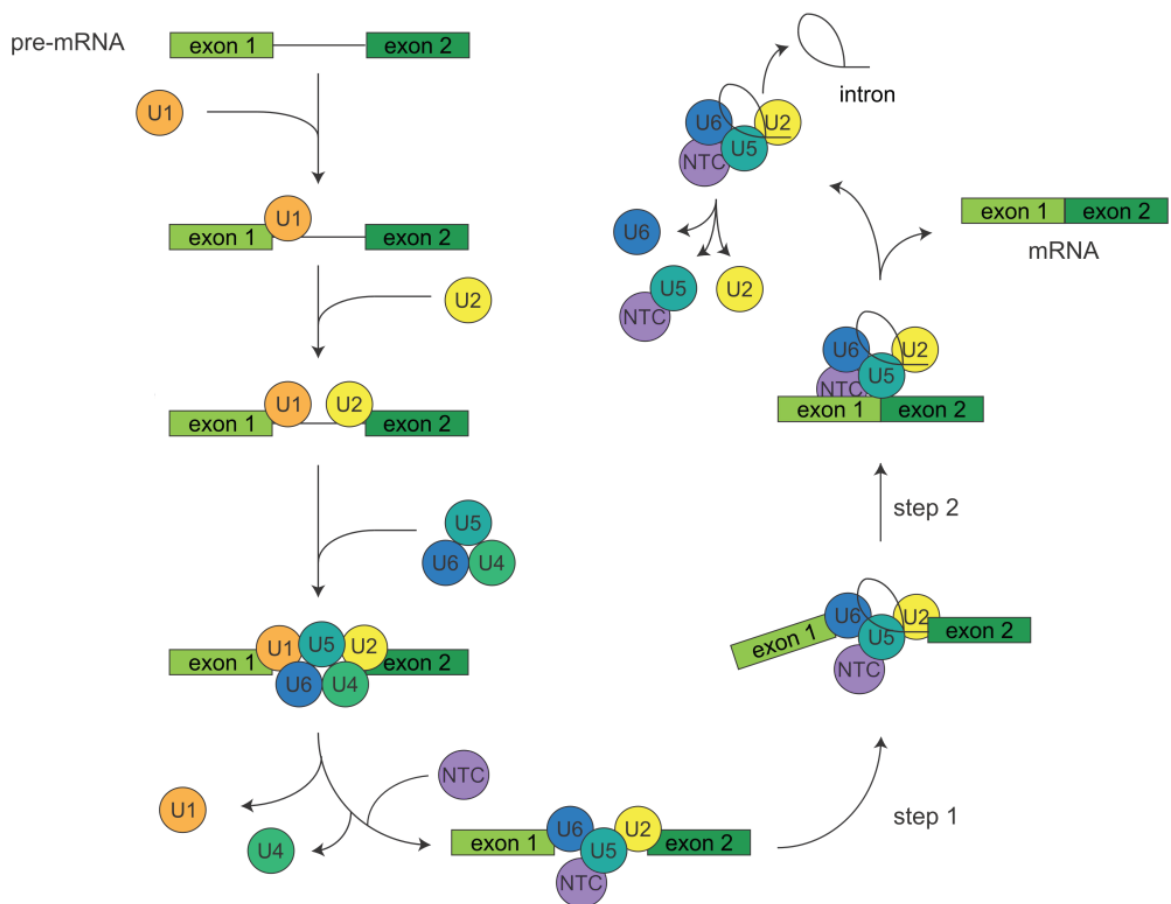


Figure 9. Splicing cycle overview (Meyer et al., 2015, modified). Green boxes – exons; black lines – introns; the U1, U2, U4, U5, and U6 – snRNP proteins (proposed to act at indicated steps of spliceosomal cycle based on homology to human proteins); and NTC – Nineteen Complex.

2.2 Alternative splicing

One of the most important processes of gene expression regulation (which leads to the enhancement of genome coding capacity and to a broader diversity of proteins in the cell) is alternative splicing (AS) (Smith and Valcarel, 2000; Blencowe, 2006; Nilsen and Graveley, 2010). By this process, different mature mRNA isoforms can be produced from one pre-mRNA. Pre-mRNAs undergo alternative splicing in about 95% of the protein-coding genes in humans (and around 60% in Arabidopsis) (Pan et al., 2006; Filichkin et al., 2010; Marquez et al., 2012). There are several types of AS events, including exon skipping (ES), alternative 5' or 3' splice-site selection, and intron retention (IR) (Fig. 10) (Graveley, 2001; Ner-Gaon, 2004). Mostly, AS occurs within the coding regions, but it does not always lead to the production of new proteins. AS events can also generate premature termination codons (PTCs) targeting mRNAs to the nonsense mediated decay (NMD) pathway, which consequently affects transcript levels in the cell (Pan et al., 2006; Ni et al., 2007). Moreover, about one-fifth of all identified AS events occur within the 5' or 3' UTRs, affecting the stability and transport of mRNAs or altering open reading frames (ORFs), for example.

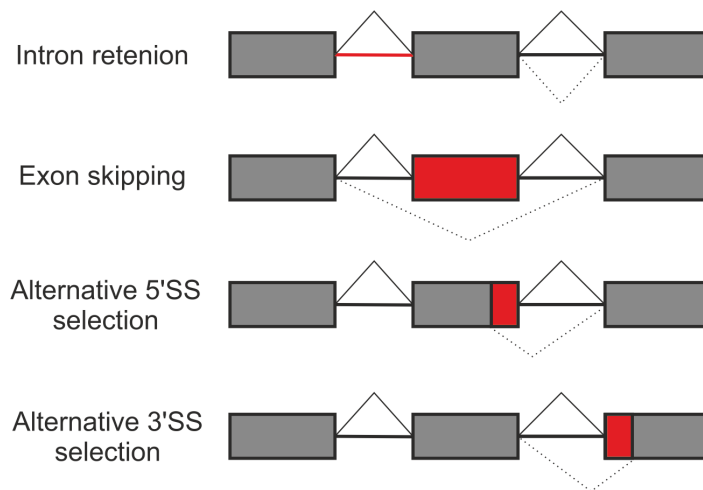


Figure 10. The most common types of alternative splicing events. Gray boxes – exons; bolded black lines – introns; black lines – constitutive splicing events; dashed lines, red lines, and red boxes – alternative splicing events.

2.3 Pre-mRNA splicing in plants

Information regarding pre-mRNA splicing in plants has recently evolved. Although the principles of this mechanism are conserved among kingdoms, mammalian introns cannot be spliced in plants, and only a few examples of plant introns spliced in HeLa cells have been found (Brown et al., 1986; Wiebauer et al., 1988; Iwata et al., 2011). This can be connected to the differences of the intron recognition systems within these two kingdoms. The most common alternative splicing event in plants is intron retention, representing about 40% of all identified AS events (Barta et al., 2012; Marquez et al., 2012). In contrast to animals (where exon skipping is the most-frequent AS event), this represents only 8% of all identified events in plants (Keren et al., 2010; Reddy et al., 2012).

Most *Arabidopsis* spliceosomal proteins were found based on the homology to human, yeast, or *Drosophila*'s spliceosome components (Wang and Brendel, 2004; Koncz et al., 2012). These splicing regulators are called splicing factors (SFs) and are involved in guiding the spliceosome components towards the proper sequences within pre-mRNAs (Kalyna et al., 2006; Wachter et al., 2012). What is more, they bind to specific exonic or intronic sequences in pre-mRNA; in this way, they increase splicing efficiency (by its interaction with splicing enhancers) or decrease it (by binding to splicing suppressors). The first identified pre-mRNA splicing regulators in plants were Serine/Arginine-rich proteins (SR) (Reddy, 2004). In *A. thaliana*, there are 18 such proteins belonging to 6 gene families (Kalyna et al., 2006; Barta et al., 2010; Duque et al., 2011; Richardson et al., 2011). Another group of splicing factors that are present in animals and plants consists of heterogeneous nuclear ribonucleoproteins (hnRNPs); e.g., polypyrimidine tract binding proteins (PTBs) (Sawicka et al., 2008; Stauffer et al., 2010; Wachter et al., 2012). Besides their role in pre-mRNA splicing, PTB proteins are also involved in regulation of polyadenylation and mRNA transport. What is interesting, plant-splicing factors may control their own pre-mRNA splicing as a response to different factors such as environmental cues and, thus, increase their transcript isoforms diversity (Kalyna et al., 2006; Stauffer et al., 2010).

3 Polyadenylation mechanism in plants

Polyadenylation of the 3' ends of transcripts is the second-most-important process (after splicing) that affects mRNA metabolism in the cell. Formation of the 3' end of mRNAs occurs in two successive steps: (1) pre-mRNA is cleaved at the specific polyA site; and (2) a polyA tail is added. Both of these stages are regulated by conserved and complex machinery comprised of 25-30 different proteins (Proudfoot, 2004; Hunt, 2008; Lutz, 2008; Millevoi and Vagner, 2009). Plant proteins involved in polyA signal recognition, cleavage, and polyadenylation were mostly identified based on the homology to their mammalian counterparts (Hunt et al., 2008).

The bases of polyadenylation signal composition and recognition have been extensively studied for many years (Hunt et al., 1987; Li and Hunt, 1997; Loke et al., 2005). Three signal elements have been identified: (1) Near Upstream Element (NUE); (2) Far Upstream Element (FUE); and (3) Cleavage Element (CE), all located within pre-mRNAs and necessary for their efficient polyadenylation. The plant NUE sequence consists of six nucleotides and is analogous to the AAUAAA signal, which is a polyadenylation signal in mammals (Proudfoot and Brownlee, 1976; Proudfoot, 1991). However, only 10% of Arabidopsis genes contain the AAUAAA signal, and other variants of this sequence are more common in plants (Loke et al., 2005). NUE signal is located 13 to 30 nucleotides upstream from the cleavage site (Hunt, 1994; Li and Hunt, 1995). The FUE signal, comprised of 60-120 nucleotides, combines UG motifs and/or the UUGUUAA sequence and is more diverse than NUE. This element controls and enhances polyA site recognition. The third signal – CE – is dinucleotide sequence YA (CA or UA) located at the cleavage site and/or within its proximity (Loke et al., 2005). The positions of these three signal elements within the 3'UTR of the plant pre-mRNA are presented in the figure below (Fig. 11).

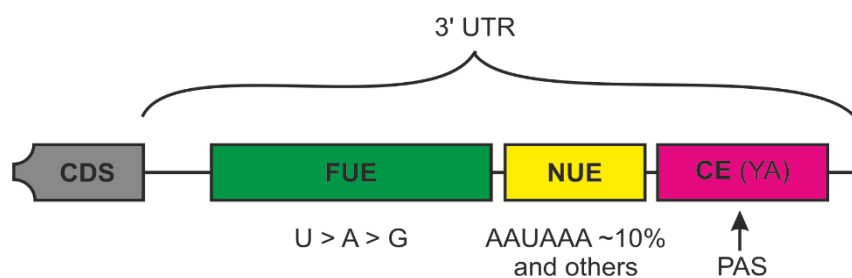


Figure 11. Plant polyadenylation signal composition. CDS – protein-coding sequence; UTR - untranslated region; FUE – Far Upstream Element; NUE – Near Upstream Element; CE – Cleavage Element; PAS – polyA site; YA – CE dinucleotide (Y = U or C).

In general, the polyadenylation signal within the NUE is recognized by multi-subunit Cleavage and Polyadenylation Specificity Factor (CPSF), while multicomponent Cleavage Stimulatory Factor (CStF) binds to the CE sequence (Fig. 12) (MacDonald et al., 1994; Murthy and Manley, 1995). The 5' end of the polyadenylation signal associates with Cleavage Factors I and II (CFI and CFII) (Venkataraman et al., 2005). There are also other cleavage and polyadenylation factors required for proper mRNA polyadenylation that bind in the closest proximity or directly to the cleavage site; for example, Simplekin and Poly(A)-binding Proteins (PABs) (Bienroth et al., 1993; Wahle, 1995; Barabino et al., 2000; Dichtl and Keller 2001). Pre-mRNA is cleaved by the CPSF73 (73-kDa subunit of CPSF) and then polyadenylated by the conserved nucleotidyltransferase - Poly(A) Polymerase (PAP) (Raabe et al., 1991; Wahle, 1991; Kyriakopoulou et al., 2001; Perumal et al., 2001; Topalian et al., 2001; Barnard et al., 2004; Ryan et al., 2004; Mandel et al., 2006).

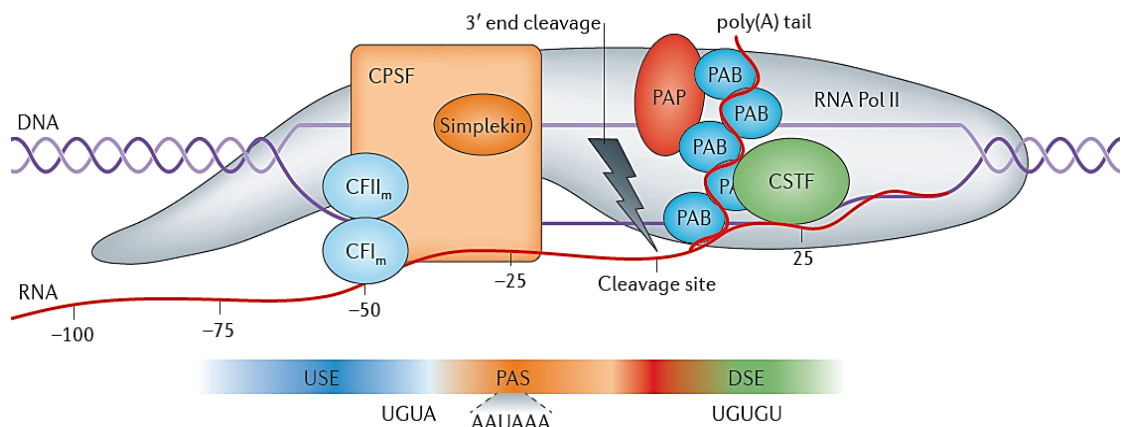


Figure 12. The main players involved in pre-mRNA polyadenylation (Elkon et al., 2013, modified). USE - Upstream Sequence Elements (=FUE); PAS – Polyadenylation Signal (=NUE); DSE - U- or GU-rich Downstream Sequence Elements (=CE).

The canonical polyA sites reside at the 3' ends of the transcripts. However, in the majority of pre-mRNAs, more than one polyA site can be selected, resulting in the alternative polyadenylation (APA) of transcripts. APA is a widespread phenomenon, generating various mRNAs with alternative 3' ends. Through alternative polyA site selection, specific fragments can be excluded/included into an mRNA sequence; therefore, the APA mechanism boosts the complexity of the cell transcriptome. This process can be closely associated with other mechanisms; i.e., transcription initiation and termination, pre-mRNA capping, and splicing (Proudfoot, 2004; Tollervey, 2004; Tian et al., 2007).

Nowadays, the competition between splicing and polyadenylation are the most-extensively studied. Interestingly, both of these processes can be mutually exclusive, when the alternative polyA site resides within the intron of pre-mRNA (Macknight et al., 2002). It was also shown that, in mammals, the U1 snRNP binding to the 5'SS prevents the selection of proximal polyA sites located in the closest proximity to this splice site, thus protecting pre-mRNAs from premature cleavage and polyadenylation (Fig. 13) (Kaida et al., 2010; Martinson, 2011; Berg et al., 2012). What is more, the U1 snRNP specific protein – the U1-70K – interacts with Poly(A) Polymerase (PAP) in HeLa cells (Gunderson et al., 1998).

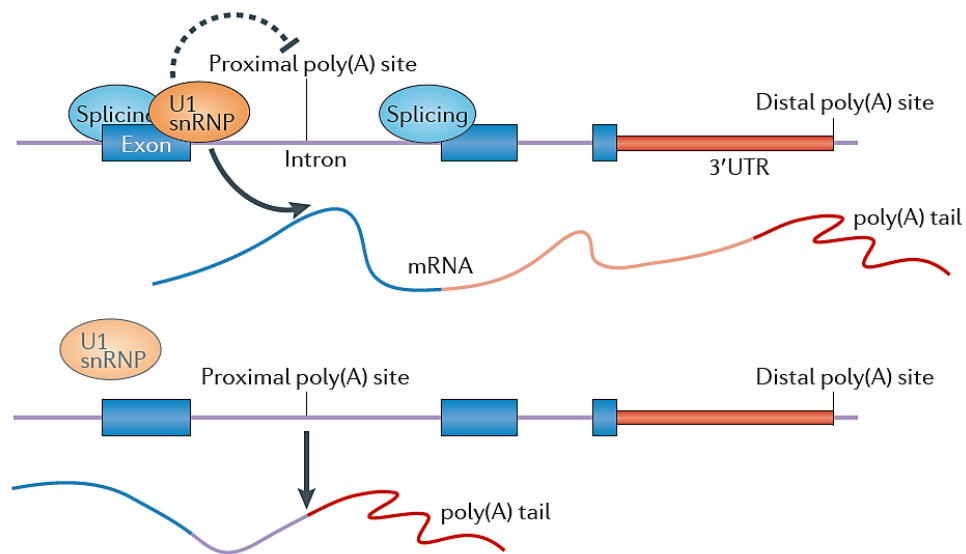


Figure 13. The interplay between the U1 snRNP and selection of proximal polyA site (Elkon et al., 2013, modified). Blue boxes – exons; orange boxes – 3' UTRs; violet lines – introns; blue and orange lines – mature mRNAs; red lines – poly(A) tails.

The proper pattern of mature mRNA polyadenylation is crucial for many processes in the cell, like mRNA transport and localization, mRNA stability and degradation, and the initiation of mRNA translation (Millevoi and Vagner, 2009). In plants (where more than 50% of pre-mRNAs possess alternative polyA signals within their sequences), it has been shown that APA influences development rate and flowering, response to environmental factors, cell metabolism, and many others (Yoshimura et al., 2002; Quesada et al., 2003; Simpson et al., 2003, 2004; Herr et al., 2006; Muralla et al., 2008; Xing et al., 2008a, 2008b; Hornyik et al., 2010; Liu et al., 2010).

4 Posttranscriptional regulation of miRNA biogenesis

As mentioned above, the structure of plant *MIR* is very diverse and complex; thus, many additional processes may influence the efficiency of miRNA biogenesis. It has been demonstrated that pri-miRNAs and pre-mRNAs of miRNA-hosting genes undergo constitutive and alternative splicing (Szarzynska et al., 2009; Bielewicz et al., 2013; Kruszka et al., 2013; Schwab et al., 2013; Szweykowska-Kulinska et al., 2013; Kruszka et al., 2014; Zielezinski et al., 2015; Barciszewska-Pacak et al., 2016; Knop and Stepien et al., 2016). What is more, the presence and activity of alternative polyA signals have been described in many Arabidopsis miRNA primary precursors (e.g., pri-miR162a, pri-miR163, pri-miR164b, pri-miR164c, pri-miR171a, and pri-miR402). Thus, it is clear that posttranscriptional processes (e.g., splicing and polyadenylation) may significantly influence miRNA maturation. What is more, the involvement of many proteins in both pre-mRNA splicing and pri-miRNA processing (like SE, CBC, STA1, GRP7, PRL1, HOS5, RS40 and RS41 (see also Table 1)) suggests that splicing and miRNA biogenesis in plants are closely related (Raczynska et al., 2010, 2014; Chaabane et al., 2012; Koster et al., 2014; Zhang et al., 2014; Chen et al., 2015).

4.1 Crosstalk between miRNA biogenesis and splicing during maturation of exonic miRNAs derived from intron-containing genes in plants

In 2013, two reports concerning the splicing effects on Arabidopsis exonic miR163, miR161, and miR172a biogenesis were published (Bielewicz et al., 2013; Schwab et al., 2013). These three miRNAs are located within the first exons of intron-containing *MIRs* (Kurihara and Watanabe, 2004; Szarzynska et al., 2009). Analyses of the transgenic lines carrying *MIR163* versions without an intron or with mutated splice sites revealed that efficient splicing is necessary for the proper production of mature miR163 (Bielewicz et al., 2013; Schwab et al., 2013). For both intron-less *MIR163* and with an inactivated 5' splice site, a decreased level of miRNA was detected. What is interesting, there was no significant effect of 3'SS mutation on miR163 biogenesis efficiency; therefore, the active 5'SS was essential for the stimulation of miR163 maturation. The same effect of the 5' splice site was also observed for miR161. Additionally, for the pri-miR163, whose pre-miRNA is located upstream of *MIR163* intron, preferential selection of the alternative intronic proximal polyA site was observed,

after the inactivation of the 5'SS (Bielewicz et al., 2013). Besides, the efficient splicing of the *MIR163* intron determined the proper Arabidopsis plant response to pathogen attack. All of this data implies the important role of splicing and alternative polyadenylation during the maturation of Arabidopsis exonic miRNAs derived from intron-containing genes.

Interesting observations were also found in *A. thaliana* dicistronic *MIR842/846*. In this gene, pre-miR846 is located within the exon, while the miR842 stem-loop structure is situated within the upstream intron (Jia and Rock, 2013). Treatment with abscisic acid (ABA) induces AS events (i.e., intron retention and the selection of alternative splice sites), resulting in the downregulation of both mature miR842 and miR846. Thus, these results indicate that the ratio between the splicing isoforms of pri-miRNA may have an impact on the final accumulation of mature miRNAs.

In monocots, the role of efficient pri-miRNA splicing for miRNA biogenesis has been shown for the *MIR444* family (Lu et al., 2008; Sunkar and Jagadeeswaran, 2008). In pri-miR444s, miRNAs and miRNA*s are located in two different exons (separated by an intron). Only the proper excision of this intron leads to the correct formation of the pre-miR444 hairpin and allows for the efficient production of miR444.

4.2 Biogenesis of miRNAs located within introns of their host genes

4.2.1. Intronic miRNA maturation in mammals

As opposed to plants, a significant number of miRNAs are located within the introns of protein-coding or non-coding RNA genes in mammals (Rodriguez et al., 2004; Kim 2005; Kim and Kim, 2007). Thus far, the connections between splicing and miRNA biogenesis have been described for several examples.

In 2011, the mechanism of the biogenesis of human miR211 located within the 6th intron of the *Melastatin* host gene was described (Janas et al., 2011). The authors demonstrated that the processing of miR211 stimulated excision of the miRNA-hosting intron. It is noteworthy to mention that the splicing of this intron is dependent on Drosha and DGCR8 activity (the main components of the nuclear mammalian microprocessor complex (see also Table 2)), since the knockdown of these factors results in the inhibition of intron 6 excision. What is more, miR211 maturation efficiency is determined by the U1 snRNP binding to the 6th intron 5'SS. Inactivation of this splice site leads to a decreased accumulation of mature miRNA. Also noteworthy, the knockdown

of the U1 snRNP components reduced the level of intronic miRNAs globally and did not affect intergenic miRNA accumulation. Based on these results, the authors suggested that mutual cooperation between the microprocessor and spliceosome regulates the proper and efficient production of at least several intronic miRNAs in mammals (Fig. 14).

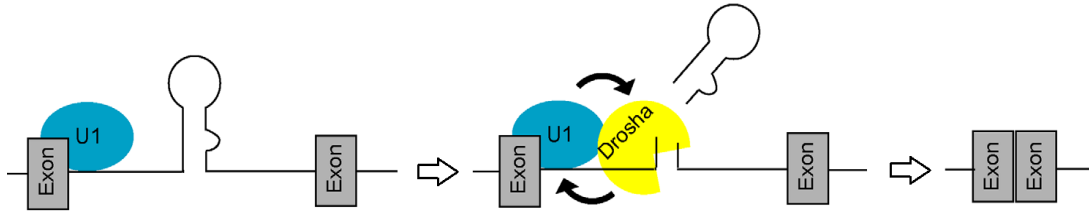


Figure 14. A model of mutual cooperation between microprocessor and spliceosome during intronic miRNA biogenesis in mammals (Janas et al., 2011, modified). Stem-loop structure – pre-miRNA.

In 2014, two reports concerning the maturation of human clustered miRNAs miR106b, miR93, and miR25 (located within the 13th intron of the *MCM7* (Minichromosome Maintenance Complex Component 7) host gene) were published (Agranat-Tamir et al., 2014; Ramalingam et al., 2014). Agranat-Tamir and her colleagues presented that the inhibition of miRNA-carrying intron excision correlated with the upregulated accumulation of all three mature miRNAs. At the same time, the knockdown of Droscha resulted in increased splicing efficiency of this intron. What is more, new AS events occurring between clustered miRNAs were identified in both reports (Agranat-Tamir et al., 2014; Ramalingam et al., 2014). The selection of alternative 3' splice sites within the 13th intron of *MCM7* pre-mRNA (affected after Droscha downregulation) altered the accumulation of all miRNAs derived from the analyzed cluster. Additionally, it was demonstrated that pre-miRNAs and components of the microprocessor complex – Droscha and DGCR8 – cosedimented with the supraspliceosomes (the large multicomponent complexes containing all five spliceosomal snRNPs as well as other non-snRNP splicing factors) (Sperling et al., 2008; Agranat-Tamir et al., 2014). On the other hand, it was previously shown that the splicing components associated/cosedimented with the microprocessor complexes and pre-miRNAs (Shiohama et al., 2007; Kataoka et al., 2009). What is more, Ramalingam and his colleagues identified independent full-length pri-miRNAs for miR106b, miR93, and miR25, suggesting that all can be transcribed as autonomous transcription units (Ramalingam et al., 2014). The presented results indicate that human intronic miRNA biogenesis may be regulated at both the transcriptional

and posttranscriptional levels via the selection of an alternative transcription start site and splicing events (Agranat-Tamir et al., 2014; Ramalingam et al., 2014).

Besides the canonical miRNA biogenesis mechanism, there are also other known pathways of pri-miRNA processing. In 2007, a class of small RNAs was described in *Drosophila melanogaster* that are generated from short introns that form pre-miRNA hairpins itself (Okamura et al., 2007; Ruby et al., 2007). Such introns are called mirtrons. MiRNA biogenesis from the mirtrons starts from intron splicing. The released intron lariat is debranched and forms a pre-miRNA hairpin, which is then transported to the cytoplasm and cleaved by Dicer to generate mature miRNA (via the canonical pathway of miRNA biogenesis). Thus, the biogenesis of mirtron-derived miRNAs (common in humans, mice and flies) is independent on Drosha and DGCR8 proteins (Ladewig et al., 2012).

4.2.2. Intronic miRNA biogenesis in plants

In contrast to animals, knowledge regarding intronic miRNA biogenesis in plants is limited. The first report concerning proposed interactions between miRNA production and miRNA-hosting intron splicing was published in 2008 (Brown et al., 2008). In this review, three possible mechanisms of cooperative or competitive crosstalk between the plant microprocessor and spliceosome were proposed (Fig. 15). In the post-splicing mechanism, the pre-miRNA hairpin is processed from an intron lariat that is released after host pre-mRNA splicing (Fig. 15, Panel A). The pre-splicing cleavage mechanism assumes that pre-miRNA is cut out from the hosting intron by the microprocessor before its splicing, resulting in an interrupted continuity of host pre-mRNA (Fig. 15, Panel B). Thus, miRNA production and mRNA maturation are mutually exclusive in this case. In the co-splicing mechanism, pre-miRNA cleavage occurs right after the splicing commitment complex is assembled, leading to the production of both host mRNA and mature miRNA (Fig. 15, Panel C).

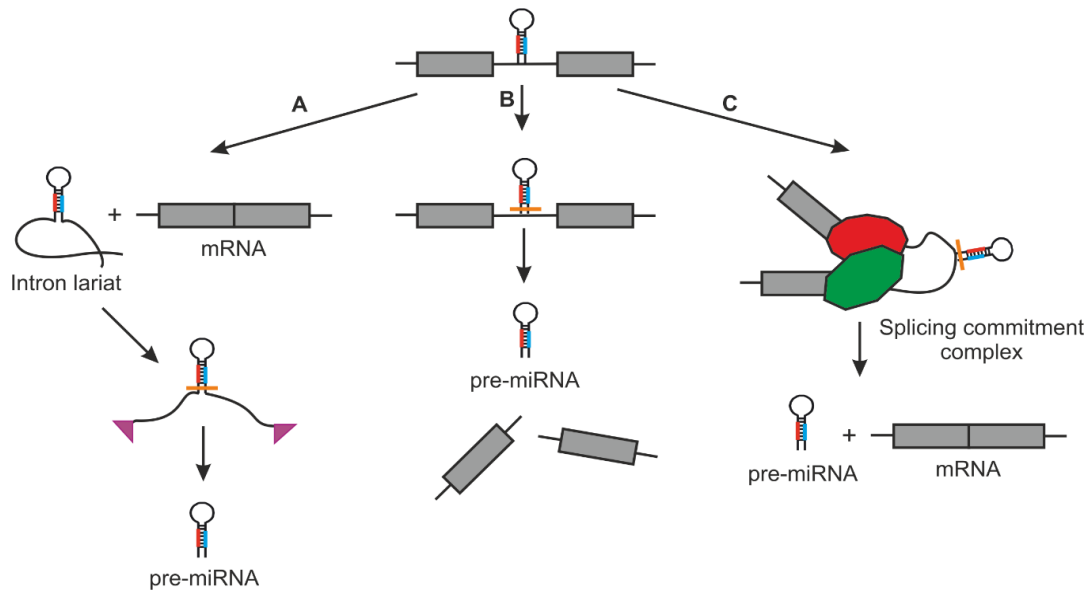


Figure 15. Schematic diagram of potential pathways of intronic miRNA processing in plants (based on Brown et al., 2008). A – post-splicing processing; B – pre-splicing processing; C – co-splicing processing. Gray boxes – exons; black lines – introns; violet arrowheads – exonucleolytic processing; orange lines – cleavage by DCL1; stem-loop structures – pre-miRNAs; red and blue lines – miRNA and miRNA*; red and green boxes – spliceosomal proteins.

In several reports, the complex splicing pattern of *MIR162a* (*At5g08185*) transcripts was described (Hirsch et al., 2006; Brown et al., 2008; Barciszewska-Pacak et al., 2016). In the second intron of this host gene, a pre-miR162a hairpin is located (see Table 3). The pre-mRNA of *At5g08185* undergoes various AS events that lead to the formation of six mRNA isoforms (Fig. 16). Only those isoforms produced as a result of the first or second AS event (AS isoforms 2 and 3) as well as the miRNA-hosting intron retained isoform (AS isoform 1) can be substrates for the plant microprocessor complex to produce mature miR162a. Other isoforms are probably non-functional. Moreover, it has been shown that drought and salinity stress treatments resulted in an increase of the level of the functional miR162-containing isoform, together with changes of the polyA site selection ratio (Barciszewska-Pacak et al., 2016). These observations were accompanied by a higher accumulation of mature miRNA. Such a regulation of miR162a biogenesis efficiency by affecting the splicing of the miRNA-hosting intron and polyadenylation site selection revealed new ways of fine-tuning the *MIR* gene expression in plants.

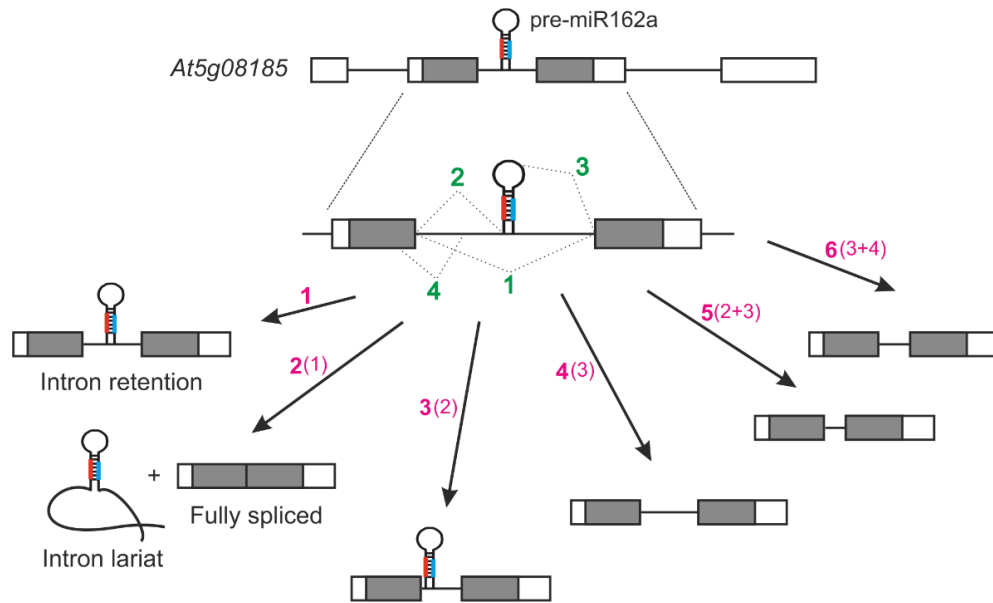


Figure 16. Schematic diagram of six splicing isoforms derived from pri-miR162a as a result of AS events. Stem-loop structure – pre-miRNA; red and blue lines – miRNA and miRNA*; white boxes – UTRs; gray boxes – protein-coding sequence; black solid lines – introns; black dashed lines – AS events; purple numbers – AS isoforms; numbers in brackets – selected AS events.

In 2012, the mechanism of Arabidopsis intronic miR400 was proposed (Yan et al., 2012). This miRNA is located within the first intron in the 5' UTR of the *At1g32583* host gene. Under control conditions, splicing of the miRNA-hosting intron was efficient and resulted in the effective production of both host mRNA and mature miR400. Under heat-stress conditions, the miR400 stem-loop structure was retained within the host mRNA as a consequence of alternative 5' splice site selection (located close to the 3' end of the first intron). Thus, intron-retained pre-miR400 was not efficiently processed to mature miRNA (whose accumulation decreased under stress conditions). Moreover, inactivation of the constitutive 5' splice site or the branch point sequence also lead to the downregulation of mature miR400 levels. The mutation of the alternative 5' splice site influenced miRNA accumulation only after heat-stress treatment. Based on these results, the authors proposed a model in which the miRNA-hosting intron lariat is the best substrate for the microprocessor complex to produce miR400, and this miRNA cannot be efficiently produced from the intron retained within the host mRNA (Fig. 17).

5 Plant miRNAs responsive to biotic and abiotic stress factors

During their growth and development, plants are exposed to a wide variety of environmental factors. Only the proper molecular response allows them to survive by adaptation or acclimation to stress conditions. Plants have developed specific mechanisms to precisely recognize climate changes and stress factors, through which they can rapidly adjust their response at the transcriptomic, cellular, and physiological levels. What is more, plants react differently to particular stresses as well as to multiplex stress factors occurring at the same time (Rizhsky et al., 2004). There are many different biotic (i.e., bacterial pathogen, viruses, fungi, insects, nematodes, etc.) and abiotic (i.e., drought, soil salinity, extreme temperatures, heavy metals, etc.) stress factors that influence the expression of many genes at both the transcriptional and posttranscriptional levels (Chao et al., 2005; Fagard et al., 2007; Si et al., 2009; Brotman et al., 2012). These stimuli may also affect mRNA translation as well as posttranslational protein modification.

Up until now, many miRNAs have been identified as regulators of proper stress response in various plant species; e.g., *Arabidopsis*, rice, barley, wheat, and potato (Kruszka et al., 2012, 2014; Pieczynski et al., 2013; Pandey et al., 2014; Barciszewska-Pacak et al., 2015; Guerra et al., 2015; Nigam et al., 2015; Zhang, 2015). By fine-tuning the levels of their miRNAs, plants try to cope with the environmental stress factors to which they are exposed. Examples of identified stress-responsive *Arabidopsis* miRNAs are presented in the table below (Tab. 4).

Table 4. Stress-responsive miRNAs in *Arabidopsis thaliana*: ↓-downregulation; ↑-upregulation; (?) - unknown

Arabidopsis miRNA	Stress factors	Target mRNAs	Regulated process	References
miR156 (↑)	Drought; salinity; UV-B; viruses	SBP-like (↓)	Leaf (size and shape) and shoot development; vegetative phase change; flowering time; male sterility	Zhou et al., 2007; Liu et al., 2008; Zhou et al., 2008
miR159/miR390 (↑)	ABA; drought; salinity; UV-B	TCPs/MYBs (↓)	Flowering time; leaf shape and size; male sterility; seed germination	Zhou et al., 2007; Liu et al., 2008; Zhou et al., 2008

miR160 (↑)	ABA; UV-B; bacterial infection	ARF10 (↓)	Seed germination; floral organ identity; auxin signaling; lateral root formation	Sunkar and Zhu, 2004; Liu et al., 2007; Zhou et al., 2007
miR166 (↑)	Drought; cold; UV-B	HD-ZIPIII (↓)	Leaf polarity and development; female sterility; cell differentiation	Zhou et al., 2007; Zhou et al., 2008; Kantar et al., 2010;
miR168 (↑)	Drought; salinity	AGO1 (↓)	miRNA biogenesis regulation; plant development	Liu et al., 2008; Dolata et al., 2016
miR169a/c (↓)	ABA; drought	NFY A5 (↑)	Regulation of stress-responsive gene expression; control of stomatal aperture	Li et al., 2008; Liu et al., 2008; Zhou et al., 2008
miR319a/b/c (↑)	Cold; drought; copper excess and deficiency; cadmium excess; salinity	TCPs (?)	Leaf shape and size; plant development; floral organ identity; flowering time	Sunkar and Zhu, 2004; Liu et al., 2008; Zhou et al., 2008; Barciszewska- Pacak et al., 2015
miR319b.2 (↑)	Copper excess and deficiency; cadmium excess; drought	RAP2.12 (?) TBL10 (?)	Unknown	Barciszewska- Pacak et al., 2015
miR393 (↑)	ABA; cold; drought; salinity; UV-B; bacterial infection	TIR1/AFB2 (↓)	Auxin signaling; lateral root formation	Sunkar and Zhu, 2004; Zhou et al., 2007; Liu et al., 2008; Zhou et al., 2008
miR395 (↑)	Drought; sulfur deficiency	APS1/3/4 (↓) SULTR2;1 (↓)	Sulfur assimilation and allocation	Kawashima et al., 2009, 2011
miR397 (↑)	Drought; copper deficiency	LAC2 (↓) LAC4 (↓) LAC17 (↓)	Copper homeostasis in the cell	Sunkar and Zhu, 2004; Abdel-Ghany and Pilon, 2008; Liu et al., 2008

miR398 (↓)	ABA; salinity; copper excess; oxidative stress; bacterial infection	CDS1/2 (↑)	Tolerance to light and heavy metals; sugar response; photosynthesis activity; ROS inactivation	Sunkar et al., 2006; Yamasaki et al., 2007
miR399 (↑)	Phosphate stress	UBC24/PHO2 (↓)	Pi homeostasis	Aung et al., 2006; Chiou et al., 2006; Pant et al., 2008
miR400 (↓)	Salinity; sulfur deficiency; copper excess and deficiency; cadmium excess; drought; heat; bacterial infection	PPR1/2 (?)	Seed germination	Yan et al., 2012; Barciszewska-Pacak et al., 2015; Park et al., 2014
miR402 (↑)	ABA; cold; salinity; heat; drought	DML3 (↓)	DNA methylation; seed germination	Sunkar and Zhu, 2004; Zhou et al., 2008; Knop and Stepien et al., 2016
miR408 (↑)	Cold; drought; copper deficiency	LAC3 (↓) LAC12 (↓) LAC13 (↓)	Copper homeostasis in the cell	Abdel-Ghany and Pilon, 2008; Liu et al., 2008; Zhou et al., 2008
miR857 (↑)	Copper deficiency	LAC7 (↓)	Copper homeostasis in the cell	Abdel-Ghany and Pilon, 2008

Abbreviations: SBP-like, SQUAMOSA PROMOTER BINDING PROTEIN-LIKE; TCP, TEOSINTE BRANCHED/CYCLOIDEA/PCF; ARF10, AUXIN RESPONSE FACTOR 10; HD-ZIPIII, THE CLASS III HOMEODOMAIN-LEUCINE ZIPPER PROTEIN; NFY, SUBUNIT OF CCAAT-BINDING COMPLEX A5; RAP2.12, RELATED TO AP2 12; TBL10, TRICHOME BIREFRINGENCE-LIKE 10; TIR10, TRANSPORT INHIBITOR RESPONSE 1; AFB2, AUXIN SIGNALING F-BOX 2; ATP1/3/4, ATP SULFURYLASE 1/3/4; SULTR2;1, SULFATE TRANSPORTER 2.1; LAC2/3/4/7/12/13/17, LACCASE 2/3/4/7/12/13/17; CDS1/2, CDP-DIACYLGLYCEROL SYNTHASE 1/2; UBC24, UBIQUITIN-CONJUGATING ENZYME 24; PHO2, PHOSPHATE 2; PPR1/2, PENTATRICOPEPTIDE REPEAT 1/2; DML3, DEMETER-LIKE PROTEIN 3.

To fully understand the role of particular miRNA under environmental conditions, identification of its target mRNA is necessary. Many miRNAs are multi-stress responsive and may regulate the expression of several target mRNAs. Moreover, miRNAs target many transcription factors, whose expression changes affect basic processes, thus reflecting plant growth and development, phase transition, and the metabolism and physiology of the cell, for example. In its response to stress treatment, the miRNA-mediated regulatory network is very complex and complicated, and the exact mechanism of its regulation is known only for a few miRNA examples. Thus, a complete understanding of miRNA biogenesis regulation and its functions in an ever-changing environment is essential for broadening our knowledge about plant tolerance to biotic and abiotic stress factors.

6 Biogenesis of miR319b and miR319b.2 in *Arabidopsis thaliana*

The *MIR319* family is highly conserved among almost all plant species and can even be found in ancient mosses (Arazi et al., 2005; Axtell and Bartel, 2005; Axtell et al., 2007; Kozomara and Griffiths-Jones, 2014). Accompanied by an elevated accumulation of mature miRNAs, the higher expression level of *MIR319s* is specific for particular tissues and developmental stages (i.e., stems, shoot apices, inflorescences, and siliques) (Palatnik et al., 2003; Sobkowiak et al., 2012). Since miR319s share high-sequence similarities to miRNAs belonging to the *MIR159* family (17 identical nucleotides within the miRNA sequences), these two families probably evolved from a common ancestor (Li et al., 2011). Moreover, both families contain three genes that encode its mature miRNAs: *MIR159a/b/c* and *MIR319a/b/c* (Palatnik et al., 2007). Nevertheless, these miRNAs regulate different target mRNAs, and their role in plant growth and development is different. The miR159s target the MYB-family transcription factor mRNAs (e.g., *MYB33* and *MYB101*) and are involved in the regulation of plant vegetative growth, flowering, male fertility, and ABA-dependent seed germination (Millar and Gubler, 2005; Reyes and Chua, 2007; Allen et al., 2007). The miR319s regulate the TCP transcription factor mRNAs (e.g., *TCP2*, *TCP3*, *TCP4*), but there are also known miR319-targeted MYB TF mRNAs (e.g., *MYB33* and *MYB65*) (Palatnik et al., 2003; Nag et al., 2009). It has been reported that miR319s control the leaf and flower development in plants, affecting growth and reproduction (Palatnik et al., 2003; Palatnik et al., 2007; Nag et al., 2009; Sobkowiak et al., 2012). MiR319s have also been identified

as stress-responsive miRNAs, since their accumulation change after abiotic-stress factor treatments (see Table 4) (Sunkar and Zhu, 2004; Liu et al., 2008; Zhou et al., 2008; Barciszewska-Pacak et al., 2015).

Primary transcripts of *MIR159* and *MIR319* possess characteristic long miRNA stem-loop structures that contain regions with high conservation (base-proximal fragment) or low conservation (loop-proximal fragment) (Palatnik et al., 2003; Bologna et al., 2009, 2013). The described features of pre-miR159 and pre-miR319 precursor hairpin structures determine their non-canonical processing to mature miRNAs, which differs from the known miRNA cleavage pathway. In the canonical mechanism common for most pri-miRNAs (called “*base-to-loop*”), DCL1 performs two cuts starting at the base and continues cleavage towards the loop of the miRNA hairpin. In the case of pre-miR159s and pre-miR319s, DCL1 begins cleavage in close proximity to the loop and handles three additional cuts towards the base direction until mature miRNAs are released (Fig. 18). This way of processing is called the “*loop-to-base*” mechanism. Additional experiments performed for pre-miR319a revealed that the upper part of the miRNA stem-loop structure is especially relevant for proper miR319a biogenesis (Bologna et al., 2009). Modification within the lower part of the pre-mRNA had a minor effect on miR319a maturation efficiency.

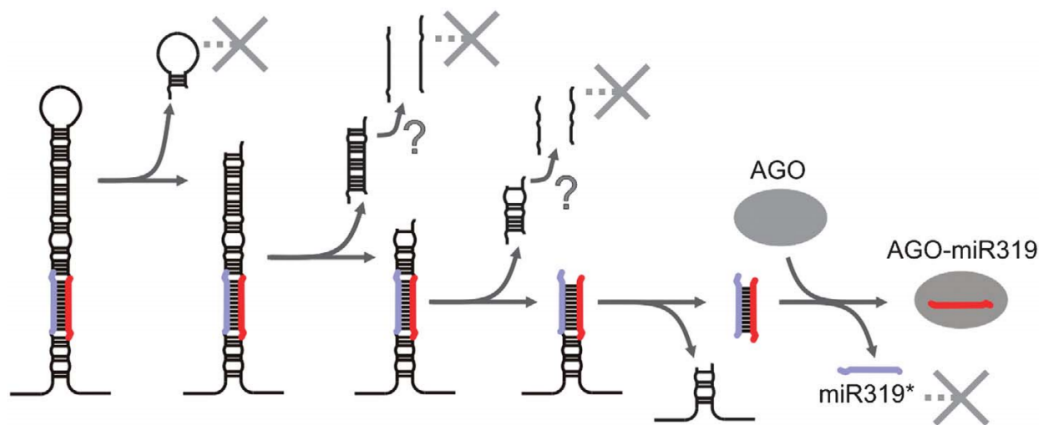


Figure 18. Pre-miR159 and pre-miR319 processing via non-canonical “*loop-to-base*” pathway (Bologna et al., 2009). Red and blue lines – miRNA and miRNA*, respectively.

Interestingly, the secondary structures of both pre-miR159 and pre-miR319 precursors possess three regions from which small RNAs can be processed. Also, in the RNA deep-sequencing results, additional small RNAs accumulated from these precursors have been detected (Rajagopalan et al., 2006; Talmor-Neiman et al., 2006; Axtell et al., 2007; Backman et al., 2008). Accumulation of these miRNAs

is considerably lower in the *hyl1-2* mutant as compared to wild-type plants, indicating that their biogenesis is regulated by the known components of miRNA biogenesis (Bologna et al., 2009). What is more, the presence of bulges in the upper part of the pre-miR319 hairpins reduced the accumulation of these small RNAs. In 2010, Zhang and colleagues reported 19 miRNA precursors from which miRNA-like small RNAs can be processed (Zhang et al., 2010). Several of them (e.g., miR447 and miR822) were shown to be processed via the classical miRNA biogenesis pathway. Among them, miR319a.2 and miR319b.2 are processed from pre-miR319a and pre-miR319b, respectively (Fig. 19), and are conserved among different plant species (e.g., Arabidopsis, rice, and Medicago). Moreover, both of these miRNAs were found in the small RNA sequencing data from bacterial-infected *A. thaliana* plants (*Pseudomonas syringae* DC3000), which may suggest that they play a significant role in plant response to biotic stress. Unfortunately, before 2012 there was no other evidence that allowed to consider these small RNAs to be functional miRNAs.

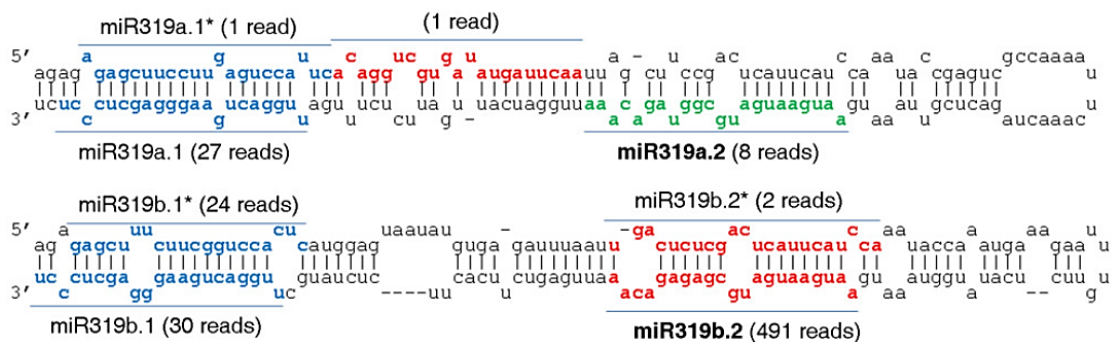


Figure 19. MiRNA-like small RNAs – miR319a.2 and miR319b.2 derived from pre-miR319a and pre-miR319b, respectively (Zhang et al., 2010, modified). MiRn.1/miRn.1* – previously annotated miRNAs/miRNAs*; miRn.2/miRn.2* – miRNA-like small RNAs. Numbers in brackets indicate number of reads mapped to particular small RNA.

In 2012, Sobkowiak and his colleagues confirmed the existence of miR319a.2 and miR319b.2 in their high-throughput sequencing (HTS) data, and moreover, discovered additional miR319c.2 generated from the pre-miR319c precursor (Sobkowiak et al., 2012). Newly identified miRNAs (like miR319a/b/c) share high-sequence similarity to each other (Fig. 20).

```

miR319a UUGGACUGAAGGGAGCUCUCCU
miR319b UUGGACUGAAGGGAGCUCUCCU
miR319c UUGGACUGAAGGGAGCUCUCCU

miR319a.2 AAUGAAUGAUGCGGAGACAA
miR319b.2 AAUGAAUGAUGCGAGAGACAA
miR319c.2 UGUGAAUGAUGCGGGAGAUUU

```

Figure 20. Sequence similarity between miR319a/b/c and miR319a.2/b.2/c.2 in *Arabidopsis thaliana* (Sobkowiak et al., 2012, modified). Nucleotides that differ between miRNAs are marked in white.

Since miR319b.2 was most-abundant within the newly identified small RNAs, it was further tested for miRNA-like features. Interestingly, the authors found a great deal of evidence suggesting that miR319b.2 is a true miRNA: (1) its accumulation decreased in the *hyl1-2* mutant as compared to wild-type plants (Fig. 21); (2) it was present in AGO-immunoprecipitates, thus it is a part of the RISC complexes; (3) miR319b.2 accumulation changed in various developmental stages and tissues (Fig. 22); (4), besides the canonical 21-nt miRNAs, the 24-nt species were also detected in inflorescence; (5) it targets the intron-containing AS isoform of transcription factor *RAP2.12* (RELATED TO APETALA 2.12) mRNA (Fig. 23). Interestingly, according to bioinformatic analyses, 12 putative mRNA targets have been predicted to be regulated by miR319b.2 (Zhang et al., 2010; Sobkowiak et al, 2012). Among them, five the best predictions have been experimentally validated (Sobkowiak et al., 2012). For the intron-containing isoform of the *RAP2.12* transcript, miRNA-mediated 3' cleavage products were detected using the 5' RACE PCR approach. What is more, the expression level of this *RAP2.12* isoform increased in miRNA biogenesis mutants as compared to wild-type plants, suggesting that it is the actual target of miR319b.2.

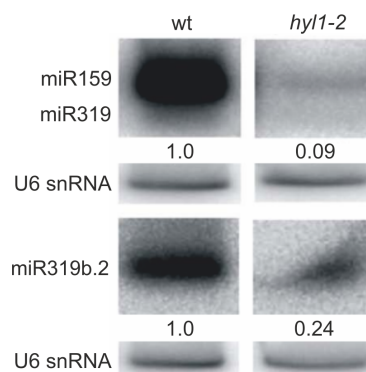


Figure 21. MiR319b.2 biogenesis depends on HYL1 activity in *A. thaliana* (Sobkowiak et al., 2012, modified). U6 snRNA was used as RNA loading control. Numbers below blot images represent band intensities in analyzed samples.

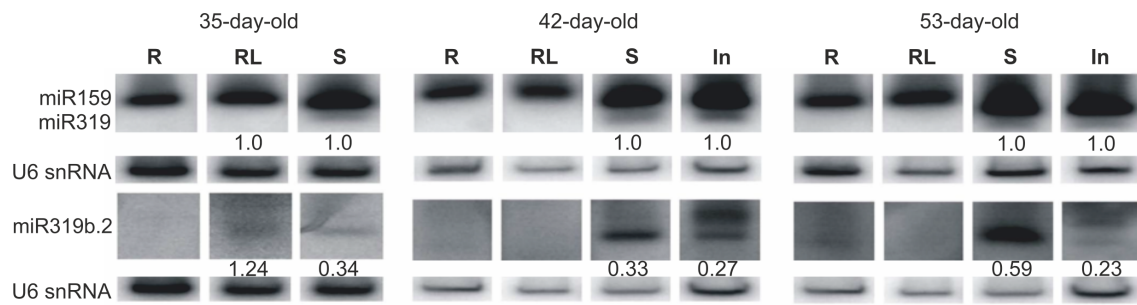


Figure 22. MiR319b.2 accumulation varies in different tissues and developmental stages of *A. thaliana* wild-type plants (Sobkowiak et al., 2012, modified). U6 snRNA was used as RNA loading control. Numbers below blot images represent miRNA band intensities in analyzed samples. Analyzed developmental stages: 35-, 42-, and 53-day-old *A. thaliana* plants. Analyzed tissues: R – roots; RL – rosette leaves; S – stems; In – inflorescences.

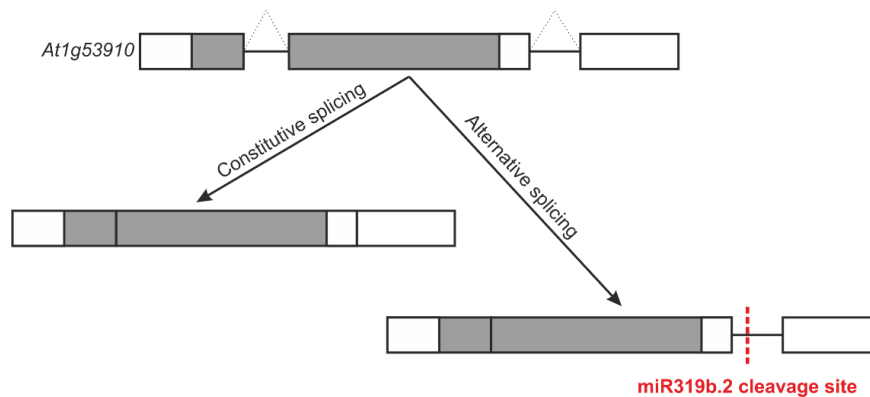


Figure 23. Alternatively spliced *RAP2.12* mRNA isoform is targeted by miR319b.2 (based on Sobkowiak et al., 2012). Boxes – exons; solid lines – introns; dashed lines – splicing events. UTRs are marked in white, while coding sequences are marked in gray. Red dashed line – miR319b.2 cleavage site.

What is more, in 2015 Barciszewska-Pacak and her colleagues identified a second target mRNA of miR319b.2 encoded by *At3g06080* (Barciszewska-Pacak et al., 2015). This gene encodes the TBL10 (Trichome Birefringence-like 10) protein (belonging to the TBL family), which may be involved in the specific O-acetylation of cell-wall polymers like cellulose (Bischoff et al., 2010). *TBL10* encodes two mRNA isoforms, and both of them can be targeted by miR319b.2 (Fig. 24). An experimentally confirmed miRNA cleavage site was located within the 5' UTR of *TBL10* mRNAs (Barciszewska-Pacak et al., 2015).

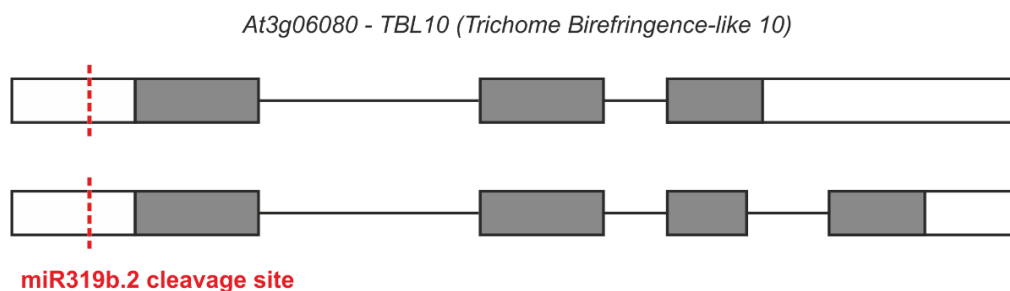


Figure 24. Two *TBL10* mRNA isoforms targeted by miR319b.2 (based on Barciszewska-Pacak et al., 2015). Boxes – exons (UTRs are marked in white, while coding sequences are marked in gray); solid lines – introns; red dashed line – miR319b.2 cleavage sites.

Mature miRNAs belonging to the *MIR319* family target the mRNAs of *TCP* genes that are involved in the regulation of cell proliferation in leaves (Aguilar-Martinez and Sinha, 2013). Thus, mutants of these miRNAs exhibit considerable phenotypical changes caused by an unbalanced level of TCP transcription factors. In 2003, the *jaw-D* Arabidopsis mutant was described, in which an overexpression of *MIR319a* accompanied by an overaccumulation of mature miR319a and extensive loss of several TCP mRNA levels were detected (Weigel et al., 2000; Palatnik et al., 2003). Accordingly to the affected cell proliferation, the *jaw-D* mutant plants were strongly altered (exhibiting, for example, crinkle, smaller and more-elliptical leaves, cotyledon epinasty, and delayed flowering) as compared to wild-type plants (Fig. 25). The insertion of wild-type TCP2 or TCP4 into the *jaw-D* mutant background only partially rescued the leaf defects of *jaw-D* mutants.



Figure 25. Phenotype comparison between Arabidopsis wild-type and *jaw-D* mutant plants (Palatnik et al., 2003, modified). In the figure, seedlings, individual leaves, and rosette leaves were compared.

Two mutants of *MIR319b* were described by Sobkowiak and his colleagues: (1) a null mutant ($\Delta miR319b$) in which T-DNA insertion was identified within the promoter region in close proximity to the 5'UTR of *MIR319b* (SALK_037093); and (2) *MIR319b* overexpressing mutant (*miR319boe*) with T-DNA insertion located downstream from *MIR319b* (SALK_059451) (Sobkowiak et al., 2012). In the $\Delta miR319b$ mutant, a decreased level of pri-miR319b and reduced levels of miRNAs (as compared to wild-type plants) (Fig. 26) were followed by growth retardation and altered rosette leaf shape (i.e., leaves are narrower and rolled inwards), with no changes in the floral organ architecture (Fig. 27). The mutant overexpressing *MIR319b* exhibited more-severe phenotypical changes than null mutant and wild-type plants (i.e., more delayed growth, arrow-shaped serrated leaves, and strong leaf curvature), which resembles the *jaw-D* mutant phenotype to a certain extent (Fig. 25 and 27). These observations were accompanied by an upregulated level of pri-miR319b and overaccumulation of mature miR319b and miR319b.2 in the *miR319boe* mutant (as compared to wild-type plants) (Fig. 26).

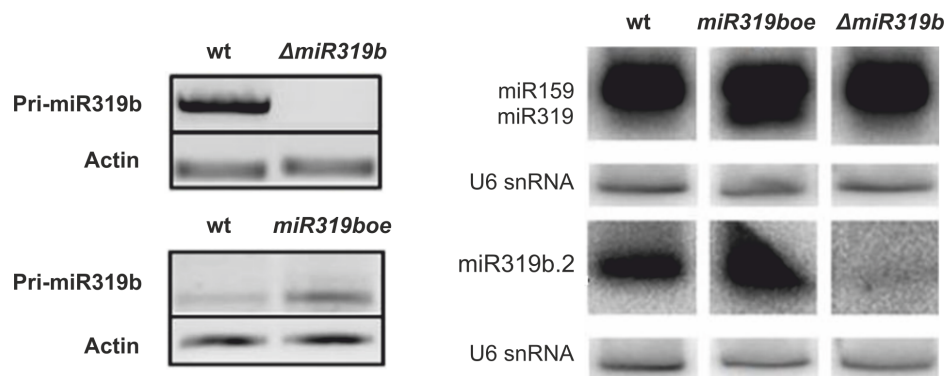


Figure 26. Pri-miR319b level and mature miR319b and miR319b.2 accumulation in Arabidopsis wild-type, $\Delta miR319b$ (SALK_037093), and $\Delta miR319boe$ (SALK_059451) plants (Sobkowiak et al., 2012, modified). Actin was used as a reference gene in a semiquantitative RT-PCR analysis, while U6 snRNA was used as RNA-loading control in N. blot experiments.



Figure 27. Phenotype comparison between 42-day-old Arabidopsis wild-type, $\Delta miR319b$ (SALK_037093), and $\Delta miR319boe$ (OE) (SALK_059451) plants (Sobkowiak et al., 2012, modified).

Both of the described *MIR319b* mutants differ significantly from the wild-type plants; however, it is still unclear which of their phenotypical features is connected to miR319b or to the newly discovered miR319b.2. Analysis of this aspect is necessary to broaden our common knowledge about the mechanisms of regulation of plant growth and development as well as the role of miR319b and miR319b.2 in these processes.

THE AIM OF THE WORK

It has been recently demonstrated that the proper splicing of the pre-miRNA-downstream-located introns is required for the efficient biogenesis of Arabidopsis exonic miRNAs encoded by intron-containing *MIR* genes (Bielewicz et al., 2013; Schwab et al., 2013). What is more, the selection of a polyadenylation site within the primary miRNA transcripts may play an important role during plant miRNA maturation (Bielewicz et al., 2013; Barciszewska-Pacak et al., 2016). Thus, the connections between the microprocessor complex, spliceosome, and polyadenylation machinery seem to be relevant for plant miRNA biogenesis. However, knowledge is limited regarding the effects of these connections for the production of plant miRNAs located within the host-gene introns. It is still unknown whether these machineries cooperate or compete with each other during the maturation of intronic miRNAs. Thus, **revealing the mechanism of *A. thaliana* intronic miRNA biogenesis was the main aim of the presented study.** Moreover, since the accumulation level of many miRNAs derived from introns was demonstrated to be regulated by environmental stimuli (Barciszewska-Pacak et al., 2015), **the effects of selected abiotic stresses on the mechanism of Arabidopsis intronic miRNA maturation were tested.**

Furthermore, as presented by Sobkowiak and his colleagues, the *MIR319b* family is important for plant growth and development (Sobkowiak et al., 2012). Within the pre-miR319b stem-loop structure, at least two functional miRNAs are located – miR319b and miR319b.2 – that differ in nucleotide sequences and targeted mRNAs. Still there is nothing known about whether the biogenesis of miR319b depends on miR319b.2 production or *vice versa*. According to this, **an additional goal of this PhD thesis was the dissection of *A. thaliana* miR319b and miR319b.2 biogenesis.**

MATERIALS AND METHODS

1 Reagents

2-Mercaptoethanol	Sigma Aldrich
Acrylamide	Sigma Aldrich
Agar (plant culture)	Sigma Aldrich
Agar (microbiological)	BioShop
Agarose	Prona
Ampicillin	BioShop
Ammonium thiocyanate	Sigma Aldrich
Ammonium nitrate	Sigma Aldrich
Ammonium peroxydisulfate (APS)	Sigma Aldrich
[$\gamma^{32}\text{P}$]-ATP	Hartmann
Bio-tryptone	BioShop
Boric acid	Sigma Aldrich
Bromophenol blue	Sigma Aldrich
Cadmium sulfate	Sigma Aldrich
Calcium chloride	Sigma Aldrich
Chloroform	Chempur
Cobalt (II) chloride	Sigma Aldrich
Copper (II) sulfate	Sigma Aldrich
Cordycepin (3'-Deoxyadenosine)	Sigma Aldrich
Deoxynucleotides - mix (dNTPs)	Sigma Aldrich
Diethyl pyrocarbonate (DEPC)	Sigma Aldrich
Dimethyl sulfoxide (DMSO)	Sigma Aldrich
Ethylenediaminetetraacetic acid (EDTA)	Sigma Aldrich
Ethanol	Chempur
Ethidium bromide	Sigma Aldrich
Formamide	Chempur
Glufosinate ammonium (BASTA)	Bayer
Glycerol	Sigma Aldrich
Herboxydiene (Gex-1A)	Cfm Oskar Tropitzsch GmbH
Hydrochloric acid (HCl)	Chempur
Isopropanol	Chempur
Iron (II) sulfate	Sigma Aldrich

Kanamycin	BioShop
MES	Sigma Aldrich
Magnesium chloride	Sigma Aldrich
Magnesium sulfate	Sigma Aldrich
Manganese (II) chloride	Sigma Aldrich
MOPS	Sigma Aldrich
Murashige & Skoog medium (MS)	Duchefa Biochemie
N, N-dimethylformamide	Sigma Aldrich
N, N'-methylene-bis-acrylamide	Sigma Aldrich
N, N, N', N'-Tetramethylethylenediamine (TEMED)	Sigma Aldrich
Orange G	Sigma Aldrich
Phenol-Tris-saturated	Roth
PIPES	Sigma Aldrich
Potassium acetate	Sigma Aldrich
Potassium chloride	Sigma Aldrich
Potassium iodide	Sigma Aldrich
Potassium nitrate	Sigma Aldrich
Potassium permanganate	Sigma Aldrich
Potassium phosphate monobasic	Sigma Aldrich
Rifampicin	BioShop
Rubidium chloride	Sigma Aldrich
Sodium acetate	Sigma Aldrich
Sodium dodecyl sulfate (SDS)	Sigma Aldrich
Silwet Gold	Chemtura
Sodium molybdate dehydrate	Sigma Aldrich
Sodium phosphate dibasic	Sigma Aldrich
Sodium phosphate monobasic	Sigma Aldrich
Sodium citrate	Sigma Aldrich
Sodium chloride	Sigma Aldrich
Sodium hypochlorite	Sigma Aldrich
Sucrose	Sigma Aldrich
Tris[hydroxymethyl]aminomethane (Tris) Base	Sigma Aldrich
Urea	Sigma Aldrich
5-bromo-4-chloro-3-indolyl-D-galactopyranoside (X-Gal)	Sigma Aldrich
Xylene Cyanol	Sigma Aldrich
Yeast extract	BioShop

2 Plant material

The presented experiments were performed using wild-type *Arabidopsis thaliana* (L.) Heynh. plants (Columbia-0). Moreover, the following *A. thaliana* homozygous mutant lines were used: *se-1* (Prigge and Wagner, 2001), *se-2* (Grigg et al., 2005), and SALK_037093 (*AmiR319b*) (Sobkowiak et al., 2012). For transient expression assays, the leaves of wild type *Nicotiana benthamiana* plants were used.

2.1 Plant growth conditions

2.1.1. Plant culture on MS medium

Arabidopsis thaliana plants were cultivated at sterile solid or liquid half-strength Murashige & Skoog medium (pH 5.5-5.6) (Tab. 4) on Petri dishes (Ø 9 cm) (Sarstedt) or in glass flasks (without agar addition), respectively. At first, the seeds were sterilized using 70% ethanol and a 1.2% sodium hypochlorite solution. After planting, the seeds were kept in 4°C in darkness for 48 hours. Next, the dishes were moved into an MLR-350H growth chamber (Sanyo), and the plants were grown under 16-hour-day conditions (approx. 150-200 $\mu\text{E}/\text{m}^2$) at a constant temperature of 22°C and 70% humidity. 10- or 14-day-old *A. thaliana* seedlings were frozen in liquid nitrogen, and stored at -80°C.

Table 4. Half-strength MS medium composition

Component	Final concentration	Amount
Murashige & Skoog medium	0.22%	1.1 g
Sucrose	1.5%	7.5 g
Plant culture agar (optionally)	1%	5 g
MiliQ water	-	up to 500 ml

Autoclaved at 121°C, 1 atm., 20 min.

2.1.2. Plant culture in soil

Arabidopsis thaliana plants were grown in “Jiffy-7 42 mm” pots (Jiffy International AS). *Nicotiana benthamiana* plants were cultivated in sterile soil “Podłoże warzywne AURA” (Hollas) (autoclaved: 121°C, 1 atm., 20 min). Seeds of both species were stratified after sowing at 4°C in darkness for 48 hours and then moved into the growth chamber. Then, plants were grown under 16-hour-day conditions (approx. 150-200 $\mu\text{E}/\text{m}^2$) at a constant temperature of 22°C and 70% humidity. *Arabidopsis thaliana* plants were collected after 35 (rosette leaves), 42 (stem), or 53 (inflorescence) days, then frozen in liquid nitrogen, and stored at -80°C. Agroinfiltration of *N. benthamiana* leaves was performed after 35-42 days of plant growth.

2.2 Plant transformation

2.2.1. Transformation of *Arabidopsis thaliana* plants using the floral dip technique

In order to obtain transgenic *Arabidopsis* lines, the *Agrobacterium tumefaciens* (AGL1)-mediated floral dip method was used (Clough and Bent, 1998). Plants were grown under 16-hour-day conditions (approx. 150-200 $\mu\text{E}/\text{m}^2$) at a constant temperature of 22°C and 70% humidity for 4-5 weeks. For transformation, *Agrobacterium tumefaciens* strains (AGL1) carrying the analyzed gene cloned into binary vector were used. Bacteria were grown in 300 ml of a liquid LB medium supplemented with the proper antibiotics at 28°C with shaking (170 rpm) for 24 hours. Next, the AGL1 culture was centrifuged (20 min., 3000 g). Cells were resuspended in a 10% sucrose solution to $\text{OD}_{600}=0.8$. Then, a Silwet Gold solution was added to 0.05% of the final concentration. Before transformation, all siliques and open flowers were removed. Then, the plants were dipped in the prepared AGL1 solution. After transformation, the plants were stored under cover for 24 hours in darkness and, next, grown under regular conditions until the seeds were ready to harvest.

2.2.2. Selection of *Arabidopsis* transgenic lines using BASTA herbicide

The selection of MIR319b transgenic lines carrying MIR319b versions cloned into binary vector pMDC123 was performed using BASTA herbicide. For this purpose, T1 generation seedlings growing in soil were sprayed four times with 300 μ M BASTA solution (dissolved in MiliQ water) at two-day intervals. After the BASTA treatment, T1 selected plants were grown until the siliques matured. Next, the seeds were collected and sown on a solid half-strength MS medium (Tab. 4) supplemented with agar and BASTA herbicide (final concentration - 6 μ g/ml). If T2 plants were homozygous, all seedlings on the plate would be green. After selection, T2 homozygous plants were transferred to soil and grown until the seeds were ready to collect. For each construct, at least three homozygous T2 lines of transgenic plants were selected.

2.2.3. Transient expression in *Nicotiana benthamiana* leaves

Nicotiana benthamiana plants were grown under 16-hour-day conditions (approx. 150-200 μ E/m²) at a constant temperature of 22°C and 70% humidity for 35-42 days. For agroinfiltration, *Agrobacterium tumefaciens* strains (AGL1) carrying the analyzed gene cloned into a binary vector were used. Bacteria were grown in 50 ml of the liquid LB medium supplemented with the proper antibiotics at 28°C with shaking (170 rpm) for 24 hours. Next, the AGL1 culture was centrifuged (20 min., 3000 g). Cells were resuspended in the buffer containing 10 mM MES (pH 5.6) and 10 mM MgCl₂ to OD₆₀₀=0.6. The prepared *Agrobacterium* solution was infiltrated into *Nicotiana* leaves using a syringe. A clear buffer was used as a mock (control). After transformation, the plants were grown for an additional 72 hours, and then the agroinfiltrated leaves were collected, frozen in liquid nitrogen, and stored at -80°C. All agroinfiltrations were performed in three biological replications.

2.3 Induction of *A. thaliana* plant response to selected abiotic stresses

All experiments were performed in three biological replications. After application of the described below abiotic stresses, plant material was collected, frozen in liquid nitrogen, and stored at -80°C.

2.3.1. Heat stress

For heat-stress treatment, wild-type *A. thaliana* 14-day-old seedlings were transferred from 22° to 37°C and incubated for 0.5, 2, 6, and 12 hours (Barciszewska-Pacak et al., 2015). Control plants, grown at 22°C, were collected at time point “0.” To confirm heat-stress response, the expression levels of two marker genes were analyzed in both the control and stressed plants: *HSP17.6* (*At5g12030*) and *HSP22.0* (*At4g10250*).

2.3.2. Salinity stress

To induce salinity stress, wild-type *A. thaliana* 14-day-old seedlings were transferred from the plates into the half-strength liquid MS medium (prepared as described in Table 4, but without the addition of agar) containing 250 mM NaCl excess (Barciszewska-Pacak et al., 2015). Control plants were grown in a standard liquid half-strength MS medium. Then, the plants were incubated at 22°C for 24 hours with constant light and shaking (150 rpm). To confirm salinity-stress response, the expression levels of three marker genes were analyzed in both the control and stressed plants: *ABF3* (*At4g34000*), *LEA4* (*At1g32560*), and *TSPO* (*At2g47770*).

2.3.3. Drought stress

For drought-stress induction, *Arabidopsis thaliana* wild-type plants were grown under control conditions (as described in 2.1.2.) in a controlled environment of 70% SWC (soil water content) until the 1.10 growth stage (Boyes et al., 2001; Barciszewska-Pacak et al., 2015). Drought stress was applied by withholding water and continued until the 30% SWC (3 days before wilting) and 20% SWC (wilting) levels were reached, respectively. Control plants were grown in 70% SWC. To confirm drought response, the expression levels of three marker genes were analyzed in both the control and stressed

plants: *RAB18* (*At5g66400*), *RD29B* (*At5g52300*), and *NCED3* (*At3g14440*) (Barciszewska-Pacak et al., 2015).

2.4 Plant treatment with transcription inhibitor – cordycepin (3'-Deoxyadenosine)

2.4.1. Heat-stressed *A. thaliana* 17-day-old seedling treatment with cordycepin

Arabidopsis seedlings were grown for 17 days in a solid half-strength MS medium (Tab. 4) under control conditions (16-hour-day conditions [approx. 150-200 $\mu\text{E}/\text{m}^2$] at a temperature of 22°C and 70% humidity). Next, the plants were exposed to 37°C for 2 hours to induce heat-stress response. The stressed seedlings were transferred into an incubation buffer (1 mM Pipes (pH 6.25), 1 mM sodium citrate, 1 mM KCl, and 15 mM sucrose) and swirled at 30 rpm at 22°C for 30 minutes (Seeley et al., 1992). Next, 3'-deoxyadenosine (Cordycepin; C3394; Sigma Aldrich) was added to a final concentration of 0.6 mM (time 0). Plant tissue samples were collected after 20, 40, 60, and 80 minutes of incubation time with cordycepin, frozen in liquid nitrogen, and stored at -80°C.

2.4.2. Agroinfiltrated *N. benthamiana* leaf disc treatment with cordycepin

Nicotiana plants were grown for about 4-5 weeks in sterile soil under control conditions (16-hour-day conditions (approx. 150-200 $\mu\text{E}/\text{m}^2$) at a temperature of 22°C and 70% humidity) and then agroinfiltrated as described above. 72 hours after transformation, small discs (\varnothing 5 mm) were cut out from the transfected leaves (n=100) and placed in a square Petri dish containing 30 ml of incubation buffer (1 mM Pipes (pH 6.25), 1 mM sodium citrate, 1 mM KCl, and 15 mM sucrose). After 30 minutes of swirling at 30 rpm, 3'-deoxyadenosine (Cordycepin; C3394; Sigma Aldrich) was added to a final concentration of 0.6 mM (time 0). Plant tissue samples were collected after 30, 60, 120, and 180 minutes of incubation time with cordycepin, frozen in liquid nitrogen, and stored at -80°C.

2.5 Plant treatment with splicing inhibitor – Herboxidiene (Gex-1A)

For herboxidiene treatment, 14-day-old *Arabidopsis* seedlings grown on plates (2.1.1) under control conditions were transferred to a liquid half-strength MS medium (Table 4, without the addition of agar) supplemented with 2 μ M DMSO and/or 4 μ M Gex-1A. Then, the seedlings were incubated at 22°C with continuous light and shaking (50 rpm). After 12 and 24 hours, plant material was collected, frozen in liquid nitrogen, and stored at -80°C. Control plant material was collected at time point “0.”

3 Bacterial cultures

3.1 Bacteria strains

The following bacterial strains were used:

- (1) competent cells of *Escherichia coli* DH5 α - for cloning and plasmid amplification;
- (2) competent *Agrobacterium tumefaciens* (AGL1) - for transformation of *Arabidopsis thaliana* plants using the floral dip method and for transient expression experiments in *Nicotiana benthamiana* leaves.

3.2 Bacterial culture media and reagents

During the performed experiments the following bacterial culture media were used:

- (1) LB (Luria-Bertani) liquid medium (Tab. 5):

Table 5. LB liquid medium composition

Component	Final concentration	Amount
Bio-tryptone	1%	5 g
Yeast extract	0.5%	2.5 g
NaCl	1%	5 g
MiliQ water	-	up to 500 ml

Autoclaved at 121°C, 1 atm., 20 min.

- (2) LB (Luria-Bertani) solid medium (Tab. 6):

Table 6. LB solid medium composition

Component	Final concentration	Amount
Bio-tryptone	1%	5 g
Yeast extract	0.5%	2.5 g
NaCl	1%	5 g
Microbiological agar	1.5%	7.5 g
MiliQ water	-	up to 500 ml

Autoclaved at 121°C, 1 atm., 20 min.

Moreover, the following bacterial culture reagents were used:

- (1) antibiotic solutions: ampicillin (50 mg/ml; dissolved in MiliQ water), kanamycin (50 mg/ml; dissolved in MiliQ water), and rifampicin (50 mg/ml; dissolved in DMSO). All antibiotic were filtered using MILLEX-HP filters ($\text{\O} 0.45 \mu\text{m}$) (Millipore);
- (2) X-Gal solution (20 mg/ml, dissolved in N, N-dimethylformamide).

3.3 *E. coli* cell transformation

3.3.1. Preparation of competent *E. coli* cells

For transformation of the *E. coli* DH5 α strain, competent bacterial cells were used. For this purpose, DH5 α cells were grown in 25 ml of the liquid LB medium (37°C/16 hours) with shaking (220 rpm) (New Brunswick Scientific Innova 4230 Refrigerated Benchtop Incubator Shaker, Eppendorf). Next, 2 ml of the bacterial culture was transferred into 100 ml of fresh liquid LB medium and grown at 37°C with shaking (220 rpm) to OD₆₀₀=0.6. Then, the culture was divided into two 50-ml sterile tubes (Falcon), placed on ice for 15 minutes, and centrifuged (15 min./2500 g/4°C). Each pellet was resuspended in 16 ml of Buffer I (Tab. 7), placed on ice for 15 minutes, and centrifuged (15 min./2500 g/4°C). Next, the pellets were resuspended in 4 ml (each) of Buffer II (Tab. 8), and the *E. coli* DH5 α competent cells were portioned per 100 μl to 1.5-ml sterile tubes (Eppendorf), and stored at -80°C. All steps were performed in a sterile environment (flow chamber MSC-Advantage™ (Thermo Fisher Scientific)).

Table 7. Buffer I composition

Component	Final concentration	Amount
RbCl	0.1 M	1.2 g
MnCl ₂ *4H ₂ O	0.99%	0.99 g
1M Potassium acetate (pH 7.5)	0.03 M	3 ml
CaCl ₂ *2H ₂ O	0.15%	0.15 g
100% Glycerol	10%	10 ml
MiliQ water	-	up to 100 ml

Filtered using MILLEX-HP filters ($\text{\O} 0.22 \mu\text{m}$) and stored at 4°C.

Table 8. Buffer II composition

Component	Final concentration	Amount
RbCl	0.1 M	1.2 g
0.5M MOPS (pH 6.8)	0.01 M	2 ml
CaCl ₂ *2H ₂ O	1.1%	1.1 g
100% Glycerol	10%	10 ml
MiliQ water	-	up to 100 ml

Filtered using MILLEX-HP filters (Ø 0.22 µm) and stored at 4°C.

3.3.2. Transformation of *E. coli* cells using heat-shock method

The *E. coli* DH5α competent cells in a 1.5-ml tube were thawed on ice. Next, ligation mix/plasmid was added into each tube (gently mixed), and the sample was incubated on ice for 30 minutes. Then, the sample was heated (42°C) for 1 minute, chilled on ice (2 min.), and finally 600 µl of the liquid LB medium (pre-warmed to 37°C) was added. The transformed bacterial culture was incubated for 1.5 hours at 37°C with shaking (350 rpm) (Thermomixer Comfort, Eppendorf).

3.3.3. Transformed *E. coli* cell growth conditions and selection

250 µl of the transformed bacterial cell suspension were grown on a solid LB medium supplemented with the proper antibiotics (final concentration - 0.05 mg/ml). For the selection of bacterial colonies carrying pGEM T-Easy plasmids, 30 µl of an X-Gal solution was added. Plates with bacterial cultures were incubated at 37°C for 16 hours. Colonies with the proper plasmids were checked using the colony PCR technique and then grown in the liquid LB medium (supplemented with the proper antibiotics to a final concentration of 0.05 mg/ml) at 37°C for 16 hours with shaking (220 rpm).

3.4 *A. tumefaciens* cell transformation

3.4.1. Preparation of competent AGL1 cells

At the beginning, AGL1 cells were grown in 25 ml of the liquid LB medium supplemented with rifampicin (0.1 mg/ml) at 28°C for 24 hours with shaking (170 rpm). Next, 5 ml of the bacterial culture was transferred into 200 ml of fresh liquid LB medium (with rifampicin – 0.1 mg/ml) and grown at 28°C with shaking (170 rpm) to OD₆₀₀=0.6. Then, the culture was divided into four 50-ml sterile tubes (Falcon), placed on ice for 15 minutes, and centrifuged (15 min./2500 g/4°C). Each pellet was then resuspended in 40 ml of pre-chilled sterile MiliQ water, placed on ice for 15 minutes, and centrifuged (15 min./2500 g/4°C). This step was repeated six times in order to fully desalt the pellets. Next, the bacterial pellets were resuspended in 5 ml (each) of chilled sterile 10% glycerol and centrifuged (15 min./2500 g/4°C). Finally, the pellets were resuspended in 1 ml of chilled sterile 10% glycerol, and the AGL1 electrocompetent cells were portioned per 50 µl to 1.5-ml sterile tubes (Eppendorf) and stored at -80°C. All steps were performed in a sterile environment (flow chamber).

3.4.2. Transformation of AGL1 cells using electroporation method

Competent AGL1 cells in the 1.5-ml tubes were thawed on ice (~15 min.). During this time, the ligation mixture was desalted using a nitrocellulose 0.025 µm filter (Millipore) for 30 minutes. Next, a desalted ligation mix/plasmid solution was added to the tube, and the mixture was transferred to a pre-chilled 0.2-cm-gap electroporation cuvette (Bio-Rad). A pulse of 2.5 kV (129 ohm resistance) was applied, and 1 ml of sterile liquid LB medium was immediately added to the bacterial cells. Then, the bacterial culture was mixed, transferred to fresh 1.5-ml tubes (Eppendorf), and incubated at 28°C for 1 hour with shaking (170 rpm).

3.4.3. Transformed AGL1 cells growth conditions and selection

250 µl of the transformed bacterial cell suspension was grown on the solid LB medium supplemented with proper antibiotics (final concentration - 0.05 mg/ml) and rifampicin (0.1 mg/ml). Plates with bacterial cultures were incubated at 28°C for 48 hours. Colonies with the proper plasmids were checked using the colony PCR technique and then grown

in the liquid LB medium (supplemented with proper antibiotics in a final concentration of 0.05 mg/ml and rifampicin – 0.1 mg/ml) at 28°C for 48 hours with shaking (170 rpm).

4 Methods used during work with ribonucleic acid (RNA)

4.1 Northern hybridization

4.1.1. RNA isolation using TRIzol reagent

For Northern blot analysis, total RNA was extracted from grinded, frozen plant material using a TRIzol reagent (Tab. 9).

Table 9. TRIzol reagent composition

Component	Final concentration	Amount
Phenol (acid-saturated)	38%	38 ml
Guanidine thiocyanate	0.8 M	11.816 g
Ammonium thiocyanate	0.4 M	7.612 g
3M Sodium acetate (pH 5)	0.1 M	3.34 ml
100% Glycerol	5%	5 ml
DEPC-treated water	-	up to 100 ml

DEPC-treated water: 1000 ml of MiliQ water was incubated with 500 μ l of Diethyl pyrocarbonate (DEPC) at 37°C (overnight) and then autoclaved twice (121°C, 1 atm., 20 min.).

Acid phenol solution: 99.66 ml of DEPC-treated water and 3.33 ml of 3M sodium acetate (3 M) were added to 100 ml of phenol. The prepared solution was incubated overnight at 4°C with shaking (600 rpm). Next, the water phase above the phenol was removed (~1 cm layer was left), and 50 μ l of 2-Mercaptoethanol was added.

To isolate the total RNA, 1 ml of the TRIzol reagent was added to 100 mg of grinded frozen plant tissue. The sample was vortexed, incubated at room temperature for 5 minutes, and centrifuged (15 min./12,000 g/4°C). Then, the extract was transferred into a fresh 2-ml sterile tube (Eppendorf), and 500 μ l of chloroform was added. The sample was vortexed, incubated at room temperature for 3 minutes, and centrifuged (15 min./12000 g/4°C). Next, the extract was transferred into a fresh 2-ml sterile tube, one-volume of chloroform was added, and the mixture was centrifuged (5 min./12,000 g/4°C). The extract was transferred into a fresh 1.5-ml sterile tube, and one-volume of isopropanol was added. The sample was incubated at room temperature for 20 minutes and then centrifuged (20 min./12,000 g/4°C). Next, the RNA pellet was washed twice with 1 ml of chilled 75% ethanol, dried at room temperature, and dissolved with 40 μ l of DEPC-treated water. The sample's integrity was checked on 2% agarose gel, and the concentration was estimated using a NanoDrop spectrophotometer (DS-11 Spectrophotometer, DeNovix).

4.1.2. RNA electrophoresis in agarose gel

To check the integrity of the isolated total RNA, agarose-gel electrophoresis was applied. For this purpose, a small-gel horizontal system (Hoefer) was used. The RNA sample was mixed with a 2x-concentrated RNA-loading buffer (Tab. 10), denatured (70°C/10 min.), and incubated on ice for 2 minutes. Then, the sample was loaded in 2% agarose gel (Tab. 12) and run in a 1x TBE buffer (diluted from the 10x TBE buffer) (Tab. 11) at a constant current of 50 mA. The intact total RNA showed sharp, clear 28S and 18S rRNA bands, and the 28S rRNA band was approximately twice as intense as the 18S rRNA band.

Table 10. 2x-concentrated RNA-loading buffer composition

Component	Final concentration	Amount
1M Tris HCl (pH 7.5)	10 mM	0.5 ml
0.5 M EDTA	2.5 mM	2.5 ml
Formamide	90%	45 ml
1% Xylen cyanol	0.01%	0.5 ml
1% Bromophenol blue	0.01%	0.5 ml
DEPC-treated water	-	up to 50 ml

Autoclaved at 121°C, 1 atm., 20 min.

Table 11. 10x TBE buffer composition

Component	Final concentration	Amount
Tris base	0.89 M	108 g
Boric acid	0.89 M	55 g
EDTA	20 mM	7.3 g
MiliQ water	-	up to 1000 ml

Autoclaved (121°C, 1 atm., 20 min.) and stored at room temperature.

Table 12. 2% agarose gel composition

Component	Final concentration	Amount
Agarose	2%	1 g
10x TBE buffer	1x	5 ml
MiliQ water	-	up to 50 ml

To the boiled and cooled mixture (~50°C) ethidium bromide solution was added (0.05 mg/100 ml).

4.1.3. RNA electrophoresis in polyacrylamide gel

RNA electrophoresis was performed using an Owl™ P10DS Dual Gel System (Thermo Fisher Scientific). The RNA sample was run on a denaturing 15% polyacrylamide gel (Tab. 13-14) and poured between clean glasses (immediately after the addition of TEMED and 10% APS). Before loading the sample, a pre-electrophoresis was performed (30 min./300V in 1x TBE buffer). Then, an RNA sample (20 µg) was mixed with one-volume of 2x-concentrated RNA-loading dye (Tab. 10), denatured (70°C/10 min.), incubated on ice for 2 minutes, and loaded onto the gel. Electrophoresis was performed at 300V in the 1x TBE buffer for 4-5 hours.

Table 13. 40% polyacrylamide solution composition

Component	Final concentration	Amount
Acrylamide	38%	38 g
N, N'-methylene-bis-acrylamide	2%	2 g
DEPC-treated water	-	up to 100 ml

Filtered using MILLEX-HP filters (Ø 0.45 µm) and stored at 4°C.

Table 14. 15% denaturing polyacrylamide gel composition

Component	Final concentration	Amount
Urea	8 M	36 g
10x TBE buffer	1x	7.5 ml
40% Polyacrylamide solution	15%	28.125 ml
DEPC-treated water	-	up to 75 ml

Filtered using MILLEX-HP filters (Ø 0.45 µm) and stored at 4°C. Right before pouring the gel between glasses, 32 µl of TEMED and 700 µl of 10% APS solution were added.

4.1.4. RNA transfer from gel to membrane

To transfer the RNA from gel to membrane, six pieces of 3-mm CHR Whatman™ blotting paper (GE Healthcare) and one piece of Amersham Hybond NX nylon membrane (GE Healthcare) were prepared. They were the same size as the gel and were soaked in a 0.5x TBE buffer (diluted from 10x TBE buffer (Tab. 11)) before using. Three pieces of blotting paper were stacked on the anode platform of the transfer cell (Pierce® Fast Semi-Dry Blotter, Thermo Fisher Scientific). Then, the membrane was placed,

and the gel was transferred to the top of the membrane. Afterwards, three more pieces of blotting paper were placed above the gel. All pieces were tightly squeezed to avoid the presence of air bubbles. Then, the cathode platform was assembled, and the transfer was carried out for 1 hour at 10 V. After transfer, the blotting papers and gel were removed, and the membrane with RNA was placed RNA-side-up in the UV-light box (Stratagene® UV, Stratalinker) to covalently attach the RNA to the membrane via UV light energy (120 kJ/cm²).

4.1.5. Radiolabeling of DNA oligonucleotides

To detect mature miRNAs, perfectly complementary DNA oligonucleotides were designed. Then, the 5' end of each oligonucleotide was radiolabeled using a T4 Polynucleotide Kinase (New England BioLabs) in the following reaction:

- 2 µl of DNA oligonucleotide (probe) (10 µM);
- 5 µl of [$\gamma^{32}\text{P}$]-ATP (6000 Ci/mmol);
- 5 µl of T4 Polynucleotide Kinase Buffer;
- 2 µl of T4 Polynucleotide Kinase (10U/µl);
- 36 µl DEPC-treated water.

The reaction mixture was incubated at first at 37°C for 30 minutes and then at 65°C for 20 minutes to inactivate the enzyme. Finally, the unincorporated [$\gamma^{32}\text{P}$]-ATP was removed from the sample using CentriPure N columns (emp Biotech GmbH) according to the manufacturer's protocol. The probe against U6 snRNA (used as a loading control) was radiolabeled in the same manner, with one exception: 2 µl of [$\gamma^{32}\text{P}$]-ATP (6000 Ci/mmol) was used for each sample.

4.1.6. Hybridization of radiolabeled oligonucleotides with RNA

To hybridize the RNA with the probe, the membrane was placed RNA-side-up in a glass hybridization bottle containing 7 ml of a pre-warmed (42°C) hybridization buffer (Tab. 15). The bottle was incubated in a hybridization oven at 42°C for 30 minutes (with rotation). Then, the hybridization buffer was replaced with a fresh portion, and the incubation was repeated. The radiolabeled DNA oligonucleotide was denatured at 85°C for 2 minutes, incubated on ice (2 min.), and added to the bottle containing

the membrane. After overnight incubation at 42°C, the hybridization solution was removed, and the membrane was washed twice for 30 minutes with a washing buffer (Tab. 16-17).

Table 15. Hybridization buffer composition

Component	Final concentration	Amount
10% SDS	3.5%	35 ml
1M Na ₂ HPO ₄	375 mM	37.5 ml
1M NaH ₂ PO ₄	125 mM	12.5 ml
DEPC-treated water	-	up to 100 ml

Filtered using MILLEX-HP filters (Ø 0.45 µm) and stored at room temperature.

Table 16. 20x SSC buffer composition

Component	Final concentration	Amount
NaCl	17.5%	175.3 g
Sodium citrate	8.8%	88.2 g
DEPC-treated water	-	up to 1000 ml

Autoclaved (121°C, 1 atm., 20 min.) and stored at room temperature.

Table 17. Washing buffer composition

Component	Final concentration	Amount
20x SSC buffer	2x	100 ml
10% SDS	1%	10 ml
DEPC-treated water	-	up to 1000 ml

Filtered using MILLEX-HP filters (Ø 0.45 µm) and stored at room temperature.

4.1.7. Hybridization signal detection

Depending on the accumulation level of the analyzed miRNA, exposition lasted from one to seven days. The hybridization signal was visualized via phosphor imaging using a Fluorescent Image Analyzer Image FLA5100 (Fuji Film Inc.). The results were analyzed using Multi Gauge software (ver. 2.4) (Fuji Film Inc.).

4.2 cDNA preparation

4.2.1. RNA isolation for cDNA preparation

The total RNA used for cDNA preparation was isolated using a Direct-zol™ RNA Mini Prep Kit (Zymo Research). To 100 mg of the frozen grinded plant tissue, 1 ml of the TRIzol reagent (Tab. 9) was added. The sample was vortexed, incubated at room temperature for 5 minutes, and centrifuged (15 min./12,000 g/4°C). The extract was transferred into a fresh 2-ml sterile tube (Eppendorf) and again centrifuged (15 min./12,000 g/4°C). This step was repeated third time. Next, the extract was transferred into a fresh 2-ml sterile tube, one-volume of 100% ethanol was added, and the mixed sample was loaded into a column. Afterwards, the RNA was isolated according to the manufacturer's protocol. RNA integrity was checked on 2% agarose gel, and the sample concentration was estimated using a NanoDrop spectrophotometer (as described in 4.1.2.).

4.2.2. Removing genomic DNA contamination from RNA sample

To remove genomic DNA contamination, 40 µg of isolated total RNA was treated with a TURBO DNase (TURBO DNA-free™ Kit, Thermo Fisher Scientific) according to the manufacturer's instructions. As previously, RNA integrity was checked on 2% agarose gel, and the sample concentration was estimated using a NanoDrop spectrophotometer.

4.2.3. First-strand cDNA synthesis for RT-PCR/RT-qPCR analysis

cDNA was synthesized for the following types of RT-PCR/RT-qPCR reactions:

- (1) gene expression analysis: reverse transcription (RT) reactions were prepared from 3 µg of the total DNase-treated RNA using an oligo-dT(18) primer (Thermo Fisher Scientific) and SuperScript III Reverse Transcriptase (Thermo Fisher Scientific), according to the manufacturer's instructions;
- (2) mature miRNA accumulation analysis: cDNA was prepared from 10 ng of the total DNase-treated RNA using a 5x RT miRNA-specific primer (Thermo Fisher Scientific) and MultiScribe™ Reverse Transcriptase (Thermo Fisher Scientific), according to the manufacturer's protocol.

4.2.4. First-strand cDNA synthesis for 5' RLM-RACE PCR and 3' RACE PCR analyses

In order to analyze the 5' ends of the transcripts, a cDNA template was performed from 1 μ g of the total DNase-treated RNA using GeneRacer™ Kit (Thermo Fisher Scientific), according to the manufacturer's instructions. After each step of the cDNA template preparation, RNA integrity was checked on 2% agarose gel (as described in 4.1.2.).

For analysis of the transcript 3' ends, cDNA was prepared from 1 μ g of the total DNase-treated RNA using a SMARTer RACE cDNA Amplification Kit (Clontech), according to the manufacturer's protocol.

5 Methods used during work with deoxyribonucleic acid (DNA)

5.1 Genomic DNA isolation

The genomic DNA used for genetic construct preparation was isolated from grinded plant tissue using a DNeasy Plant Mini Kit (Qiagen) per the manufacturer's instructions.

Genomic DNA for transgenic-line genotyping was isolated from one leaf (collected from a three-week-old plant), placed in a 1.5 ml tube (Eppendorf), and grinded using a plastic stick. Then, 400 μ l of the DNA extraction buffer (Tab. 18) was added, and the sample was vortexed and incubated at room temperature for 30 minutes. Then, it was centrifuged (15 min./14,000 g/22°C), and 300 μ l of the supernatant was transferred into a fresh 1.5-ml tube. The sample was mixed with 300 μ l of isopropanol, incubated at room temperature for 15 minutes, and centrifuged (15 min./14,000 g/22°C). Next, to wash the DNA, 300 μ l of 70% ethanol was added to the pellet, and the sample was centrifuged (5 min./14,000 g/22°C). This step was repeated yet again. Then, the DNA pellet was dried at room temperature and finally dissolved in 40 μ l of MiliQ water.

Table 18. DNA extraction buffer composition

Component	Final concentration	Amount
1M Tris HCl (pH 7.5)	200 mM	10 ml
5M NaCl	250 mM	2.5 ml
0.5M EDTA (pH 8.0)	25 mM	2.5 ml
10% SDS	0.5%	2.5 ml
MiliQ water	-	up to 50 ml

Filtered using MILLEX-HP filters (\varnothing 0.45 μ m) and stored at room temperature.

5.2 PCR reactions

5.2.1. PCR reactions using DreamTaq DNA Polymerase

The DreamTaq DNA Polymerase (Thermo Fisher Scientific) was used in all standard PCR reactions, such as genotyping or colony PCR. The following conditions were applied (Tab. 19-20):

Table 19. DreamTaq DNA Polymerase PCR reaction composition (for each reaction)

Component	Final concentration	Amount
10x DreamTaq buffer (with MgCl ₂)	1x	2 µl
4x 2.5 mM dNTP mix	0.2 mM	1.6 µl
DreamTaq DNA polymerase (5U/µl)	0.025 U/µl	0.1 µl
10 µM Forward primer	0.5 µM	1 µl
10 µM Reverse primer	0.5 µM	1 µl
DNA (template)	~ 20 ng	~ 1 µl
MiliQ water	-	up to 20 µl

NTC (Non-template control) contained water instead of DNA template.

Table 20. DreamTaq DNA Polymerase PCR reaction thermal profile

Step	Temperature	Time	Number of cycles
Initial denaturation	95°C	3 min.	1
Denaturation	95°C	30 sec.	25-35
Annealing	55-60°C	30 sec.	
Elongation	72°C	1 min./1 kb	1
Final elongation	72°C	5-15 min.	

PCR reactions were performed using a PTC-200 Peltier Thermal Cycler (MJ Research) or Veriti Thermal Cycler (Thermo Fisher Scientific). PCR products were checked on 1-1.5% agarose gel.

5.2.2. PCR reactions using Pfu DNA Polymerase

The Pfu DNA Polymerase (Thermo Fisher Scientific), with proofreading activity, was used for the preparation of all genomic constructs to amplify the genes-of-interest. The following conditions were applied (Tab. 21-22):

Table 21. Pfu DNA Polymerase PCR reaction composition (for each reaction)

Component	Final concentration	Amount
10x Pfu buffer (with MgSO ₄)	1x	2 µl
4x 2.5 mM dNTP mix	0.2 mM	1.6 µl
DreamTaq DNA polymerase (5U/µl)	0.05 U/µl	0.2 µl
10 µM Forward primer	0.5 µM	1 µl
10 µM Reverse primer	0.5 µM	1 µl
DNA (template)	50-100 ng	~ 1 µl
MiliQ water	-	up to 20 µl

NTC (Non-template control) contained water instead of DNA template.

Table 22. Pfu DNA Polymerase PCR reaction thermal profile

Step	Temperature	Time	Number of cycles
Initial denaturation	95°C	3 min.	1
Denaturation	95°C	30 sec.	
Annealing	55-60°C	30 sec.	35-40
Elongation	72°C	2 min./1 kb	
Final elongation	72°C	5-15 min.	1

PCR reactions were performed using a PTC-200 Peltier Thermal Cycler or Veriti Thermal Cycler. PCR products were checked on 1-1.5% agarose gel.

5.2.3. Quantitative real-time PCR technique (RT-qPCR)

The RT-qPCR technique was used to analyze the expression levels of pri-miRNAs and target mRNAs as well as the ratio of splicing isoforms and polyadenylation site selection. Moreover, with this approach, the accumulation of mature miRNAs was estimated. All experiments were performed using a 7900HT Fast Real-Time PCR System (Thermo Fisher Scientific) in at least three biological replicates. All of the results were analyzed using SDS 2.4 software (Thermo Fisher Scientific). The error bars were calculated using the SD Function in Microsoft Excel software. The statistical significance of the results presented was estimated using a Student's t-test or ANOVA followed by a Tukey's test (for the analysis of *se-1* and *se-2*) at three significance levels: * $p < 0.05$, ** $p < 0.01$, and *** $p < 0.001$.

5.2.3.1 Gene expression analysis using Power SYBR® Green PCR Master Mix

Standard gene expression analysis (pri-miRNAs, target mRNAs, splicing, and polyadenylation isoforms) was performed with the use of a Power SYBR® Green PCR Master Mix (Thermo Fisher Scientific), which allowed to directly monitor the level of newly synthesized double-stranded DNA (dsDNA). The following RT-qPCR reaction conditions were applied (Tab. 23-24):

Table 23. RT-qPCR reaction composition (for each reaction with total volume of 10 μ l)

Component	Final concentration	Amount
2x Power SYBR® Green PCR Master Mix	1x	5 μ l
0.5 μ M Primer mix (Forward + Reverse)	200 nM (each)	1 μ l
cDNA template	-	1 μ l

NTC (Non-template control) contained water instead of DNA template.

Table 24. RT-qPCR reaction thermal profile

Step	Temperature	Time	Number of cycles
Initial denaturation	95°C	10 min.	1
Denaturation	95°C	15 sec.	40-45
Annealing and extension	60°C	1 min.	
Dissociation curve	95°C	15 sec.	1
	60°C rising to 95 °C	30 min.	1

In each experiment, the dissociation curve was analyzed to exclude the possibility of multiple product amplification. Before the right experiment, the amplification efficiency of each primer pair was calculated by RT-qPCR analysis with the use of a 10-fold dilution series of a cDNA template mix. Next, a linear regression was calculated based on the obtained data (Ct values). Efficiency (E) was estimated from the line slope (“a” value) using the $E=10^{-1/a}$ equation. Only primer pairs with the highest (nearly equal) efficiency (max. difference of 2% was accepted) were used for further experiments.

The expression levels of splicing and polyadenylation isoforms were calculated using the relative quantification ($2^{-\Delta Ct}$), while the fold change values (for pri-miRNA and target mRNA levels) were calculated using the $2^{-\Delta\Delta Ct}$ method. The glyceraldehyde-3-phosphate dehydrogenase (GAPDH, *At1g13440*), Actin2 (*At3g18780*) (both for *A. thaliana* analyses), and HYGROMYCIN (ACI22368) (for *N. benthamiana*) were utilized as reference genes.

5.2.3.2 MiRNA accumulation level analysis using TaqMan® Universal Master Mix II with UNG

To analyze the accumulation level of mature miRNA, RT-qPCR analyses were performed according to the TaqMan® MicroRNA, & Non-coding RNA Assay (Thermo Fisher Scientific). For this purpose, TaqMan® Universal Master Mix II with UNG (Thermo Fisher Scientific), TaqMan® probes, and primers specific for mature miRNAs or the internal reference gene (TaqMan® Small RNA Assay) were used. The following RT-qPCR reaction conditions were applied (Tab. 25-26):

Table 25. RT-qPCR reaction composition (for each reaction with total volume of 20 μ l)

Component	Final concentration	Amount
2x TaqMan® Universal Master Mix II with UNG	1x	10 μ l
20x TaqMan® Small RNA Assay (probe, primers) or Internal Reference Assay	1x	1 μ l
cDNA template	-	1 μ l
MiliQ water	-	up to 20 μ l

NTC (Non-template control) contained water instead of DNA template.

Table 26. RT-qPCR reaction thermal profile

Step	Temperature	Time	Number of cycles
AmpErase® UNG activity	50°C	2 min.	1
Initial denaturation	95°C	10 min.	1
Denaturation	95°C	15 sec.	45-50
Annealing and extension	60°C	1 min.	

For the estimation of the mature miRNA accumulation level, the fold change values were calculated using the $2^{-\Delta\Delta C_t}$ method. U6 snRNA (*At3g14735*) was utilized as reference gene.

5.2.4. Site-directed mutagenesis

Mutagenesis of the identified splice sites was performed using a QuikChange® II Site-Directed Mutagenesis Kit (Agilent Technologies). As a PCR template, 20 ng of plasmid carrying the native gene version were used. Primers introducing mutations were designed using the QuikChange Primer Design online tool (Agilent Technologies). In order to avoid the formation of primer secondary structures, a Q-solution reagent (Qiagen) was used in each mutagenesis reaction. For PCR reaction, the following conditions were applied (Tab. 27-28):

Table 27. QuikChange® II Site-Directed Mutagenesis PCR reaction composition (for each reaction)

Component	Final concentration	Amount
10x Pfu Turbo buffer	1x	5 µl
4x 10 mM dNTP mix	0.2 mM	1 µl
Pfu Turbo DNA polymerase (2.5U/µl)	0.05 U/µl	1 µl
10 µM Forward primer	0.625 µM	1.25 µl
10 µM Reverse primer	0.625 µM	1.25 µl
Plasmid DNA (template)	20 ng	~ 1 µl
Q-solution	-	1 µl
MiliQ water	-	up to 50 µl

NTC (Non-template control) contained water instead of DNA template.

Table 28. QuikChange® II Site-Directed Mutagenesis PCR reaction thermal profile

Step	Temperature	Time	Number of cycles
Initial denaturation	95°C	3 min.	1
Denaturation	95°C	30 sec.	
Annealing	50-55°C	1 min.	27-30
Elongation	68°C	1 min./1 kb	
Final elongation	68°C	5-15 min.	1

PCR reactions were performed using a PTC-200 Peltier Thermal Cycler or Veriti Thermal Cycler. Further steps were performed according to the manufacturer's instructions. The results of mutagenesis were checked by DNA sequencing.

5.2.5. 5' RLM-RACE PCR and 3' RACE PCR analyses

cDNA templates for 5' RLM-RACE PCR and 3' RACE PCR analyses were performed as described above (4.2.4). PCR reactions were performed using an Advantage® 2 Polymerase Mix (Clontech). For the 5' RLM-RACE PCR experiments, reverse gene-specific primers and 5' Gene Racer primers were used ("standard" or "nested" for the first or second PCR round, respectively). PCR reactions were performed according to the following conditions (Tab. 29-32):

Table 29. Composition of 1st round of Advantage® 2 Polymerase-based 5' RLM-RACE PCR reaction (for each reaction)

Component	Final concentration	Amount
10x Advantage 2 PCR buffer	1x	5 µl
4x 10 mM dNTP mix	0.3 mM	1.5 µl
Advantage® 2 Polymerase mix	-	1 µl
10 µM Gene-specific primer	0.3 µM	1.5 µl
10 µM 5' Gene Racer primer	0.9 µM	4.5 µl
cDNA	-	~ 1 µl
MiliQ water	-	up to 50 µl

NTC (Non-template control) contained water instead of DNA template.

Table 30. Thermal profile of 1st round of Advantage® 2 Polymerase-based 5' RLM-RACE PCR reaction

Step	Temperature	Time	Number of cycles
Initial denaturation	94°C	2 min.	1
Denaturation	94°C	30 sec.	5
Elongation	72°C	1 min./1 kb	
Denaturation	94°C	30 sec.	5
Elongation	70°C	1 min./1 kb	
Denaturation	94°C	30 sec.	20-25
Annealing	60-68°C	30 sec.	
Elongation	72°C	1 min./1 kb	
Final elongation	68°C	5-15 min.	1

Table 31. Composition of 2nd round of Advantage® 2 Polymerase-based 5' RLM-RACE PCR reaction (for each reaction)

Component	Final concentration	Amount
10x Advantage 2 PCR buffer	1x	5 µl
4x 10 mM dNTP mix	0.3 mM	1.5 µl
Advantage® 2 Polymerase mix	-	1 µl
10 µM Gene-specific nested primer	0.2 µM	1 µl
10 µM Gene Racer nested primer	0.2 µM	4 µl
PCR mixture from the 1 st round	-	~ 2 µl
MiliQ water	-	up to 50 µl

NTC (Non-template control) contained water instead of DNA template.

Table 32. Thermal profile of 2nd round of Advantage® 2 Polymerase-based 5' RLM-RACE PCR reaction

Step	Temperature	Time	Number of cycles
Initial denaturation	94°C	3 min.	1
Denaturation	94°C	30 sec.	30-35
Annealing	60-68°C	30 sec.	
Elongation	72°C	1 min./1 kb	
Final elongation	72°C	5-15 min.	1

For the 3' RACE PCR experiments, the Forward-gene-specific primers and Universal Primer Mix (UPM), and the following PCR reaction conditions were used (Tab. 33-36):

Table 33. Composition of 1st round of Advantage® 2 Polymerase-based 3' RACE PCR reaction

Component	Final concentration	Amount
10x Advantage 2 PCR buffer	1x	5 µl
4x 10 mM dNTP mix	0.3 mM	1.5 µl
Advantage® 2 Polymerase mix	-	1 µl
10 µM Gene-specific primer	0.2 µM	1 µl
10x UPM	1x	5 µl
cDNA	-	2.5 µl
MiliQ water	-	up to 50 µl

NTC (Non-template control) contained water instead of DNA template.

Table 34. Thermal profile of 1st round of Advantage® 2 Polymerase-based 3' RACE PCR reaction

Step	Temperature	Time	Number of cycles
Initial denaturation	94°C	3 min.	1
Denaturation	94°C	30 sec.	5
Elongation	72°C	1 min./1 kb	
Denaturation	94°C	30 sec.	
Annealing	70°C	30 sec.	5
Elongation	72°C	1 min./1 kb	
Denaturation	94°C	30 sec.	
Annealing	68°C	30 sec.	20
Elongation	72°C	1 min./1 kb	
Final elongation	68°C	5-15 min.	

Table 35. Composition of 2nd round of Advantage® 2 Polymerase-based 3' RACE PCR reaction

Component	Final concentration	Amount
10x Advantage 2 PCR buffer	1x	5 µl
4x 10 mM dNTP mix	0.3 mM	1.5 µl
Advantage® 2 Polymerase mix	-	1 µl
10 µM Gene-specific nested Primer	0.2 µM	1 µl
10x UPM	1x	5 µl
PCR mixture from the 1 st round	-	~ 2 µl
MiliQ water	-	up to 50 µl

NTC (Non-template control) contained water instead of DNA template.

Table 36. Thermal profile of the 2nd round of Advantage® 2 Polymerase-based 3' RACE PCR reaction

Step	Temperature	Time	Number of cycles
Initial denaturation	94°C	3 min.	1
Denaturation	94°C	30 sec.	
Annealing	68°C	30 sec.	30-35
Elongation	72°C	1 min./1 kb	
Final elongation	72°C	5-15 min.	1

All PCR reactions were performed using a PTC-200 Peltier Thermal Cycler or Veriti Thermal Cycler. PCR products were checked on 1.5-2% agarose gel, ligated to the pGEM T-Easy vector (Promega) and next sequenced.

5.3 DNA electrophoresis in agarose gel

To check the PCR products, agarose-gel electrophoresis was applied using a small-gel horizontal system. A DNA sample was mixed with a 2x-concentrated (Tab. 37) or 6x-concentrated (Tab. 38) DNA-loading buffer. Then, the sample was loaded on 1-2% agarose gel (Tab. 12) (depending on PCR product length) and run in a 1x TBE buffer (diluted from the 10x TBE buffer) (Tab. 11) at a constant current of 50 mA.

Table 37. 2x-concentrated DNA-loading buffer composition

Component	Final concentration	Amount
Urea	4 M	12 g
Sucrose	50%	25 g
0.5 M EDTA	50 mM	5 ml
1% Bromophenol blue	0.1%	5 ml
1% Xylen Cyanol	0.1%	5 ml
MiliQ water	-	up to 50 ml

Autoclaved at 121°C, 1 atm., 20 min.

Table 38. 6x-concentrated DNA-loading buffer composition

Component	Final concentration	Amount
1M Tris HCl (pH 7.5)	10 mM	0.5 ml
0.5 M EDTA	25 mM	2.5 ml
100 glycerol	60%	30 ml
1% Xylen Cyanol	0.03%	1.5 ml
1% Orange G	0.15%	7.5 ml
MiliQ water	-	up to 50 ml

Autoclaved at 121°C, 1 atm., 20 min.

The length of the DNA fragments was assessed using a GeneRuler 1 kb Plus DNA Ladder (Thermo Fisher Scientific) or GeneRuler 100 bp Plus DNA Ladder (Thermo Fisher Scientific), suitable for the sizing of double-stranded DNA from 75 to 20,000 bp or from 100 to 3,000 bp, respectively.

5.4 Genetic construct preparation

5.4.1. DNA purification directly from PCR mixture or extraction from agarose gel

After PCR reaction, PCR products were purified directly from the PCR mixture or extracted from the agarose gel using a GeneJET Gel Extraction and DNA Cleanup Micro Kit (Thermo Fisher Scientific) according to the manufacturer's instructions. The DNA concentration was estimated using a NanoDrop spectrophotometer.

5.4.2. Restriction cleavage of DNA

Purified products of the PCR reactions (inserts) and vectors were digested using restriction enzymes (Thermo Fisher Scientific) according to the manufacturer's protocol. The effects of the cleavage were controlled by agarose-gel electrophoresis. Next, inserts were purified from the reaction mixture using a GeneJET Gel Extraction and DNA Cleanup Micro Kit according to the manufacturer's instructions, and the DNA concentration was estimated using a NanoDrop spectrophotometer.

5.4.3. Vector dephosphorylation

To avoid the self-ligation of the used vectors, DNA samples after restriction cleavage of the plasmids were treated with FastAP Thermosensitive Alkaline Phosphatase (Thermo Fisher Scientific) according to the manufacturer's instructions. Samples quality was checked by agarose-gel electrophoresis, and the vectors were purified from the reaction mixture using a GeneJET Gel Extraction and DNA Cleanup Micro Kit. Next, the DNA concentration was estimated using a NanoDrop spectrophotometer.

5.4.4. DNA ligation

For cloning, the purified insert was ligated into the dephosphorylated vector using T4 DNA ligase (Thermo Fisher Scientific) in the following reaction composition (Tab. 39):

Table 39. Standard ligation reaction composition

Component	Final concentration	Amount
Purified DNA insert	5:1 molecular ratio of insert to vector	1-7 μ l
Vector		1 μ l
10x Ligation buffer	1x	1 μ l
T4 DNA ligase (5 U/ μ l)	5U	1 μ l
MiliQ water	-	up to 10 μ l

The reaction was incubated for 3 hours at room temperature and next was used for the transformation of competent *E. coli* cells.

5' RLM RACE PCR and 3' RACE PCR products were directly ligated from the PCR mixture to the pGEM T-Easy vector using a T4 DNA ligase in the following reaction composition (Tab. 40):

Table 40. 5' RLM RACE PCR and 3' RACE PCR products ligation reaction composition

Component	Final concentration	Amount
PCR mixture	-	7 μ l
pGEM T-Easy vector (10 ng/ μ l)	10 ng	1 μ l
10x Ligation buffer	1x	1 μ l
T4 DNA ligase (5 U/ μ l)	5U	1 μ l
MiliQ water	-	up to 10 μ l

The reaction was incubated for 3 hours at room temperature and next was used for the transformation of competent *E. coli* cells.

5.4.5. Plasmid DNA isolation

Plasmid DNA was isolated from the liquid LB bacterial cultures using a GeneJET Plasmid Miniprep Kit (Thermo Fisher Scientific) according to the manufacturer's instructions. The DNA concentration was estimated using a NanoDrop spectrophotometer.

5.4.6. DNA sequencing

DNA sequencing was performed using the Sanger method in the Laboratory of Molecular Biology Techniques at the Faculty of Biology (Adam Mickiewicz University) in Poznan, Poland.

5.4.7. LR clonase reaction

The cloning of inserts from entry (pENTR/D-TOPO) into the destination binary vectors was performed using a Gateway LR Clonase II Enzyme Mix (Thermo Fisher Scientific) according to the manufacturer's protocol. For this purpose, 150 ng of the entry vector and 100 ng of the destination vector were used in each experiment.

5.4.8. Vectors

For cloning and construct preparation, the following vectors were used:

- (1) **pENTR™/D-TOPO®** vector (Thermo Fisher Scientific), used as an entry vector in Gateway® Technology-based cloning (Thermo Fisher Scientific);
- (2) **pMDC32**, modified **pMDC99** (carrying *Atlg77230*, *ACT2*, and *GAPDH* promoters, respectively), and **pMDC123** vectors (Curtis and Grossniklaus, 2003), used as destination vectors in Gateway® Technology-based cloning;
- (3) **pGEM T-Easy** vector (Promega), used for the cloning of 5' RLM-RACE PCR and 3' RACE PCR products.

6 Oligonucleotides

Sequences of all oligonucleotides used in this PhD thesis are presented in the tables below (Tab. 41-45).

Table 41. Primers used for construct preparation

Name	Sequence (5' → 3')	Purpose
F1	ATAAGAATGCGGCCGCGTAGAGAAGATGAAGCTAACGTGG AA	<i>Atlg77230</i> (MIR402) genomic sequence amplification
R1	TTTGGCGCGCCGAGCCCAAAAAAGAGAAATGTA	
F2	CATTAGAGCCCAAGGAGACAAGTTCGCTTTTTTTAACCAGC TG TAGCTAAATAAACCTAAA	Original constitutive 5'SS mutagenesis
R2	TTTAGGGTTTATTTAGCTACAGCTGGTTAAAAAAGCGAAC TTGTCTCCTGGGCTCTAATG	
F3	ATTTAGCTACAGCTGGTTTTGCTCAGCGAACTTGTCTCCT	gt-ca constitutive 5'SS mutagenesis
R3	AGGAGACAAGTTCGCTGAGCAAAACCAGCTGTAGCTAAAT	
F4	TTATTTAGCTACAGCTGGTTTTGGTCAGCGAACTTGTCTCCT TGG	Ggt-Cca constitutive 5'SS mutagenesis
R4	CCAAGGAGACAAGTTCGCTGACCAAAACCAGCTGTAGCTAA ATAA	
F5	GTTTATTTAGCTACAGCTGGTTTTGGACAGCGAACTTGTCTC CTTGGGCT	AGgt-TCca constitutive 5'SS mutagenesis
R5	AGCCCAAGGAGACAAGTTCGCTGTCCAAAACCAGCTGTAGC TAAATAAAC	
F6	GCCTCAGGTTTCATTCATGACATTTCTTGTAATTTTTTAC TTTGTTTATGGAACCTAAGTGAATT	Cryptic 5'SS mutagenesis
R6	AATTCACCTAAGTAGTTCCATAAACAAAGTAAAAAATTAC AAGAAATGTCATGAATGATGAACCTGAGGC	
F7	TCTTGTTTACTCATCGTGATATTGCTCTGTTTTTTGGAAAAT ACCAGGAGGCTCTAGGGAAATGG	Constitutive 3'SS mutagenesis
R7	CCATTTCCCTAGAGCCTCCTGGTATTTTCCAAAAACAAGA GCAATATCACGATGAGTAAACAAGA	

F8	CATCGTGATATTGCTCTTGAAGGAAGGAAAATACTTTTTGC TCTAGGGAAATGGGAAGCTGCTC	Cryptic 3'SS mutagenesis
R8	GAGCAGCTTCCCATTTCCCTAGAGCAAAAAAGTATTTTCCTT CCTTCAAGAGCAATATCACGATG	
F9	ATAAGAATGCGGCCGCGTAGAGAAGATGAAGCTAACGTGG AA	Deletion of pre-miR402 (step 1)
R9	TTAGGTCGTTCTTACTTTTCATCACATCACCAATGTGATCAC A	
F10	GATCACATTGGTGATGTGATGAAAAGTAAGAACGACCTAAA GTGAA	Deletion of pre-miR402 (step 2)
R10	TTTGGCGCGCCGAGCCCAAAAAAGAGAAATGTA	
F11	ATAAGAATGCGGCCGCGTAGAGAAGATGAAGCTAACGTGG AA	Deletion of pre-miR402 (step 3)
R11	TTTGGCGCGCCGAGCCCAAAAAAGAGAAATGTA	
F12	TTTTCAATTGCGTGGTAGATAAGTTTGAGTTGCAT	Insertion of pre-miR402 into 1 st exon
R12	TTTTTCAATTGTTTGATAAAGTTTTTCAGTAGCATAGTAGCA	
F13	ATAAGAATGCGGCCGCGTAGAGAAGATGAAGCTAACGTGG AA	Insertion of pre-miR402 into 2 nd intron (step 1)
R13	ACTCAAACCTTATCTACCACGATTGTACATAAATAAAAAGTAA CAATACAGAAAA	
F14	CTACTGAAAACCTTATCAAATTAGGGTACGATGAATATTCTT CAAG	Insertion of pre-miR402 into 2 nd intron (step 2)
R14	TTTGGCGCGCCGAGCCCAAAAAAGAGAAATGTA	
F15	TACTTTTATTTATGTACAATCGTGGTAGATAAGTTTGAGTTG CAT	Insertion of pre-miR402 into 2 nd intron (step 3)
R15	GAATATTCATCGTACCCTAATTTGATAAAGTTTTTCAGTAGCA TAGTAGCA	
F16	TACTTTTATTTATGTACAATCGTGGTAGATAAGTTTGAGTTG CAT	Insertion of pre-miR402 into 2 nd intron (step 4)
R16	TTTGGCGCGCCGAGCCCAAAAAAGAGAAATGTA	
F17	ATAAGAATGCGGCCGCGTAGAGAAGATGAAGCTAACGTGG AA	Insertion of pre-miR402 into 2 nd intron (step 5)
R17	TTTGGCGCGCCGAGCCCAAAAAAGAGAAATGTA	
F18	GGCCAGTGCCAAGCTTGCATTGTATTGCCTTGTACAGTTC	Insertion of the <i>Atlg77230</i> promoter region to the pMDC99
R18	GCAGGCATGCAAGCTTTCTGTTCTTCGCTCCATGAA	
F19	TTAAGCTTGCTTCATCACCTTCCCACAT	Insertion of the <i>ACT2</i> promoter region to the pMDC99 vector
R19	TTAAGCTTTTTATGGGTGGATTGTGGTG	
F20	TTAAGCTTAGCTTGAATCTCCCTCGTGA	Insertion of the <i>GAPDH</i> promoter region to the pMDC99 vector
R20	TTGGCGCGCCTTTGCGAAATTGAGATCGAGAGAG	
F21	CTGGCAGTTCCTACTCTCG	Colony PCR (pENTR/dTOPO-based constructs)
R21	GCTGCCAGGAAACAGCTATG	
F22	TTGGAGAGGACCTCGACTCT	Colony PCR (pMDC32- based constructs)
F23	GATCCAAGCTCAAGCTGCTC	
R23	TTTATGCTTCCGGCTCGTAT	Colony PCR (pMDC99- based constructs)

F24	ATAAGAATGCGGCCGCAATCTTTGAACTTCATCAGAATTGC	<i>At5g41663(MIR319b)</i> genomic sequence amplification
R24	TTTGGCGCGCCTTACAAATAAGTCATCTTTTATTGAGCG	
F25	GTGGAGGAAGAGAGCTTTCTTCGGTCAGGTTATGGAGTAAT ATGTGAGATTTAATTGA	miR319b* mutagenesis
R25	TCAATTAATCTCACATATTACTCCATAACCTGACCGAAGA AAGCTCTCTTCCCTCCAC	
F26	GAGACAAATTGAGTCTTCACTTCTCTATGCTCACCTGGAAG GGAGCTCCCTATTTTTATCTTTCTCAG	miR319b mutagenesis
R26	CTGAGAAAGATAAAAAATAGGGAGCTCCCTTCCAGGTGAGC ATAGAGAAGTGAAGACTCAATTTGTCTC	
F27	GTAATATGTGAGATTTAATTGACTCTCGACTCATTAAGTAA AATACCAAATGAAAGAATTTGTTCTCATATGGTA	miR319b.2* mutagenesis
R27	TACCATATGAGAACAAATCTTTTCAATTTGGTATTTTACTTAA TGAGTCGAGAGTCAATTAATCTCACATATTAC	
F28	CATTCATCCAAATACCAAATGAAAGAATTTGTTCTCATATG GTAAATGCTACTTAGATGCGAGAGACAAATGAGTCTTCAC T	miR319b.2 mutagenesis
R28	AGTGAAGACTCAATTTGTCTCTCGCATCTAAGTAGCATTAC CATATGAGAACAAATCTTTTCAATTTGGTATTTGGATGAATG AATGAGTCTTCACTTCTCTATGCATTTTTATCTTTCTCAGAG TACCA	
F29	TGGTACTCTGAGAAAGATAAAAATGCATAGAGAAGTGAAG ACTCAATT	miR319b* deletion
R29	GATGTTGAGTTGGTGGAGGAAGATGGAGTAATATGTGAGAT TTA	
F30	TAAATCTCACATATTACTCCATCTTCTCCACCAACTCAACA TC	miR319b deletion
R30	GAATTTGTTCTCATATGGTAAATGATTGAGTCTTCACTTCTC TATGCT	
F31	AGCATAGAGAAGTGAAGACTCAATCATTACCATATGAGAA CAAATTC	miR319b.2* deletion
R31	GTCCACTCATGGAGTAATATGTGAGATTTAATTAATACCAA ATGAAAGAATTTG	
F32	CAAATCTTTTCAATTTGGTATTAATTAATCTCACATATTACT CCATGAGTGGAC	miR319b.2 deletion
R32		
F33	GTTTTCCAGTCACGACGTT	Colony PCR of pMDC123-based constructs

Table 42. Primers used for PCR, RT-PCR, and RT-qPCR analyses

Name	Sequence (5' → 3')	Purpose
F34	TTGGTGACAACAGGTCAAGCA	3' <i>GAPDH</i> (reference gene) (RT-qPCR)
R34	AAACTTGTCGCTCAATGCAATC	
F35	GGTAACATTGTGCTCAGTGG	<i>ACTIN2</i> (reference gene) (RT-PCR and RT-qPCR)
R35	CTCGGCCTTGGAGATCCACA	
F36	ATTTGCGCTCCAACAATGTC	<i>HYGROMYCIN</i> (reference gene) (RT-qPCR)
R36	GATGTTGGCGACCTCGTATT	

F37	TGAGTTGCATAGTGGCAGTCTT	Pri-miR402 amplification (RT-qPCR)
R37	TGAAAGATGAATCTGCTGTTGG	
F38	AGGTTGGAGGGAATCATCCTC	FS of <i>Atlg77230</i> 1 st intron in <i>A. thaliana</i> (RT-qPCR)
R38	TGGTATTTTCCTTCCTCAGCG	
F39	AGGAGTTAGCATCACGTTGTTGT	IR of <i>Atlg77230</i> 1 st intron in <i>A. thaliana</i> (RT-qPCR)
R39	AATAGGCCTCGAATCATGAAAAT	
F40	GAAACTCGCAGAGTCCATTAGAG	FS of <i>Atlg77230</i> 1 st intron in <i>N. benthamiana</i> (RT-qPCR)
R40	ATGCATCACCAAGCTCAAGTAAC	
F41	AGGAGTTAGCATCACGTTGTTGT	IR of <i>Atlg77230</i> 1 st intron in <i>N. benthamiana</i> (RT-qPCR)
R41	AATAGGCCTCGAATCATGAAAAT	
F42	TTAATCTTGTTCCCGAAGATGC	FS of <i>Atlg77230</i> 2 nd intron (RT-qPCR)
R42	CCCACGATGGATCTATCTCAGT	
F43	GCGTGAAGCTTTTCTGTATTGTT	IR of <i>Atlg77230</i> 2 nd intron (RT-qPCR)
R43	GTGACGAAAACCATAGGAACTGT	
F44	GCATTATTGATCAATGCGGAT	FS of <i>Atlg77230</i> 4 th intron (RT-qPCR)
R44	TGATGTCTGAAGCTGTTCTCTCTT	
F45	GGACTACTCTTGGAAGAGCACAA	IR of <i>Atlg77230</i> 4 th intron (RT-qPCR)
R45	TTTCGTGAAACTCACATTGATCA	
F46	GGAACAAGAACCCTAAGAAACGA	<i>Atlg77230</i> proximal polyA (RT-qPCR)
R46	GATCGGTAGTTTGTCTACGATCAA	
F47	TGGGAAGCTGCTCTTAATCTTG	<i>Atlg77230</i> distal polyAs (RT-qPCR)
R47	GTTGCAGCTTTGAGTGCTTTC	
F48	CGCAGAGTCCATTAGAGCCC	All <i>MIR402</i> transcripts (stability assay) (RT-qPCR)
R48	GCTAACTCCTTCCGATGAACCA	
F49	GTTTTATCTTGTTTACTCATCGTGATATTGC	<i>MIR402</i> transcripts ended at distal polyA sites (stability assay) (RT-qPCR)
R49	GAGCAGCTTCCCATTTCCT	
F50	TTCAAGATGATATTCGCAACG	<i>DML3</i> expression level (RT-qPCR)
R50	TTCTGGTTTCTTCCGTCTTC	
F51	AAAAGTTTCCCTTGATCCTTCG	<i>THI4</i> expression level (RT-qPCR)
R51	CATTACGAATGAACGGATACGA	
F52	CGGCATACGTCAGAAAGGG	FS of <i>At5g21100</i> 1 st intron (RT-qPCR)
R52	TCGACAATGAACTTGTAAGTAAAG	
F53	GGAGACACGGTCATTATCCAC	IR of <i>At5g21100</i> 1 st intron (RT-qPCR)
R53	AATTTAGAGTTTATTGAATAACCTGACGTA	

F54	GGAAAGTCATGCCCTTCATC	FS of <i>At1g18880</i> 1 st intron (RT-qPCR)
R54	TTGTGCCACCGTAGATGTTG	
F55	ACAGAGGATGGAAAGTCATGC	IR of <i>At1g18880</i> 1 st intron (RT-qPCR)
R55	TGAAACGAACAAGAACTGATGA	
F56	TCAGTAGGGAGAGTGGATGATG	FS of <i>At3g60960</i> 1 st intron (RT-qPCR)
R56	GAATCTCTGCCTCCGCAAT	
F57	CATCAAGCCCCATAAGTTGG	IR of <i>At3g60960</i> 1 st intron (RT-qPCR)
R57	TCCTTCAGTTCGGTTTTAGCA	
F58	GAAGTCCAGCTGCCAGAAAC	<i>bar</i> gene amplification (PCR)
R58	AGGCACAGGGCTTCAAGAG	
F59	ATGTTGAGTTGGTGGAGGAAG	Pri-miR319b amplification (RT-qPCR)
R59	AAATGTGGTACTCTGAGAAAGATAAAAAT	
F60	GTCACCGGAATTTGGAAAGA	<i>TCP3</i> expression level (RT-qPCR)
R60	GGATCAAACCAAGCACGAAT	
F61	GTTTCTGTTCGCTCCTCTACTC	<i>TCP4</i> expression level (RT-qPCR)
R61	ATGGGACTGTAAGTGGACTGAAG	
F62	GGGTACCCTTCAGTCCAGTTTAT	<i>TCP10</i> expression level (RT-qPCR)
R62	CCATACTGTGATGATGAAGCAA	
F63	CCTTCAGTCCAATTCACAATCTC	<i>TCP24</i> expression level (RT-qPCR)
R63	GTGTAGCCATGAAAAGGAAATG	
F64	GTTTCCTTGACACATGTTTTTCG	<i>TBL10</i> expression level (RT-qPCR)
R64	TGAAGCAAGTAGAGGAACTTTGC	
F65	ATCCAGTTTCATGTAAATAAG	<i>RAP2.12</i> IR expression level (RT-qPCR)
R65	ACCACAACCCCTAAAAATAAG	

Table 43. Primers used for 5' RLM-RACE PCR analysis

Name	Sequence (5' → 3')	Purpose
5RLM_1	GAGAGTGAGCACGCAAAAGCAACCA	Analysis of 5' ends of pri-miR156d
5RLM_1N	GAGTGAGCACGCAAAAGCAACCATA	
5RLM_2	AGGGAGAGGGAGAGAAGGGGGTGAC	Analysis of 5' ends of pri-miR156f
5RLM_2N	GAGGGAGAGAAGGGGGTGACGATA	
5RLM_3	GATACAAGAGGCAACGCTGGATGC	Analysis of 5' ends of pri-miR162a
5RLM_3N	GCTGCCTCCAGCGACTCTCACTCTT	
5RLM_4	AATCCATTCATGAGATTATCATAAGTCACTTCG	Analysis of 5' ends of pri-miR400
5RLM_4N	AAGTCACTTCGTTTGAGAAACAACACTTTGCTT	
5RLM_5	CGGATCATCCAATGAAAGATGAATCTGC	Analysis of 5' ends of pri-miR402
5RLM_5N	TGAATCTGCTGTTGGAAATTGAGGCAAG	
5RLM_6	GGAAATTCACGAGATAAAGAGAACAAAAG	Analysis of 5' ends of pri-miR420
5RLM_6N	GTGTAGTATCCAATTTTTGCATTTCCGTG	

5RLM_7	ACCGCCTGGTTTGGTCTATGTACACCG	Analysis of 5' ends of pri-miR778
5RLM_7N	CCTCAACCCTAGGCACATGTCCCAAAT	
5RLM_8	GGTGCAGCGTTTCTTAAAGATGTTGATGG	Analysis of 5' ends of pri-miR833
5RLM_8N	ACTCCTCCGTTTGTTCACGATCACC	
5RLM_9	CAAGTATAAAGTCCTCATGTTTTTCCATCAG	Analysis of 5' ends of pri-miR837
5RLM_9N	CATAATTTTGAAACGAACAAGAACTGATG	
5RLM_10	TCCTTCTGCAACACCACAGGTGAC	Analysis of 5' ends of pri-miR838
5RLM_10N	GCCTCAATAACCTCAGGTTGTGCAAGAAG	
5RLM_11	CTCCCGCAACCATTGAGCTTCCAATC	Analysis of 5' ends of pri-miR842
5RLM_11N	AATGAAACCGGATGTGGCATCATCGT	
5RLM_12	GCCCAATGCGTAGAAGAGACCACTCA	Analysis of 5' ends of pri-miR844
5RLM_12N	TGCGTAGAAGAGACCACTCACCTCAA	
5RLM_13	GTGGTTGCGACGAAATGAAAGAAGGA	Analysis of 5' ends of pri-miR848
5RLM_13N	TGCGACGAAATGAAAGAAGGATGTGA	
5RLM_14	CGTGCTTTGTTGTAGTCCGGATCTTAGC	Analysis of 5' ends of pri-miR850
5RLM_14N	TTGTTGTAGTCCGGATCTTAGCTGACAGG	
5RLM_15	GCTCTGAGCTTTGAGCTTTGTTTCAGCA	Analysis of 5' ends of pri-miR852
5RLM_15N	CTGAGCTTTGAGCTTTGTTTCAGCA	
5RLM_16	CTTCCGGTTGCAGAGGCCAAGTAA	Analysis of 5' ends of pri-miR853
5RLM_16N	TCCAAGCTAAAGAGGGGAGCAGCAG	
5RLM_17	AGCACATGCTCGACCTATTGGAAA	Analysis of 5' ends of pri-miR862
5RLM_17N	GCACATGCTCGACCTATTGGAAA	
5RLM_18	TGGGAATTTCTTTTGGTCATATGGGGTGA	Analysis of 5' ends of pri-miR1886
5RLM_18N	GCATCGTCTACATGAAATTTCCAATCAAAG	
5RLM_19	ATAAAAGCTCTTTCTTCACAAATC	Analysis of 5' ends of pri-miR1888a
5RLM_19N	ATAAAAGCTCTTTCTTCACAAATC	
5RLM_20	GCCAAATCTTAATCTAAGATTGGGAAGA	Analysis of 5' ends of pri-miR1888b
5RLM_20N	ATCTTAGCCTAAGAATTTGGGTAAGATACCA	
5RLM_21	CTGAGCACCTCTATTGGTTTGTTCCTG	Analysis of 5' ends of pri-miR2112
5RLM_21N	GATGATGCGCAAATGCGGATATAAAGGTA	
5RLM_22	CGACTCGTTTCTATTTGTGGATTTGCTGA	Analysis of 5' ends of pri-miR3434
5RLM_22N	GAGAGACCAATGATCTGACTTTAGGAAGCC	
5RLM_23	TTTAGTGTACAGATGTAAGTGTACGCTGTG	Analysis of 5' ends of pri-miR5014
5RLM_23N	TGTTGTACAAAATAAGTGTACGAATCAAAT	
5RLM_24	ACCGTCGATCTTCGGTTCAATATCC	Analysis of 5' ends of pri-miR5024
5RLM_24N	CCGTCGATCTTCGGTTCAATATCC	
5RLM_25	ACCACGTGTCACGATCTTATGAGTTACTA	Analysis of 5' ends of pri-miR5026
5RLM_25N	TGCCACGAGTTAAATTTATCGATCTCAG	
5RLM_26	TGTTTTTGTTCGGGCTCAAGCCTA	Analysis of 5' ends of pri-miR5632
5RLM_26N	TGTTTTTCGGGCTCAAGCCTAGTTG	
5RLM_27	CCAATGGTAATGTGATGAGACCCAAA	Analysis of 5' ends of pri-miR5640
5RLM_27N	TTGGTTTTGCAAGAACAGCCAATAA	
5RLM_28	ACACATGCAAATAGTTTGTTCGAAT	Analysis of 5' ends of pri-miR5650
5RLM_28N	ACACATGCAAATAGTTTGTTCGAAT	

5RLM_29	AACGACATGGGCCAAAAGGTATCG	Analysis of 5' ends of pri-miR5656
5RLM_29N	CATGGGCCAAAAGGTATCGGAAA	
5RLM_univ	CGACTGGAGCACGAGGACACTGA	Universal primers used for 5' RLM-RACE PCR analysis
5RLM_univN	GGACACTGACATGGACTGAAGGAGTA	
F_M13	CGCCAGGGTTTTCCAGTCACGAC	Colony PCR of pGEM T-Easy-based constructs
R_M13	TCACACAGGAAACAGCTATGAC	

Table 44. Primers used for 3' RACE PCR analysis

Name	Sequence (5' → 3')	Purpose
3RACE_402	ATCGAATTTCCCGGATCTTCCTTTCG	Analysis of 3' ends of <i>MIR402</i> transcripts
3RACE_402N	CGAATTTCCCGGATCTTCCTTTCGAG	

Table 45. DNA oligonucleotides used as probes in Northern blot experiments

Name	Sequence (5' → 3')
p156d	GTGCTCACTCTCTTCTGTCA
p156f	GTGCTCACTCTCTTCTGTCA
p162a	CTGGATGCAGAGGTTTATCGA
p400	GTGACTTATAATACTCTCATA
p402	CAGAGGTTTAATAGGCTCGAA
p420	TGCATTCCGTGATTAGTTTA
p778	CGGTGTACATAAACCAAGCCA
p833	ACTAGACCGAGTACAACAAACA
p837-3p	CCATCAGTTTTTTGTTCGTTT
p838	TGTGCAAGAAGTAGAAGAAAA
p842	GGATGACGGATCTGACCATGA
p844	AGCTTATAAGCAATCTTACCA
p848	TAGCTTAGGCAGTCCCATGTCA
p850	CTTTGTTGTAGTCCGGATCTTA
p852	CAGAACTAAGGCGTTATCTT
p853	CTTCTCCAAGCTAAAGAGGGGA
p862	CTTCAAGTAGATCCAGCATAT
p1886	GATTCATCTCACTTCTCTCA
p1888a	TTCTTCACAAATCTTAACTTA
p1888b	TCTTCACAAATCTTAGCCTAA
p2112	ACATTGATATCCGCATTTGCG
p3434	AATAATAGAATCAGCCAAGT
p5014	ATGTTGTACAAAATAAGTGT
p5024	TGTTATATCTTGGCCTTGTCAT
p5026	ACGTGTCACGATCTTATGAGT
p5632	CTTATCCAATAATAATCCAA
p5640	TGAATCTAATTCCTTCTCTCA

p5650	TGTATCTAAGATCCAAAACAA
p5656	AAACCCAATCTCTACTTCAGT
pU6	TCATCCTTGCGCAGGGGCCA

7 Bioinformatic tools and databases

7.1 Programs

The following programs were used for the design, preparation, and analysis of the results from the presented experiments:

- (1) **The BLASTN tool** (Altschul et al., 1990), used to compare nucleotide sequence similarity between sequences-of-interest and deposited data concerning analyzed organisms - *A. thaliana* or *N. benthamiana*
(https://blast.ncbi.nlm.nih.gov/Blast.cgi?PROGRAM=blastn&PAGE_TYPE=BlastSearch&BLAST_SPEC=&LINK_LOC=blasttab&LAST_PAGE=blastn);
- (2) **The Folder ver. 1.11** (algorithm: RNAfold) (Hansen, 2007), used for the prediction of miRNA stem-loop secondary structures, and calculation of their stability parameters;
- (3) **The MultiGauge ver. 2.0** program (Fuji Film Inc.), used for processing and analyzing Northern blot results;
- (4) **The Primer3** program (Koressaar and Remm, 2007; Untergasser et al., 2012), used for general primer design (bioinfo.ut.ee/primer3-0.4.0/);
- (5) **The QuikChange® Primer Design** program (Agilent Technologies), used for designing primers for mutagenesis
(<http://www.genomics.agilent.com/primerDesignProgram.jsp>);
- (6) **The SDS2.4** program (Thermo Fisher Scientific), used to design experiments and analyze the RT-qPCR results.

7.2 Databases

The following databases were used:

- (1) **The ARAPORT** (Cheng et al., 2016) – used to combine information concerning the *Arabidopsis thaliana* Col-0 reference genome sequence and its associated annotation; i.e., gene structure, gene expression levels, protein functions, and interaction networks (<http://www.araport.org>);
- (2) **The miRBase** (Kozomara and Griffiths-Jones, 2014) - used to collect all known pre-miRNAs and mature miRNAs (predicted and experimentally confirmed) identified in various organisms (<http://www.mirbase.org>);
- (3) **The MIREX2** (Zielezinski et al., 2015) – used to allow for the comparative analysis of pri-miRNA expression levels and accumulation of mature miRNAs in different tissues of wild-type plants (*A. thaliana*, *H. vulgare* and *P. endivifolia*) as well as in *A. thaliana* miRNA biogenesis mutants (<http://www.combio.pl/mirex2>);
- (4) **The NCBI** (Geer et al., 2010) - used to provide open access to biomedical and genomic information (<http://www.ncbi.nlm.nih.gov>);
- (5) **The PLACE** (Higo et al., 1998) – used to collect information about plant cis-acting regulatory DNA elements (<https://sogo.dna.affrc.go.jp>);
- (6) **The TAIR** (Lamesch et al., 2011) – used to collect genetic and molecular biology information and data concerning *A. thaliana* (<http://www.arabidopsis.org>);
- (7) **The UniProtKB** (The UniProt Consortium, 2015) - used to collect information about proteins (<http://www.uniprot.org/help/uniprotkb>).

RESULTS

1 Biogenesis of intronic miRNAs in *Arabidopsis thaliana*

As previously mentioned, there are 29 identified intronic miRNAs in *Arabidopsis thaliana* (Tab. 3) (Hirsch et al., 2006; Brown et al., 2008; Yan et al., 2012; Jia and Rock, 2013; Zielezinski et al., 2015). Among them, 26 miRNAs are located within the introns of the protein-coding host genes. Three other miRNAs (miR842, miR850, and miR5026) are embedded in the introns of other non-coding RNAs. The knowledge concerning the mechanism of intronic miRNA biogenesis in plants is still incomplete. In this part of the presented PhD thesis, results concerning the effects of crosstalk between the microprocessor complex, spliceosome, and polyadenylation machinery on intronic miRNA maturation in *Arabidopsis thaliana* are presented.

1.1 Characterization of Arabidopsis intronic miRNAs

At the beginning, to select the best miRNA for further studies, the accumulation of all intronic miRNAs was checked in three developmental stages of *A. thaliana* wild-type plants. For this purpose, Northern blot technique was used. Sequences of all used probes against mature miRNAs are listed in Table 45. Plant material was collected from 10-day-old seedlings, 35-day-old rosette leaves, and 53-day-old inflorescences. In 10-day-old Arabidopsis seedlings, five miRNAs (miR156d, miR156f, miR162a, miR400, and miR850) were detected using the Northern technique (Fig. 28A). The accumulation of six miRNAs (miR156d, miR156f, miR162a, miR400, miR402, and miR778) was detected in the rosette leaves (Fig. 28B), while only three miRNAs were detected in the inflorescences (miR156d, miR156f, and miR162a) (Fig. 28C). The obtained results indicated that intronic miRNAs in Arabidopsis accumulate at very low levels, often undetectable using the standard Northern blot approach (since only 7 out of 29 intronic miRNAs were detected under the conditions tested).

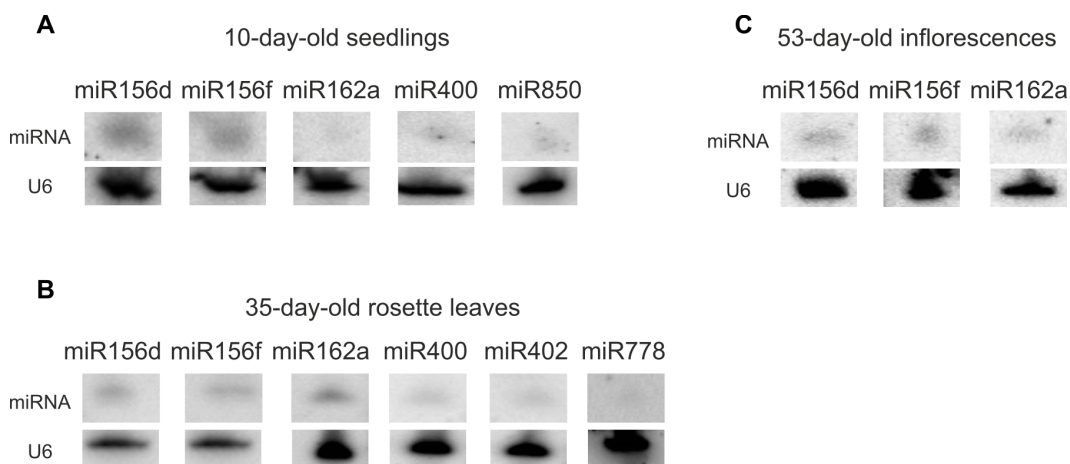


Figure 28. Northern blot analysis of the accumulation of selected mature intronic miRNAs in three developmental stages of *A. thaliana* wild-type plants: (A) 10-day-old seedlings; (B) 35-day-old rosette leaves; and (C) 53-day-old inflorescences. U6 was used as RNA loading control.

It was believed that intronic pri-miRNAs are the same transcripts as their host pre-mRNAs. Thus, the 5' RLM RACE PCR technique was applied to test this hypothesis for all Arabidopsis intronic miRNA precursors. The cDNA template was prepared from the total RNA isolated from wild-type 35-day-old rosette leaves. For each pri-miRNA, two primer sets were designed, located within the miRNA stem-loop structure (“standard” for the first PCR reaction and “nested” for the second) (Tab. 43). Finally, the sequences amplified during this experiment were aligned to the *TAIR10* database (Lamesch et al., 2011). For 25 pri-miRNAs, specific PCR products were obtained, while for the 4 other examples, only unspecific products were amplified. For the majority of analyzed pri-miRNAs, the identified transcription start sites (TSSs) were consistent with the TSSs described for their host pre-mRNAs. What is interesting, for several intronic pri-miRNA, the established 5' ends of the transcripts differed slightly from previously annotated host 5' UTR sequences (Geer et al., 2010; Lamesch et al., 2011). For the four examples (pri-miR850, pri-miR848, pri-miR5026, and pri-miR5656), the presence and activity of alternative TSSs were detected. All these results are presented in the table below (Tab. 46). Summing up, these observations suggested that Arabidopsis intronic pri-miRNAs are mostly transcribed as the same transcription units as their host pre-mRNAs. However, there are also several examples that can be independently transcribed.

Table 46. Identified transcription start sites of intronic pri-miRNAs in *A. thaliana*

No.	MiRNA	Host gene	Number of identified TSSs	Comments
1	miR156d	<i>At5g10946</i>	1	Consistent with host gene pre-mRNA TSS
2	miR156f	<i>At5g26146</i>	0	Unspecific amplification
3	miR162a	<i>At5g08185</i>	1	Consistent with host gene pre-mRNA TSS
4	miR400	<i>At1g32583</i>	1	11 bp upstream from host gene pre-mRNA TSS
5	miR402	<i>At1g77230</i>	1	Consistent with host gene pre-mRNA TSS
6	miR420	<i>At5g62850</i>	1	200 bp upstream from host gene pre-mRNA TSS
7	miR778	<i>At2g41620</i>	1	Consistent with host gene pre-mRNA TSS
8	miR833	<i>At1g78476</i>	1	Consistent with host gene pre-mRNA TSS
9	miR837	<i>At1g18880</i>	1	Consistent with host gene pre-mRNA TSS
10	miR838	<i>At1g01040</i>	1	12 bp upstream from host gene pre-mRNA TSS
11	miR842	<i>At1g61224</i>	0	Unspecific amplification
12	miR844	<i>At2g23348</i>	1	18 bp upstream from host gene pre-mRNA TSS
13	miR848	<i>At5g13890</i>	2	1 – consistent with host gene pre-mRNA TSS; 2 – 55 bp upstream from host gene pre-mRNA TSS
14	miR850	<i>At4g13495</i>	several	1 - 9 bp upstream from host gene pre-mRNA TSS; others – in the pre-miRNA-hosting intron
15	miR852	<i>At4g14500</i>	1	Consistent with host gene pre-mRNA TSS
16	miR853	<i>At3g23325</i>	1	Consistent with host gene pre-mRNA TSS
17	miR862	<i>At2g25170</i>	1	Consistent with host gene pre-mRNA TSS
18	miR1886	<i>At2g37160</i>	1	Consistent with host gene pre-mRNA TSS
19	miR1888a	<i>At5g21100</i>	1	Consistent with host gene pre-mRNA TSS
20	miR1888b	<i>At3g60960</i>	1	14 bp upstream from host gene pre-mRNA TSS
21	miR2112	<i>At1g01650</i>	1	21 bp upstream from host gene pre-mRNA TSS
22	miR3434	<i>At5g22770</i>	1	60 bp upstream from host gene pre-mRNA TSS
23	miR5014	<i>At1g65960</i>	1	100 bp downstream from host gene pre-mRNA TSS
24	miR5024	<i>At1g44100</i>	0	Unspecific amplification
25	miR5026	<i>At4g13495</i>	several	1 - 9 bp upstream from host gene pre-mRNA TSS; others – in the pre-miRNA-hosting intron
26	miR5632	<i>At2g19390</i>	1	Consistent with host gene pre-mRNA TSS
27	miR5640	<i>At1g05570</i>	0	Unspecific amplification
28	miR5650	<i>At2g48140</i>	1	Consistent with host gene pre-mRNA TSS
29	miR5656	<i>At1g05780</i>	2	1 – 30 bp upstream and 2 – 21 bp downstream from host gene pre-mRNA TSS

Based on the obtained results, miR402 was selected for further studies. The following criteria were taken into account during the selection of this miRNA:

- pri-miR402 is transcribed as the same transcription unit as its host pre-mRNA (Tab. 46);
- miR402 belongs to a single-gene family (there is no possible cross-detection of any other Arabidopsis miRNA);
- miR402 accumulation was detectable using the Northern blot approach (Fig. 28);
- the promoter region of miR402 host gene (*At1g77230*) is rich in many stress-responsive elements (identified by using the PLACE database (Higo et al., 1998));
- miR402 was described as abiotic stress-responsive miRNA (Sunkar and Zhu, 2004; Zhou et al., 2008; Kim et al., 2010; Barciszewska-Pacak et al., 2015);
- miR402 plays an important role during Arabidopsis seed germination (Kim et al., 2010).

Pre-miR402 is located within the first intron of the *At1g77230* host gene (Fig. 29). This gene encodes the uncharacterized protein rich in TPR (Tetratricopeptide Repeat) repeats.



Figure 29. Schematic structure of the *At1g77230* carrying pre-miR402 within its first intron. Boxes – exons (protein-coding sequence – gray, UTRs – white); lines – introns; red and blue lines – miRNA and miRNA*, respectively.

The highest expression level of the miR402 host gene was detected in seeds (Hruz et al., 2008). This can be connected with the role of miR402 in seed germination via targeting the *At4g34060* (DEMETER-LIKE 3 (*DML3*)) mRNA (Kim et al., 2010) (Fig. 30). The *At4g34060* gene encodes the DNA glycosylase involved in the demethylation of 5-methylcytosines with preferences for CpG and CpNpG sequences (Ortega-Galisteo et al., 2008). Thus, it is an important enzyme required for maintaining DNA methylation marks, also of genes involved in the regulation of seed viability and germination (Kim et al., 2010). It has been shown that a higher accumulation of miR402 resulted in improved Arabidopsis seed germination. This is probably due to the more-efficient cleavage of the *DML3* mRNA by miR402 that, in turn, maintains the DNA methylation of the genes identified as negative regulators of seed germination.

Moreover, there is no available null Arabidopsis mutant of *At1g77230*. There is high probability that the lack of expression of this gene along with the deficient production of mature miR402 blocks the germination of homozygous mutant seeds via the lower DNA methylation level of genes involved in the negative regulation of the germination process.



Figure 30. Schematic structure of the *At4g34060* (*DML3*) encoding target mRNA of miR402. Boxes – exons (protein-coding sequence –gray, UTRs – white) horizontal lines – introns; vertical line – miR402 cleavage site. The full-length *DML3* gene consists of 20 exons (a shortened version is presented here).

1.2 Analysis of miR402 biogenesis in selected abiotic stresses

Since it was reported, that miR402 is a multi-stress-responsive miRNA, the mechanism of its biogenesis was tested under selected abiotic stress conditions. At first, heat stress was applied. 14-day-old *A. thaliana* seedlings were treated with a high temperature (37°C). Plant material was collected after 0.5, 2, 6, and 12 hours of stress, while the control plants were collected at time point “0.” Then, the levels of pri-miR402 and mature miR402 were analyzed using RT-qPCR and Northern blot, respectively. The increased expression level of pri-miRNA was observed after at least two hours of stress treatment, which correlated with the upregulation of mature miR402 (Fig. 31A-B). Since the level of miR402 was barely detectable in Northern hybridization, an additional RT-qPCR analysis was performed to examine mature miRNA accumulation, which confirmed the observations from the Northern blot experiment (Fig. 31C).

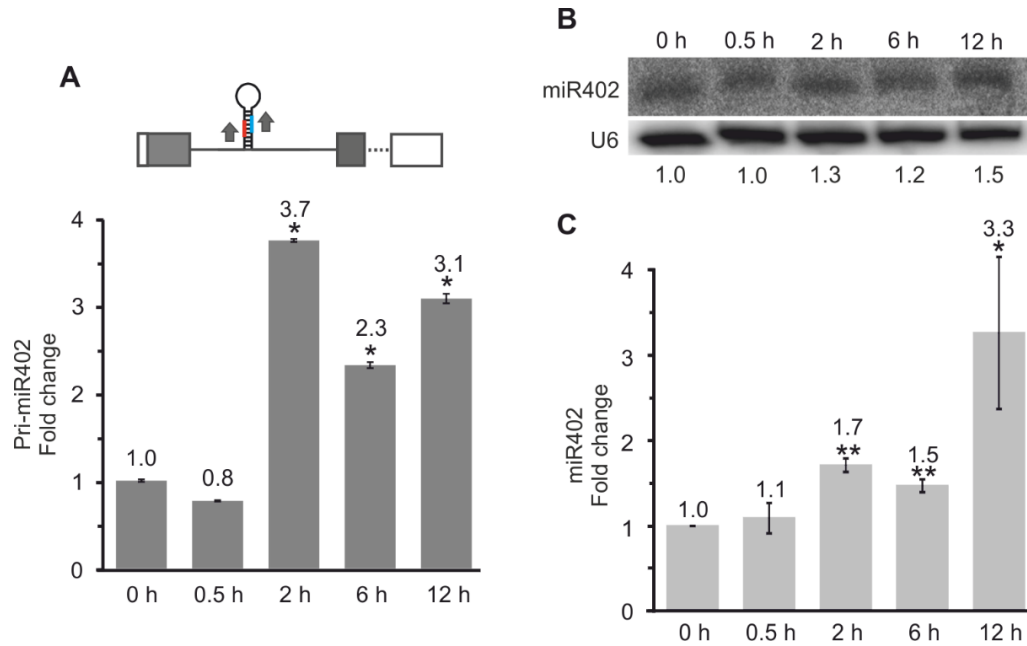


Figure 31. Pri-miR402 and miR402 levels increased under heat-stress conditions. (A) RT-qPCR analysis of pri-miR402 level. In the upper part of the panel, a scheme of the *At1g77230* is presented, with arrows indicating the primers used for amplification. (B) MiR402 accumulation measured using Northern blot. The numbers below the blot image represent the relative intensities of the miRNA bands. U6 was used as RNA loading control. (C) MiR402 level analyzed using RT-qPCR technique. (A, C) Error bars indicate SD (n=3), and asterisks point to significant differences between treated sample and control plants (*p < 0.05; **p < 0.01).

Next, the effect of high temperature on the miR402-hosting intron splicing pattern was examined using the RT-qPCR approach. The primer pair for detecting the fully spliced isoform was designed on the exon 1-exon 2 junction in order to amplify the isoform-of-interest only (Tab. 42). The primer pair for the analysis of the intron-retained isoform was designed within the first *At1g77230* intron (Tab. 42). As a result of heat-stress treatment, a lower splicing efficiency in the miRNA-carrying intron was observed (when compared to control conditions) (Fig. 32A). This correlated with the upregulated level of mature miR402 (Fig. 31B-C). Interestingly, there were no changes in the fourth *At1g77230* intron splicing isoform levels (this intron does not carry any miRNA) (Fig. 32B). According to these observations, high temperature does not equally affect the splicing efficiency of all *MIR402* introns.

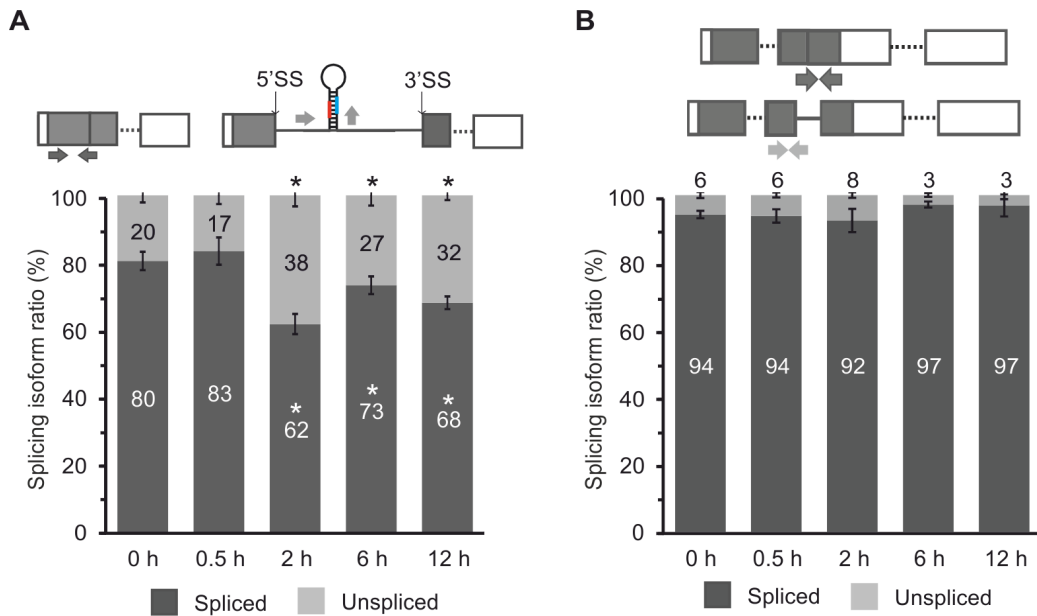


Figure 32. Heat stress inhibited splicing of the miRNA-hosting intron and did not affect fourth *Atlg77230* intron excision efficiency. RT-qPCR analysis of the splicing isoform ratio of (A) the miRNA-carrying intron and (B) the fourth *Atlg77230* intron. In the upper part of the panels, schemes of the *Atlg77230* are presented with arrows indicating the primers used for amplification. Error bars indicate SD (n=3), and asterisks point to significant differences between treated sample and control plants (*p < 0.05; white stars - for spliced isoform; black stars - for unspliced isoform).

What is more, the 3' RACE PCR approach was applied to analyze the 3' ends of *Atlg77230* transcripts. A cDNA template was prepared from 14-day-old *A. thaliana* wild-type seedlings. Two primer sets ("standard" for the first PCR reaction and "nested" for the second) were designed to anneal to the first *Atlg77230* exon (Tab. 44). As a result, three alternative polyadenylation sites were identified. The first, called the proximal polyA site, was located within the miR402-carrying intron, downstream from the miRNA stem-loop structure. The other two, identified at the 5' end of the fifth exon, were called distal polyA sites (together with the canonical polyadenylation site, located at the 3' end of *Atlg77230* transcript). The positions of the detected alternative polyadenylation sites are presented in the table below (Tab. 47). Additionally, the presence and activity of all of these polyA sites were both confirmed in the Direct RNA Sequencing data published by Sherstnev and colleagues (Sherstnev et al., 2012). Importantly, under heat-stress conditions, a more-preferable selection of the alternative proximal intronic polyadenylation site was observed (Fig. 33), which correlated with the higher accumulation of mature miR402 (Fig. 31B-C).

Table 47. Identified alternative polyadenylation sites within *Atlg77230* transcripts

No.	Name	Position (from the 5' end of <i>Atlg77230</i> transcript) in nucleotides	Sequence of the identified cleavage and polyadenylation sites (bold)
1	proximal polyA site	974	AAGTGAATT
2	distal polyA site 1	1756	TAATGAACC
3	distal polyA site 2	1889	TTTCCAGTA

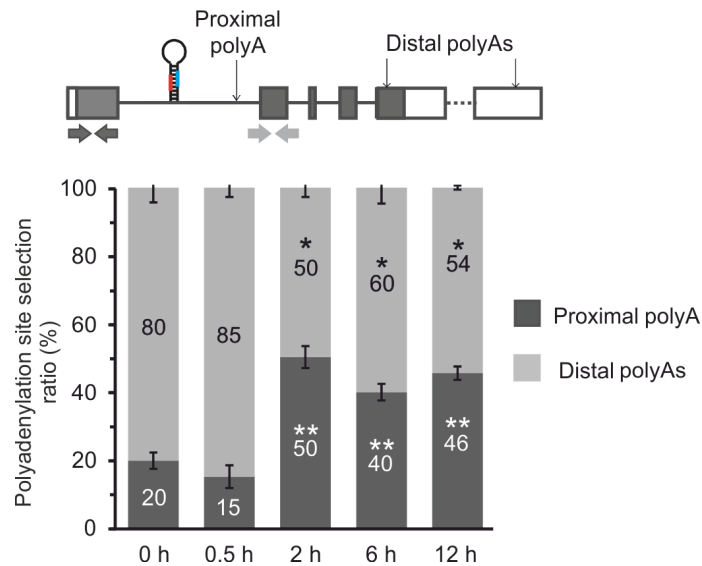


Figure 33. Heat-stress-stimulated selection of the alternative intronic proximal polyA site. RT-qPCR analysis of polyadenylation site selection of the *Atlg77230* transcripts. In the upper part of the panel, the scheme of the *Atlg77230* is presented, with arrows indicating the primers used for amplification. Error bars indicate SD (n=3), and asterisks point to significant differences between treated sample and control plants (*p < 0.05; **p < 0.01; white stars - for proximal polyA isoform; black stars - for distal polyA isoform).

Also, the level of the miR402 target *DML3* mRNA was estimated using RT-qPCR with the use of a primer pair framed miRNA-cleavage site (Tab. 42). Under heat-stress conditions, when the miR402 accumulation was upregulated (Fig. 31B-C), the level of *DML3* mRNA decreased (Fig. 34).

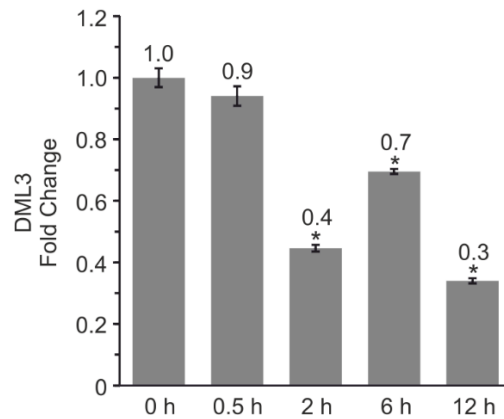


Figure 34. The *DML3* mRNA level decreased after heat-stress treatment. RT-qPCR analysis of the *DML3* transcript level. Error bars indicate SD (n=3), and asterisks point to significant differences between treated sample and control plants (*p < 0.05).

Interestingly, using bioinformatics tools, a second target mRNA for miR402 has been predicted (Dai and Zhao, 2011). It was the mRNA of *At5g54770* encoding the *THI4* protein in which the miRNA-cleavage site was located within the 3' UTR (Fig. 35). This protein is involved in thiamine biosynthesis and mitochondrial DNA damage tolerance (according to UniProt KB database). What is more, the cleavage products of this mRNA were also found in the Arabidopsis degradome data (Nuc et al., unpublished).



Figure 35. Schematic structure of the *At5g54770* (*THI4*) encoding a novel target mRNA of miR402. Boxes – exons (protein-coding sequence – gray; UTRs – white); horizontal lines – introns; vertical line – miR402 cleavage site.

Thus, the level of *THI4* mRNA was also checked by RT-qPCR using a primer pair encompassing the miRNA cleavage site (Tab. 42). After at least 2 hours of heat-stress treatment, downregulation of the *THI4* mRNA was observed (Fig. 36), which was consistent with the higher accumulation of mature miRNA (Fig. 31B-C). Based on these results, a new miR402 target mRNA (*THI4*) was identified and experimentally confirmed.

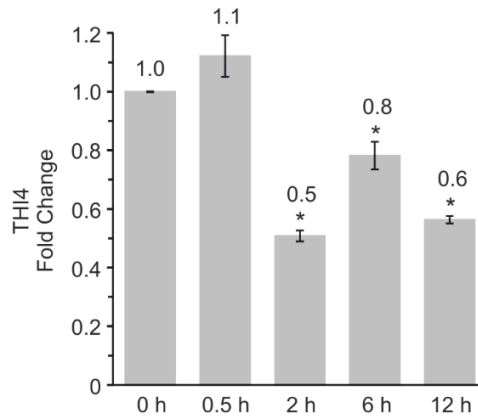


Figure 36. The *TH14* mRNA level decreased after heat-stress treatment. RT-qPCR analysis of the *TH14* transcript level. Error bars indicate SD (n=3), and asterisks point to significant differences between treated sample and control plants (*p < 0.05).

To check, whether upregulated levels of pri-miR402 and miR402 after heat-stress treatment are the results of increased precursor stability, the pri-miR402 half-life was measured with the use of cordycepin (3'-deoxyadenosine). This is an analogue of adenosine lacking the 3'-OH group, whose incorporation into pre-mRNA results in the premature termination of its synthesis (Kaczka et al., 1964; Siev et al., 1969). Thus, it is a commonly used transcription inhibitor in animal and plant cells. The procedure of half-life analysis was performed in accordance with Seeley and colleagues, but with several modifications (Seeley et al., 1992). 17-day-old *A. thaliana* seedlings were treated with high temperature (37°C) for 2 hours. Control plants were grown under standard conditions. Then, the heat-stressed and control seedlings were transferred into an incubation buffer, into which cordycepin was added (0.6 mM) 30 minutes later. Plant material was collected at the indicated time points: 0, 20, 40, 60, and 80 minutes of incubation with cordycepin. Pri-miR402 transcript levels analyzed using RT-qPCR were next plotted against time. Based on linear regression, the half-life of the transcripts was calculated for the control and stressed plants, and the stabilities of the whole pool of transcripts (as well as those terminated at distal polyA sites) were determined. There were no significant changes observed in the half-life of the pri-miR402 transcripts under stress and control conditions (Fig. 37A-B). These results proved that the higher accumulation of mature miR402 after heat-stress treatment was not an outcome of increased pri-miR402 stability.

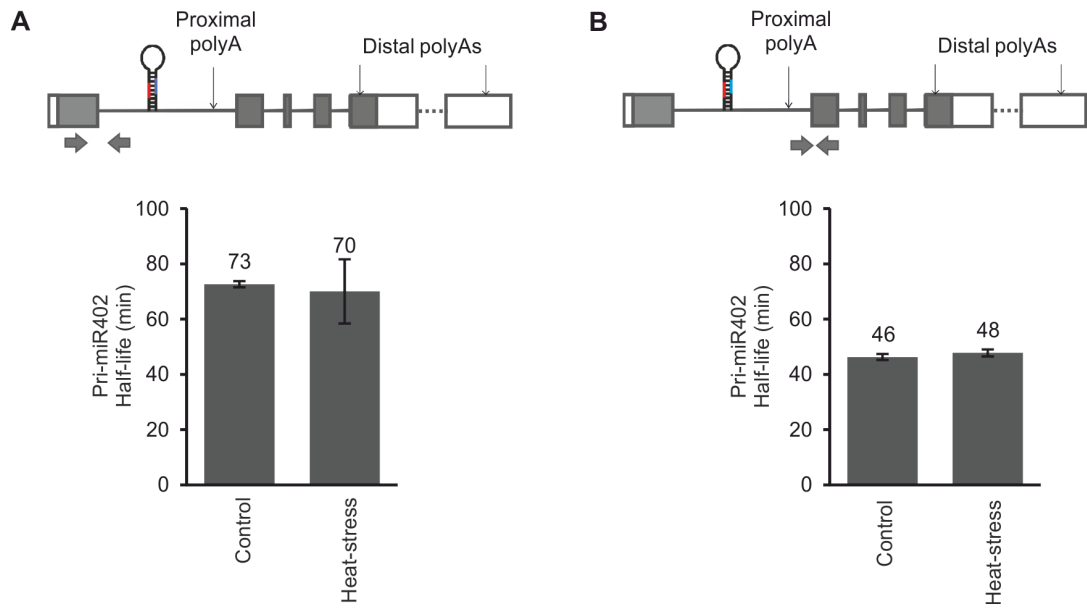


Figure 37. High temperature did not change stability of the *MIR402* transcripts. RT-qPCR analysis of the half-life of (A) the overall pool of pri-miR402 precursors and (B) the transcripts terminated at the distal polyA sites. In the upper part of the panels, schemes of the *At1g77230* are presented, with arrows indicating the primers used for amplification. Error bars indicate SD (n=3).

Additionally, the effects of other abiotic stresses on miR402 biogenesis, such as salinity and drought (mild – 30% SWC and severe – 20% SWC), were tested. As it was observed in heat stress, both salinity and severe drought caused the upregulation of the level of pri-miR402 together with an increased accumulation of mature miR402 (Fig. 38A-B).

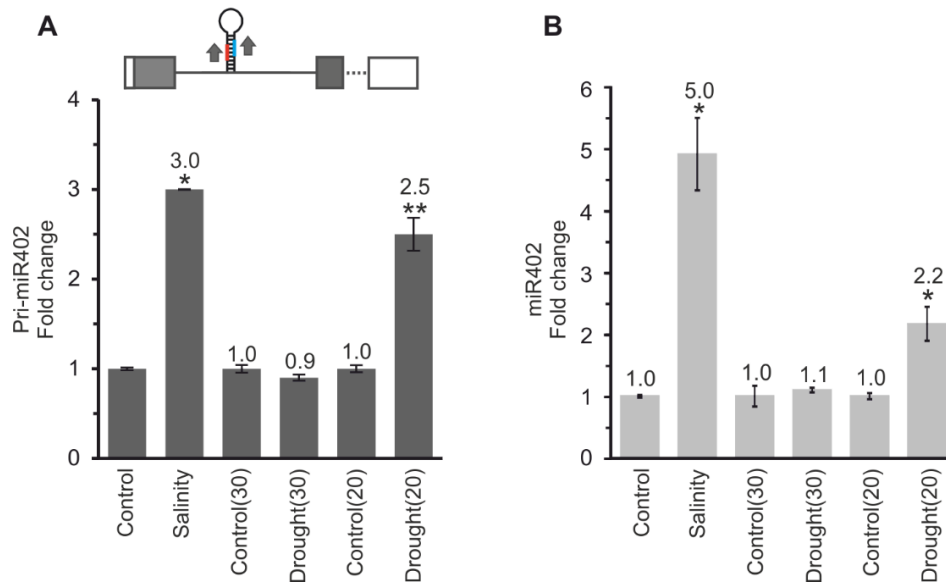


Figure 38. Pri-miR402 and miR402 levels increased under salinity and severe-drought stresses. RT-qPCR analysis of (A) the pri-miR402 level and (B) the mature miR402 accumulation. In the upper part of Panel A, the scheme of the *At1g77230* is presented, with arrows indicating the primers used for amplification. Error bars indicate SD (n=3), and asterisks point to significant differences between treated sample and control plants (*p < 0.05; **p < 0.01).

Moreover, splicing of the miRNA-hosting intron was inhibited under stress conditions (Fig. 39A). Similarly, a higher selection of the intronic proximal polyA site was detected under salinity and severe drought stresses (Fig. 39B).

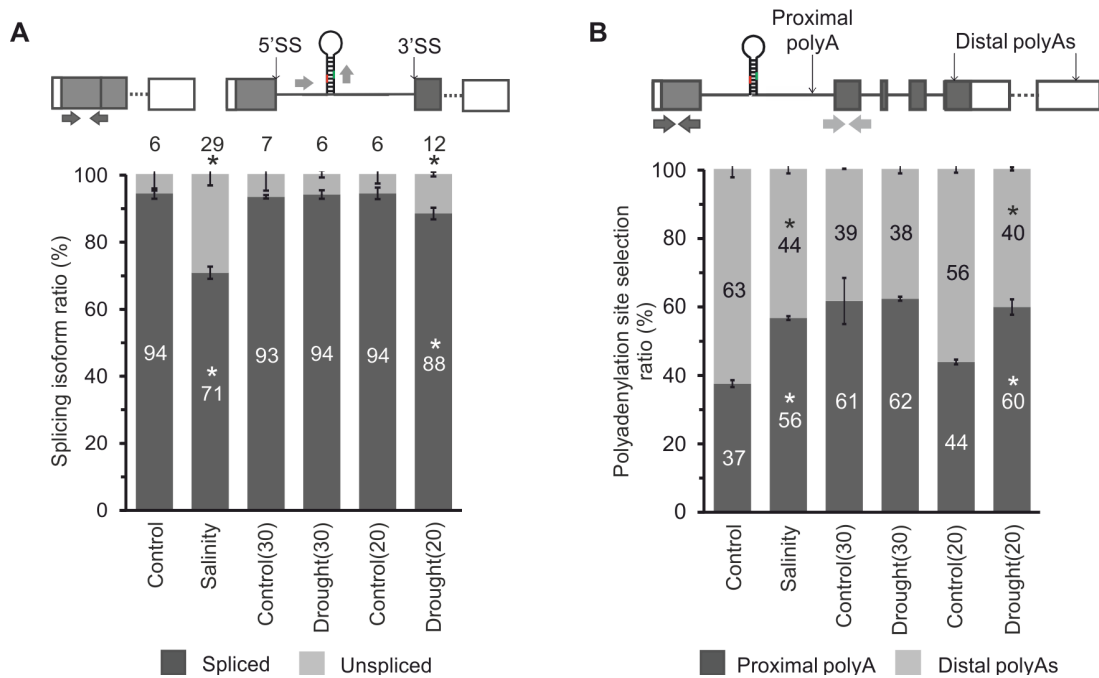


Figure 39. Abiotic stresses inhibited splicing of the miRNA-hosting intron and stimulated proximal polyA site selection. RT-qPCR analysis of (A) the miRNA-hosting intron splicing efficiency and (B) the *Atlg77230* polyadenylation site selection. In the upper part of the panels, schemes of the *Atlg77230* are presented, with arrows indicating the primers used for amplification. Error bars indicate SD (n=3), and asterisks point to significant differences between treated sample and control plants (*p < 0.05; white stars - for spliced or proximal polyA isoforms; black stars - for unspliced or distal polyA isoform).

Also, the levels of both target mRNAs (DML3 and THI4) were downregulated under stress conditions (Fig. 40), when miR402 accumulation was upregulated (Fig. 38B).

To conclude this part, the obtained results implied that intronic miR402 biogenesis is regulated by additional factors like splicing and polyadenylation machineries. Moreover, the interplay between these machineries may play an important role during a plant's response to abiotic stresses.

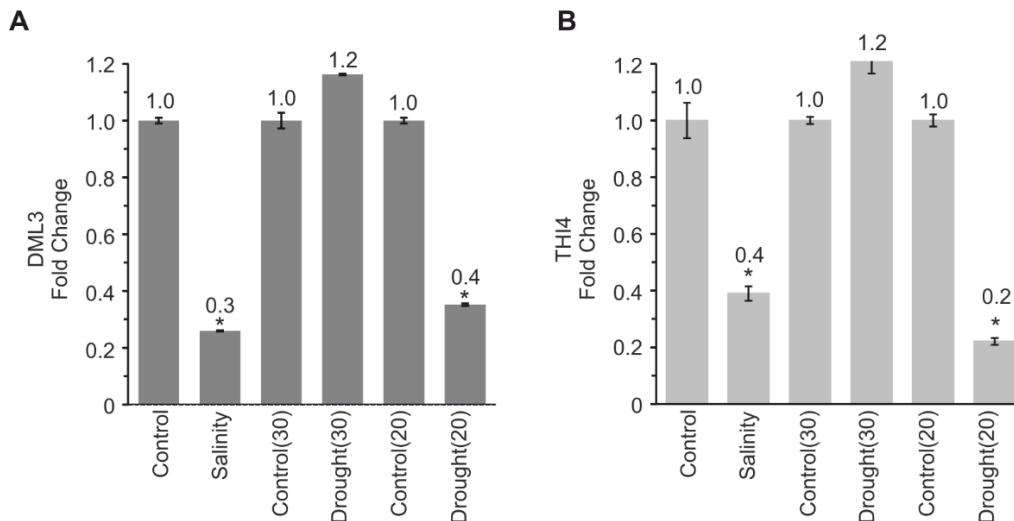


Figure 40. MiR402 target mRNA levels decreased under selected abiotic stress conditions. RT-qPCR analysis of (A) the *DML3* and (B) the *THI4* mRNA levels. Error bars indicate SD (n=3), and asterisks point to significant differences between treated sample and control plants (*p < 0.05).

1.3 Intronic miR402 biogenesis regulation after splicing inhibitor treatment (Gex-1A)

In the next step, the effect of global splicing impairment on miR402 biogenesis was examined. For this purpose, splicing inhibitor herboxidiene (Gex-1A) was used. This chemical compound was identified by Monsanto as a plant herbicide (Isaac et al., 1992; Miller-Wideman et al., 1992). Currently, it is known for its ability to decrease intron-splicing efficiency in both animal and plant cells (Hasegawa et al., 2011; Dolata and Guo et al., 2015). Herboxidiene, as described for Spliceostatin A, binds to SAP155 (a subunit of the SF3b splicing factor, which is a component of the U2 snRNP complex) and prevents SF3b association with the branch point region of introns (Hasegawa et al., 2011).

In the performed experiment, 14-day-old *A. thaliana* seedlings were incubated in a liquid half-strength MS medium supplemented with 4 μ M Gex-1A. As a control, seedlings incubated in the standard liquid half-strength MS medium or with the addition of 2 μ M DMSO were used. Plant material was collected at three time points – after 0, 12, and 24 hours of incubation. Then, the levels of pri-miR402 and mature miR402 were analyzed using RT-qPCR. Significant upregulation of pri-miRNA was observed after 12 and 24 hours of Gex-1A treatment (Fig. 41A), which correlated with higher mature miRNA accumulation (Fig. 41B).

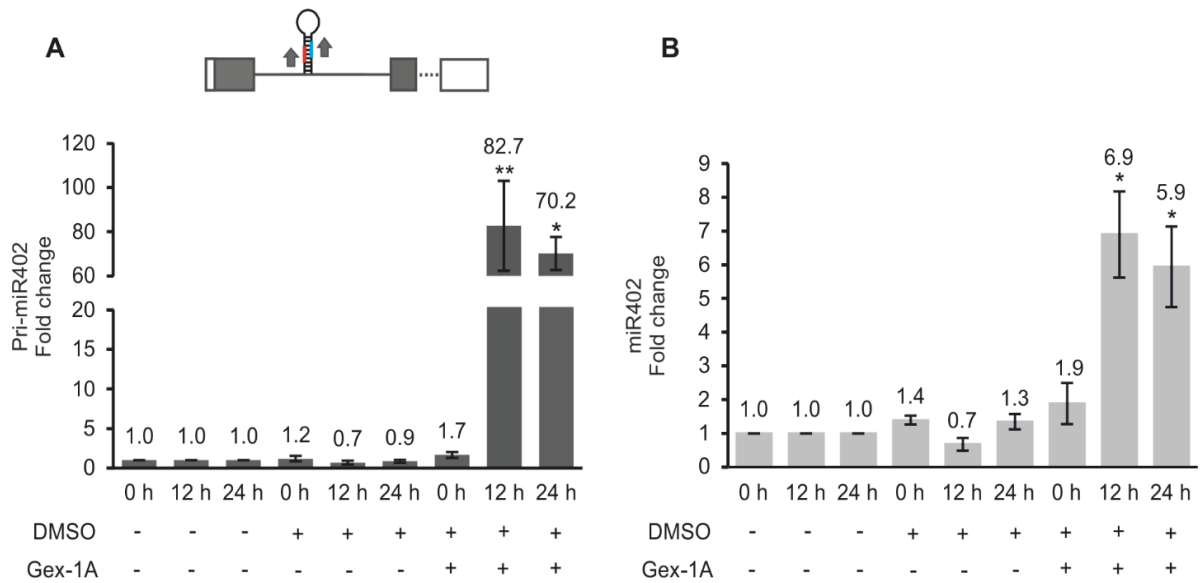


Figure 41. Gex-1A treatment increased pri-miR402 and miR402 levels. RT-qPCR analysis of (A) pri-miR402 level and (B) miR402 accumulation. In the upper part of Panel A, the scheme of the *At1g77230* is presented, with arrows indicating the primers used for amplification. Error bars indicate SD (n=3), and asterisks point to significant differences between treated sample and control plants (*p < 0.05; **p < 0.01).

Also, the splicing of the miR402-hosting intron was less efficient after herboxydiene treatment than under control conditions (Fig. 42). The same effect of splicing inhibition was detected for the third *ACTIN2* (*At3g18780*) intron as well as the fourth *MIR402* intron (Fig. 43A-B). Additionally, Gex-1A treatment induced intronic proximal polyA site selection (Fig. 44).

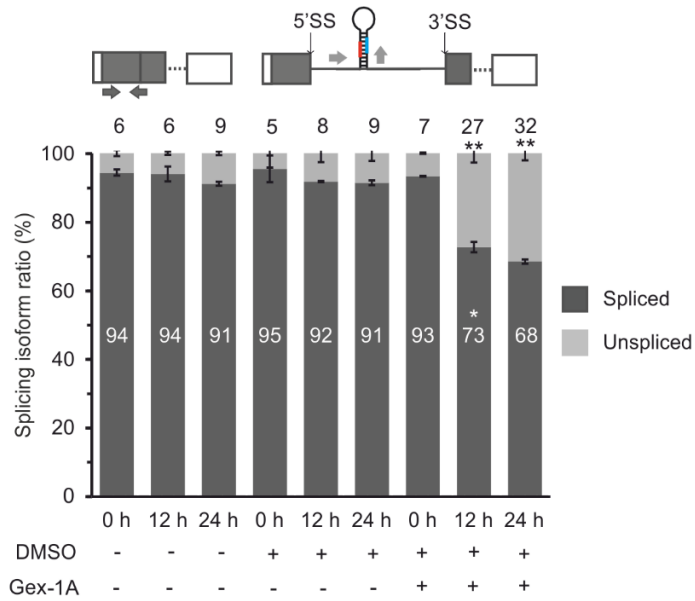


Figure 42. Gex-1A treatment inhibited splicing of the *Atlg77230* miRNA-hosting intron. RT-qPCR analysis of splicing isoform ratio of the miRNA-carrying intron. In the upper part of the panel, schemes of the *Atlg77230* are presented, with arrows indicating the primers used for amplification. Error bars indicate SD (n=3), and asterisks point to significant differences between treated sample and control plants (*p < 0.05; **p < 0.01; white stars - for spliced isoform; black stars - for unspliced isoform).

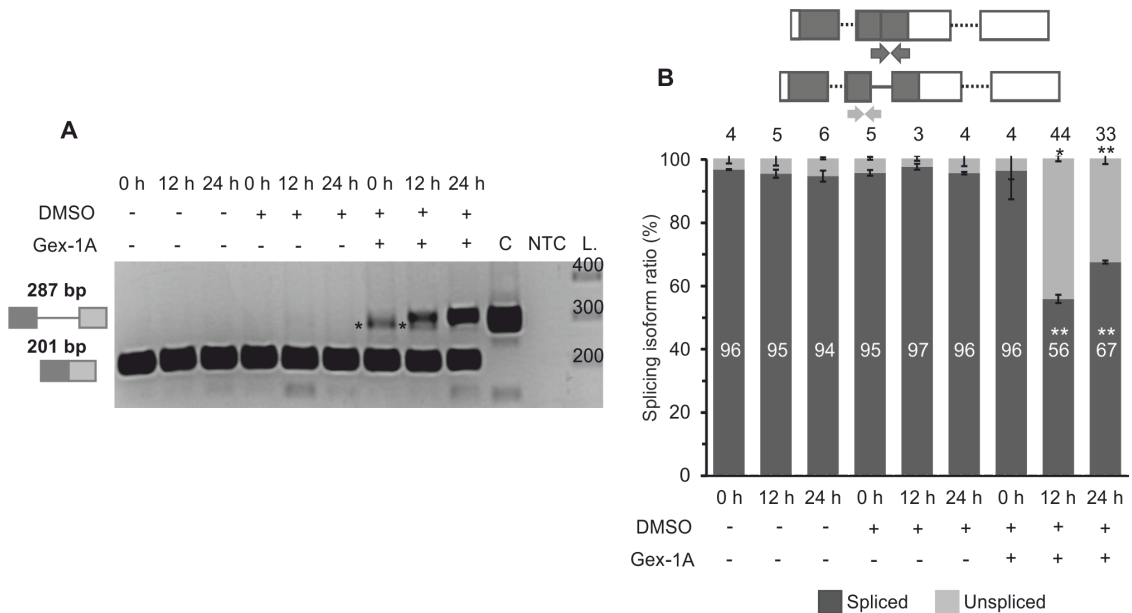


Figure 43. Gex-1A treatment inhibited splicing of the *ACTIN 2* third intron and the *Atlg77230* fourth intron. (A) RT-PCR analysis of the *At3g18780* (*ACT2*) third intron splicing efficiency. L, Gene Ruler 1 kb Plus DNA Ladder; C, genomic DNA used as a PCR template (positive control); NTC, non-template control. Asterisks indicate non-specific PCR products. (B) RT-qPCR analysis of the *Atlg77230* fourth intron splicing efficiency. In the upper part of the panel, schemes of the *Atlg77230* are presented, with arrows indicating the primers used for amplification. Error bars indicate SD (n=3), and asterisks point to significant differences between treated sample and control plants (*p < 0.05; **p < 0.01; white stars - for spliced isoform; black stars - for unspliced isoform).

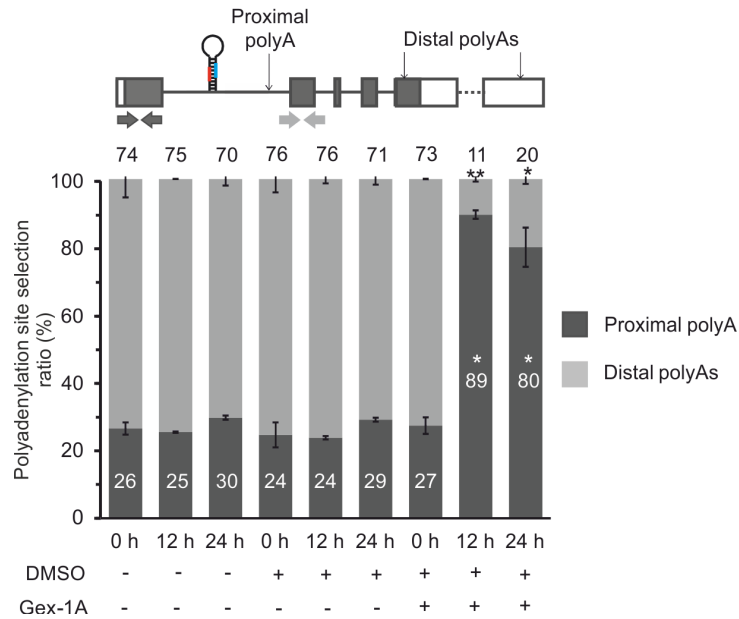


Figure 44. Gex-1A treatment stimulated selection of alternative intronic proximal polyA site in *At1g77230* transcript. RT-qPCR analysis of polyadenylation site selection of *At1g77230* transcripts. In the upper part of the panel, the scheme of the *At1g77230* is presented, with arrows indicating the primers used for amplification. Error bars indicate SD (n=3), and asterisks point to significant differences between treated sample and control plants (*p < 0.05; **p < 0.01; white stars - for proximal polyA isoform; black stars - for distal polyA isoform).

Also, a downregulation of target mRNA levels was observed under the conditions tested (Fig. 45).

To sum up, splicing inhibited by the action of herboxidiene exhibited the same effect on miR402 biogenesis as those abiotic stress factors applied in this work.

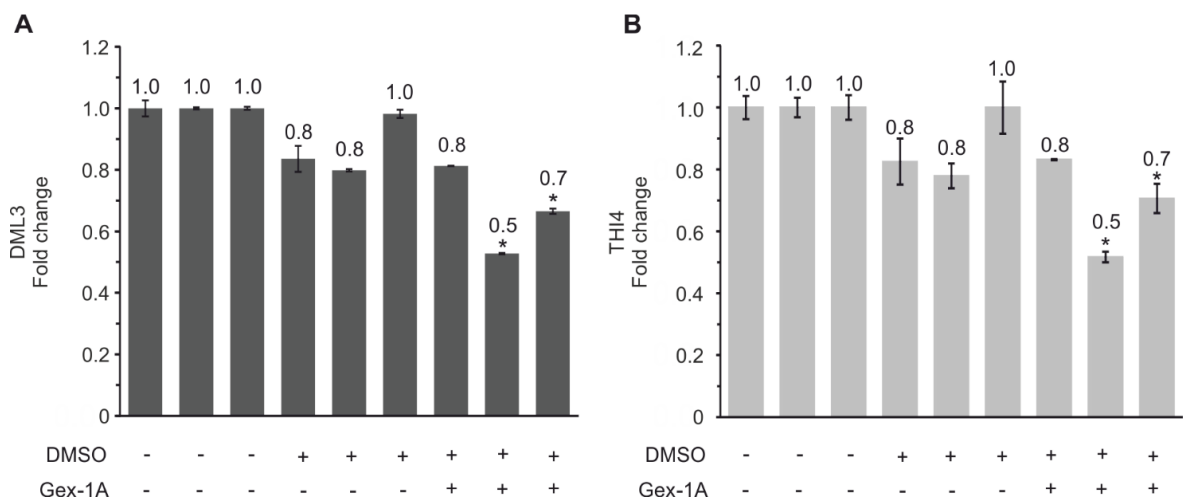


Figure 45. MiR402 target mRNA levels decreased after Gex-1A treatment. RT-qPCR analysis of (A) the *DML3* and (B) the *THI4* mRNA levels. Error bars indicate SD (n=3), and asterisks point to significant differences between treated sample and control plants (*p < 0.05).

To check the effect of Gex-1A-induced splicing inhibition on the biogenesis of other miRNAs, two additional Arabidopsis intronic miRNAs were tested: miR837-3p and miR1888b (located in the first introns of *At1g18880* and *At3g60960*, respectively). Similar to miR402, the accumulation levels of both miRNAs were upregulated after Gex-1A treatment (Fig. 46A, 47A), which was also accompanied by the decreased efficiency of miRNA-carrying intron excision (Fig. 46B, 47B).

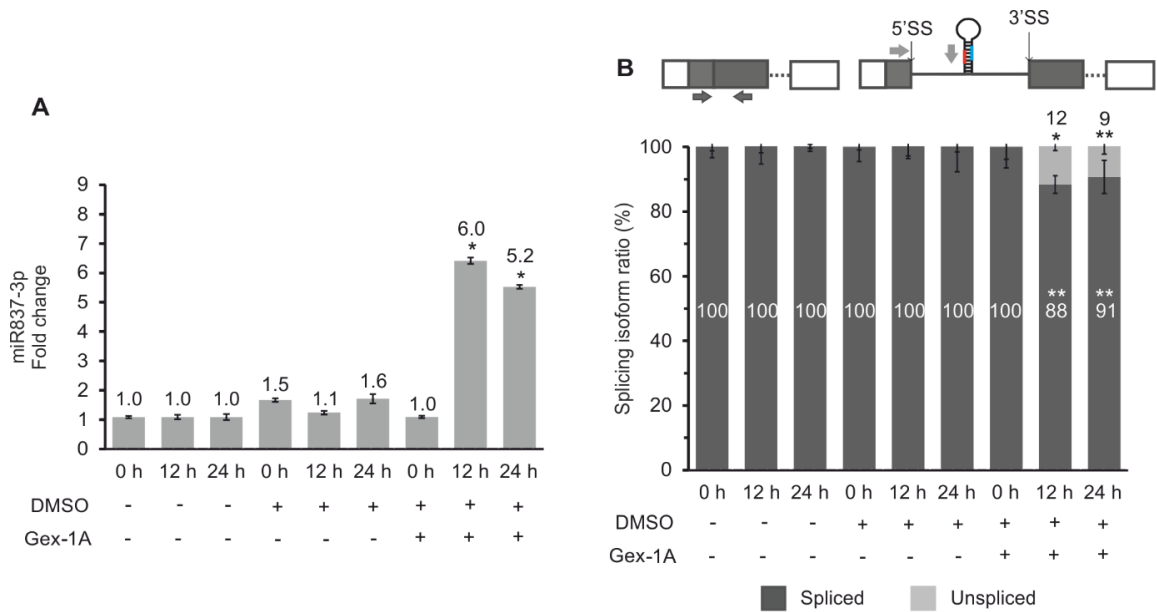


Figure 46. Gex-1A treatment increased the miR837-3p accumulation and inhibited the miRNA-carrying intron splicing. RT-qPCR analysis of (A) the miR837-3p accumulation and (B) the miRNA-hosting intron splicing efficiency. In the upper part of Panel B, schemes of the *At1g18880* are presented, with arrows indicating the primers used for amplification. Error bars indicate SD (n=3), and asterisks point to significant differences between treated sample and control plants (*p < 0.05; **p < 0.01; white stars - for spliced isoform; black stars - for unspliced isoform).

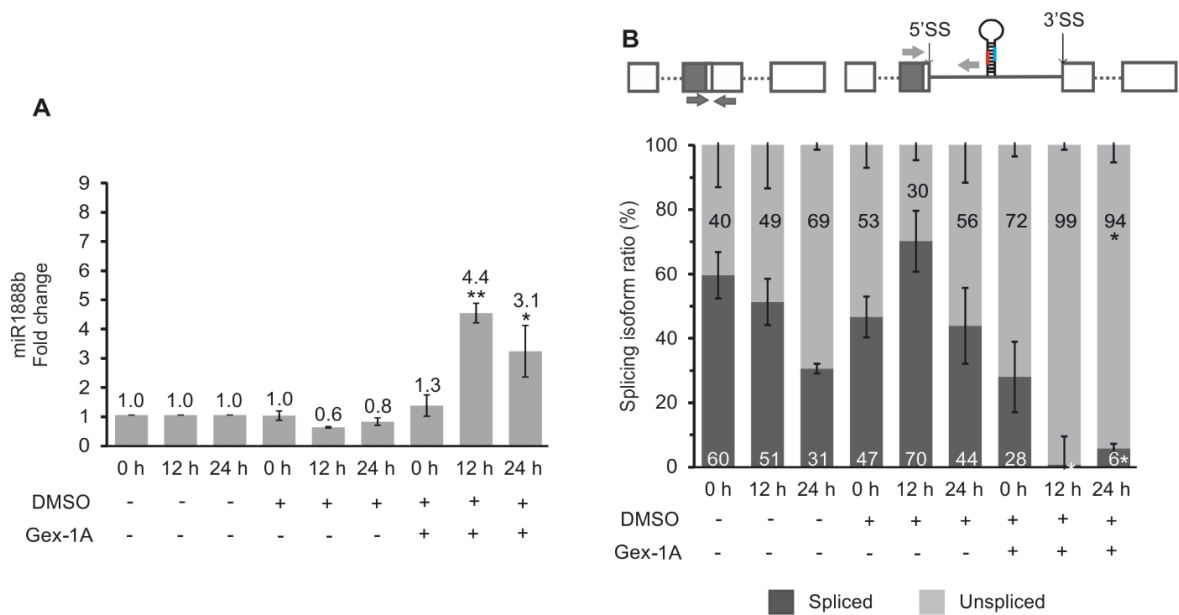


Figure 47. Gex-1A treatment increased the miR1888b accumulation and the inhibited miRNA-carrying intron splicing. RT-qPCR analysis of (A) the miR1888b accumulation and (B) the miRNA-hosting intron splicing isoform ratio. In the upper part of Panel B, schemes of the *At3g60960* are presented, with arrows indicating the primers used for amplification. Error bars indicate SD (n=3), and asterisks point to significant differences between treated sample and control plants (*p < 0.05; **p < 0.01; white stars - for spliced isoform; black stars - for unspliced isoform).

The presented results strongly suggest the existence of a novel mechanism of plant intronic miRNA biogenesis regulation, involving a competition between the spliceosome and plant microprocessor complexes.

1.4 Active 5'SS controls miR402 biogenesis

Next, deeper analyses of the miR402 biogenesis mechanism and its regulation via splicing and polyadenylation were conducted. For this purpose, *Atlg77230* mutants carrying inactivated first-intron splice sites (in every combination) were prepared. Therefore, the genomic sequence of the *MIR402* host gene was cloned into the pENTR/D-TOPO vector. Next, site-directed mutagenesis was performed to inactivate (1) the 5' ($\Delta 5'ss$), (2) the 3' ($\Delta 3'ss$); and (3) both 5' and 3' ($\Delta(5'ss+3'ss)$) splice sites (Fig. 48). Then, mutated versions of *Atlg77230* were cloned into binary vector pMDC32 (carrying the double 35S strong promoter), which is expressed in both bacteria and plants (Curtis and Grossniklaus, 2003). Since there is no Arabidopsis null mutant of *Atlg77230*, prepared genetic constructs were used in a transient expression assay in *Nicotiana*

benthamiana leaves. Moreover, mutation of the constitutive 5'SS resulted in the weak activation of the cryptic 5'SS, located downstream from the miR402 stem-loop structure. Thus, additional constructs were prepared as described above: (4) Δ cry5'ss; (5) Δ (cry5'ss+3'ss); (6) Δ (5'ss+cry5'ss); and (7) Δ (5'ss+cry5'ss+3'ss) (Fig. 48).

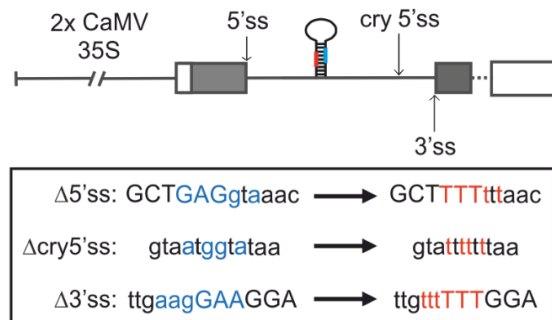


Figure 48. The scheme of the *At1g77230* native construct with mutations inactivating 5', 3', and cryptic 5' splice sites depicted in the frame. Blue and red letters point to nucleotides before and after mutagenesis, respectively. Capital letters indicate exon sequences.

The performed analyses revealed the important role of constitutive 5'SS during the maturation of miR402. Inactivation of this splice site resulted in the strong upregulation of both pri-miR402 and mature miR402 levels (Fig. 49A), together with the almost-complete inhibition of miRNA-hosting intron splicing (Fig. 49B). The cryptic 5'SS was not important for miR402 maturation since its mutation had no effect on the level of miRNA (Fig. 49).

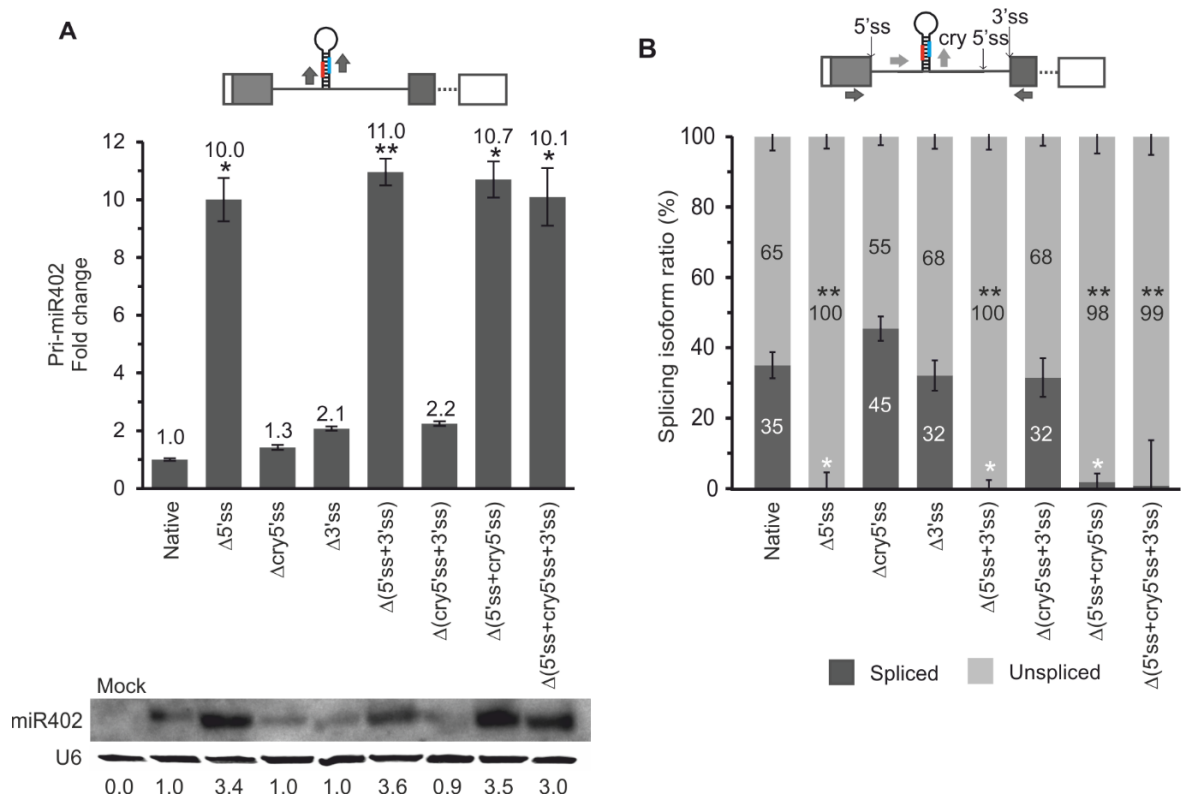


Figure 49. Inactivation of constitutive 5' splice site resulted in upregulation of pri-miR402 and mature miR402 levels, which correlated with miRNA-carrying intron splicing inhibition. (A – upper panel) RT-qPCR analysis of the pri-miR402 level; (A – lower panel) miR402 accumulation analyzed using Northern hybridization. The numbers below the blot image are the relative intensities of the miRNA bands. U6 was used as RNA loading control. The mock represents *Nicotiana* leaves infiltrated with only a buffer (negative control). (B) Splicing isoform analysis of the *Atlg77230* first intron. (A, B) At the top of the panels, schemes of the *Atlg77230* are presented, with arrows indicating the primers used for amplification. Error bars indicate SD (n=3), and asterisks point to significant differences between analyzed sample and control plants (*p < 0.05; **p < 0.01; white stars - for spliced isoform; black stars - for pri-miRNA and unspliced isoform).

Surprisingly, there were no significant changes in the splicing isoform ratio after mutation of the constitutive 3'SS (Fig. 49B). Sequencing of the RT-qPCR products revealed activation of the cryptic 3'SS, located 14 nt downstream from the constitutive one (Fig. 50A). After inactivation of both 3' splice sites ($\Delta(3'ss+cry3'ss)$), 23% of the spliced isoform was still detected (caused by the activation of another cryptic 3'SS, 9 nt downstream from the first cryptic 3'SS), correlating with a slight increase in the level of mature miR402 (Fig. 50B).

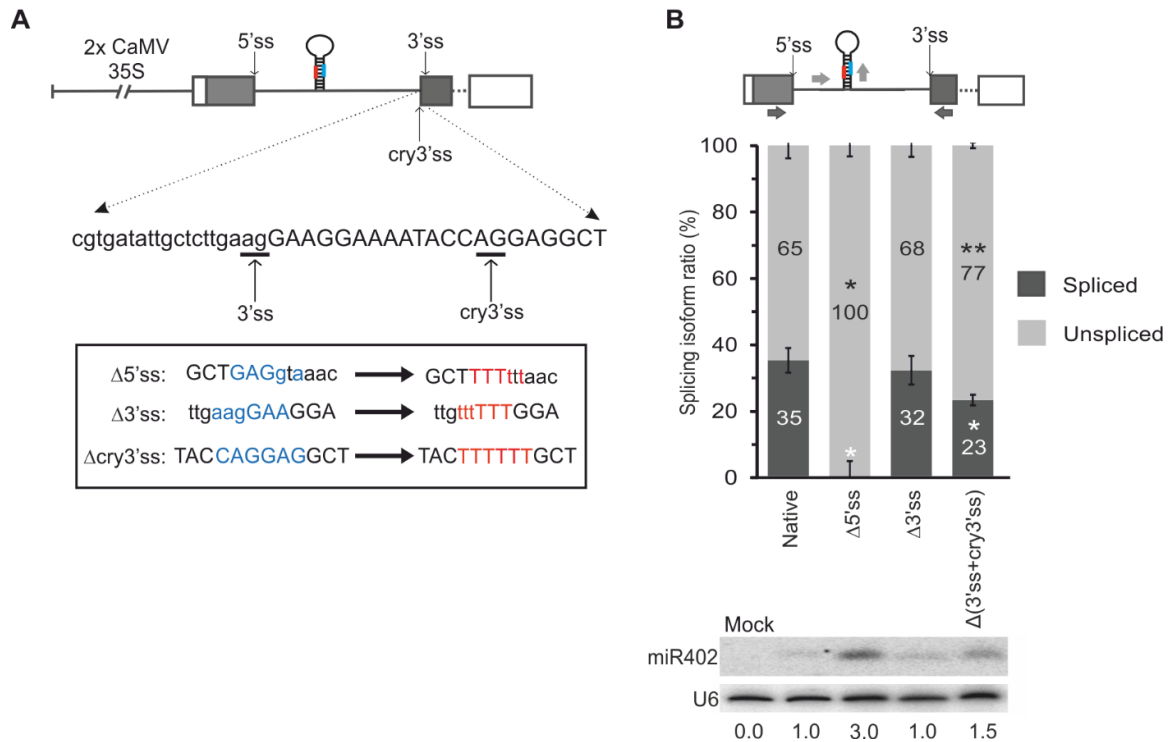


Figure 50. 3'SS played a minor role in miR402 biogenesis regulation. (A) The schematic structure of the *AtIg77230* native constructs with mutations inactivating the 5', 3', and cryptic 3' splice sites depicted in the frame. Blue and red letters point to nucleotides before and after mutagenesis, respectively; capital letters indicate exon sequence. (B) The pri-miR402 (*upper panel*) and mature miR402 (*lower panel*) levels measured using RT-qPCR and Northern blot, respectively (U6 was used as RNA loading control). The numbers below the blot image are the relative intensities of the miRNA bands. The mock represents *Nicotiana* leaves infiltrated with only a buffer (negative control). At the top of Panel B, the scheme of the *AtIg77230* is presented, with arrows indicating the primers used for amplification. Error bars indicate SD (n=3), and asterisks point to significant differences between analyzed sample and control plants (*p < 0.05; **p < 0.01; white stars - for spliced isoform; black stars - for unspliced isoform).

Moreover, analysis of the polyadenylation isoform level indicated that the abolishment of miRNA-hosting intron splicing after constitutive 5'SS inactivation correlated with the higher selection of intronic proximal polyA site (Fig. 51), which mirrored observations from stress and Gex-1A experiments in *A. thaliana*.

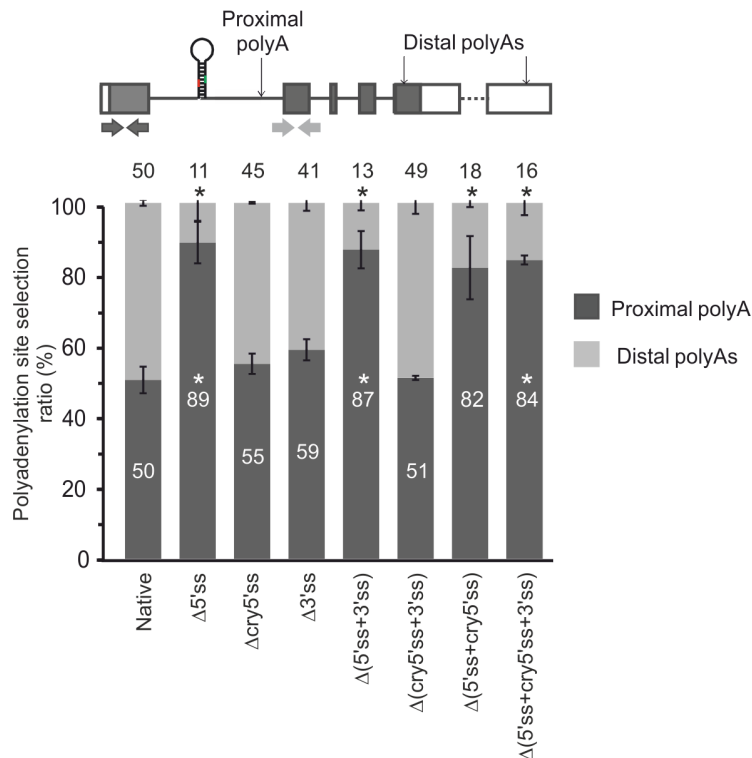


Figure 51. Inactivation of constitutive 5' splice site resulted in preferential selection of proximal polyA site. RT-qPCR analysis of polyadenylation site selection of the *Atlg77230* transcripts. In the upper part of the panel, the scheme of the *Atlg77230* is presented, with arrows indicating the primers used for amplification. Error bars indicate SD (n=3), and asterisks point to significant differences between sample and control plants (*p < 0.05; white stars - for proximal polyA isoform; black stars - for distal polyA isoform).

Previously published results demonstrated that the effect of the 5'SS mutation on miRNA biogenesis may depend on the strength of the promoter used (Bielewicz et al., 2013; Schwab et al., 2013). Thus, to exclude this possibility, *Atlg77230* genomic sequences (with native and mutated constitutive 5'SS were cloned into a modified pMDC99 vector (Curtis and Grossniklaus, 2003; Knop and Stepien et al., 2016). The original version of this vector does not carry any promoter sequence. Thus, additional promoter sequences were introduced into the pMDC99 vector: (1) the native *Atlg77230* promoter; (2) the *At3g18780* (*ACT2*) promoter; and (3) the *Atlg13440* (*GAPDH*) promoter. The MiR402 accumulation level from the construct carrying the native *MIR402* promoter was almost undetectable (Fig. 52). However, inactivation of the constitutive 5'SS in two other constructs (under the control of the *ACT2* and the *GAPDH* promoters) resulted in the upregulation of the level of mature miR402. These observations confirmed the results obtained with the use of a strong 35S promoter.

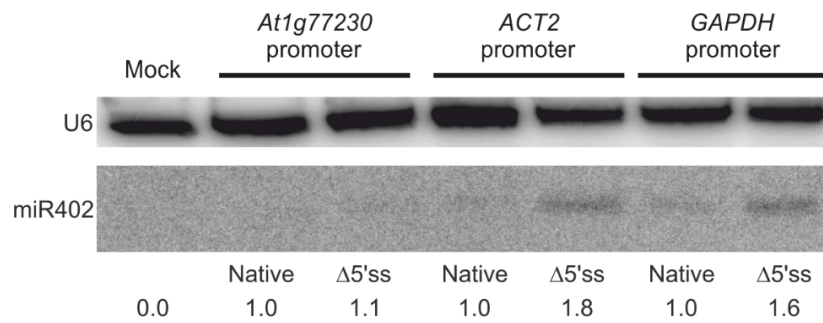


Figure 52. Increased miR402 accumulation after 5'SS inactivation did not depend on the promoter used. The accumulation of mature miR402 measured using Northern blot (U6 was used as RNA loading control). The *At1g77230* versions with active (native) and inactivated ($\Delta 5'ss$) first intron 5'SS were expressed under control of the native *At1g77230*, the *ACT2*, and the *GAPDH* promoters. The numbers below the blot image are the relative intensities of the miRNA bands. The mock represents *Nicotiana* leaves infiltrated with only a buffer (negative control).

It has also been reported that the different types of mutation introduced may affect the effect of 5'SS inactivation on miRNA maturation (Bielewicz et al., 2013; Schwab et al., 2013). In the prepared genetic constructs, the six nucleotides within the 5'SS (GAGgta) were changed to TTTttt (Fig. 48). So, it was possible that the observed alterations of miR402 biogenesis after 5'SS inactivation were caused by the binding of some proteins to created an oligo U tract. Thus, three other types of point mutation were introduced, changing two, three, or four nucleotides within the *MIR402* first intron 5' splice site sequence (Fig. 53A). All analyzed mutations triggered mature miR402 upregulation simultaneously with miRNA-hosting intron splicing inhibition (Fig. 53B).

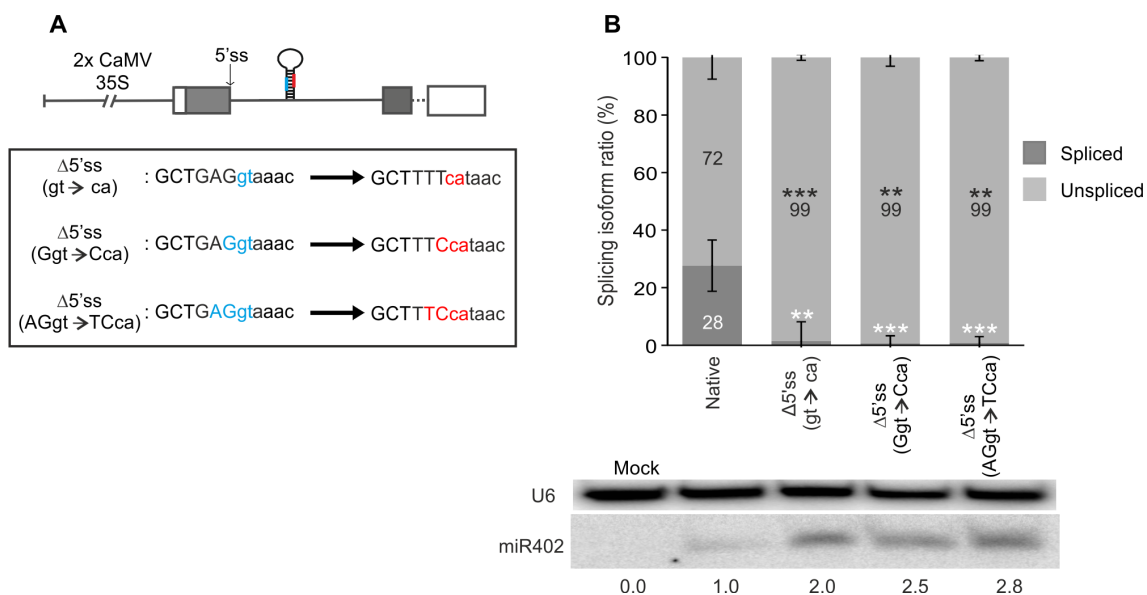


Figure 53. Upregulation of the level of mature miR402 after 5'SS inactivation does not depend on the type of 5'SS mutation introduced (A) The schematic structure of *Atlg77230* native constructs, with point mutations inactivating the 5' splice site depicted in the frame. The blue and red letters indicate nucleotides before and after mutagenesis, respectively; capital letters indicate exon sequence. (B – upper panel) RT-qPCR analysis of the miR402-hosting intron splicing isoform ratio. Native and $\Delta 5'ss$ mean the active and inactivated first *Atlg77230* intron 5' splice sites, respectively. Error bars indicate SD (n=3), and asterisks indicate significant differences between analyzed sample and control plants (**p<0.01; ***p<0.001; white stars – spliced isoforms; black stars – unspliced isoforms). (B – lower panel) The level of mature miR402 measured using Northern blot (U6 was used as RNA loading control). The numbers below the blot image are the relative intensities of the miRNA bands. The mock represents *Nicotiana* leaves infiltrated with only a buffer (negative control).

Moreover, to exclude the possibility of increased pri-miR402 stability after inactivation of the 5'SS, the cordycepin assay was applied. 72 hours after agroinfiltration, a small discs from *N. benthamiana* transfected leaves were dissected and incubated in a buffer for 30 min, and then cordycepin was added (0.6 mM). Plant material was collected after 0, 30, 60, 120, and 180 minutes of incubation with the cordycepin. The half-life of the pri-miR402 transcripts was determined as described previously for heat-stressed *Arabidopsis* seedlings (see Results section: 1.2). Based on the obtained data, there were no differences in the stability of the whole pool of pri-miR402 transcripts (Fig. 54A) nor in those terminated at the distal polyA sites (Fig. 54B) between the versions with the active and inactivated *Atlg77230* first intron 5'SS.

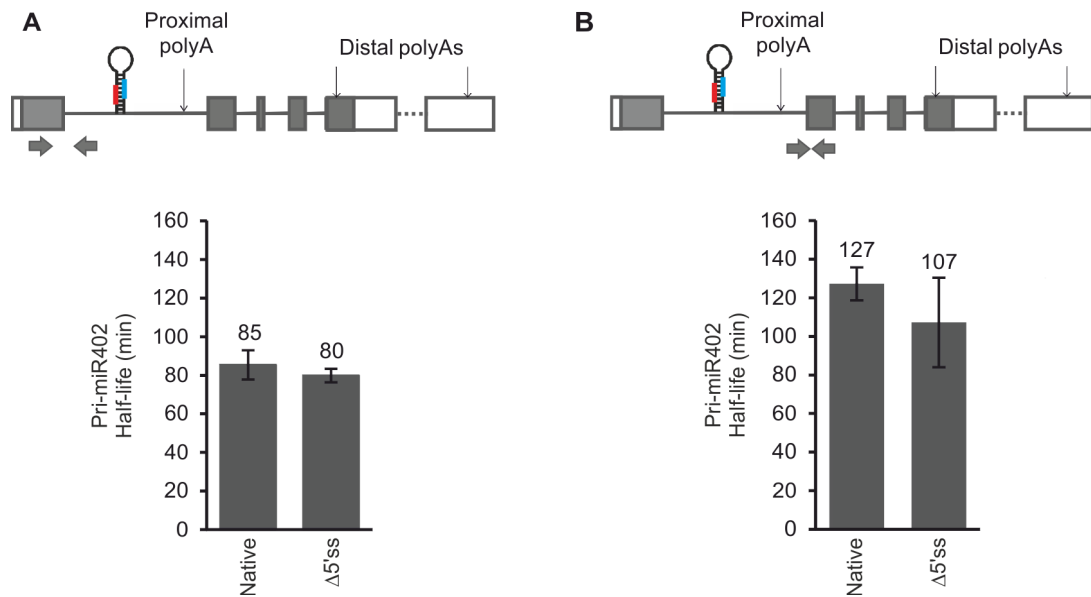


Figure 54. Inactivation of constitutive 5'SS did not change intronic miR402 precursor stability. RT-qPCR analysis of the half-life of (A) the overall pool of pri-miR402 precursors and (B) the transcripts terminated at the distal polyA sites. Native and $\Delta 5'ss$ mean the active and inactivated first *At1g77230* intron 5' splice sites, respectively. In the upper part of the panels, schemes of the *At1g77230* are presented, with arrows indicating the primers used for amplification. Error bars indicate SD (n=3).

To conclude this part, the obtained results pointed to the important role of the 5'SS and splicing inhibition during intronic miR402 biogenesis. What is important, the effect of this 5' splice site was not influenced by the type of promoter used, type of splice-site mutation introduced, nor changed pri-miR402 stability.

1.5 The effect of pre-miR402 stem-loop structure localization on miRNA biogenesis efficiency

Accordingly to the previously published results concerning the biogenesis of miR161 and miR163 located within the exons of intron-containing *MIR* genes, splicing and active 5'SS stimulate their biogenesis (Bielewicz et al., 2013). This is contrary to the observed role of the 5'SS in the maturation of intronic miR402. Thus, the main aim of the next step was to elucidate the role of the 5'SS in miRNA biogenesis regarding pre-miRNA location within the pri-miRNA transcript. For this purpose, the miR402 stem-loop structure was shifted from the first intron (variant A) to the first exon (Variant B) or second intron (Variant C) of the *At1g77230* gene (Fig. 55).

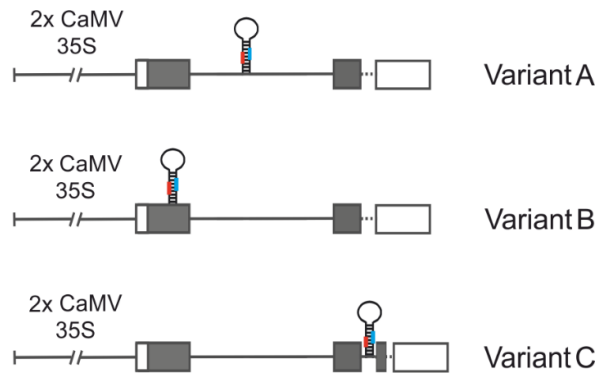


Figure 55. The schematic structure of the *At1g77230* construct versions: Variant A (pre-miR402 in first intron), Variant B (miR402 stem-loop moved to first exon), and Variant C (miR402 hairpin moved to second intron).

To prepare the constructs carrying the B and C variants, the pre-miR402 was first removed from the *MIR402* host gene using a three-step PCR approach (Fig. 56).

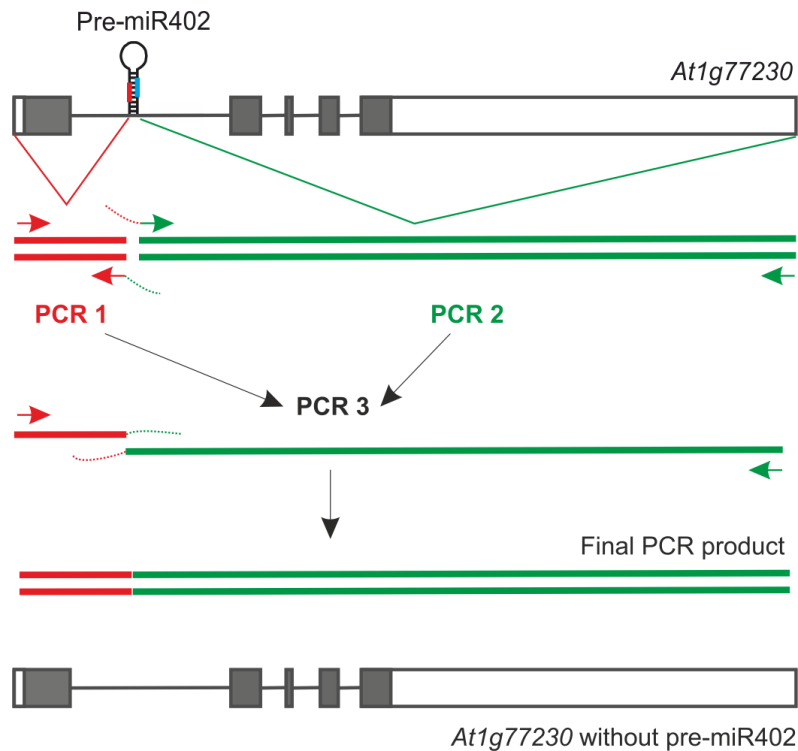


Figure 56. Schematic overview of three-step PCR approach used for deletion of the pre-miR402 stem-loop structure from *At1g77230*. Red lines – 5' fragment of *At1g77230* native version (1- 400 nt); green lines – 3' fragment of *At1g77230* native version (710 - 3649 nt); arrows – primer pairs used for fragment-of-interest amplification; dotted lines – 20-nt-long overhangs (overlapping sequences between fragments combined together).

Otherwise, pre-miR402 was amplified separately using specific primers (Tab. 41). Then, the miR402 stem-loop structure was introduced into the first exon of the *At1g77230* lacking pre-miR402 with the use of an *Mfe*I restriction site. To prepare Variant C, a five-step PCR approach was applied (Fig. 57) in which a PCR product containing the whole *At1g77230* genomic sequence without pre-miR402 was used as a template for Steps 1 and 2.

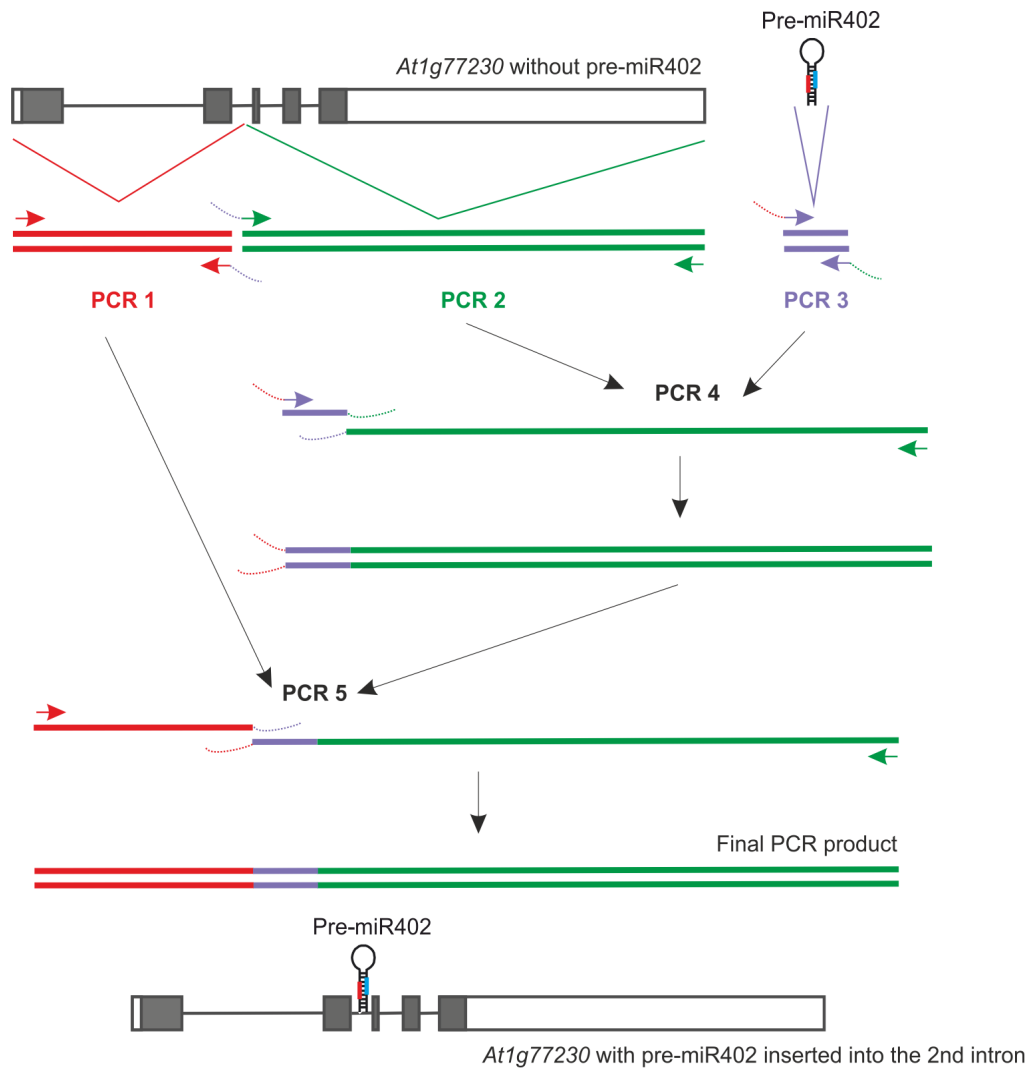


Figure 57. Schematic overview of five-step PCR approach used for insertion of the pre-miR402 stem-loop structure into *At1g77230* second intron. Red lines – 5' fragment of *At1g77230* version deprived of pre-miR402 (1 - 1211 nt); green lines – 3' fragment of *At1g77230* version lacking pre-miR402 (1212 - 3649 nt); violet lines – pre-miR402; arrows – primer pairs used for fragment-of-interest amplification; dotted lines – 20-nt-long overhangs (overlapping sequences between fragments combined together).

Modified *MIR402s* were cloned into the pENTR/D-TOPO vector. Each variant was prepared in two versions: with the active (native) and inactivated ($\Delta 5'ss$) 5' splice site of the miRNA-hosting intron. Then, all versions were transferred to the pMDC32 binary vector. As before, the transient expression assay in *Nicotiana benthamiana* leaves was performed. The analyzed pri-miR402 levels increased after inactivation of the 5'SS in both Variants A and B (Fig. 58 – upper panel). At the same time, mutation of the first-intron 5'SS caused no changes in the level of pri-miRNA in Variant C. What is important, inactivation of the 5'SS resulted in the upregulation of the level of mature miR402 in Variant A (pre-miRNA located within the first intron), while a decreased accumulation of miR402 was observed for the variant with the miRNA stem-loop structure shifted to the upstream exon (Variant B) (Fig. 58 – lower panel).

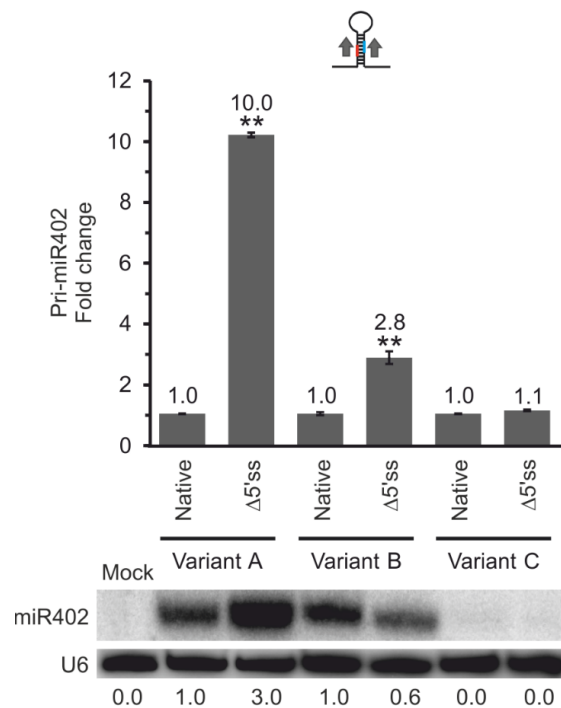


Figure 58. The effect of the 5'SS on miR402 biogenesis efficiency depended on the pre-miR402 location within its host gene. (Upper panel) RT-qPCR analysis of the pri-miR402 level. Native and $\Delta 5'ss$ mean the active and inactivated first *At1g77230* intron 5' splice sites, respectively. In the upper part of the panel, the scheme of the *At1g77230* is presented, with arrows indicating the primers used for amplification. Error bars indicate SD (n=3), and asterisks point to significant differences between analyzed sample and control plants (**p < 0.01). (Lower panel) The accumulation of mature miR402 measured using Northern blot. U6 was used as RNA loading control. The numbers below the blot image are the relative intensities of the miRNA bands. The mock represents *Nicotiana* leaves infiltrated with only a buffer (negative control).

Splicing isoform ratio analysis of the miRNA-hosting intron revealed that mutation of the 5'SS caused almost complete splicing abolishment in all variants (Fig. 59A), together with an increased selection of intronic proximal polyadenylation sites (Fig. 59B).

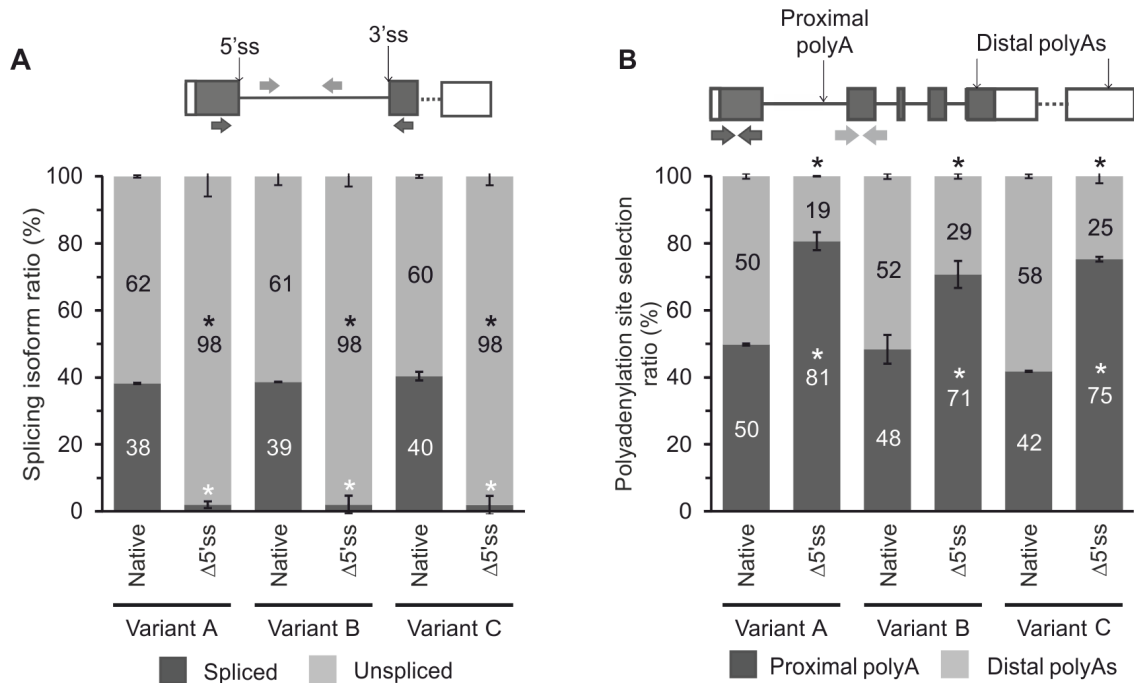


Figure 59. Effect of constitutive 5'SS inactivation on splicing efficiency and polyA site selection did not depend on pre-miR402 position within its host gene. RT-qPCR analysis of (A) the *Atlg77230* first intron splicing efficiency and (B) the proximal and distal polyA site selection. Native and Δ5'ss mean the active and inactivated first *Atlg77230* intron 5' splice sites, respectively. In the upper part of the panels, schemes of the *Atlg77230* are presented, with arrows indicating the primers used for amplification. Error bars indicate SD (n=3), and asterisks point to significant differences between analyzed sample and control plants (*p < 0.05).

Interestingly, after pre-miR402 relocation to the second intron, the accumulation of mature miRNA was almost undetectable in both versions with active and inactivated first intron 5'SS (Fig. 58 – lower panel). RT-qPCR analysis revealed that the second *Atlg77230* intron was efficiently spliced regardless of the lack or presence of the miRNA stem-loop structure within this intron (Fig. 60).

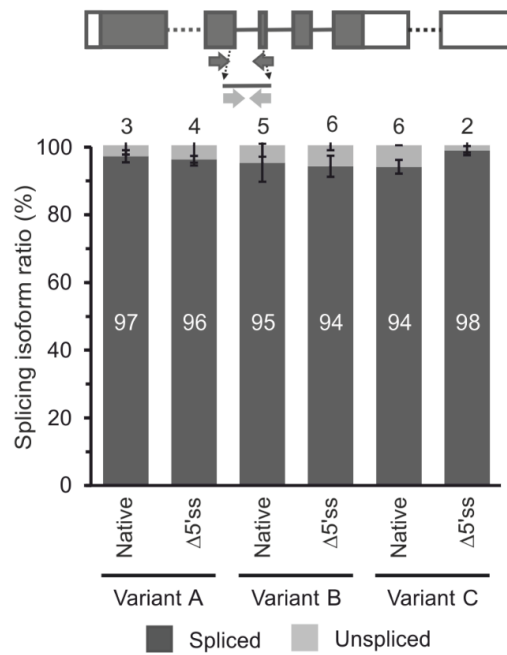


Figure 60. Pre-miR402 position did not influence the *At1g77230* second splicing efficiency. RT-qPCR analysis of *At1g77230* second intron splicing efficiency. Native and $\Delta 5'ss$ mean the active and inactivated first *At1g77230* intron 5' splice sites, respectively. In the upper part of the panels, schemes of the *At1g77230* are presented, with arrows indicating the primers used for amplification. Error bars indicate SD (n=3).

Moreover, additional experiments were conducted to exclude the possibility of different precursor stability produced from Variant A and Variant B constructs. The cordycepin assay was performed as previously described for *N. benthamiana* (see Results section: 1.4). There were no changes observed between the half-life of the native versions (with the active first intron 5'SS) of Variant A and Variant B (Fig. 61A-B). A significant increase in the stability of the whole pool of pri-miR402 transcripts was observed in Variant B after inactivation of the 5' splice site (as compared to the active 5'SS version) (Fig. 61A), which correlated with decreased miR402 accumulation (Fig. 58 – lower panel).

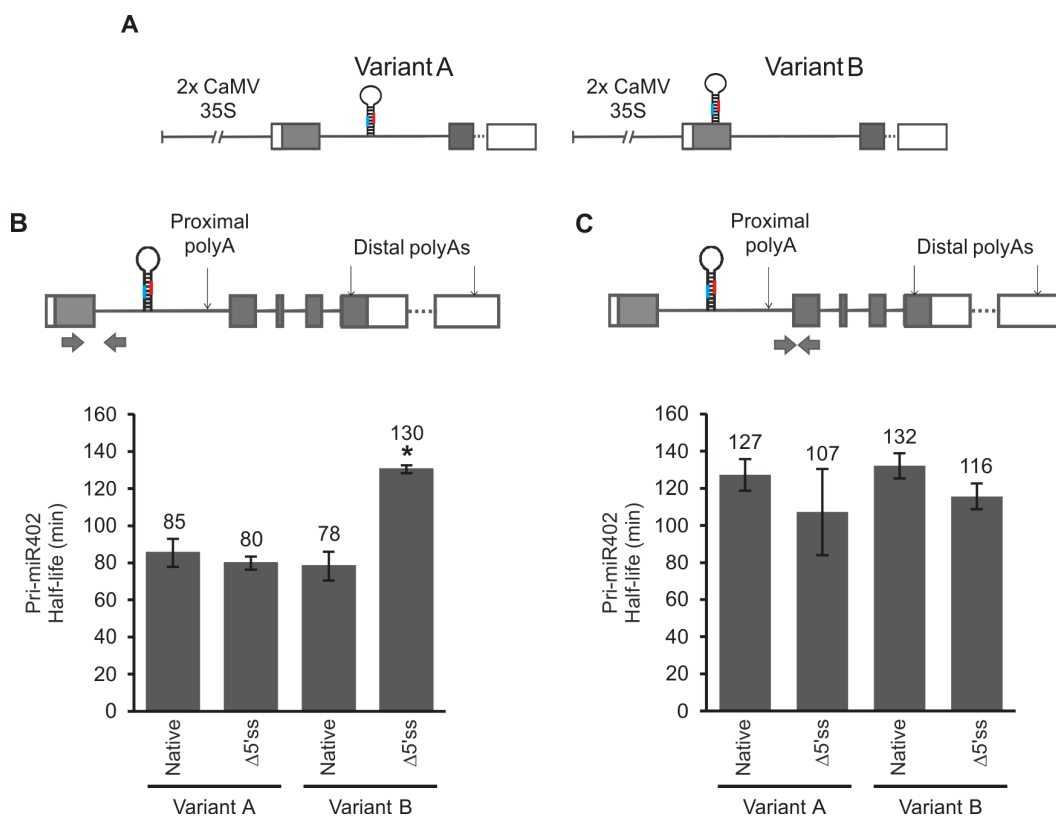


Figure 61. Inactivation of 5'SS did not decrease pri-miR402 stability. (A) The schematic structures of the *At1g77230* construct variants: A (wild-type) and B (miR402 stem-loop shifted to the first exon). The RT-qPCR analysis of the half-life of (B) the overall pool of pri-miR402s, and (C) the transcripts terminated at the distal polyA sites. Native and Δ5'ss mean the active and inactivated first *At1g77230* intron 5' splice sites, respectively. In the upper part of each panel, schemes of the *At1g77230* are presented, with arrows indicating the primers used for amplification. Error bars indicate SD (n=3), and the asterisk indicates a significant difference between analyzed sample and control plants (*p<0.05).

The presented results revealed that the position of the pre-miRNA hairpin regarding the nearest active 5'SS is the main determinant of miRNA biogenesis efficiency regulation. An active 5' splice site stimulates the maturation of upstream-located exonic miR402 while inhibiting the production of the downstream-positioned intronic miR402. This effect is not influenced by the changed pri-miR402 stability produced in either Variant A or Variant B. What is more, the described observations proved that miR402 cannot be efficiently produced from spliced-out introns.

1.6 The role of SERRATE protein in regulation of intronic miRNA maturation

Recently published data revealed that the SERRATE protein (a key component of the plant microprocessor complex) interacts with the U1 snRNP auxiliary proteins; i.e., PRP39b, PRP40a, PRP40b, and LUC7l (Knop and Stepien et al., 2016). These results supported the hypothesis about direct interactions between miRNA biogenesis and splicing machineries via the SE protein. As mentioned in the introduction, there are two viable hypomorphic Arabidopsis mutants of SE: *se-1* and *se-2* (Prigge and Wagner, 2001; Grigg et al., 2005). It has been demonstrated that the SERRATE version present in the *se-1* mutant (lacking 20 amino acids from the C-terminus) is still able to interact with its identified the U1 snRNP partners (Knop and Stepien et al., 2016). However, when SE is lacking its 40 C- terminus aa (*se-2* version), the connections between SERRATE and PRP39b, PRP40a, and PRP40b are lost.

To analyze the effect of the lack or the presence of the microprocessor – spliceosome interactions on intronic miRNA biogenesis, these two SE mutants were used. Plant material collected from 14-day-old *A. thaliana* wild-type, *se-1*, and *se-2* seedlings was analyzed for the accumulation of mature miR402 using the RT-qPCR technique. As anticipated, due to the less-efficient miRNA biogenesis (Prigge and Wagner, 2001), downregulation of the level of mature miRNA was observed in the *se-1* mutant (as compared to wild-type plants) (Fig. 62A). In the *se-2* mutant, the accumulation of miR402 was higher than in *se-1* (despite the fact that miRNA biogenesis was impaired in both mutants plants (Prigge and Wagner, 2001; Grigg et al., 2005)); however, it was lower when compared to wild-type. Importantly, the observed miRNA level changes correlated with the strongest miR402-hosting intron splicing inhibition in *se-2* in comparison to *se-1* and wild-type plants (Fig. 62B).

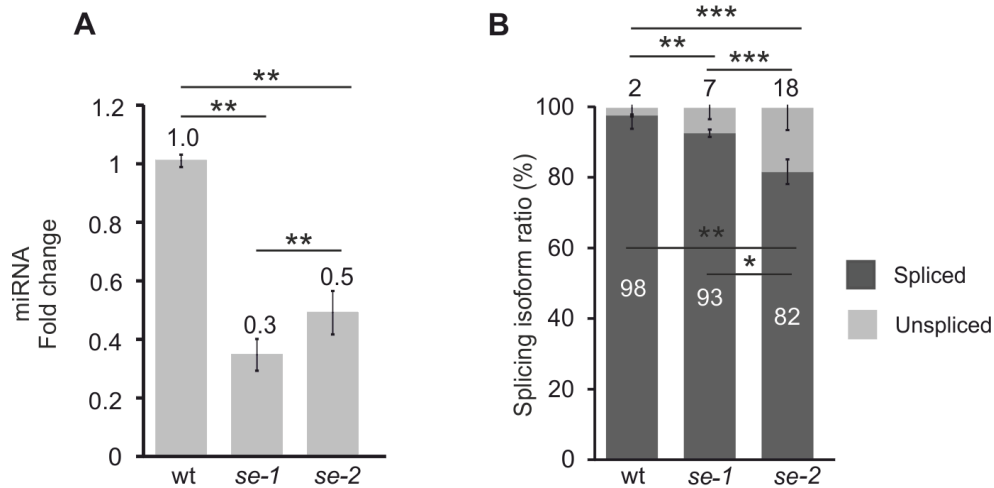


Figure 62. The SERRATE – U1 snRNP interactions affected intronic miR402 biogenesis in *A. thaliana*. RT-qPCR analysis of (A) the level of mature miR402 and (B) the splicing efficiency of the miR402-hosting intron in wild-type, *se-1*, and *se-2* plants. Error bars indicate SD (n=3), and asterisks indicate significant differences between analyzed samples and control plants (**p<0.01; ***p<0.001).

Also, the biogenesis of intronic miR1888a was analyzed in two SE mutants. The pre-miR1888a is located within the first intron of *At5g21100* host gene. The performed analysis revealed that miR1888a and miR402 are regulated by a similar mechanism, since also for miR1888a the lower miRNA-carrying intron splicing efficiency in the *se-2* mutant was observed along with an increased accumulation of mature miRNA (as compared to *se-1* plants) (Fig. 63A-B).

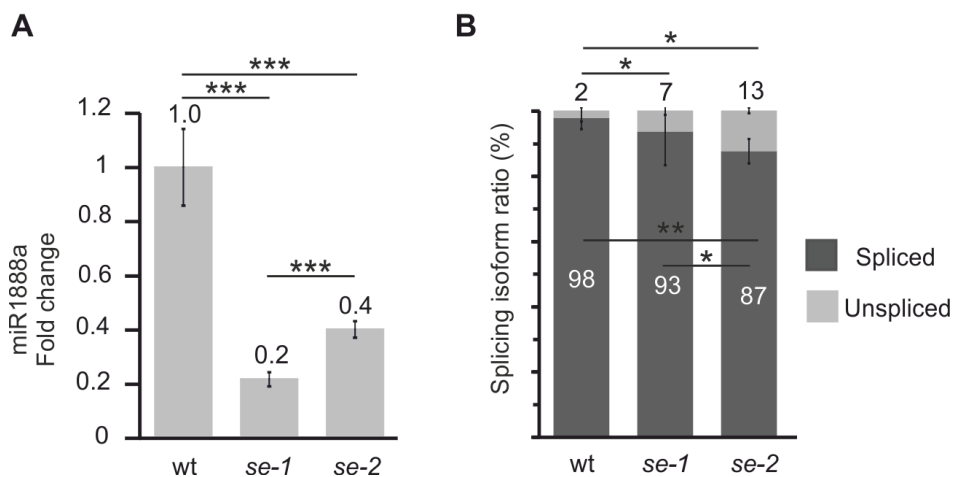


Figure 63. The SERRATE – U1 snRNP interactions affected intronic miR1888a biogenesis in *A. thaliana*. RT-qPCR analysis of (A) the level of mature miR1888a and (B) the splicing efficiency of the miR1888a-hosting intron. Error bars indicate SD (n=3), and asterisks indicate significant differences between analyzed samples and control plants (*p<0.05; **p<0.01; ***p<0.001).

The presented data confirmed that SE – the U1 snRNP interactions play an essential role in the regulation of intronic miRNA biogenesis in *Arabidopsis thaliana*. These results proved that a lack of connections between the plant microprocessor and spliceosome complexes observed in *se-2* mutants triggers strong miRNA-hosting intron splicing inhibition, which leads to the more-efficient production of mature intronic miRNAs.

2 Functional dissection of miR319b and miR319b.2 biogenesis in plants

Accordingly to the literature, the *MIR319b* family is important for plant growth and development (Sobkowiak et al., 2012). Interestingly, at least two functional miRNAs have been identified within the pre-miR319b stem-loop structure – miR319b and miR319b.2. These miRNAs possess dissimilar sequences; thus, they target different mRNAs.

2.1 Preparation of Arabidopsis transgenic lines carrying mutated versions of *MIR319b*

The basis of the presented project was to prepare genetic constructs that carry modified pre-miR319b sequences. Therefore, the primer pair was designed to amplify the genomic sequence of *At5g41663* (*MIR319b*) together with the ~2000-bp-long region located upstream from the annotated 5' *At5g41663* UTR (Fig. 64A) (Tab. 41). PCR product was next cloned into the pENTR/D-TOPO vector (pMIR319b:*MIR319b*). Then, four additional *MIR319b* gene variants were prepared: (1) with mutated miR319b and miR319b* sequences (pMIR319b:mut_319b) (Fig. 64B – *upper panel*); (2) with mutated miR319b.2 and miR319b.2* sequences (pMIR319b:mut_319b.2) (Fig. 64B – *lower panel*); (3) with deleted miR319b and miR319b* sequences (pMIR319b:del_319b) (Fig. 64C – *upper panel*); and (4) with removed miR319b.2 and miR319b.2* sequences (pMIR319b:del_319b.2) (Fig. 64C – *lower panel*).

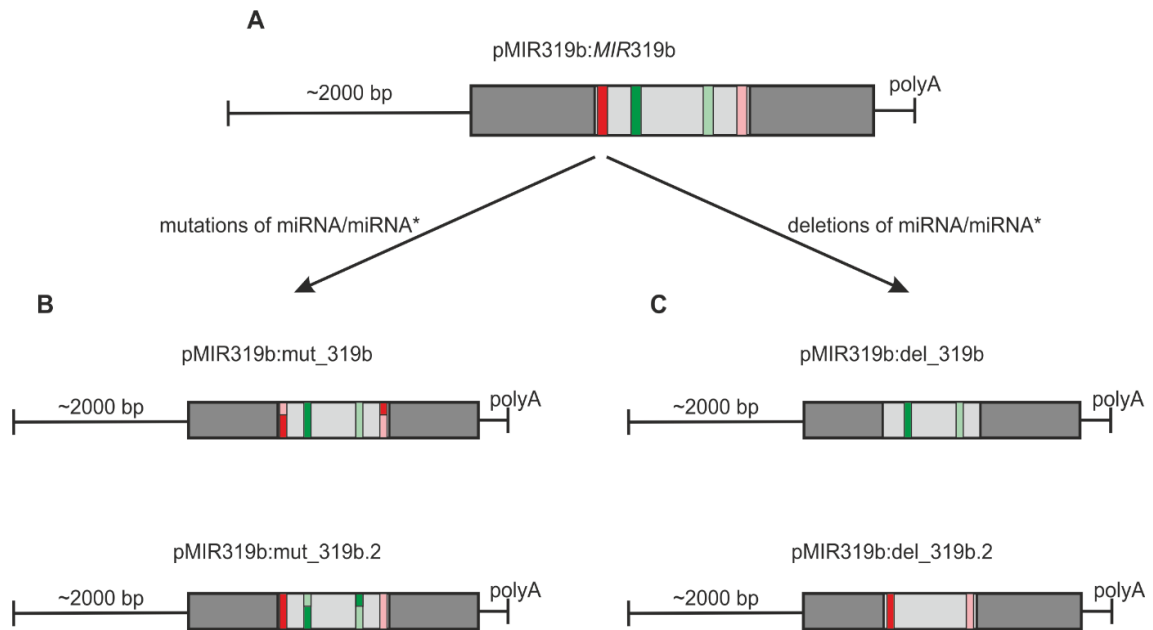


Figure 64. Schemes of (A) the pMIR319b:*MIR319b* native construct and its modifications: (B) mutations and (C) deletions of miR319b/miR319b* or miR319b.2/miR319b.2* within pre-miR319b, respectively. Boxes – exon; light gray – pre-miR319b sequence; dark and light red – miR319b* and miR319b, respectively; dark and light green – miR319b.2* and miR319b.2, respectively. 2000 bp – region containing promoter sequence of *MIR319b*. In Panel B, the exchanged fragments between miRNAs and miRNAs* are marked.

For the preparation of mutated versions of native pre-miR319b (Fig. 65A), site-directed mutagenesis was performed in order to exchange either the 3' part of miR319b* with the 5' part of miR319b (Fig. 65B) or miR319b.2*'s 3' part with miR319b.2's 5' part (Fig. 65C). These mutations were designed to inhibit the abilities of miR319b or miR319b.2 to cleave their target mRNAs. What is more, they did not significantly change the miRNA stem-loop structure stability parameters (i.e., Gibbs Free Energy - ΔG) nor the pairing of miRNA/miRNA* within the duplexes. In the other two constructs, shortened versions of the pre-miR319b stem-loop structure were prepared (Fig. 66).

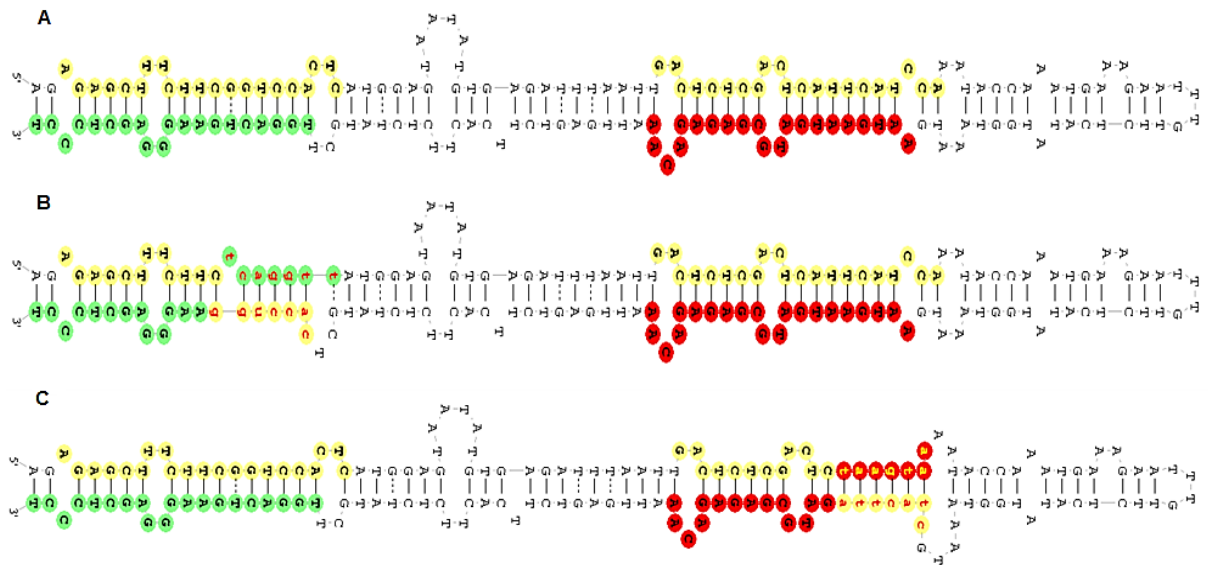


Figure 65. Schemes of (A) the native pre-miR319b stem-loop structure and its mutated variants within (B) miR319b and miR319b*, and (C) miR319b.2 and miR319b.2* sequences. Yellow – miRNAs*; green – miR319b; red – miR319b.2; red and yellow lettering – mutated parts of the miRNA/miRNA* sequences. Pre-mRNA structures designed, and Gibbs Free Energy (ΔG) calculated with Folder ver. 1.11 (algorithm: RNAfold) (Hansen, 2007). (A) $\Delta G = -80.80$; (B) $\Delta G = -72.80$; (C) $\Delta G = -81.20$.

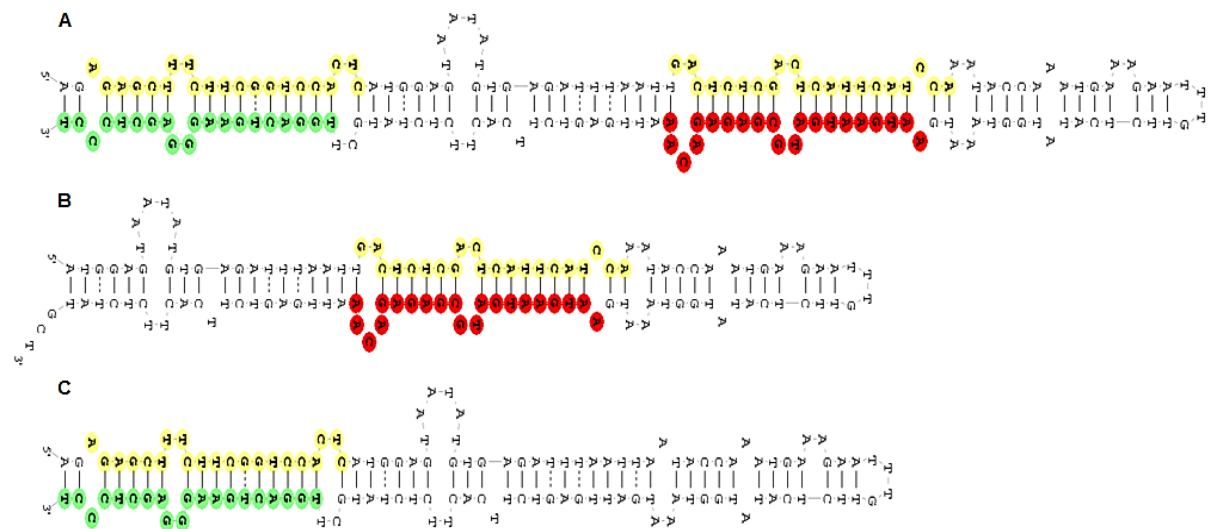


Figure 66. Schemes of (A) the native pre-miR319b stem-loop structure and its shortened variants without (B) miR319b and miR319b* sequences and (C) miR319b.2 and miR319b.2* sequences. Yellow – miRNAs*; green – miR319b; red – miR319b.2. Pre-mRNA structures designed, and Gibbs Free Energy (ΔG) calculated with Folder ver. 1.11 (algorithm: RNAfold) (Hansen, 2007). (A) $\Delta G = -80.80$; (B) $\Delta G = -46.40$; (C) $\Delta G = -59.50$.

All of the prepared constructs (the one native and four mutated variants) were next cloned into binary vector pMDC123 (without any promoter) in order to assure that the expression of *MIR319b* variants would be driven by the native promoter located within the 2000-bp-long fragment upstream from *At5g41663* (Curtis and Grossniklaus, 2003). Then, null $\Delta miR319b$ mutant plants were transformed with the prepared constructs using the *Agrobacterium tumefaciens* (AGL1)-mediated floral dip method (Clough and Bent, 2008). Transgenic lines were self-crossed until achieving a homozygous state. Since the pMDC123 vector carries the *bar* resistance gene, mutant plant selection was performed using BASTA herbicide (see Materials and Methods for details).

After the selection of the proper homozygous transgenic lines, T2-collected seeds were grown in soil for 42 days. Then, plant material from stems was harvested for further analyses. As analyzed plant material, the stems were selected accordingly to Sobkowiak and his colleagues' report, in which it was shown that both miR319b and miR319b.2 accumulated at high levels in Arabidopsis stem tissues (Sobkowiak et al., 2012). For each gene construct, three independent transgenic lines were studied. To identify the transgenes, a PCR reaction was applied in which genomic DNA isolated from one leaf of the mutant plant was used as a template. A primer pair was designed to amplify 242 bp of the *bar* gene (Tab. 42). In all of the selected lines, the presence of the transgene was confirmed (Fig. 67). Thus, all of these lines were used for further studies.

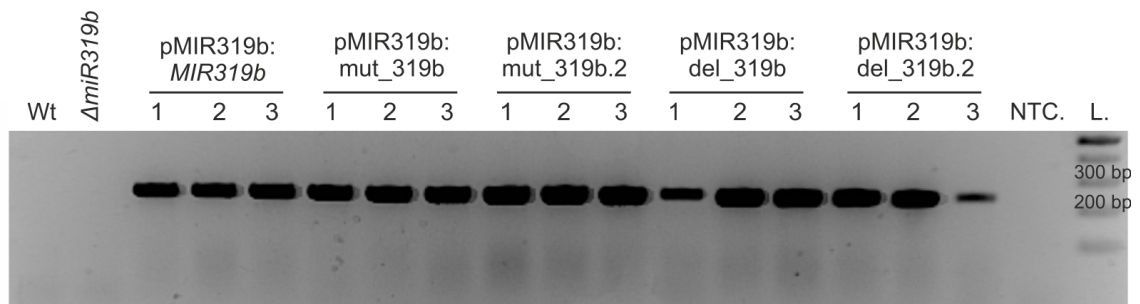


Figure 67. Genotyping of selected Arabidopsis transgenic lines carrying native, mutated, and shortened variants of *MIR319b*. Amplification of 242-bp-long *bar* gene fragment. Wt – wild-type control plants; $\Delta miR319b$ – null *MIR319b* mutant plants; 1, 2, 3 – three independent lines for each construct; NTC – non-template control; L - Gene Ruler 100 bp Plus DNA Ladder.

2.2 Detailed analysis of miR319b and miR319b.2 in selected transgenic lines

2.2.1. Analysis of pri-miR319b and mature miRNA levels in *MIR319b* transgenic lines

At first, the selected transgenic lines were tested for levels of pri-miR319b and mature miRNAs using the RT-qPCR technique. cDNA templates were prepared from the total RNA isolated from the collected 42-day-old Arabidopsis stems. The primer pair for pri-miRNA analysis was designed to amplify 220-bp-long (in the pMIR319b:*MIR319b*, pMIR319b:mut_319b, and pMIR319b:mut_319b.2 constructs) or 178-bp-long products (in lines carrying the pMIR319b:del_319b and pMIR319b:del_319b.2 constructs), respectively (Tab. 41). The obtained results confirmed a significant downregulation of the level of pri-miR319b in *AmiR319b* mutant plants (Fig. 68). Analysis of all transgenic lines revealed an upregulation of the *MIR319b* transcript level (as compared to null mutant plants). The lowest level was observed in two cases: when miR319b/miR319b* were mutated (pMIR319b:mut_319b), and when miR319b/miR319b* were removed (pMIR319b:del_319b). For lines carrying mutated or deleted miR319b.2/miR319b.2* (pMIR319b:mut_319b.2 and pMIR319b:del_319b.2), the level of pri-miR319b fluctuated the most between the lines, but it generally resembled the wild-type level.

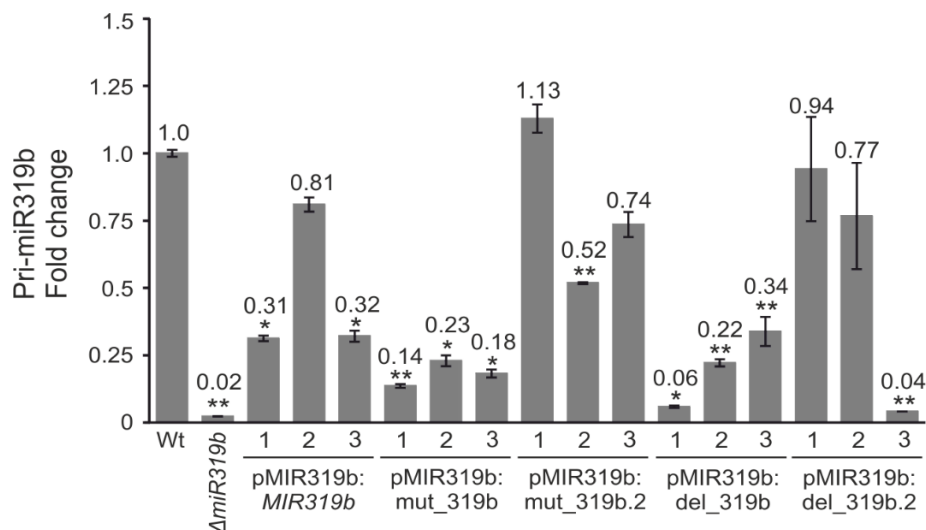


Figure 68. RT-qPCR analysis of the pri-miR319b levels in selected transgenic lines. Error bars indicate SD (n=3), and asterisks indicate significant differences between analyzed sample and wild-type control plants (*p<0.05; **p<0.01).

RT-qPCR analysis of the mature miR319b accumulation in *ΔmiR319b* showed a downregulation of the miR319b level to 42% (as compared to the wild-type plants) (Fig. 69). This was caused by the fact that the TaqMan® probe against miR319b also recognized mature miR319a. In most of the selected transgenic lines, levels of the detected miR319b were comparable to the *ΔmiR319b* mutant (but still significantly lower than in wild-type plants).

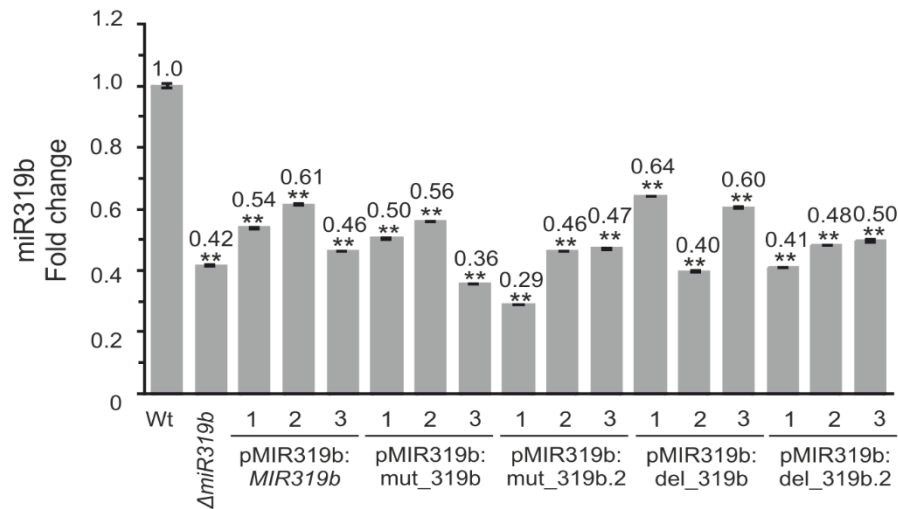


Figure 69. RT-qPCR analysis of the mature miR319b accumulation in selected transgenic lines. Error bars indicate SD (n=3), and asterisks indicate significant differences between analyzed sample and wild-type control plants (**p<0.01).

The level of miR319b.2 in the *ΔmiR319b* mutant was almost undetectable (6%, as compared to wild-type plants) (Fig. 70). The introduction of the native version of *MIR319b* (pMIR319b:*MIR319b*) caused an upregulation of the level of miR319b.2 as compared to the null mutant plants, but this level was still lower than in wild-type plants. As expected, the accumulation of mature miR319b.2 was almost untraceable in those lines carrying the mutated (pMIR319b:mut_319b.2) or deleted (pMIR319b:del_319b.2) miR319b.2/miR319b.2* sequences. Interestingly, modification of the pre-miR319b sequence by mutation (pMIR319b:mut_319b) or removal (pMIR319b:del_319b) of the miR319b/miR319b* sequences also resulted in a very low level of detected mature miR319b.2. This may suggest the existence of the mechanistic cross-regulation of the biogenesis of miR319b and miR319b.2 from the same pre-miR319b hairpin structure.

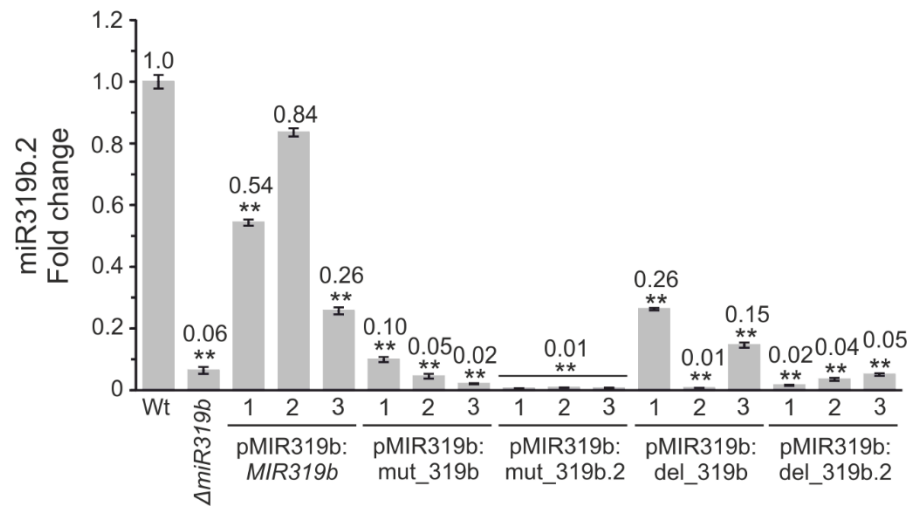


Figure 70. RT-qPCR analysis of the mature miR319b.2 accumulation in selected transgenic lines. Error bars indicate SD (n=3), and asterisks indicate significant differences between analyzed sample and wild-type control plants (**p<0.01).

2.2.2. Analysis of selected target mRNA levels

In the next step, the possibility of crosstalk between the analyzed miRNA species in regulating their target mRNA levels was tested. Primer pairs used in RT-qPCR were designed to frame the identified miRNA cleavage sites within the analyzed target mRNAs (Tab. 42).

For miR319b, four target TCP TF mRNAs were tested (*TCP3*, *TCP4*, *TCP10*, and *TCP24*). The level of *TCP3* mRNA was significantly upregulated in the *ΔmiR319b* mutant (as compared to wild-type plants) (Fig. 71). Unexpectedly, in the analyzed transgenic lines, the *TCP3* mRNA level was mostly downregulated. Only in one line (pMIR319b:del_319b.2_1) significant upregulation was observed, while in several lines, the *TCP3* mRNA levels were not affected at all.

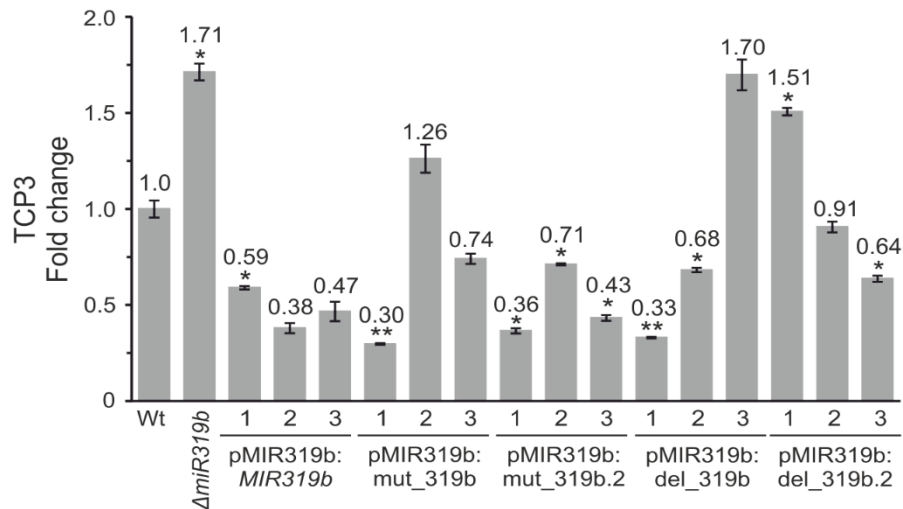


Figure 71. RT-qPCR analysis of the *TCP3* mRNA levels in selected transgenic lines. Error bars indicate SD (n=3), and asterisks indicate significant differences between analyzed sample and wild-type control plants (*p<0.05; **p<0.01).

As for *TCP3* mRNA, also the level of *TCP4* mRNA was upregulated in $\Delta miR319b$ mutant in comparison to wild-type plants (Fig. 72). Unexpectedly, introduction of the native version of *MIR319b* into mutant background (pMIR319b:*MIR319b*) resulted in downregulation of the *TCP4* mRNA level. Remarkably, its level was mostly upregulated in lines with mutated/deleted parts of the miR319b/miR319b* sequences (pMIR319b:mut_319b and pMIR319b:del_319b). The same effect was observed, when miR319b.2/miR319b.2* sequences were changed or removed (pMIR319b:mut_319b.2 and pMIR319b:del_319b.2), that correlated with decreased accumulation of the mature miR319b.2 (Fig. 70). Several lines did not exhibit significant changes of the *TCP4* mRNA levels (Fig. 72).

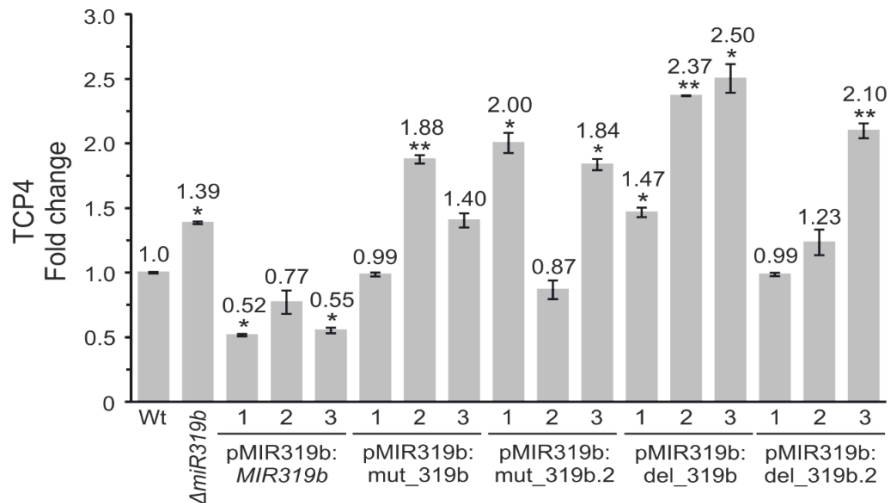


Figure 72. RT-qPCR analysis of the *TCP4* mRNA levels in selected transgenic lines. Error bars indicate SD (n=3) and asterisks indicate significant differences between analyzed sample and wild-type control plants (*p<0.05; **p<0.01).

Even higher upregulation (than for the *TCP3* and *TCP4* mRNAs) was observed for the level of *TCP10* mRNA in the $\Delta miR319b$ mutant (as compared to wild-type plants) (Fig. 73). In lines carrying native *MIR319b* (pMIR319b:*MIR319b*), the level of *TCP10* mRNA was similar to that of the control plants. What is more, in lines with mutated miR319b/miR319b* (pMIR319b:mut_319b), the level of *TCP10* mRNA fluctuated the most. It was significantly upregulated when miR319b/miR319b* were removed from the miRNA stem-loop structure (pMIR319b:del_319b). Interestingly, the level of *TCP10* mRNA was significantly elevated in those lines with mutated/deleted miR319b.2/miR319b.2* (pMIR319b:mut_319b.2 and pMIR319b:del_319b.2), which correlated with a decreased level of mature miR319b.2 (Fig. 70).

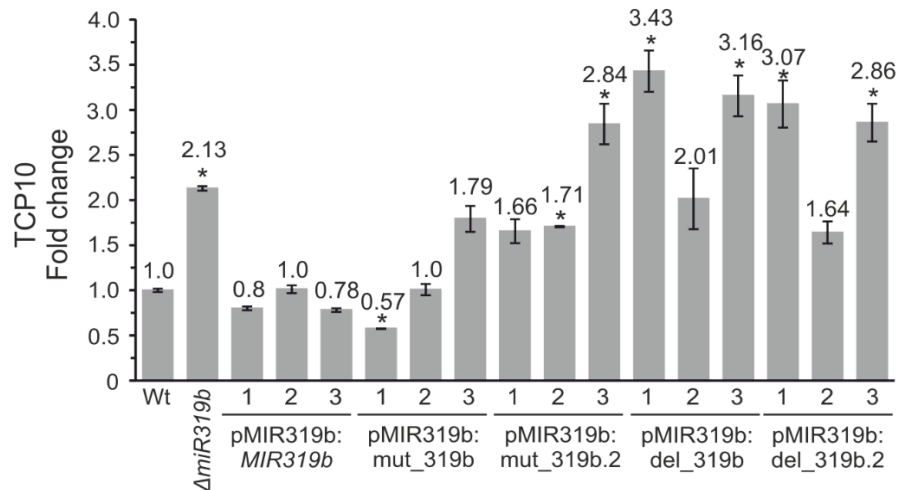


Figure 73. RT-qPCR analysis of the *TCP10* mRNA levels in selected transgenic lines. Error bars indicate SD (n=3), and asterisks indicate significant differences between analyzed sample and wild-type control plants (*p<0.05; **p<0.01).

The same effects found in *TCP10* were also observed for the *TCP24* mRNA (Fig. 74), with the highest upregulation of its level seen in those transgenic lines with deleted miR319b/miR319b* (pMIR319b:del_319b) or miR319b.2/miR319b.2* (pMIR319b:del_319b.2).

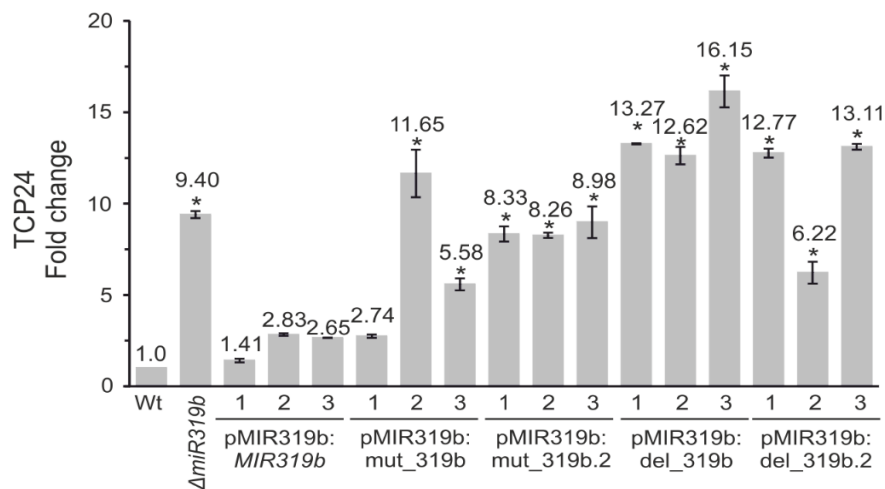


Figure 74. RT-qPCR analysis of the *TCP24* mRNA levels in selected transgenic lines. Error bars indicate SD (n=3), and asterisks indicate significant differences between analyzed sample and wild-type control plants (*p<0.05; **p<0.01).

For miR319b.2, two target mRNA that had been experimentally confirmed previously were analyzed – *TBL10* and the intron-retained (IR) isoform of *RAP2.12* (Sobkowiak et al., 2012; Barciszewska-Pacak et al., 2015). For the *TBL10* mRNA, an upregulation was observed in the $\Delta miR319b$ mutant (as compared to wild-type plants) (Fig. 75). In lines carrying native *MIR319b* (pMIR319b:*MIR319b*), the *TBL10* mRNA levels resembled the expression in control plants. Importantly, significant upregulation of this target mRNA was observed for all four *MIR319b* versions carrying the mutated/shortened variants of pre-miR319b.

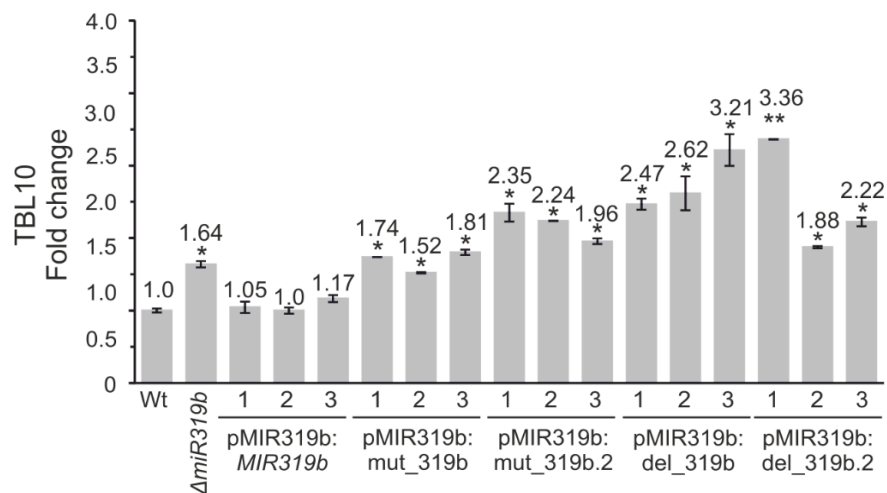


Figure 75. RT-qPCR analysis of the *TBL10* mRNA levels in selected transgenic lines. Error bars indicate SD (n=3), and asterisks indicate significant differences between analyzed sample and wild-type control plants (*p<0.05; **p<0.01).

The levels of the IR-isoform of *RAP2.12* fluctuated more than the *TBL10* mRNA in the analyzed lines (Fig. 76). Its level in the $\Delta miR319b$ mutant was upregulated (but not significantly) when compared to wild-type plants. Moreover, there was no clear effect when native *MIR319b* was introduced into the null mutant background (pMIR319b:*MIR319b*), since the analyzed mRNA levels varied relevantly between the three analyzed transgenic lines. Remarkably, these target isoform levels were mostly elevated in four other lines in which the pre-miR319b sequence was modified.

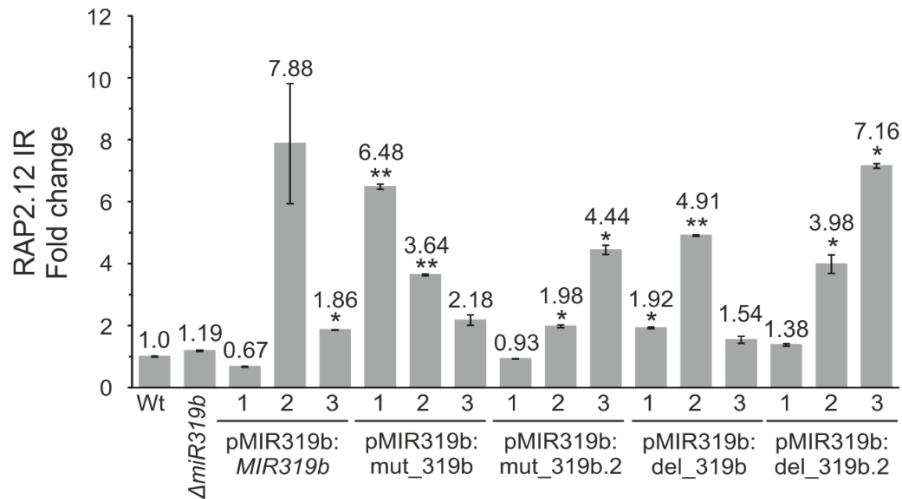


Figure 76. RT-qPCR analysis of the *RAP2.12* intron retained (IR) isoform levels in selected transgenic lines. Error bars indicate SD (n=3), and asterisks indicate significant differences between analyzed sample and wild-type control plants (*p<0.05; **p<0.01).

The presented results showed that the levels of identified miR319b target mRNAs (*TCP4*, *TCP10*, and *TCP24*) changed when miR319b.2/miR319b.2* sequences were altered (pMIR319b:mut_319b.2) or deleted from the pre-miR319b (pMIR319b:del_319b.2). Also, the levels of *TBL10* and the *RAP2.12* IR-isoform were affected in lines with changed/removed miR319b/miR319b* sequences (pMIR319b:mut_319b and pMIR319b:del_319b). Thus, it is highly probable that there is crosstalk between miR319b and miR319b.2 in the regulation of their target mRNA levels based on this data.

DISCUSSION

1 Biogenesis of intronic miRNAs in *Arabidopsis thaliana*

1.1 Plant intronic miRNA accumulation depends on developmental stage or environmental conditions tested

Among 29 identified *Arabidopsis* intronic miRNAs, only 7 species were detected in wild-type plants using the Northern blot approach in the three developmental stages tested (Fig. 28). Three of the miRNAs (miR156d, miR156f, and miR162a) were detected in all analyzed developmental stages. These miRNAs belong to multi-gene miRNA families, in which all small RNAs exhibit nucleotide-sequence similarity to each other. The *MIR156* and *MIR162* families possess ten and two miRNA members, respectively. Thus, it is highly probable that the detected hybridization signals were a sum of the accumulation levels of all miRNAs belonging to the same family (Kozomara and Griffiths-Jones, 2014). Besides, the gene structures are known for only a few members of these families, i.e., *MIR156a*, *MIR156c*, *MIR156d*, *MIR156f*, *MIR162a*, and *MIR162b* (Hirsch et al., 2006; Szarzynska et al., 2009; Zielezinski et al., 2015; Barciszewska-Pacak et al., 2016). These represent the different types of *MIR* genes that (1) encode both the intron-less and intron-containing independent transcription units; or (2) that carry pre-miRNAs within their introns. For these reasons, these miRNAs were not representative examples for further studies of the mechanism of intronic miRNA biogenesis.

On the other hand, hybridization signals were obtained only in one out of the three developmental stages analyzed for the four other detected intronic miRNAs (i.e., miR400, miR402, miR778, and miR850) (Fig. 28). It has been already presented that the genes encoding *A. thaliana* intronic miRNAs are expressed differently in an age- and tissue-dependent manner, which in turn may result in the diverse accumulation of mature miRNAs (Bielewicz et al., 2011; Zielezinski et al., 2015). Moreover, it has been reported that the levels of intronic pri-miRNAs (as well as mature miRNAs) were affected by several abiotic stresses, such as drought, salinity, heat, or metal excess or deficiency (Sunkar and Zhu, 2004; Yan et al., 2012; Barciszewska-Pacak et al., 2015). Thus, the existence of a multitude of factors responsible for the regulation of intronic

miRNA accumulation explains why these miRNAs were barely detected or even undetectable under certain conditions tested.

Based on this data, it can be concluded that the expression of intronic *MIRs* can be stage- or condition-specific (similar to the genes encoding other miRNAs, small RNAs, and mRNAs). This regulation can be connected to the miRNA functions in plant cells under control and changed environmental conditions.

1.2 Plant intronic pri-miRNAs can be transcribed as independent transcription units from their host pre-mRNAs

The performed analyses of the 5' ends of intronic pri-miRNAs using the 5' RLM-RACE PCR approach revealed that not all of these precursors are transcribed as the same transcription units as their host pre-mRNAs (Tab. 46). For 14 out of 29 examples, the identified pri-miRNA transcription start sites were consistent with the TSSs previously defined for their host genes (Lamesch et al., 2011). For 11 other intronic pri-miRNAs, the detected TSSs were located within a range of a few nt (nucleotides) to several hundred nt upstream or downstream from the described host gene TSSs. There is a possibility that the 5' UTRs of the analyzed host genes were wrongly annotated. This can be especially true for the identified differences in TSS locations ranging over about a dozen or so nucleotides (Tab. 46). However, as mentioned above, genes that encode intronic miRNAs are expressed differently in various stages or under various environmental conditions (Sunkar and Zhu, 2004; Bielewicz et al., 2011; Yan et al., 2012; Barciszewska-Pacak et al., 2015; Zielezinski et al., 2015). In the presented experiment, only one developmental stage was studied (35-day-old rosette leaves of wild-type plants). Thus, it cannot be excluded that, in other stages/conditions or in mutant plants, the selection of other new TSSs can be activated (even the same as the TSSs of their host genes). It is also probable that these pri-miRNAs are transcribed independently from their host-gene pre-mRNAs. What is more, for four intronic pri-miRNA examples, no specific amplification products were detected. This probably means that the genes encoding these miRNAs are not sufficiently expressed under the conditions tested.

Interestingly, for 6 out of the 29 analyzed precursors of intronic miRNAs, more than one active TSS was detected (Tab. 46; unpublished data). This may indicate the existence of novel mechanisms of intronic pri-miRNA level regulation via the selection of constitutive or alternative transcription start sites. For example,

5' RLM-RACE PCR analysis of the 5' ends of *MIR400* (*At1g32583*) transcripts (based on amplification from the third exon) revealed that, under control conditions, two TSSs are active – the first (TSS₁), located at the beginning of the *At1g32583* 5' UTR (consistent with the TSS identified with the use of primers annealing to the pre-miR400), and the second (TSS₂), located within the second exon (Fig. 77A) (unpublished data). However, under heat-stress conditions, only TSS₁ was active (Fig. 77B). This correlated with the lower accumulation of mature miR400 (Yan et al., 2012) and selection of the alternative 3'SS (located ~80 nt upstream from the identified TSS₂) (unpublished data).

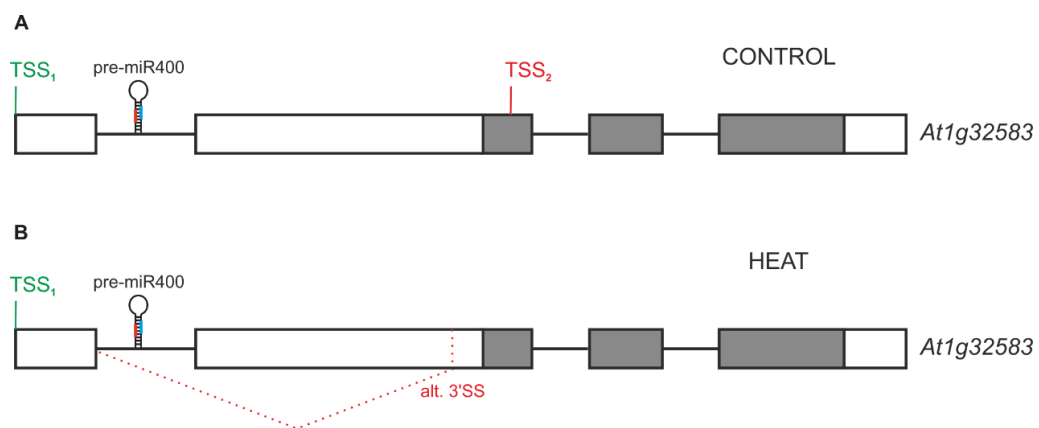


Figure 77. Heat stress affected the selection of transcription start sites within *MIR400* (*At1g32583*). Boxes – exons (protein-coding sequence – gray, UTRs – white); black lines – introns; red and blue lines – miRNA and miRNA*. Constitutive TSS₁ – green; alternative TSS₂ – red; alternative splicing event – red dashed lines.

Moreover, for intronic pre-miR850 and pre-miR5026 (both located within the same intron of the *At4g13495* host gene), several active alternative TSSs were detected (Tab. 46). Some of these are located between the miR850 and miR5026 stem-loop structures. This suggests their potential regulatory role in the uncoupling of clustered miR850 and miR5026 biogenesis by generating unique independent transcription units carrying only one pre-miRNA from one host gene. These observations are consistent with the data published by Ramalingam and colleagues for HeLa cells (Ramalingam et al., 2014). They demonstrated that the precursors of three miRNAs (i.e., pri-miR106b, pri-miR93 and pri-miR25 – located within the same intron of the *MCM7* host gene) can be products of the transcription of autonomous independent transcription units.

Taking all of this information together, the selection of a transcription start site may play an important regulatory role during the biogenesis of intronic miRNA in both

human and plant cells. What is interesting, the efficiency of TSS selection can depend on the conditions applied (like stress factors).

1.3 Splicing inhibition stimulates intronic miRNA biogenesis efficiency

It has already been reported that stress treatment causes splicing pattern changes in as many as 50% of the genes in a cell (Kazan, 2003; Wang and Brendel, 2006; Ali and Reddy, 2008; Marquez et al., 2012; Mastrangelo et al., 2012). This, in turn, may alter mRNA coding potential and eventually protein functions. Among the identified stress-affected genes, there are many examples necessary for the regulation of plant response to abiotic stresses (Filichkin et al., 2010). Besides, stress treatment induces AS changes in the splicing machinery components. It has been documented that, under stress conditions, ~100 various transcripts can be generated from only 16 genes encoding Arabidopsis SR proteins by alternative splicing (Isshiki et al., 2006; Palusa et al., 2007). What is more, since accumulation levels of many plant miRNAs have been stated to be affected by abiotic stress treatments, it is highly probable that stress factors also alter the efficiency of the microprocessor machinery assembly and action (Sunkar and Zhu 2004; Kruszka et al., 2012; Guerra et al., 2015; Nigam et al., 2015; Zhang et al., 2015).

In the presented PhD thesis, experiments performed under selected abiotic stress conditions (i.e., high temperature, salinity, and drought) revealed the complex mechanism of Arabidopsis intronic miR402 maturation. In the analyzed stresses, upregulation of the pri-miR402 and mature miRNA levels (Fig. 31, 38) correlated with the less-efficient splicing of the miR402-hosting intron (Fig. 32A, 39A). The observed effects can be consequences of the stress-induced changes of protein-protein or RNA-protein interaction stability as well as the conformational modifications of the secondary/tertiary structure of RNAs (Chursov et al., 2009; Feig, 2009). Moreover, as previously mentioned, the expression of splicing regulatory factors (like SR proteins) as well as their splicing patterns can change after stress treatment. Based on this, it can be concluded that, under stress conditions, the assembly of the splicing machinery can be affected, along with the less-efficient recognition and binding of spliceosome components and/or splicing factors to particular pre-mRNA sequences (like splice sites, branch points, or splicing enhancers/silencers).

What was interesting, high temperature did not cause any changes in the splicing efficiency of the *At1g77230* fourth intron (Fig. 32B). There are several distinct differences between the first and fourth *MIR402* introns that may play an important role in the regulation of their splicing mechanism. From them, the most important are the following: (1) the fourth intron is much shorter than the first one (so it can be lacking in splicing regulatory elements); and (2) there is no miRNA stem-loop structure present in the fourth intron (thus, its secondary structure is less complicated than in the case of the first intron). Therefore, there may be a mechanism that regulates the splicing efficiency of the *At1g77230* introns in a different manner under the conditions tested.

A similar mechanism of intronic miRNA biogenesis regulation by abiotic stress factors was described by Barciszewska-Pacak and her colleagues for Arabidopsis miR162a (Barciszewska-Pacak et al., 2016). This miRNA is located within the second intron of the *At5g08185* host gene (Hirsch et al., 2006). It was demonstrated that the proper production of miR162a requires the inhibition of splicing efficiency of the miR162a-hosting intron or diminished selection of the alternative 5'SS (located between the miRNA and miRNA* sequences), which in turn leads to the retention of the pre-miRNA-containing intron part within the host mRNA (Fig. 16). This important correlation was observed under stress conditions (i.e., salinity and drought) and was consistent with the mechanism of miR402 biogenesis regulation after stress treatment (Barciszewska-Pacak et al., 2016). In contrast, the level of intronic miR400 was mostly downregulated under abiotic stress conditions (Yan et al., 2012; Barciszewska-Pacak et al., 2015). Moreover, it was reported that, under heat-stress conditions, the less-efficient Arabidopsis miR400 production correlated with the higher selection of alternative 5'SS (located in the miRNA-carrying intron, downstream from the pre-miR400), which leads to miR400 stem-loop-structure retention as a part of the host mRNA (Yan et al., 2012). Based on this, miR400 is processed more efficiently from the released intron. The observed opposite mechanism of intronic miR400 biogenesis regulation can be caused by many additional factors when compared to the production of miR402 and miR162a (like the presence of various regulatory elements within their pri-miRNAs or differences in the structure and stability of their pre-miRNA hairpins) as well as the activity of alternative TSSs, splice sites, and polyA sites that differ between the described intronic miRNA transcripts.

Experiments of the global splicing inhibition by Gex-1A (a chemical compound preventing the U2 snRNP from binding to the pre-mRNA branch points) confirmed the results obtained in stressed *A. thaliana* seedlings (Hasegawa et al., 2011). The less-efficient splicing of the miR402-hosting intron (Fig. 42) correlated with the upregulated accumulation of mature miR402 (Fig. 41B). Literature data indicates that the spliceosome assembly is more complicated and flexible than previously thought and can occur via alternative pathways (Shcherbakova et al., 2013). The authors suggested that 5'SS sequence recognition by the U1 snRNP is not stable. The U1 snRNP complex may dynamically associate and dissociate from this splice site, until the downstream branch point and 3'SS are synthesized by RNA polymerase II. Based on these suggestions, it is possible that the U1 snRNP – 5'SS association can be stable only after the U2 snRNP binding to the BP sequence. These conclusions may explain the observed stimulatory effect of Gex-1A treatment on the production of several Arabidopsis intronic miRNAs (Fig. 41B, 46A, 47A). On the other hand, the indirect effects of global splicing inhibition by Gex-1A cannot be excluded in the presented mechanism. Since herboxidiene inhibits the excision of numerous introns in the cell, observed upregulation of miRNA levels can also be caused by the impaired maturation of the pre-mRNA transcripts of proteins important for miRNA biogenesis and splicing itself. Thus, further experiments are needed to precisely elucidate the mechanism of Gex-1A action on the miRNA production in plants.

What is more, there are also many other mechanisms (like the transcription rate) that can be regulated by stress factors (like drought, heat, and salinity), which can also affect splicing efficiency and *vice versa* (de la Mata et al., 2003; Kwek et al., 2009; Dolata et al., 2015; Barciszewska-Pacak et al., 2015).

To conclude, there are many factors acting at the transcriptional and posttranscriptional levels that can regulate the crosstalk between intronic miRNA biogenesis and the splicing of miRNA-hosting introns; in this way, they can shape the efficiency of miRNA production in plants.

1.4 Active 5' splice site controls biogenesis of intronic miR402

Analyses performed on *Nicotiana benthamiana* plants revealed the important role that the 5' splice site plays in the regulation of intronic miR402 biogenesis. Inactivation of the miR402-hosting intron 5'SS, which resulted in the almost-complete abolishment of this intron splicing, lead to the increased production of mature miR402 (Fig. 49B). Importantly, the effect of the 5'SS on miR402 maturation did not depend on the type and strength of the promoter used nor the type of 5' splice site mutation introduced (Fig. 52-53).

Furthermore, the position of the miRNA stem-loop structure in respect to the nearest active 5' splice site turned out to be pivotal for the regulation of miRNA biogenesis efficiency. When the miR402 hairpin was located downstream from the active 5'SS (pre-miR402 in the first *At1g77230* intron), inactivation of this splice site stimulated the maturation of miR402 (Fig. 58 – lower panel, Variant A). However, when the miR402 stem-loop structure was shifted to the first exon (upstream from the 5'SS), mutation of the 5' splice site inhibited the biogenesis of mature miR402 (Fig. 58 – lower panel, Variant B). These results confirmed the previously observed regulation of the biogenesis of exonic miR163 and miR161 by the 5'SSs of those introns located downstream from the pre-miRNAs (Bielewicz et al., 2013). Moreover, these effects were not caused by altered precursor stability, since there were no differences between the half-life measured for the intronic (Variant A) nor exonic (Variant B) *MIR402* transcripts, respectively (Fig. 61).

In *A. thaliana* seedlings treated with abiotic stress factors, upregulation of miR402 always correlated with higher expression levels of pri-miR402 (Fig. 31A, 38A). Interestingly, in *N. benthamiana*, pri-miR402 abundance was elevated after the mutation of the 5'SS in both Variant A (the pre-miR402 in the intron) and B (the pre-miR402 in the first exon) (Fig. 58 – upper panel). At the same time, mature miRNA levels were up- or down-regulated, respectively (Fig. 58 – lower panel). In Variant A (where primers amplifying pri-miRNA anneal within the miRNA-hosting intron sequence), the measured levels of pri-miR402 mirrored the splicing efficiency of this intron. Thus, inactivation of the 5'SS that caused splicing inhibition of the *At1g77230* first intron resulted in a higher level of pri-miR402 in Variant A. In turn, the pri-miR402 level in Variant B represent the efficiency of precursor processing to mature miR402. Since mutation of the 5'SS decreased the accumulation of miR402, the upregulated levels

of pri-miR402 represented the unprocessed precursor. This is consistent with the observations done in Arabidopsis mutant plants, in which the miRNA biogenesis pathway was defective (i.e., *hyl1-2*, *dcl1-7*, *se-1*, and *cbc*) (Zielezinski et al., 2015).

Summing up, the presented results demonstrate a new regulatory mechanism of biogenesis of Arabidopsis miRNAs derived from the intron-containing *MIR* genes. The 5'SS (located in the closest proximity to the miRNA stem-loop structure) plays main role in this regulation. Importantly, the effect of this active 5'SS depends on its position in respect to the pre-miRNA hairpin and can be stimulatory or inhibitory, respectively, when pre-miRNA is located upstream or downstream from this splice site.

1.5 Selection of polyadenylation site within pri-miRNA transcripts influences plant intronic miRNA biogenesis efficiency

Besides the less-efficient miR402-hosting intron splicing, upregulated miR402 accumulation also correlated with the higher selection of alternative proximal polyadenylation site under the stress conditions tested (Fig. 33, 39B). This polyA site was located in the miRNA-carrying intron, downstream from the pre-miRNA hairpin. Moreover, the same effect was observed when the 5'SS of the first *At1g77230* intron was inactivated (Fig. 51, 59B). This can be explained by the known supplementary role of the U1 snRNP complex in preventing the pre-mRNAs from premature cleavage and polyadenylation (Kaida et al., 2010). The authors discovered that, when the U1 snRNP is bound to the 5'SS of the pre-mRNA, it inhibits the action of the polyadenylation machinery at cryptic polyA sites located within the first few kilobases from this 5' splice site.

However, the preferable selection of the proximal polyA site in *MIR402* transcripts did not always correlate with the more-efficient production of mature miR402. In both variants, the proximal polyA site was selected more often after inactivation of the *At1g77230* first intron 5'SS in the construct with intronic (Variant A) and exonic (Variant B) pre-miR402 localization (Fig. 59B). At the same time, the accumulation of miR402 was upregulated or downregulated in Variant A or Variant B, respectively (Fig. 58 – *lower panel*). Similar observations were presented by Bielewicz and colleagues for Arabidopsis miR163 (Bielewicz et al., 2013). They demonstrated that, after inactivation of the 5'SS of the pre-miR163-downstream intron, the splicing inhibition

correlated with the preferential selection of a proximal intronic polyadenylation site and, at the same time, a decreased accumulation of mature miR163.

Taking all of this data into consideration, activity of the 5'SS located closest to the pre-miRNA hairpin predominantly regulates the biogenesis efficiency of Arabidopsis miRNAs encoded by the intron-containing *MIR* genes. This is caused by the changed splicing efficiency of these introns but not always by the selection of polyadenylation sites.

1.6 SERRATE is key player in a crosstalk between the plant microprocessor and spliceosome

The presented data indicates that splicing and intronic miRNA biogenesis are coupled in plants. Thus, it is clear that there is a crosstalk between the spliceosome and plant microprocessor in plant cells. Moreover, many proteins that are involved in miRNA maturation, like CBP20, CBP80, SE, etc. (see also Table 1), were additionally shown to regulate the splicing of both pre-mRNAs and pri-miRNAs (Laubinger et al., 2008; Raczynska et al., 2010, 2014). Among them, SERRATE was found to be an interacting partner of many other proteins participating in miRNA biogenesis, like CPL1, TOUGH, NOT2, RACK1, and PRL1 (Manavella et al., 2012; Ren et al., 2012; Wang et al., 2012; Speth et al., 2013; Zhang et al., 2014). Therefore, SE looks like the best candidate for being a key communicator between different RNA metabolism machineries, like between the microprocessor and spliceosome in plants.

Recently published data has proven these assumptions by revealing interactions between the SERRATE protein and the four U1 snRNP auxiliary components; i.e., PRP39b, PRP40a, PRP40b, and LUC7l (Knop and Stepien et al., 2016). The experiments presented in this work confirmed the perfect colocalization and direct interactions between these proteins, both *in vitro* (by a pull-down assay) and *in vivo* in the plant cell (by the FRET-FLIM technique in *A. thaliana* protoplasts). It was also described in the introduction that SE comprises of the structured core and two unstructured termini located at the N- and C- protein ends (Machida et al., 2011). The core part of SERRATE was demonstrated to interact with HYL1 and CBC (Raczynska et al., 2014). For interactions with RNA and DCL1, the core part and N-terminus of SE are required (Iwata et al., 2013). The latest data indicated that SERRATE connects with the U1 snRNP auxiliary partners

by N- and C- unstructured tails (Knop and Stepien et al., 2016). Based on this data, it is possible that SE interacts with components of the microprocessor and spliceosome at the same time.

It has also been reported that the SERRATE version lacking 40 amino acids from the C-terminus (present in *se-2* mutant plants) is not able to interact with the U1 snRNP components (PRP39b, PRP40a, and PRP40b) (Grigg et al., 2005; Knop and Stepien et al., 2016). In *se-1* mutant plants (where the SE protein is shorter by 20 aa from the C-tail), communication between the microprocessor and spliceosome still occurs (Prigge and Wagner, 2001; Knop and Stepien et al., 2016). The results presented within this PhD thesis describe the downregulation of intronic mature miR402 and miR1888a levels in the *se-1* mutant when compared to wild-type plants (Fig. 62A, 63A), which was caused by miRNA biogenesis impairment in *se-1* (Prigge and Wagner, 2001; Zielezinski et al., 2015). Interestingly, the accumulation of miR402 and miR1888a increased in *se-2* plants, which correlated with the less-efficient splicing of the miRNA-carrying introns when compared to *se-1* (Fig. 62B, 63B). In contrast, it was demonstrated that the inhibition of splicing of the pri-mRNA-downstream located intron in *se-2* plants correlated with an even-lower decreased accumulation of mature miRNAs for exonic miRNAs (miR163 and miR171b) when compared to *se-1* mutant (Fig. 78) (Knop and Stepien et al., 2016).

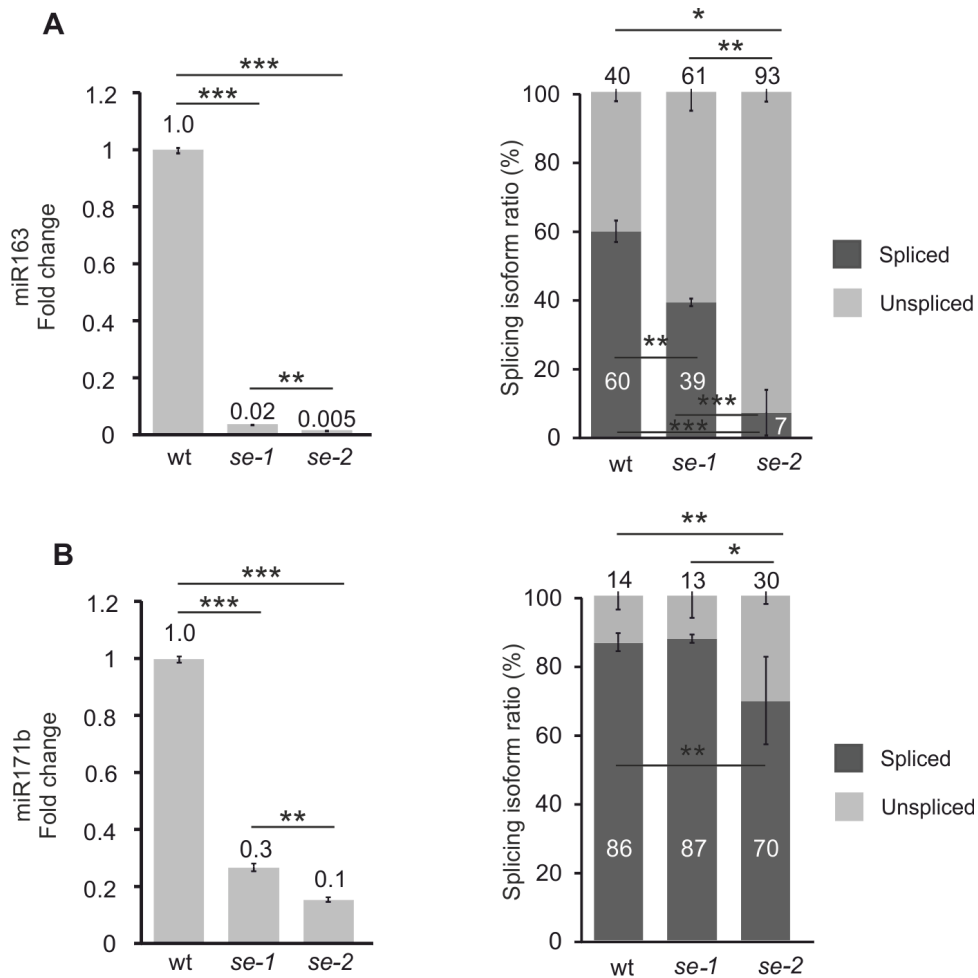


Figure 78. The interactions between SERRATE and the U1 snRNP auxiliary proteins affect exonic miRNA biogenesis in *A. thaliana* (Knop and Stepien et al., 2016). (A) RT-qPCR analysis of the level of mature miR163 and splicing efficiency of the pre-miR163-downstream located intron. (B) RT-qPCR analysis of the level of mature miR171b and splicing efficiency of the pre-miR171b-downstream located intron. (A-B) Error bars indicate SD (n=3), and asterisks indicate significant differences between analyzed samples and control plants (*p<0.05; **p<0.01; ***p<0.001).

These observations pointed to the essential role of the microprocessor – spliceosome communication during the biogenesis of Arabidopsis miRNAs encoded by intron-containing *MIR* genes. What is more, the effect of these connections depends on the position of the stem-loop structure regarding the nearest place of binding of the U1 snRNP complex, so the 5' splice site. Based on the results presented within this PhD thesis as well as data in the literature, the following models of plant miRNA biogenesis regulation can be proposed (Fig. 79). For intronic miRNA, when the 5' splice site located upstream from the miRNA stem-loop structure is active, SE interacts strongly with the U1 snRNP complex and poorly with other components of the plant microprocessor complex. As a result, the splicing of the miRNA-hosting intron

is stimulated, and miRNA biogenesis is less efficient (Fig. 79A – *upper panel*). After inactivation of this 5'SS, the U1 snRNP binding is blocked; thus, SE fully participates in the microprocessor formation. Therefore, excision of the miRNA-carrying intron is inhibited, and the miRNA biogenesis is stimulated (Fig. 79A – *lower panel*). For exonic miRNAs whose introns are located downstream from the pre-miRNA hairpin, SE and other proteins of the plant microprocessor bind to the precursor after stem-loop structure formation. When the 5'SS is active, binding of the U1 snRNP stabilizes interactions between SE and other microprocessor components, which in turn results in the more-efficient production of miRNA (Fig. 79B – *upper panel*). On the other hand, the lack of the U1 snRNP caused by inactivation of the 5' splice site leads to the less-stable formation of the plant microprocessor, which alters pri-miRNA processing (Fig. 79B – *lower panel*).

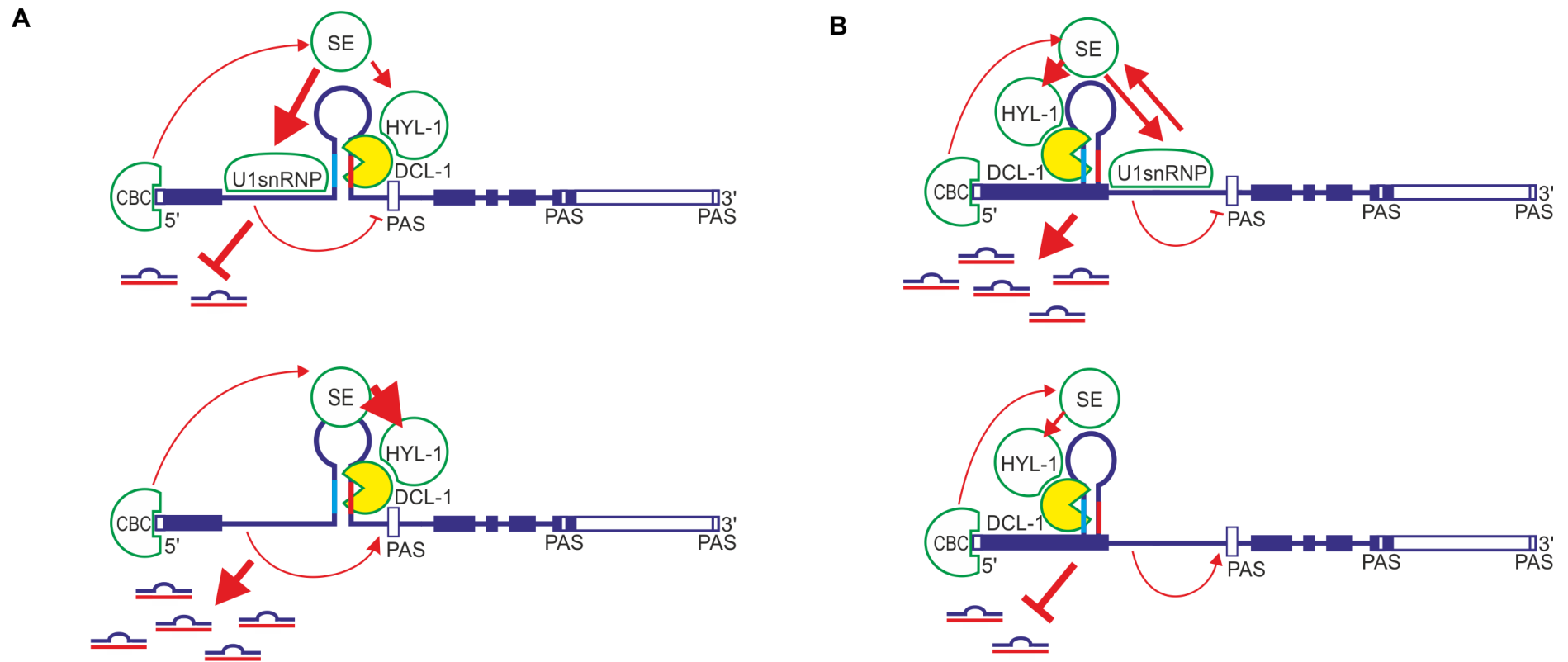


Figure 79. Proposed model of the crosstalk between the plant microprocessor complex and spliceosome during biogenesis of (A) intronic and (B) exonic miRNAs in *A. thaliana* (Knop and Stepien et al., 2016). Boxes – exons (dark blue – coding sequence), lines – introns, light blue and red lines – miRNA and miRNA*, thick arrows – strong interactions, thin arrows – weak interactions, no-headed arrow – inhibition, open boxes – proximal and distal polyadenylation sites (PAS). CBC, CAP-BINDING COMPLEX; SE, SERRATE; HYL1, HYPOPLASTIC LEAVES 1; DCL1, DICER-LIKE1.

1.7 Co-transcriptional regulation of intronic miRNA biogenesis in plants

Besides the regulation of intronic miRNA biogenesis at the posttranscriptional level, there are additional possibilities of pri-miRNA coordination worthy of consideration. In 2008, evidence concerning co-transcriptional processing of miRNA precursors in human cells was presented (Morlando et al., 2008). It was demonstrated that Drosha may associate with the chromatin of some *MIR* genes and that the processing of miRNA precursors occurs co-transcriptionally, before the miRNA-carrying intron is spliced out from the host pre-mRNA. Besides, in many mammalian long non-coding RNA transcripts possessing miRNAs, termination of transcription can be conducted via microprocessor cleavage of the precursor (Dhir et al., 2015). Moreover, it was presented that the AGO1 protein in animals interacts with RNA Pol II and, therefore, is able to regulate the expression and splicing of many genes in the cell (Ameyar-Zazoua et al., 2012; Huang et al., 2013; Allo et al., 2014).

Importantly, it was reported that inactivation of the Elongator complex (a multi-subunit complex interacting with elongating RNA Pol II) in plants resulted in a decreased level of RNA polymerase II associated with the *MIR* genes (Otero et al., 1999; Fang et al., 2015). This correlated with downregulated pri-miRNA levels. What is more, there are several proteins (like CDC5, NOT2, and CDF2) that were described to regulate *MIR* transcription and, thus, influence pri-miRNA and mature miRNA levels (Wang et al., 2013; Zhang et al., 2013; Sun et al., 2015). Recently published data has indicated that AGO1 can also be involved in the regulation of *MIR* gene transcription in plants (Dolata et al., 2016). The authors presented that AGO1 can interact with the newly synthesized *MIR* transcripts, which in turn results in the premature dissociation of RNA Pol II from miRNA genes and eventually a decreased expression level of pri-miRNAs.

Based on these findings, miRNA biogenesis can be coordinated at both the transcriptional and posttranscriptional levels. However, knowledge regarding all of the possibilities of plant miRNA maturation mechanism regulation is still incomplete.

2 Functional dissection of miR319b and miR319b.2 biogenesis in plants

The second part of the presented PhD thesis concerns the biogenesis of miR319b and miR319b.2. These miRNAs belong to a specific, highly conserved *MIR319b* family (Arazi et al., 2005; Axtell and Bartel, 2005; Axtell et al., 2007). Expression of Arabidopsis *MIR319b* was identified as tissue- and age-dependent, with the highest levels found in adult plants (in stems and inflorescences) (Palatnik et al., 2003; Sobkowiak et al., 2012). Mature miR319b has been demonstrated to control the expression level of a broad range of genes encoding TCP transcription factors (Palatnik et al., 2003; Nag et al., 2009). Therefore, this miRNA is involved in the regulation of many developmental processes, like leaf and flower morphogenesis or plant reproduction. Moreover, miR319b was reported to be a multi stress-responsive miRNA (Sunkar and Zhu, 2004; Liu et al., 2008; Zhou et al., 2008; Barciszewska-Pacak et al., 2015).

Especially interesting in the *MIR319b* family is the fact that two functional mature miRNAs are located within one pre-miR319b structure: miR319b and miR319b.2 (Zhang et al., 2010; Sobkowiak et al., 2012). This is a unique and characteristic feature of plant pre-miR319 precursors that (besides pre-miR319b) is also true for pre-miR319a and pre-miR319c (from which miR319a and miR319a.2 or miR319c and miR319c.2 derive, respectively). Among these additional miRNAs, miR319b.2 has been reported to accumulate at the highest level, which changes under abiotic stress conditions (Sobkowiak et al., 2012; Barciszewska-Pacak et al., 2015). Interestingly, it has been shown that miR319b.2 targets the AS-isoform of the *RAP2.12* transcription factor and *TBL10*. Therefore, miR319b and miR319b.2 differ in nucleotide sequence and targeted mRNAs even though they originate from the same pre-miRNA hairpin. On the other hand, these miRNAs can be functionally connected, since TCPs control the jasmonate biogenesis pathway and regulate leaf aging, while *RAP2.12* has been shown to be involved in a plant's senescence and response to osmotic stress (Schomer et al., 2008; Papdi et al., 2008; Shan et al., 2011). Therefore, it was particularly interesting to check whether miR319b and miR319b.2 biogenesis is mechanistically coupled and to find out if these miRNAs may function in a synergistic or antagonistic way via the cross-regulation of their target mRNA levels or the metabolic pathways in which these mRNAs are involved.

To analyze these issues, five *Arabidopsis* transgenic lines carrying native, mutated, or shortened versions of pre-miR319b (transformed into a Δ *miR319b* mutant) were generated (Fig. 64-66). Introduction of the native version of *MIR319b* (*At5g41663*) (pMIR319b:*MIR319b*) into the null mutant background resulted in the reconstitution of the miRNA precursor wild-type level in only one out of three transgenic lines (Fig. 68). Such a discrepancy was observed despite the fact that *MIR319b* expression ought to be controlled by the native *At5g41663* promoter. Moreover, the lowest levels of pri-miR319b were detected in those lines carrying mutated or deleted miR319b/miR319b* sequences (pMIR319b:mut_319b and pMIR319b:del_319b). In the case of miR319b.2/miR319b.2* sequence mutation or removal (pMIR319b:mut_319b.2 or pMIR319b:del_319b.2), the pri-miRNA levels resembled that of the wild-type plant the most. Mature miR319b levels in all of the analyzed transgenic lines were downregulated when compared to wild-type plants (and similar to the mature miRNA level detected in the null Δ *miR319b* mutant) (Fig. 69). This may suggest that miR319b cannot be efficiently produced in any of the transgenic lines prepared, even in those lines carrying native *MIR319b*. However, these results were not quite informative, especially due to the identical nucleotide sequences of mature miR319a and miR319b (Palatnik et al., 2007). Up until now, there has been no available method of miRNA detection that allows us to distinguish between these two miRNA species. MiR319b.2 levels in those lines with the introduced native *MIR319b* version were lower than in wild-type control plants (but still higher than in the other lines analyzed) (Fig. 70). As expected, in those lines with modified miR319b.2/miR319b.2* sequences (pMIR319b:mut_319b.2 and pMIR319b:del_319b.2), the accumulation levels of miR319b.2 were undetectable. What was particularly interesting, the mutation or deletion of miR319b/miR319b* sequences (pMIR319b:mut_319b and pMIR319b:del_319b) resulted in the strong inhibition of mature miR319b.2 production.

Based on these observations, several conclusions can be drawn. Since the significant downregulation of pri-miR319b levels correlated with lower levels of mature miRNAs in those lines with altered miR319b/miR319b* sequences (pMIR319b:mut_319b and pMIR319b:del_319b), it is possible that the introduced modifications reduced the *MIR319b* transcription rate. It is likely that any transcription regulatory elements (like the TF binding sites) can be located within those miR319b or miR319b* sequences whose alterations may affect RNA Pol II processivity.

On the other hand, these modifications can decrease *MIR319b* transcript stability, which in turn results in the downregulation of pri-miRNA and miRNA levels. To analyze such possibilities, additional experiments are required, such as a comparison of (1) RNA polymerase II occupancy on the *MIR319b* gene body; and (2) pri-miR319b stabilities between the generated transgenic lines. Besides, miRNA/miRNA*-sequence manipulations may lead to the less-stable folding of the miR319b stem-loop structure, which in turn affects the efficiency of biogenesis in both miRNAs. This can be relevant in such a case, since the pre-miR319b part containing miR319b and miR319b* seems to be the most-stable fragment of the pre-miRNA hairpin formed. Predominantly shortening of pre-miRNA structure may significantly influence the efficiency of mature miRNA biogenesis from the pri-miR319b precursor. This aspect is even more interesting in light of the specific mechanism of pre-miR319b hairpin processing that involves the “loop-to-base” direction of DCL1 cleavage (Bologna et al., 2009, 2013). There is a high probability that the mutation/removal of miRNA/miRNA* sequences from pre-miR319b changes the direction of precursor processing, therefore causing miR319b or miR319b.2 production efficiency to be lower. To confirm this assumption, some supplementary experiments are needed in order to elucidate the processing mechanism of pre-miR319b in all of the generated transgenic lines. For this purpose, the 5' RACE PCR approach can be used, which allows for the detection of pre-miRNA cleavage products (as presented by Bologna and colleagues (Bologna et al., 2009).

The analyses of miR319b target mRNA levels revealed that the levels of *TCP4*, *TCP10*, and *TCP24* (targeted by miR319b) were mostly upregulated in those lines carrying modified pre-miR319b structures, which was also observed in those lines with alterations introduced within their miR319b.2/miR319b.2* sequences (Fig. 72-74). For the *TCP3* target mRNA, there was no obvious regulation observed under the conditions tested (Fig. 71). Moreover, upregulation of both miR319b.2 target mRNAs (*TBL10* and the IR-isoform of *RAP.12*) was observed in each transgenic line carrying the modified pre-miR319b hairpin (Fig. 75-76). These results indicate that there is a possibility of cross-regulation of the target mRNAs between miR319b and miR319b.2. However, in order to prove that the observed effect is direct or indirect, further experiments are required.

Taking all this data together, it has been presented that the introduced modification within the pre-miR319b structure may change the precursor processing mechanism and/or efficiency, and eventually the accumulation of mature miRNAs.

Therefore, it looks like the biogenesis of miR319b seems to be influenced by the processing efficiency of miR319b.2 and *vice versa*. However, further experiments are still necessary to fully understand the mutual dependences between these two miRNAs during their biogenesis. What is more, it has been presented that the *A. thaliana* null $\Delta miR319b$ mutant exhibits growth retardation and altered leaf shape (as compared to wild-type plants) (Sobkowiak et al., 2012). Thus, it would be worth analyzing whether the phenotypes of the generated transgenic lines differ from the phenotypes of the $\Delta miR319b$ mutant and wild-type plants. Such experiments are required to finally dissect the miR319b and miR319b.2 functions in plant-development regulation.

CONCLUSIONS

- 1 Many *A. thaliana* intronic miRNAs accumulate at different levels in an age- and environmental condition-dependent manner.
- 2 The majority of the characterized Arabidopsis intronic pri-miRNAs seem to be transcriptionally linked to their host pre-mRNAs, and their transcription is regulated from the same promoter regions. For several intronic *MIR* transcripts, alternative transcription start sites have been identified.
- 3 The selection of a transcription start site may play an important regulatory role during the maturation of intronic miRNAs.
- 4 Abiotic stress treatment stimulates the production of Arabidopsis intronic miR402, which correlates with miRNA-hosting intron splicing inhibition and alternative intronic proximal polyadenylation site selection.
- 5 The active 5' splice site of the miRNA-hosting intron plays an important role in the regulation of intronic miR402 biogenesis efficiency.
- 6 The effect of the active 5' SS on miRNA maturation clearly depends on the position of the miRNA stem-loop structure in regards to this splice site. This effect can be inhibitory or stimulatory when the pre-miRNA hairpin is located downstream or upstream from the nearest 5'SS, respectively.
- 7 The competition between the microprocessor and spliceosome as well as the selection of polyadenylation sites can play essential roles in the regulation of plant intronic miRNA biogenesis.
- 8 The biogenesis of *Arabidopsis thaliana* miR319b and miR319b.2 seems to be mechanistically coupled. Moreover, mature miR319b and miR319b.2 can cross-regulate their target mRNA levels.
- 9 Modifications of the miR319b/miR319b*-containing part of the pre-miR319b hairpin alter mature miR319b.2 production efficiency. The alterations introduced within this part of the miRNA stem-loop structure can influence the *MIR319b* transcription rate, pri-miR319b half-life, folding of the pre-miR319b stem-loop structure, and/or direction of pri-miR319b processing by the microprocessor complex.

FUTURE PERSPECTIVES

1. Analysis of biogenesis efficiency of Arabidopsis miRNAs derived from intron-containing *MIR* genes in splicing mutants

The results presented in this PhD thesis, along with the many experiments performed by others, demonstrate the important role of splicing during miRNA biogenesis in *Arabidopsis thaliana* (Bielewicz et al., 2013; Schwab et al., 2013; Barciszewska-Pacak et al., 2016). Therefore, it would be interesting to check the efficiency of maturation of all known Arabidopsis miRNAs derived from intron-containing genes in selected mutants of the splicing machinery. Bielewicz and colleagues have already observed a decreased accumulation of mature miR163 in several SR protein mutants (e.g., *rs31*, *rs2z33*, *sr34*, and *scl30a*) (Bielewicz et al., 2013). Some preliminary experiments have also revealed that levels of the selected intronic miRNAs were affected in these mutants (unpublished data). Moreover, it would be worth checking the efficiency of miRNA biogenesis in *A. thaliana* mutants with altered levels of the U1 snRNP or the U2 snRNP complexes.

2. Analysis of miRNA maturation in mutants of polyadenylation machinery in *A. thaliana*

As it was shown, the selection of polyadenylation sites within pri-miRNA transcripts can influence the biogenesis efficiency of Arabidopsis miRNAs. Moreover, it has already been demonstrated in the Department of Gene Expression that the accumulation levels of several miRNAs derived from intron-containing *MIR* genes were affected in polyadenylation machinery mutants (Szewc et al., unpublished data). Thus, it would be worth performing a wider analysis of the effect of polyadenylation mechanism alterations on the biogenesis efficiency of all plant miRNAs, using *A. thaliana* mutants of Poly(A) Polymerases (PAPs), Cleavage Stimulatory Factors (CstFs), and/or Cleavage and Polyadenylation Specificity Factors (CPSFs), for example.

3. Analysis of interactions between the microprocessor, spliceosome and polyadenylation machinery in plants

The presented results point to the existence of communications between the microprocessor, spliceosome, and polyadenylation machinery in plants. The effects of these interactions can differently shape the efficiency of miRNA biogenesis. It has already been reported that SE is involved in the crosstalk between miRNA biogenesis and the splicing machineries of *A. thaliana* (Knop and Stepien et al., 2016). These studies should be extended in order to find key interactors between the polyadenylation machinery and microprocessor and/or spliceosome complexes. Such analyses are currently ongoing in the Department of Gene Expression.

4. Global analysis of polyadenylation patterns of Arabidopsis *MIR* transcripts under selected abiotic stress conditions

As already demonstrated, the selection of polyadenylation sites of several Arabidopsis pri-miRNAs was affected under several abiotic stresses tested (Barciszewska-Pacak et al., 2016; Knop and Stepien et al., 2016). On the other hand, the efficiency of *A. thaliana* miRNA maturation changed significantly after stress treatment (Guerra et al., 2015; Nigam et al., 2015; Zhang, 2015; Barciszewska-Pacak et al., 2015, 2016). Therefore, it would be interesting to check for global changes of polyadenylation patterns of *MIR* transcripts and their effect on miRNA biogenesis under selected abiotic stresses.

5. Analysis of the presence and role of cryptic U1 snRNP-binding sites within *MIR* genes

The presented results (as well as recently published reports) have revealed that inactivation of the 5' splice site also resulted in the higher selection of alternative proximal polyA sites in plants (Bielewicz et al., 2013). This is in agreement with experiments performed in human cells, which demonstrated a new function of the U1 snRNP in protecting pre-mRNAs from premature cleavage and polyadenylation (Kaida et al., 2010; Martinson, 2011; Berg et al., 2012). Interestingly, within many transcripts (also pri-miRNAs), there are many cryptic U1 snRNP binding sites that can be identified using bioinformatics tools. Since the presence of the U1 snRNP

significantly influences plant miRNA biogenesis efficiency, it would be worth analyzing whether the U1 snRNP can also bind within intron-less *MIR* transcripts, and in that way regulate the maturation of miRNAs deriving from such genes.

6. Analysis of influence of transcription start-site selection on plant miRNA biogenesis

As presented for *MIR* transcripts, the selection of alternative transcription start sites has been observed (Zielezinski et al., 2015). The activity of constitutive and/or alternative TSSs can be an important regulatory mechanism of plant miRNA biogenesis and may depend on age or environmental conditions. Since such regulation was presented to be involved in the uncoupling biogenesis of miR106b-miR93-miR25 clustered miRNAs in human cells, such a mechanism can also occur in plant cells (Ramalingam et al., 2014). Notably, there are several identified clustered miRNAs in *A. thaliana* (Zielezinski et al., 2015); therefore, it would be interesting to analyze the importance of TSS selection in the regulation of plant miRNA biogenesis under various conditions.

7. Analysis of the role of transcription rate and pri-miRNA stability during biogenesis of miR319b and miR319b.2 in generated *MIR319b* transgenic lines

The results obtained in the second part of the presented PhD thesis revealed the downregulation of the pri-miR319b and the miR319b.2 levels in transgenic lines carrying the mutated/deleted miR319b/miR319* sequences. Therefore, it would be worth analyzing whether the observed effects can be caused by a reduced rate of *MIR319b* transcription or lower pri-miRNA stability in generated transgenic lines. To check the efficiency of transcription, the chromatin immunoprecipitation (ChIP) approach can be applied to compare RNA polymerase II processivity through the *MIR319b* gene between selected mutant lines. Moreover, the cordycepin assay should be used to perform a pri-miR319b half-life comparison between the generated transgenic lines.

8. Analysis of direction of pri-miR319b processing mechanism in generated *MIR319b* transgenic lines

Bologna and colleagues demonstrated that the pre-miR319b hairpin is processed to miRNA/miRNA* duplexes in a specific manner (called the “*loop-to-base*” mechanism) (Bologna et al., 2009, 2013). DCL1 performs four cuts, starting from the loop and proceeding towards the base of the hairpin. On the other hand, most pre-miRNAs are processed in the opposite direction – from the base to the loop of the hairpin structure (the “*base-to-loop*” mechanism). The direction of DCL1 cleavage depends on the structural features of pre-miRNA stem-loops. Based on this, modifications introduced within the pre-miR319b sequence might influence the proper folding of the pre-miR319b stem-loop structure, which in turn could result in a changed mechanism of pre-miRNA processing to mature miRNAs. Therefore, additional experiments are currently in progress in order to elucidate the direction of DCL1 cleavage of modified *MIR319b* transcripts in the generated transgenic lines.

9. Comparison of phenotype features between selected *MIR319b* transgenic lines, *ΔmiR319b* null mutant, and wild-type plants

In 2012, Sobkowiak and colleagues described a phenotype of the *A. thaliana* null *ΔmiR319b* mutant (Sobkowiak et al., 2012). This mutant exhibits significant developmental changes (like growth retardation and different leaf shape) when compared to wild-type plants. Therefore, it would be interesting to carry on a phenotypical analysis of those generated transgenic lines with mutated/shortened versions of pre-miR319b. The results of such an analysis can be helpful in discovering which phenotype features of the *ΔmiR319b* mutant are caused by a lack of miR319b and which by the absence of miR319b.2 in the plant cell.

10. Analysis of miR319b and miR319b.2 biogenesis mechanism under selected abiotic stress conditions

Since both miR319b and miR319b.2 have been shown to be responsive to stress treatment (Sunkar and Zhu, 2004; Liu et al., 2008; Zhou et al., 2008; Barciszewska-Pacak et al., 2015), it would be worth analyzing the biogenesis of these miRNAs in detail under selected abiotic stress conditions.

LITERATURE

- Abdel-Ghany SE, Pilon M. (2008). MicroRNA-mediated systemic down-regulation of copper protein expression in response to low copper availability in Arabidopsis. *J Biol Chem* 283:15932–15945
- Addo-Quaye C, Eshoo TW, Bartel DP, Axtell MJ. (2008). Endogenous siRNA and miRNA targets identified by sequencing of the Arabidopsis degradome. *Curr Biol* 18:758–762
- Agranat-Tamir L, Shomron N, Sperling J, Sperling R. (2014). Interplay between pre-mRNA splicing and microRNA biogenesis within the supraspliceosome. *Nucleic Acids Res* 42:4640–4651
- Aguilar-Martinez JA, Sinha N. (2013). Analysis of the role of Arabidopsis class I TCP genes AtTCP7, AtTCP8, AtTCP22, and AtTCP23 in leaf development. *Front Plant Sci* 4:406
- Alaba S, Piszczalka P, Pietrykowska H, Pacak AM, Sierocka I, Nuc PW, Singh K, Plewka P, Sulkowska A, Jarmolowski A. (2015). The liverwort *Pellia endiviifolia* shares microtranscriptomic traits that are common to green algae and land plants. *New Phytol* 206:352–367
- Ali GS, Golovkin M, Reddy AS. (2003). Nuclear localization and in vivo dynamics of a plantspecific serine/arginine-rich protein. *Plant J* 36:883–893
- Ali GS, Reddy AS. (2008). Regulation of alternative splicing of pre-mRNAs by stresses. *Curr Top Microbiol Immunol* 326:257–275
- Allen RS, Li J, Stahle MI, Dubroue A, Gubler F, Millar AA. (2007). Genetic analysis reveals functional redundancy and the major target genes of the Arabidopsis miR159 family. *Proc Natl Acad Sci USA* 104:16371–16376
- Allo M, Agirre E, Bessonov S, Bertucci P, Acuña LG, Buggiano V, Bellora N, Singh B, Petrillo E, Blaustein M. (2014). Argonaute-1 binds transcriptional enhancers and controls constitutive and alternative splicing in human cells. *Proc Natl Acad Sci USA* 111:15622–15629
- Altschul SF, Gish W, Miller W, Myers EW, Lipman DJ. (1990). Basic local alignment search tool. *J Mol Biol* 215:403–410
- Ameyar-Zazoua M, Rachez C, Souidi M, Robin P, Fritsch L, Young R, Morozova N, Fenouil R, Descostes N, Andrau JC, Mathieu J, Hamiche A, Ait-Si-Ali S, Muchardt C, Batsche E, Harel-Bellan A. (2012). Argonaute proteins couple chromatin silencing to alternative splicing. *Nat Struct Mol Biol* 19:998–1004
- Arazi T, Talmor-Neiman M, Stav R, Riese M, Huijser P, Baulcombe DC. (2005). Cloning and characterization of micro-RNAs from moss. *Plant J* 43:837–848

- Aukerman MJ, Sakai H. (2003). Regulation of Flowering Time and Floral Organ Identity by a MicroRNA and Its APETALA2-Like Target Genes. *Plant Cell* 15:2730–2741
- Aung K, Lin SI, Wu CC, Huang YT, Su CL, Chiou TJ. (2006). Pho2, a phosphate overaccumulator, is caused by a nonsense mutation in a microRNA399 target gene. *Plant Physiol* 141:1000–1011
- Axtell MJ, Bartel DP. (2005). Antiquity of microRNAs and their targets in land plants. *Plant Cell* 17:1658–1673
- Axtell MJ, Snyder JA, Bartel DP. (2007). Common functions for diverse small RNAs of land plants. *Plant Cell* 19:1750–1769
- Backman TW, Sullivan CM, Cumbie JS, Miller ZA, Chapman EJ, Fahlgren N, Givan SA, Carrington JC, Kasschau KD. (2008). Update of ASRP: the arabidopsis small RNA project database. *Nucleic Acids Res* 36:D982–D985
- Baek D, Park HC, Kim MC, Yun D-J. (2013). The role of Arabidopsis MYB2 in miR399f-mediated phosphate-starvation response. *Plant Signal Behav* 8:e23488
- Barabino SM, Blencowe BJ, Ryder U, Sproat BS, Lamond AI. (1990). Targeted snRNP depletion reveals an additional role for mammalian U1 snRNP in spliceosome assembly. *Cell* 63:293–302
- Barabino SM, Ohnacker M, Keller W. (2000). Distinct roles of two Yth1p domains in 3'-end cleavage and polyadenylation of yeast pre-mRNAs. *EMBO J* 19:3778–3787
- Barciszewska-Pacak M, Knop K, Jarmolowski A, Szweykowska-Kulinska Z. (2016). *Arabidopsis thaliana* microRNA162 level is posttranscriptionally regulated via splicing and polyadenylation site selection. *Acta Biochim Pol* epub, No. 2016_1349, doi: 10.18388/abp.2016_1349
- Barciszewska-Pacak M, Milanowska K, Knop K, Bielewicz D, Nuc P, Plewka P, Pacak AM, Vazquez F, Karlowski W, Jarmolowski A, Szweykowska-Kulinska Z. (2015). Arabidopsis microRNA expression regulation in a wide range of abiotic stress responses. *Front Plant Sci* 6:410
- Barnard DC, Ryan K, Manley JL, Richter JD. (2004). Symplekin and xGLD-2 are required for CPEB-mediated cytoplasmic polyadenylation. *Cell* 119:641–651
- Barta A, Kalyna M, Reddy AS. (2010). Implementing a rational and consistent nomenclature for Serine/Arginine-rich protein splicing factors (SR Proteins) in plants. *Plant Cell* 22:2926–2929
- Barta A, Marquez Y, Brown JWS. (2012). Challenges in plant alternative splicing. *Alternative Pre-mRNA Splicing: Theory and Protocols*, C.W.J. Smith and R. Lührmann, eds (Weinheim, Germany: Wiley-VCH Verlag), 79–89.
- Baumberger N, Baulcombe D. (2005). Arabidopsis ARGONAUTE1 is an RNA Slicer that selectively recruits microRNAs and short interfering RNAs. *P Natl Acad Sci USA* 102:11928–11933

- Berg MG, Singh LN, Younis I, Liu Q, Pinto AM, Kaida D, Zhang Z, Cho S, Sherrill-Mix S, Wan L, Dreyfuss G. (2012). U1 snRNP determines mRNA length and regulates isoform expression. *Cell* 150:53-64
- Bernal M, Casero D, Singh V, Wilson GT, Grande A, Yang H, Dodani SC, Pellegrini M, Huijser P, Connolly EL, Merchant SS, Kramer U. (2012). Transcriptome sequencing identifies SPL7-regulated copper acquisition genes FRO4/FRO5 and the copper dependence of iron homeostasis in Arabidopsis. *Plant Cell* 24:738–761
- Bielewicz D, Dolata J, Zielezinski A, Alaba S, Szarzyńska B, Szczesniak M, Jarmolowski A, Szweykowska-Kulinska Z, Karlowski WM. (2011). mirEX: a platform for comparative exploration of plant pri-miRNA expression data. *Nucleic Acids Res* 40:D191–D197
- Bielewicz D, Kalak M, Kalyna M, Windels D, Barta A, Vazquez F, Szweykowska-Kulinska Z, Jarmolowski A. (2013). Introns of plant pri-miRNAs enhance miRNA biogenesis. *EMBO Rep* 14:622-628
- Bienroth S, Keller W, Wahle E. (1993). Assembly of a processive mRNA polyadenylation complex. *EMBO J* 12:585–594
- Bischoff V, Nita S, Neumetzler L, Schindelasch D, Urbain A, Eshed R, Persson S, Delmer D, Scheible WR. (2010). TRICHOME BIREFRINGENCE and its homolog *At5g01360* encode plant-specific DUF231 proteins required for cellulose biosynthesis in *Arabidopsis thaliana*. *Plant Physiol* 153:590–602
- Blencowe, B.J. Alternative splicing: New insights from global analyses. *Cell* 126:37–47
- Bollman KM, Aukerman MJ, Park MY, Hunter C, Berardini TZ, Poethig RS. (2003). HASTY, the Arabidopsis ortholog of exportin 5/MSN5, regulates phase change and morphogenesis. *Development* 130:1493–1504
- Bologna NG, Mateos JL, Bresso EG, Palatnik JF. (2009). A loop-to-base processing mechanism underlies the biogenesis of plant microRNAs miR319 and miR159. *EMBO J* 28:3646–3656
- Bologna NG, Schapire AL, Zhai J, Chorostecki U, Boisbouvier J, Meyers BC, Palatnik JF. (2013). Multiple RNA recognition patterns during microRNA biogenesis in plants. *Genome Res* 23:1675–1689
- Borchert GM, Lanier W, Davidson BL. (2006). RNA polymerase III transcribes human microRNAs. *Nat Struct Mol Biol* 13:1097-1101
- Boyes DC, Zayed AM, Ascenzi R, McCaskill AJ, Hoffman NE, Davis KR, Gorlach J. (2001). Growth stage-based phenotypic analysis of Arabidopsis: a model for high throughput functional genomics in plants. *Plant Cell* 13:1499–1510
- Brennecke J, Stark A, Russell RB, Cohen SM. (2005). Principles of microRNA-target recognition. *PLoS Biol* 3:e85

- Brotman Y, Lisec J, Méret M, Chet I, Willmitzer L, Viterbo A. (2012). Transcript and metabolite analysis of the Trichoderma induced systemic resistance response to *Pseudomonas syringae* in *Arabidopsis thaliana*. *Microbiology* 158:139–146
- Brown JW, Marshall DF, Echeverria M. (2008). Intronic noncoding RNAs and splicing. *Trends in Plant Sci* 13:335–342
- Brown JW, Smith P, Simpson CG. (1996). Arabidopsis consensus intron sequences. *Plant Mol Biol* 32:531–535
- Brown JWS, Feix G, Frendewey D. (1986). Accurate in vitro splicing of two pre-mRNA plant introns in a HeLa cell nuclear extract. *Embo J* 5:2749–2758
- Carrington JC, Ambros V. (2003). Role of microRNAs in plant and animal development. *Science* 301:336–338
- Cech TR. (1990). Self-Splicing of Group I Introns. *Annu Rev Biochem* 59:543–568.
- Chaabane SB, Liu R, Chinnusamy V, Kwon Y, Park JH, Kim SY, Zhu JK, Yang SW, Lee BH. (2012). STA1, an Arabidopsis pre-mRNA processing factor 6 homolog, is a new player involved in miRNA biogenesis. *Nucleic Acids Res* 41:1984–1997
- Chan SP, Kao DI, Tsai WY, Cheng SC. (2003). The Prp19p-associated complex in spliceosome activation. *Science* 302:279–282
- Chao DY, Luo YH, Shi M, Luo D, Lin HX. (2005). Salt-responsive genes in rice revealed by cDNA microarray analysis. *Cell Res* 15:796–810
- Chen HC, Cheng SCh. (2012). Functional roles of protein splicing factors. *Biosci Rep* 32:345–359
- Chen T, Cui P, Chen H, Ali S, Zhang S, Xiong L. (2013). A KH-domain RNA-binding protein interacts with FIERY2/CTD phosphatase-like 1 and splicing factors and is important for pre-mRNA splicing in Arabidopsis. *PLoS Genet* 9:e1003875
- Chen T, Cui P, Xiong L. (2015). The RNA-binding protein HOS5 and serine/arginine-rich proteins RS40 and RS41 participate in miRNA biogenesis in Arabidopsis. *Nucleic Acids Res* 43:8283–8298
- Cheng C, Krishnakumar V, Chan A, Schobel S, Town CD. (2016). Araport11: a complete reannotation of the *Arabidopsis thaliana* reference genome. *bioRxiv* 047308; doi: <http://dx.doi.org/10.1101/047308>
- Chiou TJ, Aung K, Lin SI, Wu CC, Chiang SF, Su CL. (2006). Regulation of phosphate homeostasis by microRNA in Arabidopsis. *Plant Cell* 18:412–421
- Cho SK, Ben Chaabane S, Shah P, Poulsen CP, Yang SW. (2014). COP1 E3 ligase protects HYL1 to retain microRNA biogenesis. *Nat Commun* 5:5867

- Chursov A, Kopetzky SJ, Leshchiner I, Kondofersky I, Theis FJ, Frishman D, Shneider A. (2012). Specific temperature-induced perturbations of secondary mRNA structures are associated with the cold-adapted temperature-sensitive phenotype of influenza A virus. *RNA Biol* 9:1266–1274
- Clough SJ, Bent AF. (1998). Floral dip: a simplified method for *Agrobacterium*-mediated transformation of *Arabidopsis thaliana*. *Plant J* 16:735–743
- Company M, Arenas J, Abelson J. (1991). Requirement of the RNA helicase-like protein PRP22 for release of messenger RNA from spliceosomes. *Nature* 349:487–493
- Curtis MD, Grossniklaus UA. (2003). Gateway Cloning Vector Set for High-Throughput Functional Analysis of Genes in Planta. *Plant Physiol* 133: 462–469
- Dai X, Zhao PX. (2011). psRNATarget: a plant small RNA target analysis server. *Nucleic Acids Res* 39:W155–W159
- Dhir A, Dhir S, Proudfoot NJ, Jopling CL. (2015). Microprocessor mediates transcriptional termination of long noncoding RNA transcripts hosting microRNAs. *Nat Struct Mol Biol* 22:319–327
- Dichtl B, Keller W. (2001). Recognition of polyadenylation sites in yeast pre-mRNAs by cleavage and polyadenylation factor. *EMBO J* 20:3197–3209
- Dolata J, Bajczyk M, Bielewicz D, Niedojadlo K, Niedojadlo J, Pietrykowska H, Walczak W, Szweykowska-Kulinska Z, Jarmolowski A. (2016). Salt stress reveals a new role for ARGONAUTE1 in miRNA biogenesis at the transcriptional and posttranscriptional levels. *Plant Physiol* 172:297–312
- Dolata J, Guo Y, Kolowerzo A, Smolinski D, Brzyzek G, Jarmolowski A, Swiezewski S. (2015) NTR1 is required for transcription elongation checkpoints at alternative exons in *Arabidopsis*. *EMBO J* 34:544–558
- Dong Z, Han MH, Federoff N. (2008). The RNA-binding proteins HYL1 and SE promote accurate in vitro processing of pri-miRNA by DCL1. *Proc Natl Acad Sci USA* 105:9970–9975
- Duan CG, Fang YY, Zhou BJ, Zhao JH, Hou WN, Zhu H, Ding SW, Guo HS. (2012). Suppression of *Arabidopsis* ARGONAUTE1-mediated slicing, transgene-induced RNA silencing, and DNA methylation by distinct domains of the Cucumber mosaic virus 2b protein. *Plant Cell* 224:259–274
- Duque P. (2011). A role for SR proteins in plant stress responses. *Plant Signal Behav* 6:49–54
- Elkon R, Ugalde AP, Agami R. (2013). Alternative cleavage and polyadenylation: extent, regulation and function. *Nat Rev Genet* 14:496–506

- Fagard M, Dellagi A, Roux C, Périno C, Rigault M, Boucher V, Shevchik VE, Expert D. (2007). *Arabidopsis thaliana* expresses multiple lines of defense to counterattack *Erwinia chrysanthemi*. *Mol Plant Microbe Interact* 20:794–805
- Fang X, Cui Y, Li Y, Qi Y. (2015). Transcription and processing of primary microRNAs are coupled by Elongator complex in *Arabidopsis*. *Nat Plants* 1:15075
- Fang Y, Spector DL. (2007). Identification of nuclear dicing bodies containing proteins for microRNA biogenesis in living *Arabidopsis* plants. *Curr Biol* 17:818–823
- Feig AL. (2009). Studying RNA-RNA and RNA-Protein Interactions by Isothermal Titration Calorimetry. *Method Enzymol* 468:409–422
- Fica SM, Tuttle N, Novak T, Li NS, Lu J, Koodathingal P, Dai Q, Staley JP, Piccirilli JA. (2013). RNA catalyses nuclear pre-mRNA splicing. *Nature* 503:229–234
- Filichkin SA, Priest HD, Givan SA, Shen R, Bryant DW, Fox SE, Wong WK, Mockler TC. (2010). Genome-wide mapping of alternative splicing in *Arabidopsis thaliana*. *Genome Res* 20:45–58
- Fujioka Y, Utsumi M, Ohba Y, Watanabe Y. (2007). Location of a possible miRNA processing site in SmD3/SmB nuclear bodies in *Arabidopsis*. *Plant Cell Physiol* 48:1243–1253
- Gandikota M, Birkenbihl RP, Höhmann S, Cardon G, Saedler H, Huijser P. (2007). The miRNA156/157 recognition element in the 3' UTR of the *Arabidopsis* SBP box gene SPL3 prevents early flowering by translational inhibition in seedlings. *Plant J* 49:683–693
- Geer LY, Marchler-Bauer A, Geer RC, Han L, He J, He S, Liu C, Shi W, Bryant SH. (2010). The NCBI BioSystems database. *Nucleic Acids Res* 38:D492–496
- German MA, Pillay M, Jeong DH, Hetawal A, Luo S, Janardhanan P, Kannan V, Rymarquis LA, Nobuta K, German R, De Paoli E, Lu C, Schroth G, Meyers BC, Green PJ. (2008). Global identification of microRNA-target RNA pairs by parallel analysis of RNA ends. *Nat Biotechnol* 26:941–946
- Graveley BR. (2001). Alternative splicing: increasing diversity in the proteomic world. *Trends Genet* 17:100–107
- Gregory RI, Chendrimada TP, Cooch N, Shiekhattar R. (2005). Human RISC couples microRNA biogenesis and posttranscriptional gene silencing. *Cell* 123:631–640
- Grigg SP, Canales C, Hay A, Tsiantis M. (2005). SERRATE coordinates shoot meristem function and leaf axial patterning in *Arabidopsis*. *Nature*, 437:1022–1026
- Guerra D, Crosatti C, Khoshro HH, Mastrangelo AM, Mica E, Mazzucotelli E. (2015). Post-transcriptional and post-translational regulations of drought and heat response in plants: a spider's web of mechanisms. *Front Plant Sci* 6:57

- Gunderson SI, Polycarpou-Schwarz M, Mattaj IW. (1998). U1 snRNP inhibits pre-mRNA polyadenylation through a direct interaction between U1 70K and poly (A) polymerase. *Mol Cell* 1:255–264
- Han J, Lee Y, Yeom KH, Kim YK, Jin H, Kim VN. (2004). The Drosha-DGCR8 complex in primary microRNA processing. *Genes Dev* 18:3016–3027 (B)
- Han MH, Goud S, Song L, Fedoroff N. (2004). The Arabidopsis double-stranded RNA-binding protein HYL1 plays a role in microRNA-mediated gene regulation. *Proc Natl Acad Sci USA* 101:1093–1098 (A)
- Hansen T. (2007). Folder Version 1.11 Beta. Denmark: MBI, University of Aarhus. Available at: <http://www.ncrnalab.dk/rnafolder/>
- Hasegawa M, Miura T, Kuzuya K, Inoue A, Ki SW, Horinouchi S, Yoshida T, Kunoh T, Koseki K, Mino K, Sasaki R, Yoshida M, Mizukami T. (2011). Identification of SAP155 as the target of GEX1A (Herboxidiene), an antitumor natural product. *ACS Chem Biol* 6:229–233
- Henderson IR, Zhang X, Lu C, Johnson L, Meyers BC, Green PJ, Jacobsen SE. (2006). Dissecting *Arabidopsis thaliana* DICER function in small RNA processing, gene silencing and DNA methylation patterning. *Nat Genet* 38:721–725
- Herr AJ, Molnar A, Jones A, Baulcombe DC. (2006). Defective RNA processing enhances RNA silencing and influences flowering of Arabidopsis. *Proc Natl Acad Sci USA* 103:14994–15001
- Higo K, Ugawa Y, Iwamoto M, Higo H. (1998) PLACE: A database of plant cis-acting regulatory DNA elements. *Nucleic Acids Res.* 26:358–359
- Hiraguri A, Itoh R, Kondo N, Nomura Y, Aizawa D, Murai Y, Koiwa H, Seki M, Shinozaki K, Fukuhara T. (2005). Specific interactions between Dicer-like proteins and HYL1/DRB-family dsRNA binding proteins in *Arabidopsis thaliana*. *Plant Mol Biol* 57:173–188
- Hirsch J, Lefort V, Vankersschaver M, Boualem A, Lucas A, Thermes C, d'Aubenton-Carafa Y, Crespi M. (2006). Characterization of 43 non-protein-coding mRNA genes in Arabidopsis, including the MIR162a-derived transcripts. *Plant Physiol* 140:1192–1204
- Hornyik C, Terzi LC, Simpson GG. (2010). The spen family protein FPA controls alternative cleavage and polyadenylation of RNA. *Dev Cell* 18:203–213
- Hruz T, Laule O, Szabo G, Wessendorp F, Bleuler S, Oertle L, Widmayer P, Gruissem W, Zimmermann P. (2008). Genevestigator V3: a reference expression database for the meta-analysis of transcriptomes. *Adv Bioinformatics* 2008:420747
- Huang V, Zheng J, Qi Z, Wang J, Place RF, Yu J, Li H, Li LC. (2013). Ago1 Interacts with RNA polymerase II and binds to the promoters of actively transcribed genes in human cancer cells. *PLoS Genet* 9:e1003821

- Hubberten HM, Drozd A, Tran BV, Hesse H, Hoefgen R. (2012) Local and systemic regulation of sulfur homeostasis in roots of *Arabidopsis thaliana*. *Plant J* 72:625–635
- Hunt AG, Chu NM, Odell JT, Nagy F, Chua NH. (1987). Plant-cells do not properly recognize animal gene polyadenylation signals. *Plant Mol Biol* 8:23–35
- Hunt AG, Xu R, Addepalli B, Rao S, Forbes KP, Meeks LR, Xing D, Mo M, Zhao H, Bandyopadhyay A. (2008). Arabidopsis mRNA polyadenylation machinery: comprehensive analysis of protein–protein interactions and gene expression profiling. *BMC Genomics* 9:220
- Hunt AG. (1994). Messenger RNA 3' end formation in plants. *Annu Rev Plant Physiol Plant Mol Biol* 45:47–60
- Hunt AG. (2008). Messenger RNA 3' end formation in plants. *Curr Top Microbiol Immunol* 326:151–177
- Iki T, Yoshikawa M, Meshi T, Ishikawa M. (2012). Cyclophilin 40 facilitates HSP90 mediated RISC assembly in plants. *EMBO J* 31:267–278
- Iki T, Yoshikawa M, Nishikiori M, Jaudal MC, Matsumoto-Yokoyama E, Mitsuhara I, Ishikawa M. (2010). In vitro assembly of plant RNA-induced silencing complexes facilitated by molecular chaperone HSP90. *Mol Cell* 39:282–291
- Isaac BG, Ayer SW, Elliott RC, Stonard RJ. (1992). Herboxidiene: a potent phytotoxic polyketide from *Streptomyces* sp. A7847. *J Org Chem* 57:7220–7226
- Isshiki M, Tsumoto A, Shimamoto K. (2006). The serine/arginine-rich protein family in rice plays important roles in constitutive and alternative splicing of pre-mRNA. *Plant Cell* 18:146–158
- Iwata H, Gotoh O. (2011). Comparative analysis of information contents relevant to recognition of introns in many species. *BMC Genomics* 12:45
- Iwata H, Gotoh O. (2011). Comparative analysis of information contents relevant to recognition of introns in many species. *BMC Genomics* 14:1902–1910
- Iwata Y, Takahashi M, Fedoroff NV, Hamdan SM. (2013). Dissecting the interactions of SERRATE with RNA and DICER-LIKE 1 in Arabidopsis microRNA precursor processing. *Nucleic Acids Res* 41:9129–9140
- Izaurrealde E1, Lewis J, McGuigan C, Jankowska M, Darzynkiewicz E, Mattaj IW. (1994). A nuclear cap binding protein complex involved in pre-mRNA splicing. *Cell* 78:657–668
- Izaurrealde E, Lewis J, Gamberi C, Jarmolowski A, McGuigan C, Mattaj IW. (1995). A cap-binding protein complex mediating U snRNA export. *Nature* 376:709–712
- Janas MM, Khaled M, Schubert S, Bernstein JG, Golan D, Veguilla RA, Fisher DE, Shomron N, Levy C, Novina CD. (2011). Feed-forward microprocessing and splicing activities at a microRNA-containing intron. *PLOS Genetics* 7:e1002330

- Jia F, Rock CD. (2013). MIR846 and MIR842 comprise a cisgenic MIRNA pair that is regulated by abscisic acid by alternative splicing in roots of *Arabidopsis*. *Plant Mol Biol* 81:447–460
- Joshi PK, Gupta D, Nandal DK, Khan Y, Mukherjee SK, Sanan-Mishra N. (2012). Identification of mirtrons in rice using MirtronPred: a tool for predicting plant mirtrons. *Genomics* 99:370–375
- Kaczka EA, Trenner NR, Arison B, Walker RW, Folkers K. (1964). Identification of cordycepin, a metabolite of *Cordyceps militaris*, as 3'-deoxyadenosine. *Biochem Biophys Res Commun* 14:456–457
- Kaida D, Berg MG, Younis I, Kasim M, Singh LN, Wan L, Dreyfuss G. (2010). U1 snRNP protects pre-mRNAs from premature cleavage and polyadenylation. *Nature* 468:664–668
- Kalyana M, Lopato S, Voronin V, Barta A. (2006). Evolutionary conservation and regulation of particular alternative splicing events in plant SR proteins. *Nucleic Acids Res* 34:4395–4405
- Kandels-Lewis S, Seraphin B. (1993). Involvement of U6 snRNA in 5' splice site selection. *Science* 262:2035–2039
- Kantar M, Lucas S, H. Budak H. (2010). miRNA expression patterns of *Triticum dicoccoides* in response to shock drought stress. *Planta* 233:471–484
- Karlowski WM, Zielezinski A, Carrere J, Pontier D, Lagrange T, Cooke R. (2010). Genome-wide computational identification of WG/GW Argonaute-binding proteins in *Arabidopsis*. *Nucleic Acids Res* 38:4231–4245
- Kataoka N, Fujita M, Ohno M. (2009). Functional association of the Microprocessor complex with the spliceosome. *Mol Cell Biol* 29:3243–3254
- Kawashima CG, Matthewman CA, Huang S, Lee BR, Yoshimoto N, Koprivova A, Rubio-Somoza I, Todesco M, Rathjen T, Saito K, Takahashi H, Dalmay T, Kopriva S. (2011). Interplay of SLIM1 and miR395 in the regulation of sulfate assimilation in *Arabidopsis*. *Plant J* 66:863–876
- Kawashima CG, Yoshimoto N, Maruyama-Nakashita A, Tsuchiya YN, Saito K, Takahashi H, Dalmay T. (2009). Sulphur starvation induces the expression of microRNA-395 and one of its target genes but in different cell types. *Plant J* 57:313–321
- Kazan K. (2003). Alternative splicing and proteome diversity in plants: the tip of the iceberg has just emerged. *Trends Plant Sci* 8:468–471
- Keren H, Lev-Maor G, Ast G. (2010). Alternative splicing and evolution: Diversification, exon definition and function. *Nat Rev Genet* 11:345–355
- Ketting RF, Fischer SEJ, Bernstein E, Sijen T, Hannon GJ, Plasterk RHA. (2001). Dicer functions in RNA interference and in synthesis of small RNA involved in developmental timing in *C. elegans*. *Genes Dev* 15:2654–2659

- Kierzkowski D, Kmiecik M, Piontek P, Wojtaszek P, Szweykowska-Kulinska Z, Jarmolowski A. (2009). The Arabidopsis CBP20 targets the cap-binding complex to the nucleus, and is stabilized by CBP80. *Plant J* 56:814–825
- Kim VN. (2005). MicroRNA biogenesis: coordinated cropping and dicing. *Nat Rev Mol Cell Biol* 6:376–385
- Kim Y-K, Kim VN. (2007). Processing of intronic microRNAs. *EMBO J* 26:775–783
- Kim JY, Kwak KJ, Jung HJ, Lee HJ, Kang H. (2010). MicroRNA402 affects seed germination of *Arabidopsis thaliana* under stress conditions via targeting DEMETERLIKE Protein3 mRNA. *Plant Cell Physiol* 51:1079–1083
- Kim YJ, Zheng B, Yu Y, Won SY, Mo B, Chen X. (2011). The role of Mediator in small and long noncoding RNA production in *Arabidopsis thaliana*. *EMBO J* 30:814–822
- Kmiecik M, Simpson CG, Lewandowska D, Brown JW, Jarmolowski A. (2002). Cloning and characterization of two subunits of *Arabidopsis thaliana* nuclear cap-binding complex. *Gene* 283:171–183
- Knop K, Stepien A, Barciszewska-Pacak M, Taube M, Bielewicz D, Michalak M, Borst JW, Jarmolowski A, Szweykowska-Kulinska Z. (2016). Active 5' splice sites regulate the biogenesis efficiency of Arabidopsis microRNAs derived from intron-containing genes. *Nucleic Acids Res* doi: 10.1093/nar/gkw895
- Koncz C, deJong F, Villacorta N, Szakonyi D, Koncz Z. (2012). The spliceosome-activating complex: Molecular mechanisms underlying the function of a pleiotropic regulator. *Front Plant Sci* 3:9
- Koressaar T, Remm M. (2007). Enhancements and modifications of primer design program Primer3. *Bioinformatics* 23:1289–1291
- Koster T, Meyer K, Weinholdt C, Smith LM, Lummer M, Speth C, Grosse I, Weigel D, Staiger D. (2014). Regulation of pri-miRNA processing by the hnRNP-like protein AtGRP7 in Arabidopsis. *Nucleic Acids Res* 42:9925–9936
- Kozomara A, Griffiths-Jones S. (2014) miRBase: annotating high confidence microRNAs using deep sequencing data. *Nucleic Acids Res* 42:D68–D73
- Kruszka K, Pacak A, Swida-Barteczka A, Nuc P, Alaba S, Wroblewska Z, Karlowski W, Jarmolowski A, Szweykowska-Kulinska Z. (2014). Transcriptionally and post-transcriptionally regulated microRNAs in heat stress response in barley. *J Exp Bot* 65:6123–6135
- Kruszka K, Pacak A, Swida-Barteczka A, Stefaniak AK, Kaja E, Sierocka I, Karlowski W, Jarmolowski A, Szweykowska-Kulinska Z. (2013). Developmentally regulated expression and complex processing of barley pri-microRNAs. *BMC Genomics* 14:34

- Kruszka K, Pieczynski M, Windels D, Bielewicz D, Jarmolowski A, Szweykowska-Kulinska Z, Vazquez F. (2012). Role of microRNAs and other sRNAs of plants in their changing environments. *J Plant Physiol* 169:1664–1672
- Kurihara Y, Takashi Y, Watanabe Y. (2006). The interaction between DCL1 and HYL1 is important for efficient and precise processing of pri-miRNA in plant microRNA biogenesis. *RNA* 12:206–212
- Kurihara Y, Watanabe Y. (2004). Arabidopsis micro-RNA biogenesis through Dicer-like 1 protein functions. *Proc Natl Acad Sci USA* 101:12753–12758
- Kwek KY, Murphy S, Furger A, Thomas B, O’Gorman W, Kimura H, Proudfoot NJ, Akoulitchev A. (2002). U1 snRNA associates with TFIIF and regulates transcriptional initiation. *Nat Struct Mol Biol* 9:800–805
- Kyriakopoulou CB, Nordvarg H, Virtanen A. (2001). A novel nuclear human poly(A) polymerase, PAP γ . *J Biol Chem* 276:33504–33511
- Ladewig E, Okamura K, Flynt AS, Westholm JO, Lai EC. (2012). Discovery of hundreds of mirtrons in mouse and human small RNA data. *Genome Res* 22:1634–1645
- Lamesch P, Berardini TZ, Li D, Swarbreck D, Wilks C, Sasidharan R, Muller R, Dreher K, Alexander DL, Garcia-Hernandez M, Karthikeyan AS, Lee CH, Nelson WD, Ploetz L, Singh S, Wensel A, Huala E. (2011). The Arabidopsis Information Resource (TAIR): improved gene annotation and new tools. *Nucleic Acids Res* 40:D1202–1210
- Laubinger S, Sachsenberg T, Zeller G, Busch W, Lohmann JU, Ratsch G, Weigel D. (2008). Dual roles of the nuclear cap-binding complex and SERRATE in pre-mRNA splicing and microRNA processing in *Arabidopsis thaliana*. *Proc Natl Acad Sci USA* 105:8795–8800
- Lee RC, Feinbaum RL, Ambros V. (1993). The *C. elegans* heterochronic gene lin-4 encodes small RNAs with antisense complementarity to lin-14. *Cell* 75:843–854
- Lee Y, Ahn C, Han J, Choi H, Kim J, Yim J, Lee J, Provost p, Radmark o, Kim S, Kim VN. (2003). The nuclear RNase III Drosha initiates microRNA processing. *Nature* 425:415–419
- Lee Y, Kim M, Han J, Yeom KH, Lee S, Baek SH, Kim VN. (2004). MicroRNA genes are transcribed by RNA polymerase II. *EMBO J* 23:4051–4060
- Lewandowska D, Simpson CG, Clark GP, Jennings NS, Barciszewska-Pacak M, Lin CF, Makalowski W, Brown JW, Jarmolowski A. (2004). Determinants of plant U12-dependent intron splicing efficiency. *Plant Cell* 16:1340–1352
- Lewis BP, Shih IH, Jones-Rhoades MW, Bartel DP, Burge CB. (2003). Prediction of mammalian microRNA targets. *Cell* 115:787–798
- Li Y, Li C, Ding G, Jin Y. (2011). Evolution of MIR159/319 microRNA genes and their post-transcriptional regulatory link to siRNA pathways. *BMC Evol Biol* 11:122

- Li S, Liu L, Zhuang X, Yu Y, Liu X, Cui X, Ji L, Pan Z, Cao X, Mo B, Zhang F, Raikhel N, Jiang L, Chen X. (2013). MicroRNAs inhibit the translation of target mRNAs on the endoplasmic reticulum in Arabidopsis. *Cell* 153:562–574
- Li J, Yang Z, Yu B, Liu J, Chen X. (2005). Methylation protects miRNAs and siRNAs from a 3' end uridylation activity in Arabidopsis. *Curr Biol* 15:1501–1507
- Li QQ, Hunt AG. (1995). A near upstream element in a plant polyadenylation signal consists of more than six bases. *Plant Mol Biol* 28:927–934
- Li QQ, Hunt AG. (1997). The polyadenylation of RNA in plants. *Plant Physiol* 115:321–325
- Li S, Yang X, Wu F, He Y. (2012). HYL1 controls the miR156-mediated juvenile phase of vegetative growth. *J Exp Bot* 63:2787–2798
- Li WX, Oono Y, Zhu J, He XJ, Wu JM, Iida K, Lu XY, Cui X, Jin H, Zhu JK. (2008). The Arabidopsis NFYA5 transcription factor is regulated transcriptionally and posttranscriptionally to promote drought resistance. *Plant Cell* 20:2238–2251
- Li Y, Li C, Ding G, Jin Y. (2011). Evolution of MIR159/319 microRNA genes and their post-transcriptional regulatory link to siRNA pathways. *BMC Evol Biol* 11:122
- Liu C, Axtell MJ, Fedoroff NV (2012). The helicase and RNaseIIIa domains of Arabidopsis Dicer-Like1 modulate catalytic parameters during microRNA biogenesis. *Plant Physiol* 159:748–758
- Liu F, Marquardt S, Lister C, Swiezewski S, Dean C. (2010). Targeted 3' processing of antisense transcripts triggers Arabidopsis FLC chromatin silencing. *Science* 327:94–97
- Liu HH, Tian X, Li YJ, Wu CA, Zhen CC. (2008). Microarray-based analysis of stress-regulated microRNAs in *Arabidopsis thaliana*. *RNA* 14:836–843
- Liu J, Rivas FV, Wohlschlegel J, Yates JR, Parker R, Hannon GJ. (2005). A role for the P-body component, GW182, in microRNA function. *Nature Cell Biol* 7:1261–1266
- Liu PP, Montgomery TA, Fahlgren N, Kasschau KD, Nonogaki H, Carrington JC. (2007). Repression of AUXIN RESPONSE FACTOR10 by microRNA160 is critical for seed germination and post-germination stages. *Plant J* 52:133–146
- Lobbes D, Rallapalli D, Schmidt DD, Martin C, Clarke J. (2006). SERRATE: a new player on the plant microRNA scene. *EMBO Rep* 7:1052–1058
- Loke JC, Stahlberg EA, Strenski DG, Haas BJ, Wood PC, Li QQ. (2005). Compilation of mRNA polyadenylation signals in Arabidopsis revealed a new signal element and potential secondary structures. *Plant Physiol* 138:1457–1468
- Lu C, Fedoroff N. (2000). A mutation in the Arabidopsis HYL1 gene encoding a dsRNA binding protein affects responses to abscisic acid, auxin, and cytokinin. *Plant Cell* 12:2351–2366

- Lu C, Jeong DH, Kulkarni K, Pillay M, Nobuta K, German R, Thatcher SR, Maher C, Zhang L, Ware D, Liu B, Cao X, Meyers BC, Green PJ. (2008). Genome-wide analysis for discovery of rice microRNAs reveals natural antisense microRNAs (nat-miRNAs). *Proc Natl Acad Sci USA* 105:4951–4956
- Lutz CS. (2008). Alternative polyadenylation: a twist on mRNA 3' end formation. *ACS Chem Biol* 3:609–617
- MacDonald CC, Wilusz J, Shenk T. (1994). The 64-kilodalton subunit of the CstF polyadenylation factor binds to pre-mRNAs downstream of the cleavage site and influences cleavage site location. *Mol Cell Biol* 14:6647–6654
- Machida S, Chen HJ, Yuan YA. (2011). Molecular insights into miRNA processing by *Arabidopsis thaliana* SERRATE. *Nucleic Acids Res* 39:7828–7836
- Macknight R, Duroux M, Laurie R, Dijkwel P, Simpson G, Dean C. (2002). Functional significance of the alternative transcript processing of the Arabidopsis floral promoter FCA. *Plant Cell* 14:877–888
- Manavella PA, Hagmann J, Ott F, Laubinger S, Franz M, Macek B, Weigel D. (2012). Fastforward genetics identifies plant CPL phosphatases as regulators of miRNA processing factor HYL1. *Cell* 151:859–870
- Mandel CR, Kaneko S, Zhang H, Gebauer D, Vethantham V, Manley JL, Tong L. (2006). Polyadenylation factor CPSF-73 is the pre-mRNA 3'-end-processing endonuclease. *Nature* 444:953–956
- Marquez Y, Brown JW, Simpson C, Barta A, Kalyna M. (2012). Transcriptome survey reveals increased complexity of the alternative splicing landscape in Arabidopsis. *Genome Res* 22:1184–1195
- Martinson HG. (2011). An active role for splicing in 3'-end formation. *Wiley Interdiscip Rev RNA* 2:459–470
- Mastrangelo AM, Marone D, Laido G, De Leonardis AM, De Vita P. (2012). Alternative splicing: enhancing ability to cope with stress via transcriptome plasticity. *Plant Sci* 185–186:40–49
- de la Mata M, Alonso CR, Kadener S, Fededa JP, Blaustein M, Pelisch F, Crame P, Bentley D, Kornblihtt AR. (2003). A slow RNA polymerase II affects alternative splicing in vivo. *Mol Cell* 12:525–532
- Meister G, Landthaler M, Patkaniowska A, Dorsett Y, Teng G, Tuschl T. (2004). Human Argonaute2 mediates RNA cleavage targeted by miRNAs and siRNAs. *Mol Cell* 15:185–197
- Meister G, Landthaler M, Peters L, Chen PY, Urlaub H, Lührmann R, Tuschl T. (2005). Identification of novel argonaute-associated proteins. *Curr Biol* 15:2149–2155

- Meng Y, Shao C, Ma X, Wang H, Chen M. (2012). Expression-based functional investigation of the organ-specific microRNAs in Arabidopsis. *PLoS One* 7:e50870
- Meng Y, Shao Ch. (2012). Large-Scale Identification of Mirtrons in Arabidopsis and Rice. *PLoS One* 7:e31163
- Merchan F, Boualem A, Crespi M, Frugier F. (2012). Plant polycistronic precursors containing non-homologous microRNAs target transcripts encoding functionally related proteins. *Genome Biol* 10:R136
- Meyer K, Koester T, Staiger D. (2015). Pre-mRNA Splicing in Plants: In Vivo Functions of RNA-Binding Proteins Implicated in the Splicing Process. *Biomolecules* 5:1717–1740
- Millar AA, Gubler F. (2005). The Arabidopsis GAMYB-like genes, MYB33 and MYB65, are microRNA-regulated genes that redundantly facilitate anther development. *Plant Cell* 17:705–721
- Miller-Wideman M, Makkar N, Tran M, Isaac B, Biest N, Stonard R. (1992). Herboxidiene, a new herbicidal substance from *Streptomyces chromofuscus* A7847. Taxonomy, fermentation, isolation, physico-chemical and biological properties. *J Antibiot* (Tokyo) 45:914–921
- Millevoi S, Vagner S. (2009). Molecular mechanisms of eukaryotic pre-mRNA 3' end processing regulation. *Nucleic Acids Res* 38:2757–2774
- Moore MJ, Query CC, Sharp CA. (1993). Splicing of Precursors to mRNA by the Spliceosome. *The RNA World* (Cold Spring Harbor Monograph Archive)
- Morlando M, Ballarino M, Gromak N, Pagano F, Bozzoni I, Proudfoot NJ. (2008). Primary microRNA transcripts are processed co-transcriptionally. *Nat Struct Mol Biol* 15:902–909
- Muralla R, Chen E, Sweeney C, Gray JA, Dickerman A, Nikolau BJ, Meinke D. (2008). A bifunctional locus (BIO3- BIO1) required for biotin biosynthesis in Arabidopsis. *Plant Physiol* 146:60–73
- Murthy KG, Manley JL. (1995). The 160-kD subunit of human cleavage-polyadenylation specificity factor coordinates pre-mRNA 3'-end formation. *Genes Dev* 9:2672–2683
- Nag A, King S, Jack T. (2009). MiR319a targeting of TCP4 is critical for petal growth and development in Arabidopsis. *Proc Natl Acad Sci USA* 106:22534–22539
- Ner-Gaon H, Halachmi R, Savaldi-Goldstein S, Rubin E, Ophir R, Fluhr R. (2004). Intron retention is a major phenomenon in alternative splicing in Arabidopsis. *Plant J* 39:877–885
- Ni JZ, Grate L, Donohue JP, Preston C, Nobida N, O'Brien G, Shiue L, Clark TA, Blume JE, Ares M, Jr. (2007). Ultraconserved elements are associated with homeostatic control of splicing regulators by alternative splicing and nonsense-mediated decay. *Genes Dev* 21:708–718

- Nigam D, Kumar S, Mishra DC, Rai A, Smita S, Saha A. (2015). Synergistic regulatory networks mediated by microRNAs and transcription factors under drought, heat and salt stresses in *Oryza sativa* spp. *Gene* 555:127–139
- Nilsen TW, Graveley BR. (2010). Expansion of the eukaryotic proteome by alternative splicing. *Nature* 463:457–463
- Okamura K, Hagen JW, Duan H, Tyler DM, Lai EC. (2007). The mirtron pathway generates microRNA-class regulatory RNAs in *Drosophila*. *Cell* 130:89–100
- Ortega-Galisteo AP, Morales-Ruiz T, Ariza RR, Roldan-Arjona T. (2008). Arabidopsis DEMETER-LIKE proteins DML2 and DML3 are required for appropriate distribution of DNA methylation marks. *Plant Mol Biol* 67:671–681
- Otero G, Fellows J, Li Y, de Bizemont T, Dirac AM, Gustafsson CM, Erdjument-Bromage H, Tempst P, Svejstrup JQ. (1999). Elongator, a multisubunit component of a novel RNA polymerase II holoenzyme for transcriptional elongation. *Mol Cell* 3:109–118
- Palatnik JF, Allen E, Wu X, Schommer C, Schwab R, Carrington JC, Weigel D. (2003). Control of leaf morphogenesis by microRNAs. *Nature* 425:257–263
- Palatnik JF, Wollmann H, Schommer C, Schwab R, Boisbouvier J, Rodriguez R, Warthmann N, Allen E, Dezulian T, Huson D, Carrington JC, Weigel D. (2007). Sequence and expression differences underlie functional specialization of Arabidopsis microRNAs miR159 and miR319. *Dev Cell* 13:115–125
- Palusa SG, Ali GS, Reddy ASN. (2007). Alternative splicing of pre-mRNAs of Arabidopsis serine/arginine-rich proteins: regulation by hormones and stresses. *Plant J* 49:1091–1107
- Pan Q, Saltzman AL, Kim YK, Misquitta C, Shai O, Maquat LE, Frey BJ, Blencowe BJ. (2006). Quantitative microarray profiling provides evidence against widespread coupling of alternative splicing with nonsense mediated mRNA decay to control gene expression. *Genes Dev* 20:153–158
- Pandey R, Joshi G, Bhardwaj AR, Agarwal M, Katiyar-Agarwal S. (2014). A comprehensive genome-wide study on tissue-specific and abiotic stress-specific miRNAs in *Triticum aestivum*. *PLoS ONE* 9:e95800
- Pant BD, Buhtz A, Kehr J, Scheible WR. (2008). MicroRNA399 is a long-distance signal for the regulation of plant phosphate homeostasis. *Plant J* 53:31–38
- Papdi C, Abraham E, Joseph MP, Popescu C, Koncz C, Szabados L. (2008). Functional Identification of Arabidopsis Stress Regulatory Genes Using the Controlled cDNA Overexpression System. *Plant Physiol* 147:528–542
- Park YJ, Lee HJ, Kwak KJ, Lee K, Hong SW, Kang H. (2014). MicroRNA400-Guided Cleavage of Pentatricopeptide Repeat Protein mRNAs Renders *Arabidopsis thaliana* More Susceptible to Pathogenic Bacteria and Fungi. *Plant Cell Physiol* 55:1660–1668

- Park W, Li J, Song R, Messing J, Chen X. (2002). CARPEL FACTORY, a Dicer homolog, and HEN1, a novel protein, act in microRNA metabolism in *Arabidopsis thaliana*. *Curr Biol* 12:1484–1495
- Park MY, Wu G, Gonzalez-Sulser A, Vaucheret H, Poethig RS. (2005). Nuclear processing and export of microRNAs in Arabidopsis. *Proc Natl Acad Sci USA* 102:3691–3696
- Parker JS, Roe SM, Barford D. (2004). Crystal structure of a PIWI protein suggests mechanisms for siRNA recognition and slicer activity. *EMBO J* 23:4727–4737
- Patel AA, Steitz JA. (2013). Splicing double: insights from the second spliceosome. *Nat Rev Mol Cell Biol* 4:960–970
- Perumal K, Sinha K, Henning D, Reddy R. (2001). Purification, characterization and cloning of the cDNA of human signal recognition particle RNA 3'-adenylating enzyme. *J Biol Chem* 276:21791–21796
- Pieczynski M, Marczewski W, Hennig J, Dolata J, Bielewicz D, Piontek P, Wyrzykowska A, Krusiewicz D, Strzelczyk-Zyta D, Konopka-Postupolska D, Krzeslowska M, Jarmolowski A, Szweykowska-Kulinska Z. (2013). Down-regulation of CBP80 gene expression as a strategy to engineer a drought-tolerant potato. *Plant Biotechnol J* 11:459–469
- Prigge MJ, Wagner DR. (2001). The Arabidopsis SERRATE gene encodes a zinc-finger protein required for normal shoot development. *Plant Cell* 13:1263–1280
- Proudfoot N. (1991). Poly(a) signals. *Cell* 64:671–674
- Proudfoot N. (2004). New perspectives on connecting messenger RNA 3' end formation to transcription. *Curr Opin Cell Biol* 16:272–278
- Proudfoot NJ, Brownlee GG. (1976). The 3' non-coding region sequences in eukaryotic messenger RNA. *Nature* 263:211–214
- Qin H, Chen F, Huan X, Machida S, Song J, Yuan YA. (2010). Structure of the *Arabidopsis thaliana* DCL4 DUF283 domain reveals a noncanonical double-stranded RNA-binding fold for protein-protein interaction. *RNA* 16:474–481
- Quesada V, Macknight R, Dean C, Simpson GG. (2003). Autoregulation of FCA pre-mRNA processing controls Arabidopsis flowering time. *EMBO J* 22:3142–3152
- Raabe T, Bollum FJ, Manley JL. (1991). Primary structure and expression of bovine poly(A) polymerase. *Nature* 353:229–234
- Raczynska KD, Simpson CG, Ciesiolka A, Szewc L, Lewandowska D, McNicol J, Szweykowska-Kulinska Z, Brown JW, Jarmolowski A. (2010). Involvement of the nuclear cap-binding protein complex in alternative splicing in *Arabidopsis thaliana*. *Nucleic Acids Res* 38:265–278

- Raczynska KD, Stepien A, Kierzkowski D, Kalak M, Bajczyk M, McNicol J, Simpson CG, Szweykowska-Kulinska Z, Brown JW, Jarmolowski A. (2014). The SERRATE protein is involved in alternative splicing in *Arabidopsis thaliana*. *Nucleic Acids Res* 42:1224–1244
- Rajagopalan R, Vaucheret H, Trejo J, Bartel DP. (2006). A diverse and evolutionarily fluid set of microRNAs in *Arabidopsis thaliana*. *Genes Dev* 20:3407–3425
- Ramalingam P, Palanichamy JK, Singh A, Das P, Bhagat M, Kassab MA, Sinha S, Chattopadhyay P. (2014). Biogenesis of intronic miRNAs located in clusters by independent transcription and alternative splicing. *RNA* 20:76–87
- Reddy AS, Rogers MF, Richardson DN, Hamilton M, Ben-Hur A. (2012). Deciphering the plant splicing code: Experimental and computational approaches for predicting alternative splicing and splicing regulatory elements. *Front Plant Sci* 3:18
- Reddy AS. (2004). Plant serine/arginine-rich proteins and their role in pre-mRNA splicing. *Trends Plant Sci* 9:541–547
- Reddy AS. (2007). Alternative splicing of pre-messenger RNAs in plants in the genomic era. *Annu Rev Plant Biol* 58:267–294
- Reinhart B.J, Weinstein EG, Rhoades MW, Bartel B, Bartel DP. (2002). MicroRNAs in plants. *Gene Dev* 16:1616–1626
- Reis RS, Hart-Smith G, Eamens AL, Wilkins MR, Waterhouse PM. (2015). Gene regulation by translational inhibition is determined by Dicer partnering proteins. *Nat Plants* 1:14027
- Ren G, Chen X, Yu B. (2012). Uridylation of miRNAs by hen1 suppressor1 in Arabidopsis. *Curr Biol* 22:695–700 (B)
- Ren G, Xie M, Dou Y, Zhang S, Zhang C, Yu B. (2012) Regulation of miRNA abundance by RNA binding protein TOUGH in Arabidopsis. *Proc Natl Acad Sci USA* 109:12817–12821 (A)
- Reyes JL, Chua NH (2007). ABA induction of miR159 controls transcript levels of two MYB factors during Arabidopsis seed germination. *Plant J* 49:592–606
- Rhoades MW, Reinhart BJ, Lim LP, Burge CB, Bartel B, Bartel DP. (2002). Prediction of plant microRNA targets. *Cell* 110:513–520
- Richardson DN, Rogers MF, Labadorf A, Ben-Hur A, Guo H., Paterson AH, Reddy AS. (2011). Comparative analysis of Serine/Arginine-rich proteins across 27 eukaryotes: Insights into sub-family classification and extent of alternative splicing. *PLoS ONE* 6:e24542.
- Rizhsky L, Davletova S, Liang HJ, Mittler R. (2004). The zinc finger protein Zat12 is required for cytosolic ascorbate peroxidase 1 expression during oxidative stress in Arabidopsis. *J Biol Chem* 279:11736–11743

- Rodriguez A, Griffiths-Jones S, Ashurst JL, Bradley A. (2004). Identification of mammalian microRNA host genes and transcription units. *Genome Res* 14:1902–1910
- Ruby JG, Jan CH, Bartel DP. (2007). Intronic microRNA precursors that bypass Drosha processing. *Nature* 448:83–86
- Ryan K, Calvo O, Manley JL. (2004). Evidence that polyadenylation factor CPSF-73 is the mRNA 3' processing endonuclease. *RNA* 10:565–573
- Sakharkar MK, Chow VT, Kanguane P. (2004). Distributions of exons and introns in the human genome. *In Silico Biol* 4:387–393
- Sawicka K, Bushell M, Spriggs KA, Willis AE. (2008). Polypyrimidine-tract-binding protein: a multifunctional RNA-binding protein. *Biochem Soc Trans* 36:641–647
- Schauer SE, Jacobsen SE, Meinke DW, Ray A. (2002). DICER-LIKE1: blind men and elephants in Arabidopsis development. *Trends Plant Sci* 7:487–491
- Schommer C, Palatnik JF, Aggarwal P, Chetelat A, Cubas P, Farmer EE, Nath U, Weigel D. (2008). Control of jasmonate biosynthesis and senescence by miR319 targets. *PLoS Biol* 6:e230
- Schwab R, Speth C, Laubinger S, Voinnet O. (2013). Enhanced microRNA accumulation through stem loop-adjacent introns. *EMBO Rep* 14:615–621
- Schwer B, Gross CH. (1998). Prp22, a DEXH-box RNA helicase, plays two distinct roles in yeast pre-mRNA splicing. *EMBO J* 17:2086–2094
- Seeley KA, Byrne DH, Colbert JT. (1992). Red light-independent instability of oat phytochrome mRNA in vivo. *Plant Cell* 4:29–38
- Shan X, Li C, Peng W, Gao B. (2011). New perspective of jasmonate function in leaf senescence. *Plant Signal Behav* 6:575–577
- Sherstnev A, Duc C, Cole C, Zacharaki V, Hornyik C, Oszolak F, Milos P, Barton GJ, Simpson GG. (2012). Direct Sequencing of *Arabidopsis thaliana* RNA reveals patterns of cleavage and polyadenylation. *Nat Struct Mol Biol* 19:845–852
- Shcherbakova I, Hoskins AA, Friedman LJ, Serebrov V, Corrêa IR Jr, Xu MQ, Gelles J, Moore MJ. (2013). Alternative spliceosome assembly pathways revealed by single-molecule fluorescence microscopy. *Cell Rep* 5:151–165
- Shiohama A, Sasaki T, Noda S, Minoshima S, Shimizu N. (2007). Nucleolar localization of DGCR8 and identification of eleven DGCR8-associated proteins. *Exp Cell Res* 313:4196–4207
- Si Y, Zhang C, Meng S, Dane F. (2009). Gene expression changes in response to drought stress in *Citrullus colocynthis*. *Plant Cell Rep* 28:997–1009

- Siev M, Weinberg R, Penman S. (1969). The selective interruption of nucleolar RNA synthesis in HeLa cells by cordycepin. *J Cell Biol* 41:510–520
- Simpson CG, Thow G, Clark GP, Jennings SN, Watters JA, Brown JW. (2002). Mutational analysis of a plant branchpoint and polypyrimidine tract required for constitutive splicing of a mini-exon. *RNA* 8:47–56
- Simpson GG, Dijkwel PP, Quesada V, Henderson I, Dean C. (2003). FY is an RNA 3end-processing factor that interacts with FCA to control the Arabidopsis floral transition. *Cell* 113:777–787.
- Simpson GG, Quesada V, Henderson IR, Dijkwel PP, Macknight R, Dean C. (2004). RNA processing and Arabidopsis flowering time control. *Biochem Soc Trans* 32:565–566
- Smith CWJ, Valcarel J. (2000). Alternative pre-mRNA splicing: The logic of combinatorial control. *Trends Biochem Sci* 25:381–388
- Sobkowiak L, Karlowski W, Jarmolowski A, Szweykowska-Kulinska Z. (2012). Non-Canonical Processing of Arabidopsis pri-miR319a/b/c Generates Additional microRNAs to Target One RAP2.12 mRNA Isoform. *Front Plant Sci* 3:46
- Soltis PS, Liu X, Marchant DB, Visger CJ, Soltis DE. (2014). Polyploidy and novelty: Gottlieb's legacy. *Philos Trans R Soc Lond B Biol Sci* 369(1648)
- Song L, Han MH, Lesicka J, Fedoroff N. (2007). Arabidopsis primary microRNA processing proteins HYL1 and DCL1 define a nuclear body distinct from the Cajal body. *Proc Natl Acad Sci USA* 104:5437–5442
- Sperling J, Azubel M, Sperling R. (2008). Structure and function of the Pre-mRNA splicing machine. *Structure* 16:1605–1615
- Speth C, Willing EM, Rausch S, Schneeberger K, Laubinger S. (2013). RACK1 scaffold proteins influence miRNA abundance in Arabidopsis. *Plant J* 76:433–445
- Stauffer E, Westermann A, Wagner G, Wachter A. (2010). Polypyrimidine tract-binding protein homologues from Arabidopsis underlie regulatory circuits based on alternative splicing and downstream control. *Plant J* 64:243–255
- Stepien A, Knop K, Dolata J, Taube M, Bajczyk M, Barciszewska-Pacak M, Pacak A, Jarmolowski A, Szweykowska-Kulinska Z. (2016). Post-transcriptional coordination of splicing and miRNA biogenesis in plants. *Wiley Interdiscip Rev RNA* doi: doi: 10.1002/wrna.1403
- Sun Z, Guo T, Liu Y, Liu Q, Fang Y. (2015). The Roles of Arabidopsis CDF2 in Transcriptional and Posttranscriptional Regulation of Primary MicroRNAs. *PLoS Genet* 11:e1005598
- Sunkar R, Jagadeeswaran G. (2008). In silico identification of conserved microRNAs in large number of diverse plant species. *BMC Plant Biol* 8:3

- Sunkar R, Kapoor A, Zhu JK. (2006). Posttranscriptional induction of two Cu/Zn superoxide dismutase genes in *Arabidopsis* is mediated by downregulation of miR398 and important for oxidative stress tolerance. *Plant Cell* 18:2051–2065
- Sunkar R, Zhu JK. (2004). Novel and stress-regulated microRNAs and other small RNAs from *Arabidopsis*. *Plant Cell* 16:2001–2019
- Szarzynska B, Sobkowiak L, Pant BD, Balazadeh S, Scheible WR, Mueller-Roeber B, Jarmolowski A, Szweykowska-Kulinska Z. (2009). Gene structures and processing of *Arabidopsis thaliana* HYL1-dependent pri-miRNAs. *Nucleic Acids Res* 37:3083–3093
- Szweykowska-Kulinska Z, Jarmolowski A, Vazquez F. (2013). The crosstalk between plant microRNA biogenesis factors and the spliceosome. *Plant Signal Behav* 8:e26955
- Takahashi H, Watanabe-Takahashi A, Smith FW, Blake-Kalff M. (2000). The roles of three functional sulphate transporters involved in uptake and translocation of sulphate in *Arabidopsis thaliana*. *Plant J* 23:171–182
- Talmor-Neiman M, Stav R, Frank W, Voss B, Arazi T. (2006). Novel micro-RNAs and intermediates of micro-RNA biogenesis from moss. *Plant J* 47:25–37
- Tian B, Pan Z, Lee JY. (2007). Widespread mRNA polyadenylation events in introns indicate dynamic interplay between polyadenylation and splicing. *Genome Res* 17:156–165
- Tollervey D. (2004). Molecular biology: termination by torpedo. *Nature* 432:456–457
- Topalian SL, Kaneko S, Gonzales MI, Bond GL, Ward Y, Manley JL. (2001). Identification and functional characterization of neo-poly(A) polymerase, an RNA processing enzyme overexpressed in human tumors. *Mol Cell Biol* 21:5614–5623
- Tsuzuki M, Takeda A, Watanabe Y. (2014). Recovery of dicer-like 1-late flowering phenotype by miR172 expressed by the noncanonical DCL4-dependent biogenesis pathway. *RNA* 20:1320–1327
- The UniProt Consortium. (2015). UniProt: a hub for protein information *Nucleic Acids Res* 43:D204–D212
- Untergasser A, Cutcutache I, Koressaar T, Ye J, Faircloth BC, Remm M, Rozen SG. (2012). Primer3 - new capabilities and interfaces. *Nucleic Acids Res* 40:e115
- Vazquez F, Blevins T, Ailhas J, Boller T, Meins F, Jr. (2008). Evolution of *Arabidopsis* *MIR* genes generates novel microRNA classes. *Nucleic Acids Res* 36:6429–6438
- Vazquez F, Gascioli V, Cr  t   P, Vaucheret H. (2004). The nuclear dsRNA binding protein HYL1 is required for microRNA accumulation and plant development, but not posttranscriptional transgene silencing. *Curr Biol* 14:346–351

- Venkataraman K, Brown KM, Gilmartin GM. (2005). Analysis of a noncanonical poly(A) site reveals a tripartite mechanism for vertebrate poly(A) site recognition. *Genes Dev* 19:1315–1327
- Voinnet O. (2009). Origin, biogenesis, and activity of plant microRNAs. *Cell* 136:669–687
- Wachter A, Ruhl C, Stauffer E. (2012). The role of polypyrimidine tract-binding proteins and other hnRNP proteins in plant splicing regulation. *Front Plant Sci* 3:81
- Wahle E. (1991). A novel poly(A)-binding protein acts as a specificity factor in the second phase of messenger RNA polyadenylation. *Cell* 66:759–768
- Wahle E. (1995). Poly(A) tail length control is caused by termination of processive synthesis. *J Biol Chem* 270:2800–2808
- Wang BB, Brendel V. (2004). The ASRG database: identification and survey of *Arabidopsis thaliana* genes involved in pre-mRNA splicing. *Genome Biol* 5:R102
- Wang BB, Brendel V. (2006) Genomewide comparative analysis of alternative splicing in plants. *Proc Natl Acad Sci USA* 103:7175–7180
- Wang B, Duan C-G, Wang X, Hou Yj, Yan J, Gao C, Kim JH, Zhang H, Zhu JK. (2015). HOS1 Regulates Argonaute1 by Promoting the Transcription of the MicroRNA Gene MIR168b in Arabidopsis. *Plant J* 81:861–870
- Wang L, Song X, Gu L, Li X, Cao S, Chu C, Cui X, Chen X, Cao X. (2013). NOT2 proteins promote polymerase II dependent transcription and interact with multiple MicroRNA biogenesis factors in Arabidopsis. *Plant Cell* 25:715–727
- Weigel D, Ahn JF, Blazquez MA, Borevitz JO, Christensen SK, Fankhauser C, Ferrandiz C, Karadailsky I, Malancharuvil EJ, Neff MM, Nguyen JT, Sato S, Wang ZY, Xia Y, Dixon RA, Harrison MJ, Lamb CJ, Yanofsky MF, Chory J. (2000). Activation tagging in Arabidopsis. *Plant Physiol* 122:1003–1014
- Wiebauer K, Herrero JJ, Filipowicz W. (1988). Nuclear pre-mRNA processing in plants: Distinct modes of 3'-splice-site selection in plants and animals. *Mol Cell Biol* 8:2042–2051
- Wightman B, Ha I, Ruvkun G. (1993). Posttranscriptional regulation of the heterochronic gene *lin-14* by *lin-4* mediates temporal pattern formation in *C. elegans*. *Cell* 75:855–862
- Wu F, Yu L, Cao W, Mao Y, Liu Z, He Y. (2007). The N-terminal double-stranded RNA binding domains of Arabidopsis HYPONASTIC LEAVES1 are sufficient for pre-microRNA processing. *Plant Cell* 19:914–925
- Wu X, Shi Y, Li J, Xu L, Fang Y, Li X, Qi Y. (2013). A role for the RNA-binding protein MOS2 in microRNA maturation in Arabidopsis. *Cell Res* 23:645–657
- Xie Z, Allen E, Fahlgren N, Calamar A, Givan SA, Carrington JC. (2005). Ex Arabidopsis MIRNA genes. *Plant Physiol* 138:2145–2154

- Xing D, Li QQ. (2011). Alternative polyadenylation and gene expression regulation in plants. *Wiley Interdiscip Rev RNA* 2:445–458
- Xing D, Zhao H, Li QQ. (2008). Arabidopsis CLP1-SIMILAR PROTEIN3, an ortholog of human polyadenylation factor CLP1, functions in gametophyte, embryo, and postembryonic development. *Plant Physiol* 148:2059–2069 (B)
- Xing D, Zhao H, Xu R, Li QQ. (2008). Arabidopsis PCFS4, a homologue of yeast polyadenylation factor Pcf11p, regulates FCA alternative processing and promotes flowering time. *Plant J* 54:899–910 (A)
- Yamasaki H, Abdel-Ghany SE, Cohu CM, Kobayashi Y, Shikanai T, Pilon MJ. (2007). Regulation of copper homeostasis by micro-RNA in Arabidopsis. *J Biol Chem* 282:16369–16378
- Yamasaki H, Hayashi M, Fukazawa M, Kobayashi Y, Shikanai T. (2009). SQUAMOSA Promoter Binding Protein-Like7 is a central regulator for copper homeostasis in Arabidopsis. *Plant Cell* 21:347–361
- Yan K, Liu P, Wu CA, Yang GD, Xu R, Guo QH, Huang JG, Zheng CC. (2012). Stress-induced alternative splicing provides a mechanism for the regulation of microRNA processing in *Arabidopsis thaliana*. *Mol Cell* 48:521–531
- Yang L, Liu Z, Lu F, Dong A, Huang H. (2006). SERRATE is a novel nuclear regulator in primary microRNA processing in Arabidopsis. *Plant J* 47:841–850
- Yang SW, Chen HY, Yang J, Machida S, Chua NH, Yuan YA. (2010). Structure of Arabidopsis HYPONASTIC LEAVES1 and its molecular implications for miRNA processing. *Structure* 18:594–605
- Yang X, Zhang H, Li L. (2011). Global analysis of gene-level microRNA expression in Arabidopsis using deep sequencing data. *Genomics* 98:40–46
- Yi R, Qin Y, Macara IG, Cullen BR. (2003). Exportin-5 mediates the nuclear export of pre-microRNAs and short hairpin RNAs. *Genes Dev* 17:3011–3016
- Yoshimura K, Yabuta Y, Ishikawa T, Shigeoka S. (2002). Identification of a cis element for tissue-specific alternative splicing of chloroplast ascorbate peroxidase pre-mRNA in higher plants. *J Biol Chem* 277:40623–40632
- Yu B, Bi L, Zheng B, Ji L, Chevalier D, Agarwal M, Ramachandran V, Li W, Lagrange T, Walker JC, Chen X. (2008). The FHA domain proteins DAWDLE in Arabidopsis and SNIP1 in humans act in small RNA biogenesis. *Proc Natl Acad Sci USA* 105:10073–10078
- Zhan X, Wang B, Li H, Liu R, Kalia RK, Zhu J-K, Chinnusamy V. (2012). Arabidopsis proline-rich protein important for development and abiotic stress tolerance is involved in microRNA biogenesis. *Proc Natl Acad Sci USA* 109:18198–18203

- Zhang S, Liu Y, Yu B. (2014). PRL1, an RNA-binding protein, positively regulates the accumulation of miRNAs and siRNAs in Arabidopsis. *PLoS Genet* 10:e1004841
- Zhang S, Liu Y, Yu B. (2015). New insights into pri-miRNA processing and accumulation in plants. *Wiley Interdiscip Rev RNA* 6:533–545
- Zhang S, Xie M, Ren G, Yu B. (2013). CDC5, a DNA binding protein, positively regulates posttranscriptional processing and/or transcription of primary microRNA transcripts. *Proc Natl Acad Sci USA* 110:17588–17593
- Zhang W, Gao S, Zhou X, Xia J, Chellappan P, Zhou X, Zhang X, Jin H. (2010). Multiple distinct smallRNAs originate from the same microRNA precursors. *Genome Biol* 11:R81
- Zhou X, Wang G, Sutoh K, Zhu JK, Zhang W. (2008). Identification of cold-inducible microRNAs in plants by transcriptome analysis. *Biochim Biophys Acta* 1779:780–788
- Zhou X, Wang G, Zhang W. (2007). UV-B responsive microRNA genes in *Arabidopsis thaliana*. *Mol Syst Biol* 3:103
- Zielezinski A, Dolata J, Alaba S, Kruszka K, Pacak A, Swida-Barteczka A, Knop K, Stepień A, Bielewicz D, Pietrykowska H, Sierocka I, Sobkowiak L, Lakomiak A, Jarmolowski A, Szweykowska-Kulinska Z, Karłowski WM. (2015). mirEX 2.0 - an integrated environment for expression profiling of plant microRNAs. *BMC Plant Biol* 15:144